aman ta zabal zazu

Universidad del País Vasco

Euskal Herriko Unibertsitatea

Departamento de Fisiología
Facultad de Medicina y Odontología

Novel insights in the pathogenesis of primary biliary cholangitis and cholangiocarcinoma

Tesis presentada por
OIHANE ERICE AZPARREN

San Sebastián, 19 de Mayo de 2017

Novel insights in the pathogenesis of primary biliary cholangitis and cholangiocarcinoma

Tesis presentada por
Oihane Erice Azparren

Para la obtención del título de doctor en
***Investigación Biomédica* por la**
Universidad del País Vasco/Euskal Herriko Unibertsitatea

Tesis dirigida por
Dr. D. Jesús María Bañales Asurmendi
Dra. Dña. María Jesús Perugorria Montiel

Sponsor:

AKNOWLEDGEMENTS
AGRADECIMIENTOS

Hace ya más de cuatro años que me embarqué en la aventura de la tesis, un viaje lleno de emociones del que me llevo grandes recuerdos. El camino a la meta que es la tesis suele ser duro en ciertas ocasiones, pero con la ayuda de todos los que me han rodeado ha sido mucho más ameno, y aún recuerdo incluso mi primer día como si fuese ayer.

Comienzo agradeciendo a mis directores de tesis, Txus y Matxus. Gracias por haberme acogido en el grupo y haberme dado la oportunidad de aprender tantas cosas, tanto a nivel profesional como personal, mostrando siempre un gran entusiasmo por la ciencia.

Agradezco también a la Asociación Española Contra el Cáncer (AECC), especialmente a la Junta de Gipuzkoa por haberme concedido la beca gracias a la cual he podido desarrollar este trabajo. Además he podido conocer un poco más de cerca la labor que ejercen. El trabajo de los trabajadores y voluntarios es muy importante para la sociedad. Por todo ello, muchas gracias. Gracias al Instituto de Investigación Sanitaria Biodonostia y a la Universidad del País Vasco (UPV/EHU) por darme la oportunidad de llevar a cabo la tesis doctoral.

Por supuesto agradezco a todo el equipo de *hepato*. Al principio éramos muy pocos, pero es ya tanta la gente que ha ido pasando por el laboratorio que es difícil nombraros a todos y resumir lo mucho que cada uno me habéis aportado. Gracias a todos vosotros las largas horas en cultivos, en la sala de revelado o junto al dichoso citómetro (sí sí, el de la barbie) han sido muy divertidas en muchas ocasiones. Con vosotros he aprendido infinidad de cosas, como por ejemplo a calmarme en los momentos de más estrés, a sacar las mayores risas de los peores resultados (como esos films totalmente transparentes o con *agujeritos* sospechosos), y a ser como las *amatxos*, que encuentran todo sin que apenas sepan de su existencia. Agradezco también a los colaboradores que han participado en el desarrollo de mis estudios y a toda la gente de Biodonostia, siempre dispuestos a ayudar dentro del trabajo y a hacer planes fuera de él. Jamás olvidaré los cafés y vivencias compartidos con todo el equipo de Biodonostia.

No puedo olvidarme de mi *kuadrilla*. A pesar del poco tiempo que pasamos juntas en los últimos años, siempre estáis ahí, haciendo que esas largas de horas de trabajo queden en el olvido al menos durante esos *ratikos* únicos. No

me olvido de los demás amigos por hacerme pasar grandes momentos. Las escapadas a Iruña siempre han sido lo más deseado para poder estar con vosotr@s.

Por último, y de manera especial, agradezco a mi familia. A mi aita y mi ama sobre todo, ya que gracias a ellos y a su gran esfuerzo he podido llevar a cabo todo lo que me he propuesto. Esto no habría sido posible sin vosotros. Gracias a vuestro apoyo incondicional, vuestro cariño, consuelo y sabios consejos. Me entristece no haber podido estar en todos y cada uno de esos momentos que me hubiese gustado, aunque como bien sabéis, 'nuestra mesa siempre tendrá cuatro patas'. Esa cuarta pata es mi hermana, Edur. Agradezco tus consejos y ánimos, mostrando siempre el lado más optimista de la vida. Estoy orgullosa de ti, de cómo eres y de quien eres. Muchas gracias también a Mikel, Juana e Iñaki, por vuestro apoyo y cariño en todo momento y por esas interesantes charlas de fin de semana. A Ibai, no podría incluir aquí todo lo que tengo que agradecerte. Estos años fuera de los nuestros has sido mi apoyo diario, tanto en lo personal como en lo profesional. Me has dado serenidad en los momentos difíciles, has sido ese hombro en que buscar cariño y siempre estás ahí para todo lo que necesito, con tu gran paciencia, consiguiendo que paso a paso vaya ganando confianza en mí misma. Estoy orgullosísima de cada uno de vosotros y tremendamente agradecida de teneros siempre cerca de un modo u otro.

ABBREVIATIONS

5-FU	5-Fluorouracil
6-EMCA	6α-ethyl-23(S)-methyl-3α,7α,12α-trihydroxyl-5β-cholan-24-oic acid
7AAD	7-aminoactinomycin D
ABCG2	ATP-binding cassette sub-family G member 2
AE2	Anion exchanger 2
AIH	Autoimmune hepatitis
ALP	Alkaline phosphatase
ALT	Alanine aminotransferase
AMAs	Anti-mitochondrial autoantibodies
ANAs	Antinuclear antibodies
ANOVA	Analysis of variance
ASBT	Apical sodium-dependent bile salt transporter
AST	Aspartate aminotransferase
ATF6	Activating transcription factor 6
ATP	Adenosine triphosphate
BA	Bile acid
BAX	Bcl-2-associated X protein
BCA	Bicinchoninic acid
BCL2	B-cell lymphoma 2
BIRC5	Baculoviral inhibitor of apoptosis repeat-containing 5
BRAF	V-Raf murine sarcoma viral oncogene homolog B
BSA	Bovine serum albumin
BSEP	Bile salt export pump
BSIA	Bile salt-induced apoptosis
BTEB2	Basic transcription element binding protein 2
CA	Cholic acid
CA19-9	Carbohydrate antigen 19-9
CA125	Carbohydrate antigen 125
CA242	Carbohydrate antigen 242
Ca^{2+}_i	Intracellular calcium
CAF	Cancer-associated fibroblast
cAMP	Cyclic adenosine monophosphate
CAR	Constitutive androstane receptor
CCA	Cholangiocarcinoma
CD25	Cluster of differentiation 25
Cdc25A	Cell division cycle 25 homolog A
Cdc42	Cell division control protein 42 homolog
CDCA	Chenodeoxycholic acid
CDK	Cyclin-dependent kinase
cDNA	Complementary DNA
CEA	Carcinoembryonic antigen
CFSE	Carboxyfluorescein succinimidyl ester
CFTR	Cystic fibrosis transmembrane conductance regulator

CHOP	CCAAT-enhancer-binding protein homologous protein
Cis	Cis-Diammineplatinum (II) dichloride or Cisplatin
CisGem	Cisplatin plus gemcitabine
CK7	Cytokeratin 7
CK19	Cytokeratin 19
CK20	Cytokeratin 20
Cl^-	Chloride
CMV	Cytomegalovirus
CRISPR	Clustered regularly interspaced short palindromic repeats
CT	Computed tomography
CYFRA21-1	Cytokeratin fragment 21-1
CYP27A1	Sterol 27-hydroxylase
CYP7A1	Cytochrome P450 7A1
CYP7B1	Oxysterol 7α-hydroxylase
CYP8B1	Cytochrome P450 family 8 subfamily B member 1
DAB	*3,3-diaminobenzidine*
DAPI	40,6-diamidino-2-phenyindole
DCA	Deoxycholic acid
dCCA	Distal CCA
DEX	Dexamethasone
DHE	Dihydroethidium
DMEM/F-12	Dulbecco’s modified Eagle’s medium/Ham’s F-12
DMSO	Dimethyl sulfoxyde
DNA	Deoxyribonucleic acid
dNTPs	Deoxy-nucleotide-triphosphate mix
dsOligo	Double stranded oligo
DTT	Dithiothreitol
ECAR	Extracellular acidification rate
EDTA	Ethylenediaminetetraacetic acid
EGF	Epidermal growth factor
EGFR	Epidermal growth factor receptor
EGTA	Ethylene glycol tetraacetic acid
EKLF	Erythroid Krüppel-like factor
EMT	Epithelial-mesenchymal transition
ER	Endoplasmic reticulum
ERCP	Endoscopic retrograde cholangiopancreatography
ERK	Extracellular-signal regulated kinase
ERK1/2	Extracellular signal-regulated kinases 1/2
EUS	Endoscopic ultrasound
FBS	Fetal bovine serum
FBW7	F-box and WD repeat domain-containing 7
FCCP	Carbonyl cyanide-P-trifluoromethoxyphenylhydrazone
FDA	Food and drug administration
FGF19	Fibroblast growth factor 19

FGFR	Fibroblast growth factor receptor
free-dH_2O	Ultrapure DNase/RNase-free distilled water
FXR	Farnesoid X receptor
GAPDH	Glyceraldehyde-3-phosphate dehydrogenase
GCDCA	Glycochenodeoxycholic acid
Gem	Gemcitabine
GEO	Gene Expression Omnibus
GFP	Green fluorescent protein
GGT	Gamma glutamil transferase
GLP-1	Glucagon-like peptide-1
GO	Gene ontology
GPBAR1	G protein-coupled bile acid receptor 1
gRNA	Guide RNA
GRP78	Glucose-regulated protein 78
GTPase	Guanosine triphosphate hydrolase
H_2O_2	Hydrogen peroxide
H3	Histone 3
HBV	Viral hepatitis B
HCC	Hepatocellular carcinoma
HCO_3^-	Bicarbonate
HCV	Viral hepatitis C
HDAC	Histone deacetylases
HEPES	4-(2-hydroxyethyl)-1-piperazineethanesulfonic acid
HIF1α	Hypoxia-inducible factor 1-alpha
HPC	Hepatic progenitor cells
HRP	Horseradish peroxidase
HSC	Hepatic stellate cell
iCCA	Intrahepatic CCA
IDH1	Isocitrate dehydrogenases 1
IDH2	Isocitrate dehydrogenases 2
IF	Inmunofluorescence
IFNγ	Interferon gamma
IG	Intraductal growing
IgM	Immunoglobulin M
IKLF	Intestinal enriched Krüppel-like factor
IL-6	Interleukin-6
IL-8	Interleukin-8
InsP3R3	Type III inositol 1,4,5-trisphosphate receptor
IRE1	Inositol-requiring enzyme 1
iTRAQ	Isobaric Tags for Relative and Absolute Quantitation
KLF	Krüppel-like factor
KLF5	Krüppel-like factor 5
KOH	Potassium hydroxide
KRAS	Ki-ras2 Kirsten rat sarcoma viral oncogene homolog

LB	Lysogeny broth
LCA	Lithocholic acid
MCL1	Myeloid cell leukemia
MEK	Mitogen-activated protein kinase
MEM	Minimum Essential Medium
MF	Mass-forming
MiR	MicroRNA
MiR-506	MicroRNA-506
miR-neg	MicroRNA-negative
MMP9	Matrix metalloproteinase 9
MOC	Mechanisms of chemoresistance
MOI	Multiplicity of infection
MRC	Magnetic resonance cholangiography
MRI	Magnetic resonance imaging
mRNA	Messenger RNA
MRP2	Multidrug-resistance associated protein 2
MRP3	Multidrug-resistance associated protein 3
MRP4	Multidrug-resistance associated protein 4
MUC5AC	Mucin 5AC
NASH	Non-alcoholic steatohepatitis
NHC	Normal human cholangiocyte
NHR	Nuclear hormone receptor
NP40	Nonidet P40 Substitute
NTCP	Na^+-taurocholate cotransporting polypeptide
O/N	Overnight
OATP	Organic anion transporting polypeptides
OCA	Obeticholic acid
OCR	Oxygen consumption rate
OCT4	Octamer-binding transcription factor 4
ORF	Open reading frame
OST α/β	Organic solute transporter α/β
OXPHOS	Oxidative phosphorylation
P/S	Penicillin-streptomycin
PAM	Protospacer adjacent motif
PBC	Primary biliary cholangitis
PBS	Phosphate buffered saline
PCA	Perchloric acid
pCCA	Perihilar CCA
PCNA	Proliferating cell nuclear antigen
PCR	Polymerase chain reaction
PDC-E2	E2 component of the pyruvate dehydrogenase complex
PDGF	platelet-derived growth factor
PERK	PPKR-like ER kinase
pH2AX	Phosphorylated histone H2A variant X

PHA-M	Phytohaemagglutinin M form
PI	Periductal infiltrating
PI3K	Phosphatidyl inositol 3-kinase
PKA	Protein kinase A
PMBCs	Peripheral blood mononuclear cells
PSC	Primary sclerosing cholangitis
PTC	Percutaneous transhepatic cholangiography
PXR	Pregnane X receptor
qPCR	Quantitative polymerase chain reaction
Rac1	Ras-related C3 botulinum toxin substrate 1
RAR	Retinoic acid receptor
Rho	Ras homolog
RIPA	Radio-immunoprecipitation assay
RNA	Ribonucleic acid
ROS	Reactive oxygen species
RPMI	Roswell park memorial institute medium
RT-PCR	Reverse transcription-PCR
RXRα	Retinoid X receptor α
SDS	Sodium dodecyl sulfate
SDS-PAGE	SDS-polyacrilamide gel electrophoresis
SEM	Standard error of the mean
SGLT1	Sodium/glucose cotransporter 1
sgRNA	Single guide RNA
SHP	Short heterodimer partner
shRNA	Short hairpin RNA
SIRT1	Sirtuin-1
SLC4A2	Cl^-/HCO_3^- exchanger
SMAD4	Smad family member 4
SOX2	Sry (sex-determining region y) box 2
Sp1	Specificity protein 1
SR	Secretin receptor
T3	3, 3' 5-triiodo-L-thyronine
TAA	Thioacetamide
TACE	Transarterial chemoembolization
TAM	Tumor-associated macrophages
TAN	Tumor adjacent normal
TARE	Transarterial radioembolization
TBE	Tris-borate-EDTA buffer
TBS-Tween	Tris-buffered saline-5% tween
TCGA	The Cancer Genome Atlas
TF	Transcription factor
TGFβ	Transforming growth factor beta
Th	T-helper
TNFα	Tumor necrosis factor-alpha

TP53	Tumor protein p53
TUDCA	Tauroursodeoxycholic acid
UCP	Uncoupling protein
UDCA	Ursodeoxycholic acid
uHTS	Ultra-high-throughput screening
UPR	Unfolded protein response
UTR	Untranslated region
UV	Ultraviolet
VDR	Vitamin D_3 receptor
VEGF	Vascular endothelial growth factor
WB	Western blot
WST-1	Water soluble tetrazolium salt 1
WWP1	WW domain containing E3 ubiquitin protein ligase 1
XBP1	X-box binding protein 1
ZO-1	Zonula occludens-1

INDEX

I. INTRODUCTION

I.1 *The liver and the biliary tract*

The liver is the biggest organ in the human body and one of the most important for the maintenance of physiological homeostasis [1]. The liver performs key metabolic functions including cholesterol production, glucose storage, protein, amino acid, and lipid metabolism, detoxification processes as well as bile production [2]. The bile is a vital aqueous secretion unique in the liver which owns important functions such as the emulsion of incoming dietary fat, immunological protection of the organism from enteric infections and the excretion of toxic substances [i.e. bilirubin and bile acids (BAs)] as well as elimination of cholesterol [3]. The liver is mainly composed by two epithelial cell types, i.e. hepatocytes and cholangiocytes, which represent ~70% and ~3-5% of total liver cells, respectively, and are responsible for the formation of bile [3, 4] (Figure I.1). Hepatocytes generate and secrete the primary bile into the canaliculus (a thin lumen formed between the apical membranes of two adjacent hepatocytes). Then, bile drains into the bile ducts (formed by cholangiocytes) for its transport and modification in the way to the duodenum [3]. The liver also contains other important non-parenchymal cells: i) Kupffer cells (specialized liver macrophages with immunological and phagocytic functions), ii) hepatic stellate cells (involved in liver remodeling processes associated with hepatic fibrosis) and iii) sinusoidal endothelial cells (which allow the communication of portal blood with hepatocytes) [1].

The biliary tree has a heterogeneous structure, going from the canals of Hering to the main bile duct, and is consisted of both intrahepatic and extrahepatic bile ducts. The canals of Hering are localized intralobularly, lined by immature cholangiocytes (also considered hepatic progenitor cells, HPCs), and, among other functions, they collect the canalicular bile. The canals of Hering continue into the bile ductules, which are entirely lined by mature cholangiocytes. Bile ductules converge into the interlobular bile ducts, which are located in the portal space, and then continue into ducts of major size [5-7]. The intrahepatic bile ducts correspond to the structure going from the ductule-canalicular junction with the canals of Hering to the segmental ducts, whereas the extrahepatic bile ducts include: hepatic ducts (right, left and common hepatic ducts), gallbladder, cystic duct, common bile duct and hepato-

pancreatic ampulla [6]. The size of the ducts increases throughout the biliary tree, from the liver to the intestine, and cholangiocytes lining small *vs* large ducts are functionally heterogeneous [6, 8] (Figure I.1).

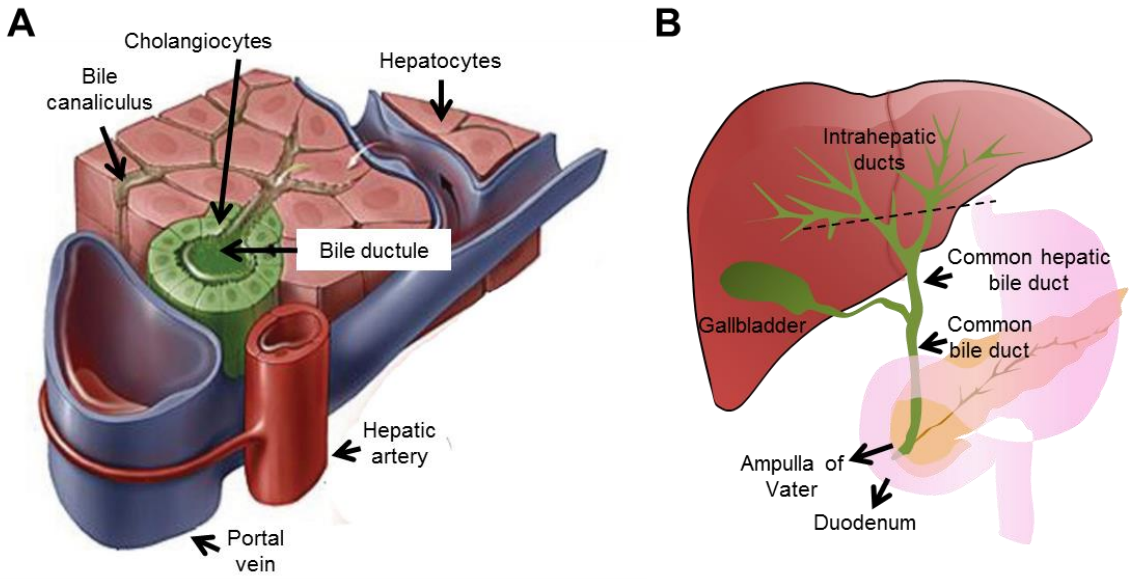

Figure I.1. Liver and biliary tree architecture. (A) The liver is mainly composed by hepatocytes, which form the canaliculi. Within the liver, bile ducts – which are lined by cholangiocytes – form the portal triad together with the adjacent hepatic artery and portal vein. **(B)** The biliary tree consists of a network of intrahepatic and extrahepatic tubular ductules that end up in the duodenum (Adapted from Tabibian *et al*., 2013 and Erice *et al*., 2015).

I.2 *Bile duct epithelial cells: cholangiocytes*

Cholangiocytes represent a small proportion of all liver cells but are very important in health and disease. They account for up to ~30-40% of the total bile flow, contributing to the fluidization and alkalinization of bile. Cholangiocytes contain an array of transmembrane carriers, located either at the apical or at the basolateral side, that regulate bile composition [3, 9-11]. This system includes channels (like water channels: aquaporins), transporters (e.g. SGLT1: Na^+-glucose transporter) and exchangers (e.g. SLC4A2: Cl^-/HCO_3^- exchanger) [9-11]. During the bile transit along the bile ducts, water and other electrolytes are secreted and/or absorbed, being bicarbonate secretion one of the most important processes [4]. The secretin receptor (SR), the cystic fibrosis transmembrane conductance regulator (CFTR) and the Cl^-/HCO_3^- anion exchanger 2 (AE2) altogether promote the biliary bicarbonate secretion, which

is the driving force for the movement of water and protects cholangiocytes against the damaging effect of toxic apolar hydrophobic BAs (a mechanism termed as the “biliary bicarbonate umbrella”) [12, 13]. Cholangiocytes can communicate and interact with other cell types in the bile ducts and can therefore respond to endogenous and exogenous stimuli, such as xenobiotics, microorganisms or drugs [14, 15]. Moreover, cholangiocytes contribute to the maintenance of tissue homeostasis by modulating key cellular processes [14, 15].

Cholangiocytes can be damaged by the interaction with exotoxins, endotoxins, microorganisms, xenobiotics or other environmental factors and respond to these by developing a reactive phenotype, generating a pro-inflammatory microenvironment. Cells are able to repair potential acute injuries regressing to a normal phenotype, a process dependent on cell genetics, epigenetic mechanisms and posttranscriptional regulation. However, if the insult persists over time, chronic biliary inflammation may lead to the development of certain cholangiopathies [15] (Figure I.2).

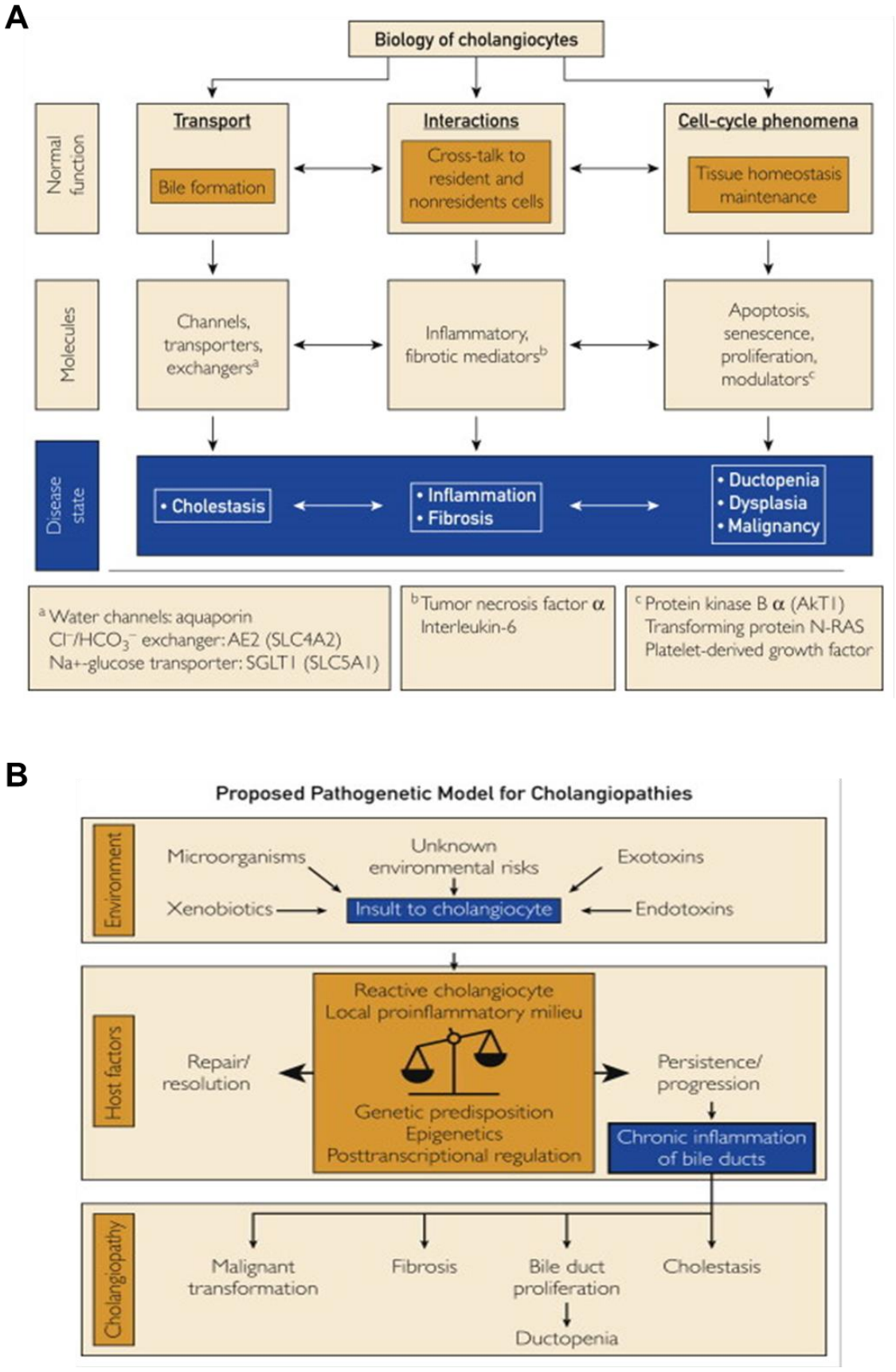

Figure I.2. Cholangiocytes in health and disease. (A) Biology of cholangiocytes. **(B)** Cholangiocytes response to injury. (Adapted from Lazaridis and LaRusso, 2015).

I.3 *Cholangiopathies*

Diseases affecting cholangiocytes are known as cholangiopathies, a term comprising genetic and acquired biliary malignancies. Alterations in the main physiological functions of cholangiocytes result in a pathological state, involving the following processes: *i*) abnormalities in bile formation, which results in cholestasis, *ii*) dysfunctions in the interaction with other cells, that might led to inflammation and fibrosis, and *iii*) dysregulations in cell-cycle phenomena, which can promote the development of ductopenia, dysplasia or malignancy [15]. Under different insults, cholangiocytes activate proliferative mechanisms to repair and compensate the loss of cells (i.e. ductopenia), by a process known as “ductular reaction”, in which HPCs in the canals of Hering might also contribute [16-18]. A neuroendocrine transdiferentiation of cholangiocytes is stimulated and autocrine and paracrine factors are released leading to fibrogenesis by the activation of portal fibroblasts and hepatic stellate cells [4] (Figure I.3). Among the molecules secreted by injured cholangiocytes, pro-inflammatory cytokines [i.e. interleukin-6 (IL-6), interleukin-8 (IL-8), tumor necrosis factor α (TNFα)], growth factors [i.e. platelet-derived growth factor (PDGF), vascular endothelial growth factor (VEGF), and transforming growth factor-beta (TGFβ] and morphogens (i.e. Hedgehog and Notch) are found, which, apart from regulating cholangiocyte functions themselves, also stimulate innate and adaptative immune responses contributing to the tissue response to injury [15, 19]. Finally, the chronic fibrosis might progress to the development of cirrhosis [20].

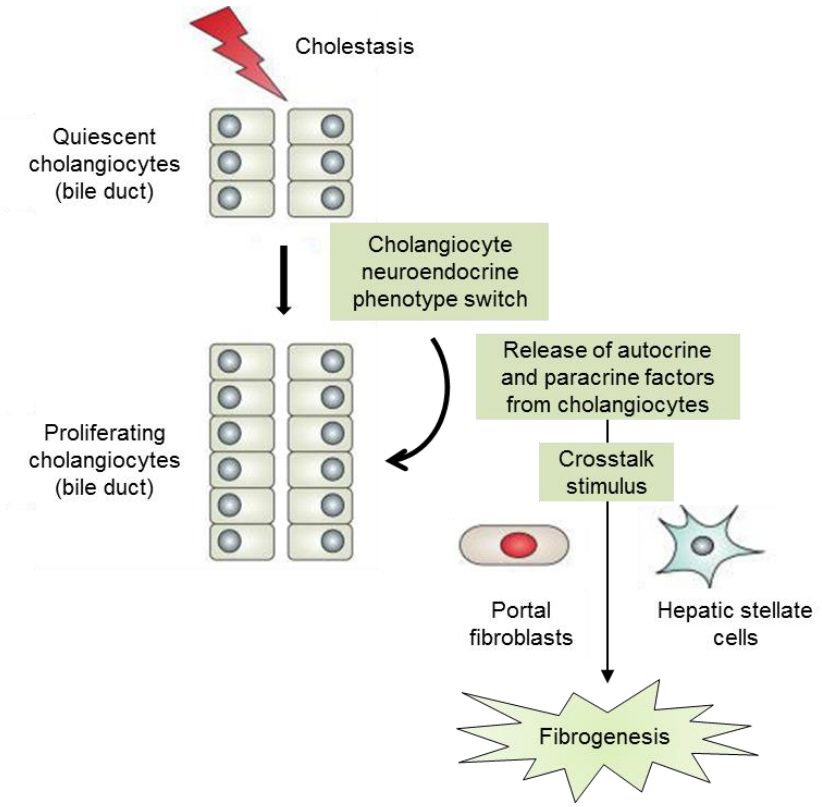

Figure I.3. Response of cholangiocytes to injury. Injury or cholestasis result in cholangiocyte activation, leading to their proliferation and stimulation of the neuroendocrine transdifferentiation of cholangiocytes. Their proliferation is regulated in an autocrine/paracrine manner and fibrogenic responses of portal fibroblasts and hepatic stellate cells are activated, resulting in activated myofibroblasts and in fibrogenesis. (Adapted from Glaser *et al* 2009).

Cholangiopathies are usually classified based on their etiology into: *i*) immune-associated, *ii*) infectious, *iii*) genetic, *iv*) vascular, *v*) idiopathic, *vi*) neoplastic or *vii*) drug-induced [9, 15] (Figure I.4). These biliary diseases are commonly characterized by inflammation and cholestasis, but they also have their own particularities [15]. In general, cholangiopathies account for high morbidity and mortality, and the available therapeutic options usually show short-term and modest beneficial effects, liver transplantation being the only curative option in many cases [15]. Therefore, it is important to elucidate the mechanisms involved in the development and progression of these diseases in order to find potential targets for therapy. The present dissertation aimed to analyze new mechanisms of pathogenesis in primary biliary cholangitis (PBC; an immune-associated cholangiopathy) and cholangiocarcinoma (CCA; the neoplastic biliary disease) in order to further search for new therapeutic targets and to test novel treatment strategies.

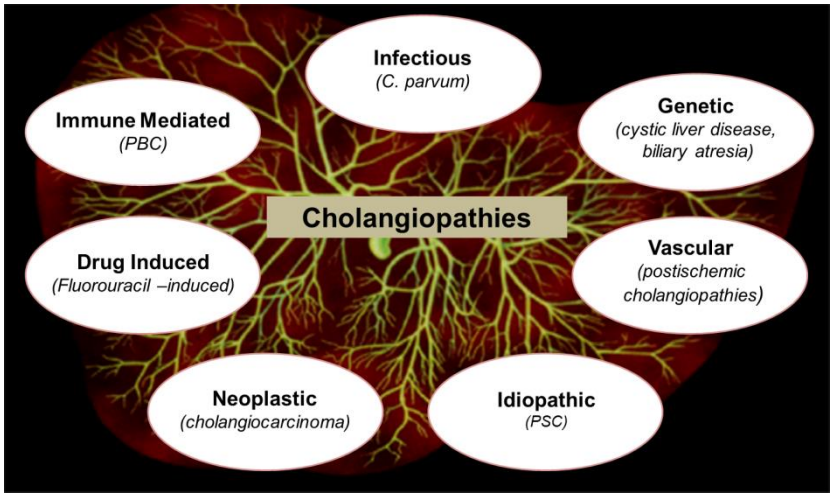

Figure I.4. Classification of cholangiopathies according to their etiology (Kindly provided by Prof. N. Larusso (Mayo Clinic).

I.3.1 *Primary biliary cholangitis (PBC)*

The first human diseases associated with autoimmune phenomena were described during 1950s, and the liver was one of the first organs described to be affected by these type of diseases [21]. Liver diseases associated to autoimmune phenomena include autoimmune hepatitis (AIH), primary sclerosing cholangitis (PSC) and primary biliary cholangitis (PBC) [21], the last two primarily targeting bile duct cells. To date, their etiopathogenesis still remains poorly understood.

I.3.1.1 *General features*

Primary biliary cholangitis (PBC), previously named as primary biliary cirrhosis [22], is a chronic cholestatic liver disease associated with autoimmune phenomena targeting the small intrahepatic bile ducts [22-24]. PBC is characterized by progressive impairment and destruction of bile duct epithelial cells together with increased portal inflammation and fibrosis [25] that, without treatment, may ultimately result in liver cirrhosis [26-29] (Figure I.5).

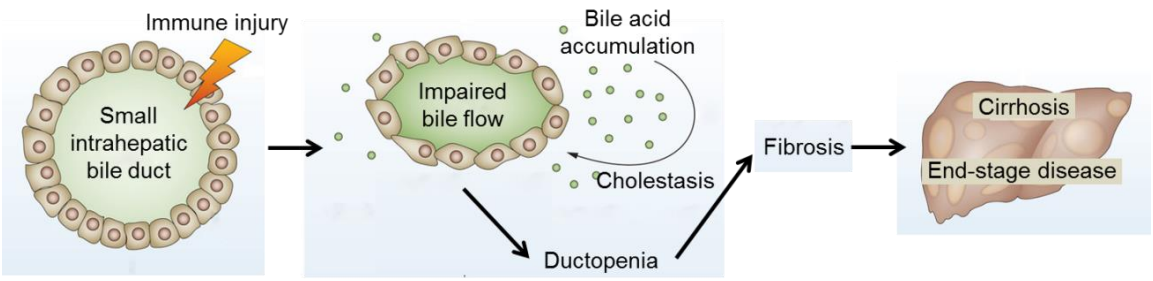

Figure I.5. Stages of PBC pathogenesis. Immune-mediated biliary injury leads to impaired bile flow, cholestasis and ductopenia. Intrahepatic accumulation of toxic bile acids causes fibrosis that may progress to cirrhosis and end-stage liver disease (Adapted from Dyson *et al*., 2015).

PBC etiology is considered multifactorial but the specific causes still remain unknown. The prevalence of PBC in Europe is estimated in 35 per 100,000 individuals but there is high variability between countries, being more popular in northern than in southern countries [30]. This rare disease is usually diagnosed in middle aged (~50 years old) women, [31] with a female/male ratio of 10/1 [32]. Geographical differences have been reported regarding genetic susceptibility and environmental factors which may promote the development and progression of PBC [30]. The individual role of each of these factors separately is not clear, but a correlation of genetic and environmental factors mediated by epigenetic modifications has been reported in PBC [33]. PBC-associated main symptoms include pruritus and fatigue, which significantly affect the life quality of these patients [30].

I.3.1.2 *PBC diagnosis*

PBC is usually diagnosed by a combination of different approaches. PBC patients are characterized by increased serum levels of biliary markers of injury such as alkaline phosphatase (ALP) and gamma glutamil transferase (GGT), as well as by mildly elevated levels of hepatocellular damage markers [i.e. aminotranferases such as alanine aminotransferase (ALT) or aspartate aminotransferase (AST)]. In addition, increased serum levels of immunoglobulins, mainly immunoglobulin M (IgM) also occurs. Of note, ~95% of PBC patients are characterized by the presence of anti-mitochondrial autoantibodies (AMAs) against the E2 component of the pyruvate dehydrogenase complex (PDC-E2) in serum, which is considered the serological hallmark of the disease, and a proportion also develop antinuclear antibodies (ANAs) [30, 34, 35]. Histological analysis of liver biopsy can also be used to further confirm the diagnosis, although this is not commonly indicated. Liver imaging by magnetic resonance or by endoscopy allows the exclusion of other liver or biliary tract diseases such as PSC [34].

I.3.1.3 *PBC therapeutic options*

Despite the autoimmune features of PBC, treatment with classical immunosuppressants is inefficient. By contrast, a chronic daily administration of ursodeoxycholic acid (UDCA), a choleretic BA, is the first option treatment approved by the food and drug administration (FDA) for PBC patients. UDCA improves the prognosis in ~2/3 of patients when treated in early stages of the disease [24, 36-38]. UDCA is a hepatoprotective BA that induces choleresis by stimulating the hepatobiliary secretion of bicarbonate, which further induces the alkalinization and fluidization of bile and prevents the damaging effect of hydrophobic BAs on the biliary epithelium [24, 37, 38]. On the other hand, obeticholic acid (OCA), a farnesoid X receptor (FXR) agonist, has recently been approved either in combination with UDCA – for those patients with an inadequate response to UDCA – or as monotherapy – for UDCA intolerant patients – [39]. OCA improves serum ALP levels, but may provoke adverse side effects such as pruritus, fatigue, abdominal pain and discomfort [39]. Ultimately, liver transplantation can be required in certain cases [40].

I.3.2 *Cholangiocarcinoma (CCA)*

I.3.2.1 *General features*

Cholangiocarcinoma (CCA) includes a heterogeneous group of malignancies affecting cholangiocytes at any point of the biliary tree [41, 42]. CCAs are usually classified according to their anatomical location as intrahepatic (iCCA), perihilar (pCCA) or distal CCA (dCCA) [43, 44], which share some features but also have important inter- and intra-tumoral differences that may impact on the pathogenesis and outcome [45]. Taken together, CCAs represent the second most frequent primary liver tumor after hepatocellular carcinoma (HCC) and correspond to ~3% of all gastrointestinal cancers [41, 43]. Overall, CCA is a rare cancer (incidence < 6/100,000) although its incidence is increasing worldwide and differs along the geographic distribution [46-48]. In this regard, Eastern countries such as Thailand, China and Korea show higher rates (>6/100.000) than Western countries (<4/100.000) [48], which is associated to infections with endemic parasites (i.e. *Opistorchis viverrini* and *Clonorchis*

sinensis) [48]. CCA is generally diagnosed in the elderly (~60-70 years-old) and is more frequent in men than in women [49].

I.3.2.2 *Classification*

The classification of CCA has been widely discussed and several classifications have been proposed taking into account different aspects of these tumors. Based on the anatomical location, the most recent classification grouped CCAs as iCCA (involving second degree bile ducts), pCCA (referring to CCAs between second degree bile ducts and the cystic duct) and dCCA (which corresponds to CCAs arising between the cystic duct and the ampulla of Vater) (Figure I.6A) [49]. Among them, pCCA is the most frequent type (~50%) followed by dCCA (~40%) and iCCA (~10%) [43]. CCAs have been also classified based on their gross appearance. In this sense, iCCAs can grow following three different patterns: *i*) mass-forming (MF), which is the most frequent form, *ii*) periductal infiltrating (PI), and *iii*) intraductal growing (IG) [50-54] (Figure I.6B). PI or IG growth patterns have been described for pCCA and dCCA, even if pCCA most frequently adopt a nodular+PI growth pattern [53, 55, 56]. Histological classifications of CCA also exist. Most pCCA and dCCA are mucinous adenocarcinomas, whereas iCCAs are highly heterogeneous, being the two main subtypes known as bile ductular type (mixed) – arising from small intrahepatic bile ducts – and bile duct type (mucinous) – arising from large intrahepatic bile ducts – [45, 57-60]. The histological subtyping has been suggested as an important classification method, as it underlines different aspects such as cell of origin, etiology, risk factors, molecular profile, clinical outcome and response to treatment [45].

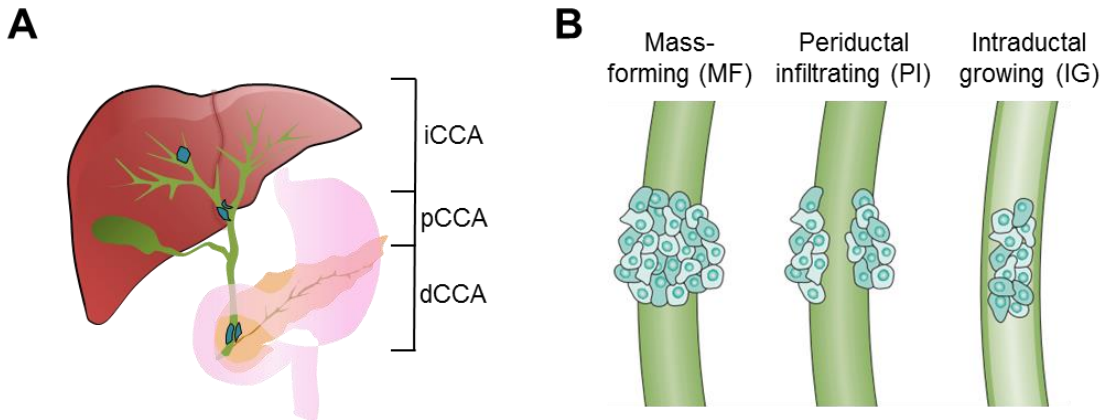

Figure I.6. CCA classification. (A) CCAs are classified as intrahepatic (iCCA), perihilar (pCCA) or distal (dCCA) depending on their anatomical location. **(B)** CCAs are also classified into mass-forming, periductal infiltrating or intraductal growing according to the gross appearance (Adapted from Erice *et al*., 2015 and Banales *et al*., 2016).

I.3.2.3 *CCA development*

Different risk factors have been described for CCA, although the majority of cases are not associated to any of them [43, 61, 62]. Environmental factors such as the infection with liver flukes (i.e. *Opistorchis viverrini* and *Clonorchis sinensis*) is a common risk factor in East Asia and the leading cause of the high CCA incidence in these countries, due to their tradition of eating uncooked fish [48, 52, 63-67]. In Europe, the association between CCA (mainly pCCA) and PSC or viral hepatitis C (HCV) is more frequent [63, 66]. Other relevant risk factors include cirrhosis, viral hepatitis B (HBV), hepatolithiasis, nonalcoholic steatohepatitis (NASH), biliary malformations and congenital diseases, such as choledocal cysts, Caroli's disease and congenital hepatic fibrosis [44, 66, 68-71]. Of note, biliary obstruction leads to BA accumulation, an event that has been suggested as a potential factor promoting CCA development [72]. Other common risk factors include smoking, alcohol consumption, obesity or diabetes [73-75]. Exposure to toxics or environmental factors such as nitrosamine-contaminated food, asbestos, dioxins, vinyl-chlorides and, in the past, thorotrast may also be related to CCA development [62].

I.3.2.4 *Cholangiocarcinogenesis*

The process of biliary tumorigenesis involves the malignant transformation of cholangiocytes due to genetic and epigenetic alterations in key signaling pathways that contribute to well-known hallmarks of cancer such as proliferation, survival, resistance to apoptosis, replicative immortality, angiogenesis, invasion and metastasis, metabolic deregulation, inflammation and immune-modulation [43, 75, 76]. Furthermore, different transcription factors (TFs) involved in the regulation of these important sets of mechanisms are altered in CCA, contributing to the tumorigenic process [77].

Genetic alterations in key pathways such as DNA repair (*TP53*) [78-80], WNT/β-catenin (*CTNNB1*) pathway [81], tyrosine kinase signaling (*KRAS,*

BRAF, SMAD4 and *FGFR2*) [44, 79, 80, 82-84] or isocitrate dehydrogenases 1 and 2 (*IDH1* and *IDH2*) [49, 85, 86] have been described in CCA [43, 45]. The fibroblast growth factor receptor (FGFR) has arisen as another potential target for CCA treatment [82, 87]. In addition, epigenetic modifications in CCA include histone modifications, DNA methylation and non-coding RNAs (i.e. miRNAs) [45]. Moreover, CCAs are highly desmoplastic tumors [88], and cancer-associated fibroblasts (CAFs), tumor-associated macrophages (TAM) and vascular cells are present in the tumor microenvironment [45, 89] promoting tumor growth [90].

I.3.2.5 *CCA detection*

CCAs are generally asymptomatic in early stages and are usually diagnosed when the disease is widespread. Different symptoms might appear during tumor progression. Malaise, cachexia, abdominal pain, night sweats, fatigue and/or jaundice can occur associated to iCCA, although 20-25% of iCCA are diagnosed incidentally [45]. In pCCA and dCCA the biliary obstruction-associated cholangitis might bring out symptoms, such as jaundice (typically painless) and/or pruritus [75]. In PSC patients, CCA may emerge as a rapid deterioration of the patient or as an incidental finding at transplant [63, 91-94].

Diagnosis is usually made by a combination of non-specific biomarkers in serum/biopsy and imaging methods [43]. Histologically, no specific markers have been validated and a differential diagnosis of iCCA *vs* HCC or metastasis is difficult [53, 95, 96]. Serum non-specific markers include the carcinoembryonic antigen (CEA) and/or the carbohydrate antigen 19-9 (CA19-9) [48]. In tissue, a combination of biliary, hepatic and tumor markers [i.e. cytokeratins 7, 19 and 20 (CK7, CK19, CK20), carbohydrate antigens 125 and 242 (CA125, CA242), cytokeratin fragment 21-1 (CYFRA21-1), or mucin 5AC (MUC5AC)] is usually analyzed [43, 45, 48, 97]. Overall, imaging methods for CCA diagnosis consist on computed tomography (CT) and cross-sectional imaging studies, and more specifically for each CCA subtype on: magnetic resonance imaging (MRI) for iCCA; magnetic resonance cholangiography (MRC) for pCCA and dCCA; percutaneous transhepatic cholangiography (PTC) for pCCA; endoscopic retrograde cholangiopancreatography (ERCP) and

endoscopic ultrasound (EUS) for dCCA [43]. Late diagnosis compromises the therapeutic options, leading to poor prognosis [45, 62].

I.3.2.6 *CCA treatment options*

Currently, the only potential curative options for CCA are the surgical resection of the tumor and liver transplantation. However, the advanced stage of these cancers at diagnosis highly compromises the use of these therapeutic approaches. For instance, only tumors without vascular infiltration and metastatic dissemination, and not affecting the normal liver function are suitable for surgical resection [98]. However, the 5-year survival rate after resection is low (11-44% depending on the CCA subtype) [95]. Liver transplantation for CCA is in general controversial and not recommended, since rapid tumor recurrence and low survival rates (10-25%) have been observed [48, 49]. Usually, tumor transplantation is followed by neoadjuvant therapy including chemotherapies such as gemcitabine, cisplatin or 5-fluorouracile [48, 99]. The role of loco-regional therapies, such as transarterial chemoembolization (TACE) and transarterial radioembolization (TARE), have shown promising results but the efficacy in CCA patients is not clear and further studies are needed [45]. In addition, conventional radiotherapy or chemotherapy (i.e. combination of gemcitabine and cisplatin) [48, 49, 100] have usually poor success due to the highly chemoresistant nature of these tumors, which show a multidrug resistance phenotype based on the activation of different mechanisms of chemoresistance (MOC) [101]. MOCs affect different aspects of the drugs, such as transport, activation and targets, but are also involved in repair mechanisms and apoptosis [45]. Other palliative strategies include biliary stent placement in an attempt to restore the biliary drainage and relief cholestasis [102-104].

To sum up, owing to the heterogeneity of CCAs and the lack of effective therapeutic options, there is an urgent need to understand in detail the molecular mechanisms involved in the pathogenesis of CCA. Individual characterization (i.e. genomic, epigenetic and molecular) of each tumor may provide valuable information on pathogenesis, prognosis and chemosensitivity. This information may help selecting the best therapeutic option for each patient as well as unraveling new potential targets for therapy.

As aforementioned, the present dissertation is focused in PBC and CCA, and, indeed, three independent studies are developed. In the first chapter, the role of the microRNA-506 in the etiopathogenesis of PBC is analyzed. On the other hand, the other two chapters aimed to elucidate two different aspects of CCA. First, we attempted to elucidate the role of two BA receptors, FXR and TGR5, in CCA progression, and second, we wanted to study the role of the Krüppel-like factors (KLFs), particularly KLF5, in CCA.

III. CHAPTER 1

ROLE OF MIR-506 IN PRIMARY BILIARY CHOLANGITIS

1 - Introduction

1.I.1 *Primary biliary cholangitis (PBC)*

Primary biliary cholangitis (PBC) is a chronic cholestatic liver disease associated with autoimmune phenomena targeting small and medium intrahepatic bile ducts [22, 25]. PBC is characterized by progressive impairment and destruction of bile duct epithelial cells (i.e. cholangiocytes) together with increased portal inflammation (Figure 1.I.1) and fibrosis. In the absence of treatment, the disease may progress to liver cirrhosis needing liver transplantation [22, 25].

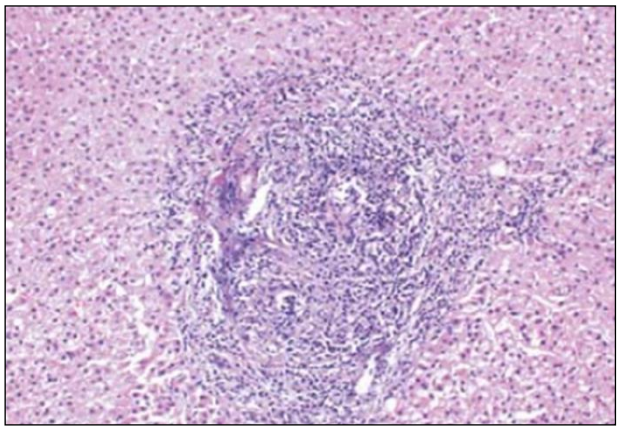

Figure 1.I.1. Liver histology of a PBC portal tract. Haematoxylin-eosin staining of a liver tissue section showing damaged bile ducts and portal inflammation. The portal triad is infiltrated by lymphocytes (Adapted from Kaplan and Gerswin, 2005).

1.I.1.1 *PBC and autoimmunity*

PBC is considered a multifactorial disease but its etiology remains still obscure. PBC mainly affects middle-aged women and most of the patients (~95%) develop anti-mitochondrial autoantibodies (AMA) specific against PDC-E2 [22, 25]. Indeed, the presence of AMAs in serum of PBC patients is considered a serological hallmark [30, 34]. Despite the autoimmune events, treatment of PBC patients with classical immunosuppressants is inefficient. Currently, and as aforementioned (see general introduction), UDCA is the best well-established FDA-approved treatment seen to contribute to the alkalinization and fluidization of bile and protect the biliary epithelium from hydrophobic bile acids [22, 25].

Furthermore, OCA has recently received a conditional approval for PBC patients, in combination with UDCA or as a monotherapy [39].

In PBC, AE2 deficiency results in sensitivity to apolar hydrophobic bile acids, leading to cholangiocyte apoptosis [109] which might result in the attraction of proinflammatory cytokines and the subsequent local inflammation [110].

1.I.1.2 *PBC and cholestasis*

Cholangiocytes own important functions in bile formation, and under an injury, damaged cholangiocytes get their normal biological functions impaired. Bile flow is altered and a cholestatic microenvironment is favored, with the resultant accumulation of cytotoxic bile acids [40]. Cholestasis in PBC patients is linked to impaired biliary bicarbonate secretion [111, 112]. The main bicarbonate extruder in normal human cholangiocytes is the Cl^-/HCO_3^- anion exchanger 2 (AE2/SLC4A2), which is located into the apical membrane promoting the secretin-stimulated biliary bicarbonate secretion and regulating the intracellular pH (pHi) homeostasis [113-115]. PBC patients exhibit a lack of response to secretin associated with decreased expression of AE2 in cholangiocytes which results in cholestasis [105]. However, UDCA treatment restores the secretin response and improves cholestasis in PBC patients. The etiopathogenic role of the characteristic AE2 downregulation in both liver and peripheral blood mononuclear cells (PBMCs) of PBC patients is highlighted by the fact that *Ae2*$^{-/-}$ mice develop spontaneously several hepatobiliary and immunological PBC-like features, including specific AMA against PDC-E2 [116]. The expression of AE2 in cholangiocytes is upregulated under the combination of UDCA and glucocorticoids, treatment employed for patients that do not respond to UDCA monotherapy [114].

On the other hand, type III inositol 1,4,5-trisphosphate receptor (InsP3R3) is an integral membrane protein located in the subapical portion of the endoplasmic reticulum (ER) of cholangiocytes. InsP3R3 functions as a major intracellular calcium (Ca^{2+}_i) release channel and its activation promotes biliary bicarbonate secretion [117, 118]. Like AE2, the expression of InsP3R3 was also found downregulated in PBC cholangiocytes inducing cholestasis [119].

Notably, the characteristic downregulation of both AE2 and InsP3R3 in PBC cholangiocytes is mediated, at least partially, by microRNA-506 (miR-506) [105, 120].

1.I.1.3 *PBC and microRNAs*

PBC patients have an altered hepatic microRNA (miR) expression pattern compared to normal controls [121, 122] (Figure 1.I.2A). MiRs were first described in early 1990s [123, 124] and consist on a group of highly conserved non-coding RNAs containing about 18-23 nucleotides. The main function of these small molecules is that they are able to post-transcriptionally regulate the expression of multiple genes. MiRs directly bind to the 3'UTR region of genes, causing translational repression [125, 126]. In this regard, the role of miRs in multiple diseases has been reported, including the pathophysiology of the biliary tree [127]. Among the altered miRs in PBC, the miR-506 was upregulated in PBC livers compared to normal controls. Our group further studied miR-506 overexpression in PBC. In this regard, miR-506 is overexpressed in the bile ducts of PBC patients compared to normal and PSC liver tissue samples [105] (Figure 1.I.2B) and directly targets both AE2 and InsP3R3 mRNAs in cholangiocytes, leading to impaired biliary secretory functions [105, 120] (Figure 1.I.2C).

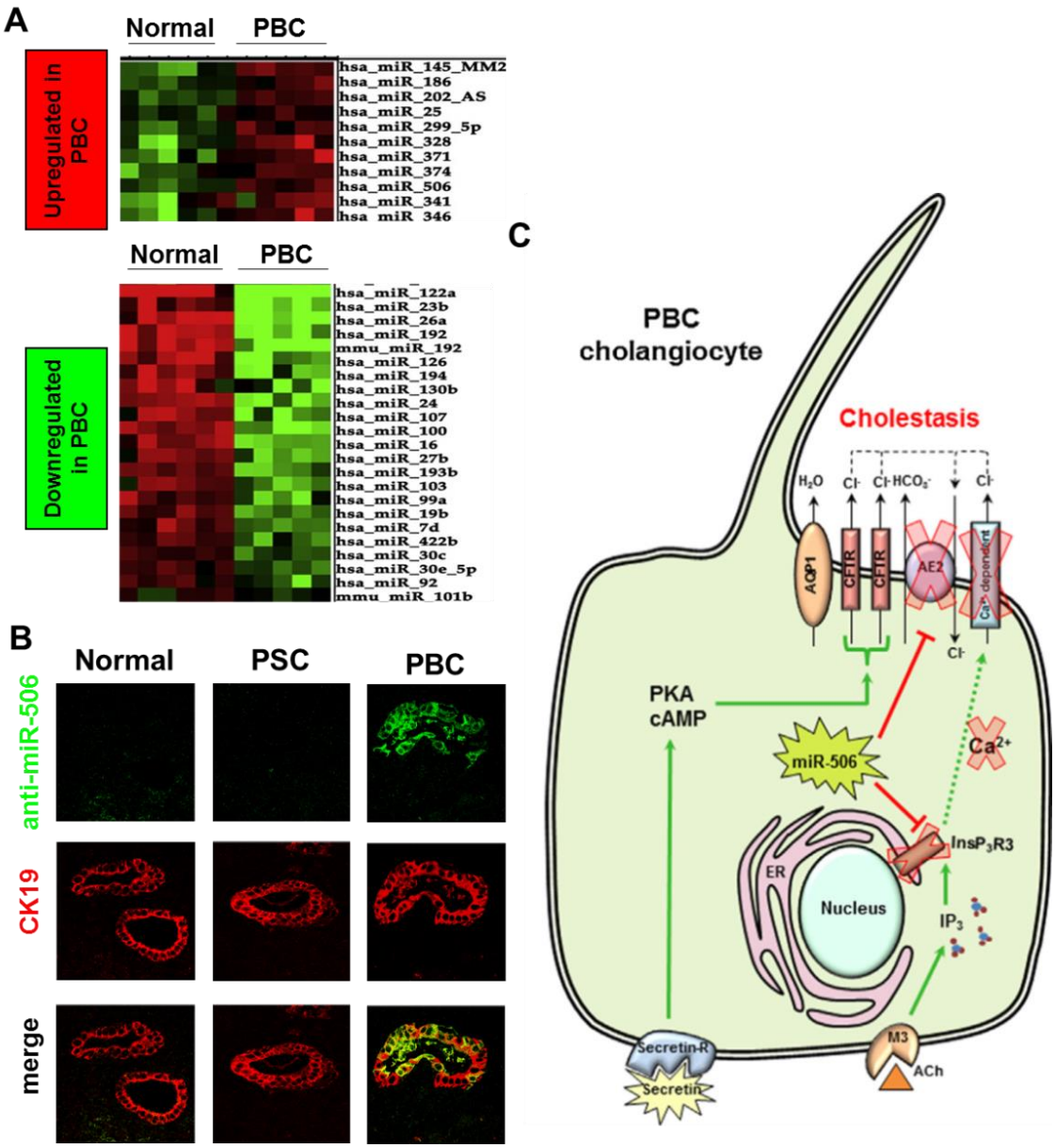

Figure 1.I.2. PBC cholangiocytes are characterized by increased miR-506 expression, which directly targets both AE2 and $InsP_3R3$ leading to cholestasis. (A) MiRNA microarray in normal and PBC human livers (Adapted from Padgett *et al*., 2009). **(B)** In situ hybridization of miR-506 (green) and immunofluorescence of CK19 (red) in liver tissue from normal PSC and PBC patients (Adapted from Banales *et al*., 2012). **(C)** Proposed mechanism of action of miR-506 in PBC cholangiocytes (Adapted from Esparza-Baquer *et al*., 2016).

1 - Hypothesis and Objectives

MiR-506 seems to have a pivotal role in the etiopathogenesis of PBC but the mechanisms that regulate its expression in cholangiocytes and the direct functional effects of miR-506 in cholangiocytes are still unknown. In this study, we aimed to investigate the role of different factors –such as pro-inflammatory cytokines, bile acids and estrogens– in the regulation of miR-506 expression in cholangiocytes and the effect of miR-506 in cholangiocyte pathophysiology and in PBC immune regulation. Therefore, we proposed the following objectives:

I. Analysis of the regulation of miR-506 promoter activity in cholangiocytes.
II. Determination of the direct effect of miR-506 in cholangiocyte pathophysiology.
III. Elucidation of the role of miR-506 on PBC immune regulation.

1 - Materials and Methods

1.M.1 *Cloning of hsa-miR-506 promoter in a luciferase expression vector*

Three different sizes of the human miR-506 gene (hsa-miR-506; NCBI Gene ID: 574511) promoter were cloned in a luciferase expression vector. Briefly, 3229, 1936 or 993 bp of the 5'-flanking region of hsa-miR-506 (Z1-hsa-miR-506pr, Z2-hsa-miR-506pr and Z3-hsa-miR-506pr, respectively) were cloned using genomic DNA obtained from a healthy individual and the promoter of cytomegalovirus (CMV) associated to the luciferase gene was inserted in the expression vector pEXP-gck as a positive control (Figures 1.M.1 A-C). First, hsa-miR-506pr constructs were amplified by high fidelity PCR using the AccuPrime Pfx DNA polymerase (Invitrogen). Specific oligonucleotide primers, shown in Table 1.M.1, with appropriate attB sites were added to obtain cDNA adapted for cloning using Gateway® technology. PCR products were recombined with pDONR™221 P1-P5r vector (Invitrogen). Next, these vectors were again recombined in a Multisite Gateway cloning reaction with a promoter-less destination vector (pDEST/pL) containing the coding sequence of firefly luciferase (Luc2), as previously described [128].

Table 1.M.1. Primers used for high fidelity PCR.

Primer code	Sequence 5'-3'
miR-506-Z1	*Forward* 5'-CGTCGTTGATACATGACTGACATAAAGT-3' *Reverse* 5'- GGTGGTGGCACTGACCATCT-3'
miR-506-Z2	*Forward* 5'- GTGTCGTCTATCCCTGATACGTGCT-3' *Reverse* 5'- GGTGGTGGCACTGACCATCT-3'
miR-506-Z3	*Forward* 5'- TCCCTTCCCCAGACTCTGGT-3' *Reverse* 5'- GGTGGTGGCACTGACCATCT-3'

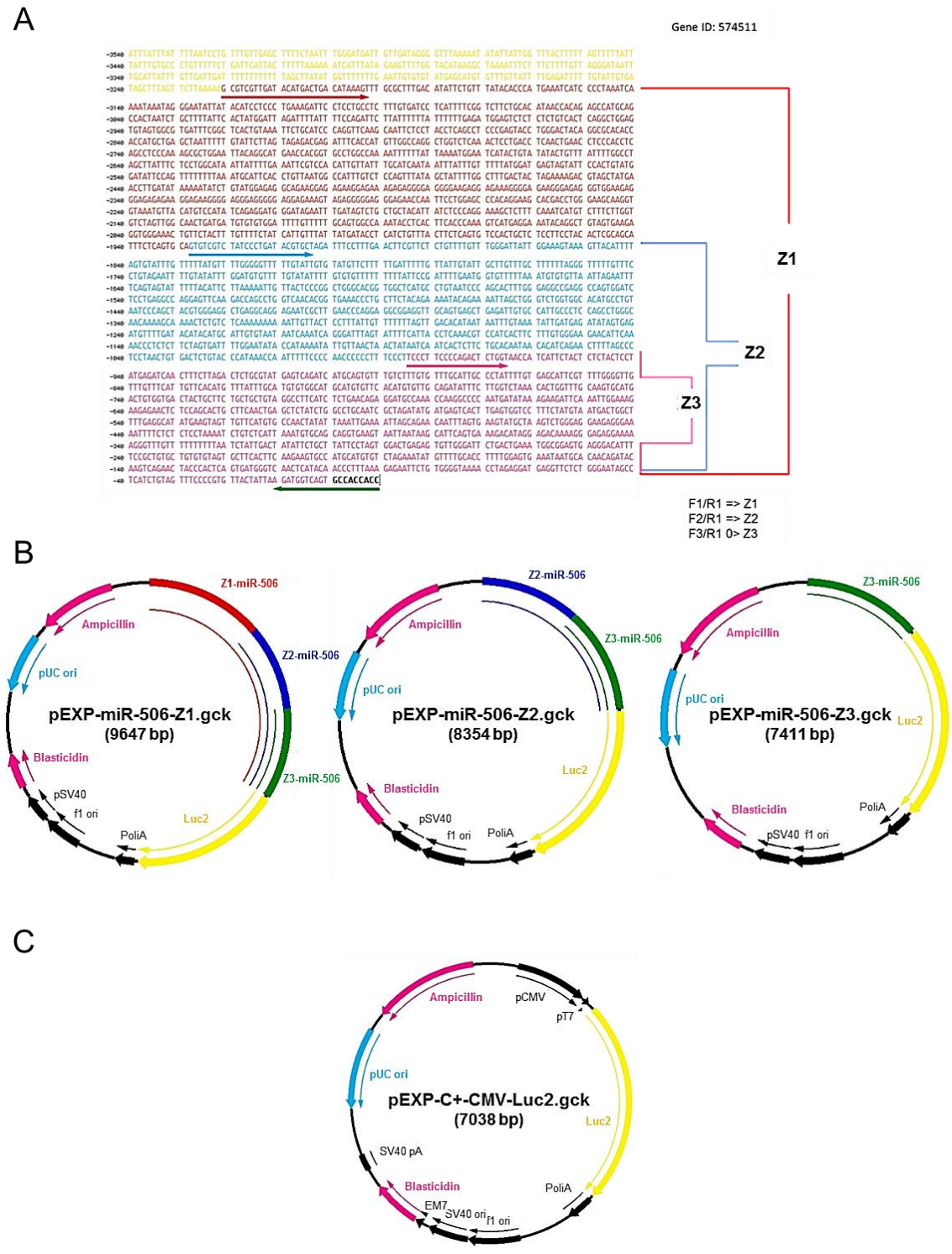

Figure 1.M.1. Promoter cloning. (A) Three fragments of different length of the sequence located immediately 5'-upstream of miR-506 were cloned [i.e. Z1 (3229 bp), Z2 (1936 bp) and Z3 (993 bp)]. **(B)** Cloning of promoter regions were performed in a pEXP-gck expression vector containing the luciferase gene. **(C)** The cytomegalovirus (CMV) promoter was used as a positive control of luciferase gene expression.

1.M.2 *Luciferase reporter assays*

H69 human cholangiocytes were transfected with Z1, Z2 or Z3 recombinant vectors using Lipofectamine 2000 (Life Technologies). Briefly, cells were seeded in a 24-well plate with fully-supplemented DMEM/F-12 medium (Table I.2) and incubated O/N. The following day, cells were washed twice with PBS, and 500 µL of transfection mix (1 µg DNA, 2.5 µL lipofectamine and 3 mL Opti-MEM) were added to each well. The transfection mix was replaced 6 h later by DMEM+10% FBS alone or together with each particular treatment condition. Luciferase activity was assessed 24 h after transfection using the *Luciferase Assay Kit, E151A* (Promega), by adding 50 µL of Lysis Buffer into each well. Luciferase activity was measured in a NOVOstar Apparatus (BMG LABTECH) and normalized to the total protein concentration.

1.M.2.1 *Cell treatments*

The effect of different pro-inflammatory cytokines [i.e. interleukins (IL) 1β, 6, 8, 12, 17, 18, tumor necrosis factor alpha (TNFα), and interferon gamma (IFNγ)], pro-fibrotic factors [i.e. transforming growth factor beta 1 (TGFβ1)], estrogens (i.e. 17β-estradiol), glucocorticoids [i.e. dexamethasone (DEX)], growth factors [i.e. epidermal growth factor (EGF)] and bile acids [i.e. cholic acid (CA), ursodeoxycholic (UDCA) and tauroursodeoxycholic (TUDCA)] in the luciferase activity of Z1, Z2 or Z3 promoters was tested. For that purpose, H69 cells were transfected and cultured as previously mentioned adding the stimuli together with lipofectamine and Opti-MEM. The concentration used for each treatment is specified in Table 1.M.2.

Table 1.M.2. Stimuli used for the analysis of miR-506 promoter activity.

Stimuli	Concentration	Comercial
IL-18	100 ng/mL	MBL
IL-17	100 ng/mL	Sigma
IL-8	50 ng/mL	R&D
IL-12	50 ng/mL	R&D
IL-6	50 ng/mL	Sigma
IL1β	10 ng/mL	R&D
TGFβ1	100 ng/mL	R&D
TNFα	100 ng/mL	Sigma
INFγ	100 ng/mL	Abcam
CA	100 µM	Sigma
UDCA	100 µM	ACROS Organics
TUDCA	100 µM	Calbiochem
DEX	100 µM	Sigma
EGF	40 ng/mL	Sigma
17β-est	100 µM	Sigma

1.M.3 *Generation of human cholangiocytes overexpressing miR-506 in culture*

H69 human cholangiocytes were stably transfected with recombinant vectors containing miR-506 (H69-miR-506), a miR-negative (H69-miR-neg) control sequence (Thermo Fisher Scientific), or just with vehicle (H69), as we previously described [105, 120]. Then, transfected cells were continuously selected with blasticidin (Invitrogen) in fully-supplemented DMEM/F-12 medium.

1.M.4 *Gene and miR-506 expression*

The quantification of miR-506 expression was performed using the *TaqMan MicroRNA Reverse Transcription Kit* and commercial miR-specific primers (miR-506 Mature miRNA sequence UAAGGCACCCUUCUGAGUAGA; Applied Biosystems). TaqMan Universal PCR Master Mix no AmpErase was used for qPCR. Z30 small nuclear RNA control (Z30 Control sequence TGGTATTGCCATTGCTTCACTGTTGGCTTTGACCAGGGTATGATCTCTTAATCTTCTCTCTGAGCTG; Applied Biosystems) was used as normalizing control.

On the other hand, gene expression (mRNA) was determined by qPCR from RNA isolated and retrotranscribed as described in general materials and methods section (see above). *GAPDH* was used as a housekeeping control. The primers used in this study are shown in Table 1.M.3.

Table 1.M.3. Primers used for qPCR of human mRNAs.

Primers	Sequences
UCP1	*Forward* 5'-CTCACCGCAGGGAAAGAA-3' *Reverse* 5'-GGTTGCCCAATGAATACTGC-3'
UCP2	*Forward* 5'-GTTCTACACCAAGGGCTCTGA-3' *Reverse* 5'-AATCGGACCTTTACCACATCC-3'
Cytokeratin 7	*Forward* 5'-ATCTTTGAGGCCCAGATTGC-3' *Reverse* 5'-TTGATCTCATCATTCAGGGC-3'
ZO1	*Forward* 5'-CGGTCCTCTGAGCCTGTAAG-3' *Reverse* 5'-GGATCTACATGCGACGACAA-3'
N-cadherin	*Forward* 5'-TCCTGCTTATCCTTGTGCTGA-3' *Reverse* 5'-CGGATTCCCACAGGCTTGAT-3'
IL8	*Forward* 5'-GTGCAGTTTTGCCAAGGAGT-3' *Reverse* 5'-ACTTGTCCACAACCCTCTGC-3'
p21	*Forward* 5'-CGATGGAACTTCGACTTTGTCA-3' *Reverse* 5'-GCACAAGGGTACAAGACAGTG-3'
IRE1	*Forward* 5'-AGGGACAGGAGGGAATCGTA-3' *Reverse* 5'-CAGTCCCTAATGCCACACCT-3'
CHOP	*Forward* 5'-TCTTCATACATCACCACACC-3' *Reverse* 5'-CTTGTGACCTCTGCTGGTTC-3'
ATF6	*Forward* 5'-GCTGGATGAAGTTGTGTCAGAG-3' *Reverse* 5'-TGTTCCAACATGCTCATAGGTC-3'
PERK	*Forward* 5'-CAGGCAAAGGAAGGAGTCTG-3' *Reverse* 5'-AACAACTCCAAAGCCACCAC-3'
XBP-1	*Forward* 5'GCAGGTGCAGGCCCAGTTGTCAC-3' *Reverse* 5'CCCCACTGACAGAGAAAGGGAGG-3'
GAPDH	*Forward* 5'-CCAAGGTCATCCATGACAAC-3' *Reverse* 5'-TGTCATACCAGGAAATGAGC-3'

1.M.5 *Mass spectrometry-based quantitative proteomics*

Shotgun comparative proteomic analysis of H69, H69-miR-neg and H69-miR-506 cells was performed using iTRAQ (isobaric Tags for Relative and Absolute Quantitation) [129]. Peptide labeling, peptide fractionation and mass-spectrometry analysis were performed as previously described [130]. After MS/MS analysis, protein identification and relative quantification were performed with the ProteinPilot™ software (version 4.5; Sciex) using the

Paragon™ algorithm as the search engine [131]. Although relative quantification and statistical analysis were provided by the ProteinPilot software, an additional 1.3-fold change cutoff for all iTRAQ ratios (ratio <0.77 or >1.3) and a p-value lower than 0.05 were selected to classify proteins as up- or down-regulated. Functional analysis of proteins was determined by gene ontology (GO) enrichment using the Panther Classification System database (http://pantherdb.org/).

1.M.6 *Western blotting*

Changes in protein expression were detected by western blot using 40 µg of whole cell extracts as described in general materials and methods section (see above). Samples were electrophoresed in 7.5% (for AE2) or 12.5% (PDC-E2, p21 and cleaved caspase-3) SDS-PAGE. β-actin was used as a protein normalizing control. The antibodies used are shown in Table 1.M.4.

Table 1.M.4. Antibodies used for western blot and/or immunofluorescence.

Antibody	Company	Reference	Use
Goat polyclonal anti-AE2	Santa Cruz	sc-46710	WB (1:250 Room Tº)
Goat polyclonal anti-PDC-E2	Santa Cruz	sc-16890	WB (1:250 4ºC) IF (1:50)
Rabbit polyclonal anti-PDC-E2	Santa Cruz	sc-32925	WB (1:250 4ºC)
Rabbit polyclonal anti-p21	Abcam	ab7960	WB (1:1,000 4ºC)
Rabbit monoclonal anti-Cleaved Caspase-3	Cell signaling	9664	WB (1:500 4ºC)
Rabbit monoclonal anti-pH2AX	Cell signaling	9718	WB (1:500 4ºC)
Mouse monoclonal anti-β-actin	Sigma	A5316	WB (1:1,000 4ºC)
Anti-rabbit IgG, HRP-linked Antibody	Cell signaling	7074	WB (1:5,000 Room Tº)
Anti-mouse IgG, HRP-linked Antibody	Cell signaling	7076	WB (1:5,000 Room Tº)
Donkey anti-goat IgG, HRP-linked Antibody	Santa Cruz	sc-2020	WB (1:5,000 Room Tº)
Donkey anti-Goat IgG (H+L) Cross-Adsorbed Secondary Antibody, Alexa Fluor 568	ThermoFisher	A11057	IF (1:1,000)

Abbreviations: WB, western blot; IF, immunofluorescence; Room Tº, room temperature

1.M.7 *Flow-cytometry based-cell proliferation*

The evaluation of cell proliferation was carried out in H69, H69-miR-neg and H69-miR-506 cholangiocytes using the Cell Proliferation Dye eFluor® 670 as described in general materials and methods section (see above). In particular, $3.5x10^4$ cells per well were seeded and cultured for 72 h in collagen-coated 12-well plates in fully-supplemented DMEM/F-12 medium (Table I.2) and then analyzed by flow cytometry in a Guava Easycyte 8HT flow-cytometer.

1.M.8 *Determination of cell adhesion properties*

Cell adhesion was evaluated in H69, H69-miR-neg and H69-miR-506 cholangiocytes. $5x10^4$ cells were seeded in collagen-coated 12-well plates and cultured at 37ºC for 3 h in fully-supplemented DMEM/F-12 medium (Table I.2). Cells were then fixed and stained with 4% formaldehyde and 0.5% crystal violet in PBS for 20 min and washed with water. Once dried, cell staining was dissolved with 10% acetic acid in PBS and the absorbance was measured at 595 nm in a Multiskan Ascent® spectrophotometer (Thermo).

1.M.9 *Cell migration*

Cell migration was tested in H69, H69-miR-neg and H69-miR-506 cholangiocytes using transwell migration chambers as described in general materials and methods section (see above). In particular, $3.5x10^4$ cells were seeded in the top side of the chambers and were cultured for 48 h. Pictures of the migrated cells were taken on random fields of the bottom side of the chamber and staining was dissolved for measuring absorbance at 550 nm in a Multiskan Ascent® spectrophotometer (Thermo).

1.M.10 *Oxidative stress detection by dihydroethidium staining*

Dihydroethidium (DHE) staining was used to detect reactive oxygen species (ROS) in H69, H69-miR-neg and H69-miR-506 cholangiocytes. For this purpose, $2x10^4$ cells per well were seeded in coverslips in 24-well plates and these were grown for 48 h. Cells were stained with 15 µM DHE (Molecular

Probes, ThermoFisher) for 10 min at 37ºC in darkness, fixed with 1% paraformaldehyde in PBS and mounted using Vectashield (Vector Laboratories). Pictures were taken using a fluorescence microscope (Leica DM IRB).

1.M.11 *Evaluation of apoptosis by flow cytometry in cholangiocytes overexpressing miR-506 in culture*

The cytotoxicity of the hydrophobic BAs chenodeoxycholic acid (CDCA, Sigma) and glycochenodeoxycholic acid (GCDCA, Sigma) was evaluated in H69, H69-miR-neg and H69-miR-506 cholangiocytes by flow-cytometry using annexin V and propidium iodide, as described in general materials and methods (see above). In particular, $2.5x10^4$ cells per well were seeded; the day after, cells were treated and cultured for 48 h. Untreated cells were used as control. Cells were then stained and analyzed in a Guava Easycyte 8HT flow-cytometer.

1.M.12 *Mitochondrial function assessment by Seahorse Analyzer*

An XF96 Extracellular Flux Analyzer (Seahorse Bioscience) was employed for measuring oxygen consumption and extracellular acidification rates (OCR and ECAR, respectively). The *XF Cell Mito Stress Test Kit* was used for that purpose, as described in general materials and methods section (see above). In the present study, $1x10^4$ H69, H69-miR-neg or H69-miR-506 cholangiocytes were seeded and cultured for 48 h in fully-supplemented DMEM/F-12 medium (Table I.2) for further Seahorse analysis.

1.M.13 *Metabolic activity determination by ATP measurement*

Levels of ATP in H69, H69-miR-neg and H69-miR-506 cells were measured using the *ATP Assay Kit* (Abcam; ab83355) following manufacturer's instructions. Briefly, cells were cultured in fully-supplemented DMEM/F-12 media (Table I.2) in P150 plates (Corning) until confluence. Then, cells were trypsinized as usual and $3x10^6$ H69, H69-miR-neg or H69-miR-506 cells were separated in triplicates in different 1.5 mL Eppendorf tubes for further processing. Cells were pelleted (1,500 rpm for 5 min) and washed with 1 mL of cold PBS. Pellets were quickly resuspended in 100 µL of ATP Assay Buffer by

repeated up and down and vortexed for cell lysis. Samples were centrifuged at 14,000 rpm for 2 min at 4ºC and supernatant was harvested and placed into a new tube. Next, deproteinization was performed as follows: 25 µL of ice-cold 4 M perchloric acid (PCA) were added, samples were vortexed and incubated for 5 min on ice. Tubes were centrifuged at 13,000 g for 2 min at 4ºC. Supernatant was placed into a new tube and 34 µL of cold 2 M potassium hydroxide (KOH) were added and briefly vortexed. The pH was adjusted to pH 6.5 - 8 using PCA, samples were centrifuged at 13,000 g for 15 min at 4ºC and supernatant was transferred into another tube. An ATP reaction mix containing ATP Assay Buffer (44 µL), ATP Probe (2 µL), ATP converter (2 µL) and Developer mix (2 µL) was prepared for all the samples and for the standard curve, which was prepared in parallel. The standard curve was prepared as indicated by the manufacturer's using 1 mM ATP and ATP Assay Buffer at six different concentrations. Additionally, a background reaction mix containing ATP Assay Buffer (46 µL), ATP Probe (2 µL) and Developer mix (2 µL) was also prepared. Next, 40 µL of the reaction mix and 40 µL of each sample (including the standard curve) were placed in each well of a 96-well plate and incubated for 30 min at room temperature in darkness. Absorbance was measured at 570 nm in a Multiskan Ascent spectrophotometer (Thermo).

1.M.14 *PDC-E2 detection by immunofluorescent microscopy*

H69, H69-miR-neg and H69-miR-506 cholangiocytes were cultured on glass coverslips O/N. Next, cells were fixed with cold methanol for 10 min at -20°C and permeabilized with a 0.5% Tween in PBS solution for 20 min at room temperature. PDC-E2 (Santa Cruz) primary antibody at 1:50 dilution was incubated for 1 h at room temperature. A fluorescent red-conjugated secondary antibody (Life Technologies, 1:1000 dilution) was incubated for 1 h and 30 min at room temperature and *Vectra System* (Vector Laboratories) was used for nuclei staining and cell mounting. PDC-E2 cellular expression was observed in a fluorescence microscope (Leica DM IRB). See Table 1.M.4.for antibody specifications.

1.M.15 *Co-culture of human cholangiocytes with peripheral blood mononuclear cells (PBMCs) of PBC patients*

H69, H69-miR-neg or H69-miR-506 human cholangiocytes were co-cultured with PBMCs isolated from a PBC patient. Briefly, H69, H69-miR-neg or H69-miR-506 cholangiocytes ($5x10^3$ cells per well) were plated in collagen-coated 96-well plates in fully-supplemented DMEM/F-12 medium (Table I.2). After O/N attachment, culture media was changed to RPMI (Gibco) supplemented with 10% FBS/1% P/S. After 48 h, PBMCs were isolated from a middle-aged female PBC patient using a density gradient media. Briefly, peripheral blood was diluted to 50% with physiological serum and carefully added to Lymphoprep™ (Fresenius Kabi Norge) (3/4 parts of Lymphoprep regarding the total peripheral blood volume). Samples were centrifuged at 2500 rpm for 30 min at room temperature. The PBMC fraction was carefully harvested using a Pasteur pipet and placed in a new tube containing physiological serum. Samples were centrifuged at 1,500 rpm for 10 min and supernatant was carefully removed. Pellet was washed with physiological serum and centrifuged at 1500 rpm for 10 min. Supernatant was carefully removed. If erythrocytes were not present, the pellet was resuspended in RPMI supplemented with 10% FBS/1% P/S and counted as usual. In the presence of erythrocytes, an intermediate step for erythrocyte lysis was performed, incubating samples for 10 min with RBC Lysis Solution (QIAGEN) and doing a subsequent washing.

Once PBMCs were isolated, cells were stained with *CellTrace™ CFSE Cell Proliferation Kit* (Invitrogen) following manufacturer's instructions and then $1.5x10^5$ PBMCs in RPMI supplemented with 10% FBS/1% P/S were added to H69, H69-miR-neg or H69-miR-506 human cholangiocytes for 96 h. Afterwards, PBMCs were harvested and stained with the lymphocyte activation marker CD25 (BD Biosciences) and the cell death marker 7AAD (Life technologies) for 20 min and analyzed in a Guava Easycyte 8HT flow cytometer. For the analysis, PBMCs were gated and the 7AAD-positive cells were discarded for testing both CFSE and CD25. Phytohaemagglutinin M form (PHA-M) (Gibco) and dimethyl sulfoxide (DMSO) (Sigma) were used as positive and negative controls for lymphocyte activation and proliferation, respectively. The research protocol was approved by the *Clinical Research Ethics Committee* of the

Donostia Hospital, and the patient signed a written consent for the use of her blood samples for biomedical research.

1.M.15.1 *Cytokine evaluation in the cell cultures*

The supernatant of both cell cultures and cell co-cultures were harvested and levels of IL-17A and IL-23 cytokines were evaluated using *Milliplex Map human high sensitivity T cell panel – Immunology multiplex assay* (Millipore), following manufacturer's instructions.

1.M.16 ***Statistical analysis***

Results were statistically analyzed as stated in general materials and methods section (see above). For comparisons between two groups, parametric *unpaired t-test* or non-parametric *Mann-Whitney test* were used. For comparisons between more than two groups, parametric *One-Way analysis of variance* (ANOVA) test followed by *a posteriori Bonferroni test* were used. Differences were considered significantly different when $p<0.05$.

1 – Results

1.R.1 *Regulation of miR-506 promoter activity in human cholangiocytes*

We previously reported that miR-506 expression is upregulated in PBC cholangiocytes compared to normal human cholangiocytes [105]. Here, the regulatory activity of the miR-506 promoter was evaluated in human cholangiocytes using recombinant luciferase reporter vectors containing a fragment of the promoter region. Three fragments of different length of the sequence located immediately 5'-upstream of miR-506 were cloned and assayed [i.e. Z1 (3229 bp), Z2 (1936 bp) and Z3 (993 bp)] (Figure 1.R.1A) in the presence or absence of different pro-inflammatory, pro-fibrotic and/or pro-mitotic molecules found overexpressed in PBC livers. As a positive control, a recombinant vector containing the cytomegalovirus (CMV) promoter was used (Figure 1.R.1A). Under basal conditions, the recombinant luciferase vector containing the Z1 (the longest fragment) miR-506 promoter showed higher expression of luciferase compared to both Z2 and Z3 fragments, whereas no differences in the activities were observed between Z2 and Z3 fragments (Figure 1.R.1A). The presence of pro-inflammatory cytokines IL-8, IL-12, IL-17, IL-18 or TNF-α all induced the luciferase expression in human cholangiocytes transfected with the Z1 recombinant vector (Figure 1.R.1B). Of note, these effects were absent in cells transfected with Z2- or Z3-promoter fragment (Figure 1.R.1C). On the other hand, other pro-inflammatory (i.e. IL-6, IL-1β and IFNγ) and pro-fibrotic (i.e. TFGβ1) cytokines did not affect miR-506 Z1-promoter activity in cholangiocytes (Figure 1.R.1D). Finally, the presence of bile acids (i.e. CA, UDCA and TUDCA), estrogens (i.e. 17β-estradiol), glucocorticoids (i.e. DEX) and growth factors (i.e. EGF) neither affected the Z1-promoter activity in human cholangiocytes (Figure 1.R.1D).

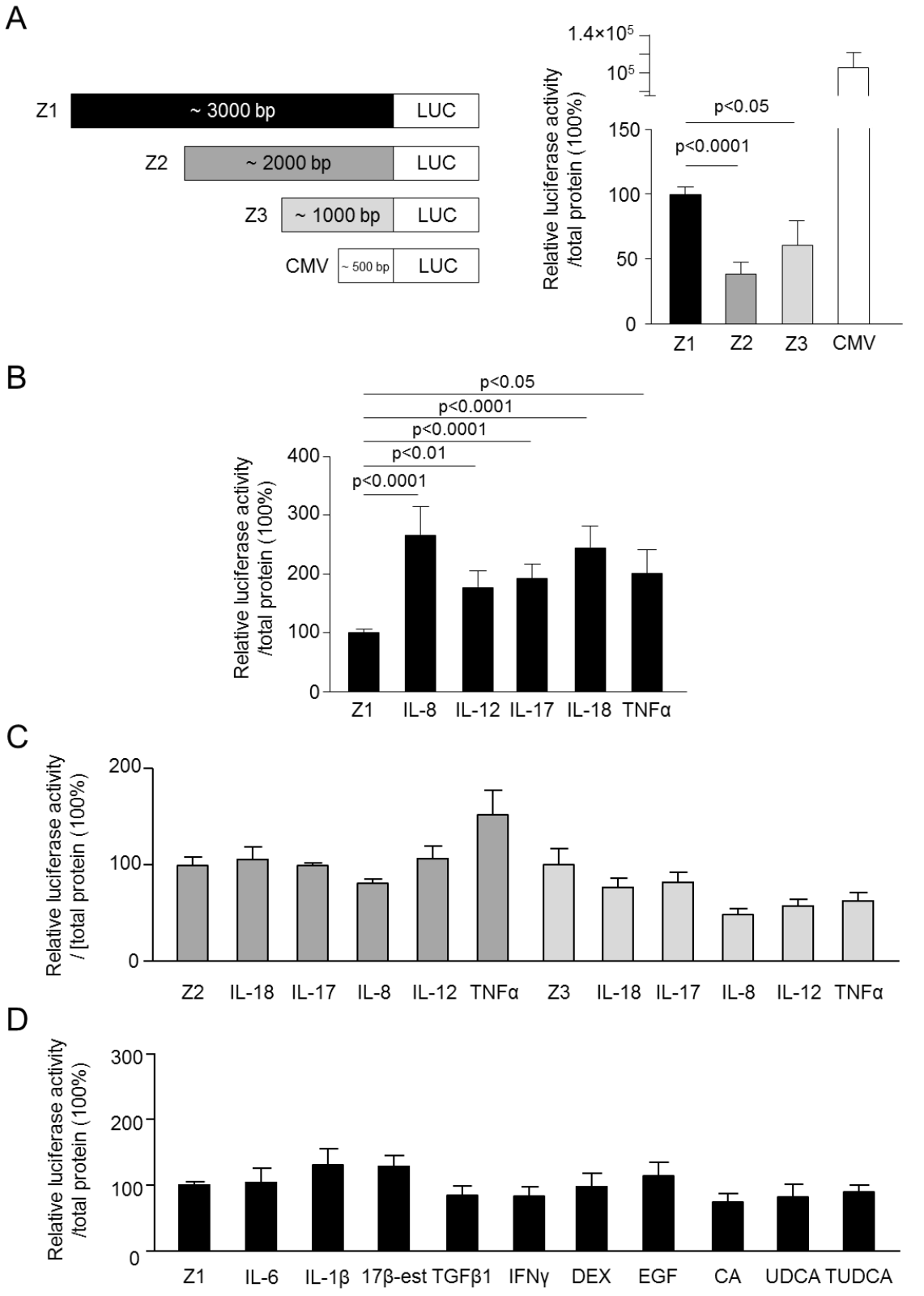

Figure 1.R.1. MiR-506 promoter activity in cholangiocytes. (A) Three fragments of different length (i.e. 3229, 1936 and 993 bp) located 5'-upstream hsa-miR-506, named as Z1, Z2 and Z3 respectively, were cloned upstream of the beginning of transcription of firefly luciferase (Luc2) coding sequence. Z1 promoter show higher luminescent levels compared to Z2 and Z3 (n=10). CMV promoter was used as a positive control (n=10). **(B)** Interleukins 8, 12, 17 and 18, as well

as TNFα, increased the luciferase activity of promoter Z1 (n=10). **(C)** Interleukins 8, 12, 17 and 18, and TNFα, did not alter the luciferase activity of Z2 and Z3 promoter sequences (n=10). **(D)** Interleukin 6 and 1β, 17β-estradiol, TGFβ1, IFNγ, DEX, EGF and bile acids (CA, UDCA, TUDCA) did not influence Z1 promoter luciferase activity (n=10).

1.R.2 *Generation of miR-506 overexpressing H69 human cholangiocytes*

H69 cholangiocytes overexpressing miR-506 (H69-miR-506) or a negative control (H69-miR-neg) sequence under the regulation of a CMV promoter were generated [105, 120]. We first verified that the expression of the miR-506 precursor (pre-miR-506) resulted in an augmented expression of the mature miR-506 sequence compared to cells transfected with the pre-miR-neg or vehicle (Figure 1.R.2).

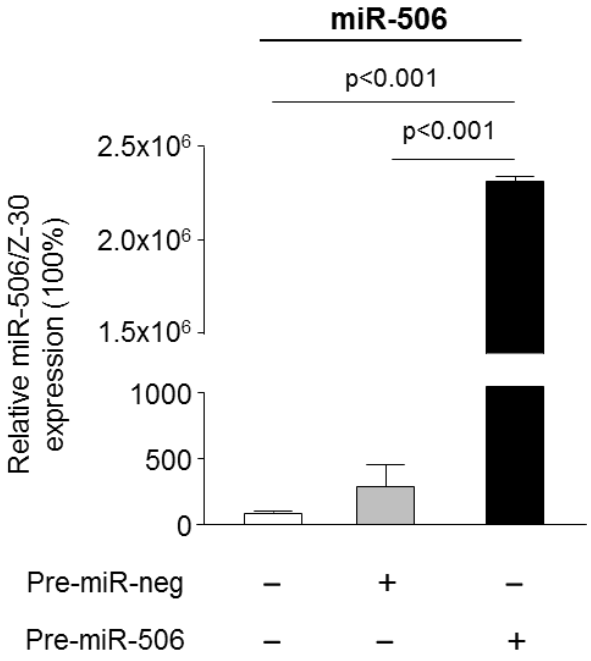

Figure 1.R.2. Analysis of miR-506 expression in H69, H69-miR-neg and H69-miR-506 cholangiocytes. H69 cells transfected with a miR-506 precursor have increased expression levels of mature miR-506 compared to H69 cells transfected with a negative control vector (miR-neg) or vehicle (H69). Z-30 was used as a housekeeping control.

1.R.3 *Effect of miR-506 on AE2 protein expression in cholangiocytes*

Our group previously reported that transient overexpression of miR-506 in H69 cholangiocytes results in the downregulation of AE2 protein expression and

activity [105]. As predicted, stable transfection of H69 cholangiocytes with recombinant vectors that overexpress miR-506 also diminished AE2 protein expression compared to cells transfected with miR-neg or vehicle (Figure 1.R.3).

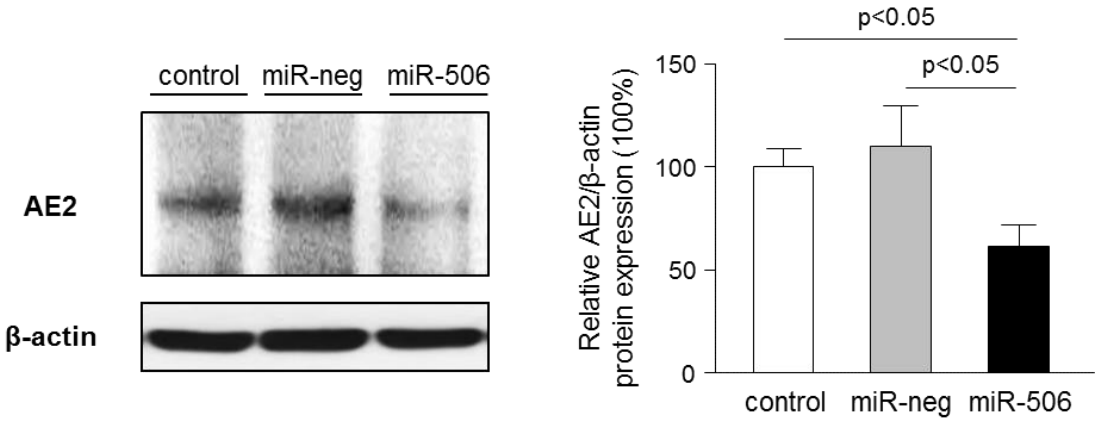

Figure 1.R.3. MiR-506 decreases AE2 protein expression in cholangiocytes. Representative western blot and corresponding quantification showing that miR-506 overexpression in H69 cells leads to downregulation of AE2 protein expression compared to controls. Bar-graph shows AE2 quantification using β-actin as a loading control (n=5).

1.R.4 *Proteomic profile associated to overexpression of miR-506 in H69 human cholangiocytes*

To elucidate the pathophysiological impact of miR-506 in cholangiocytes, a proteomic analysis was performed in H69, H69-miR-neg and H69-miR-506 cells. Overexpression of miR-506 in human cholangiocytes prompted the dysregulation of multiple proteins compared to control conditions (Figure 1.R.4A). The dysregulated proteins are involved in different biological processes such as biological adhesion (i.e. COLGALT1), biological regulation (i.e. ATP1A1, DDX3X and KPNA2) and cellular component organization or biogenesis (i.e. GSPT1, RPS19, OPA1, HSPA8, LMNA, CCT7 and ACTN1), among others (Figure 1.R.4B), but particularly in metabolic processes with altered mitochondrial proteins (i.e. ALDH2, ACO2, OPA1, PDHB, SLC25A3, NNT, ATP5H and ACLY) (Figure 1.R.4C).

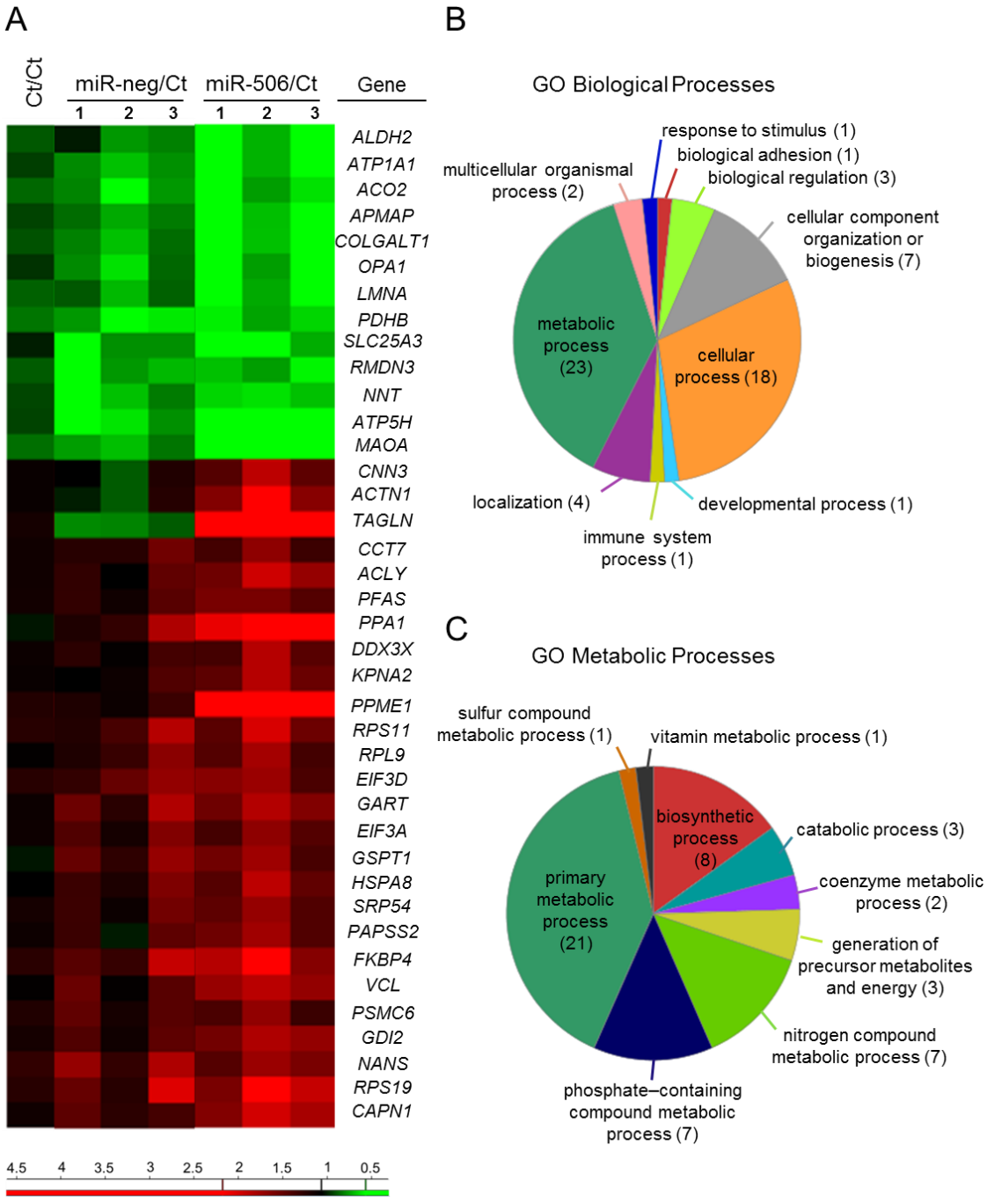

Figure 1.R.4. Proteomic profile associated to miR-506 overexpression in cholangiocytes. **(A)** Heatmap of the differentially-expressed proteins. **(B-C)** Functional classification of dysregulated proteins using the Panther Classification System database (http://pantherdb.org/), and classifications based on **(B)** biological or **(C)** metabolic processes.

1.R.5 *Role of miR-506 on the biliary phenotype, and on cholangiocyte proliferation, adhesion and migration*

PBC cholangiocytes are characterized by dedifferentiation, linked to decreased expression of biliary [132] and epithelial markers and acquisition of

mesenchymal markers [133, 134]. In this regard, we found that H69-miR-506 cells exhibited downregulation of biliary [i.e. cytokeratin 7 (CK7)] and epithelial (i.e. ZO-1) markers and increased expression of mesenchymal (i.e. N-cadherin) and pro-inflammatory (i.e. IL-8) markers compared to controls (Figure 1.R.5A). On the other hand, miR-506 decreased cell proliferation (Figure 1.R.5B), which was associated with upregulation of the cell cycle inhibitor p21 at mRNA and

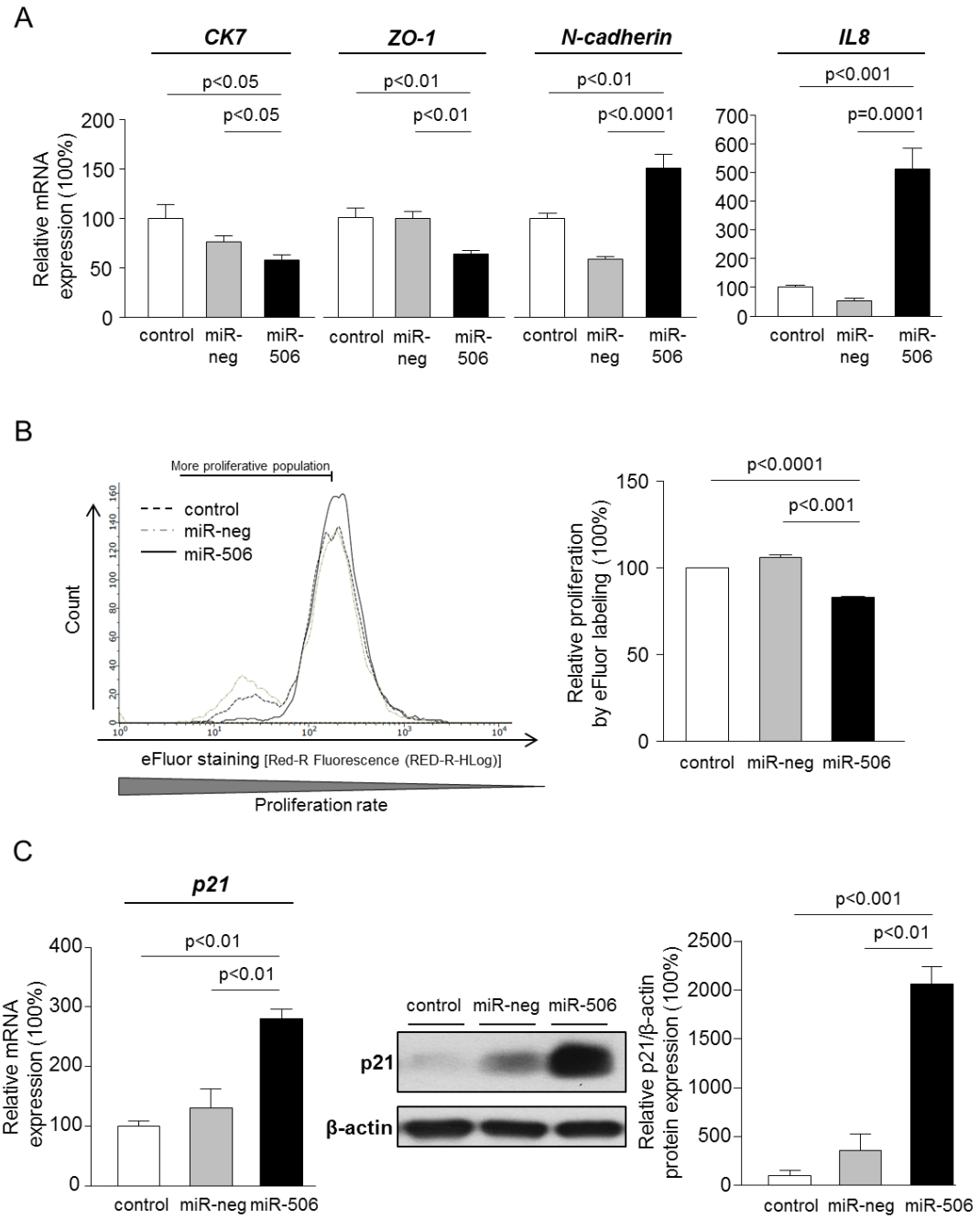

protein level compared to controls (Figure 1.R.5C).

Figure 1.R.5. MiR-506 induces cholangiocyte dedifferentiation and inhibits cell proliferation. (A) Bar-graph showing the mRNA expression levels of biliary [i.e. *cytokeratin 7* (*CK7*)], epithelial (i.e. *ZO-1*), mesenchymal (i.e. *N-cadherin*) and pro-inflammatory (i.e. *IL-8*) markers in H69-miR-506 cells compared to controls (n=6). GAPDH was used as housekeeping control. **(B)** Representative flow cytometry-based histograms and quantification of proliferation (n=3). **(C)** *p21* mRNA expression (n=6) (with *GAPDH* used as housekeeping control) and representative western blot of p21 protein expression. Bar-graph shows p21 quantification, using β-actin as loading control (n=3).

This altered phenotype was also associated with decreased adhesion and migration properties of cholangiocytes (Figure 1.R.6).

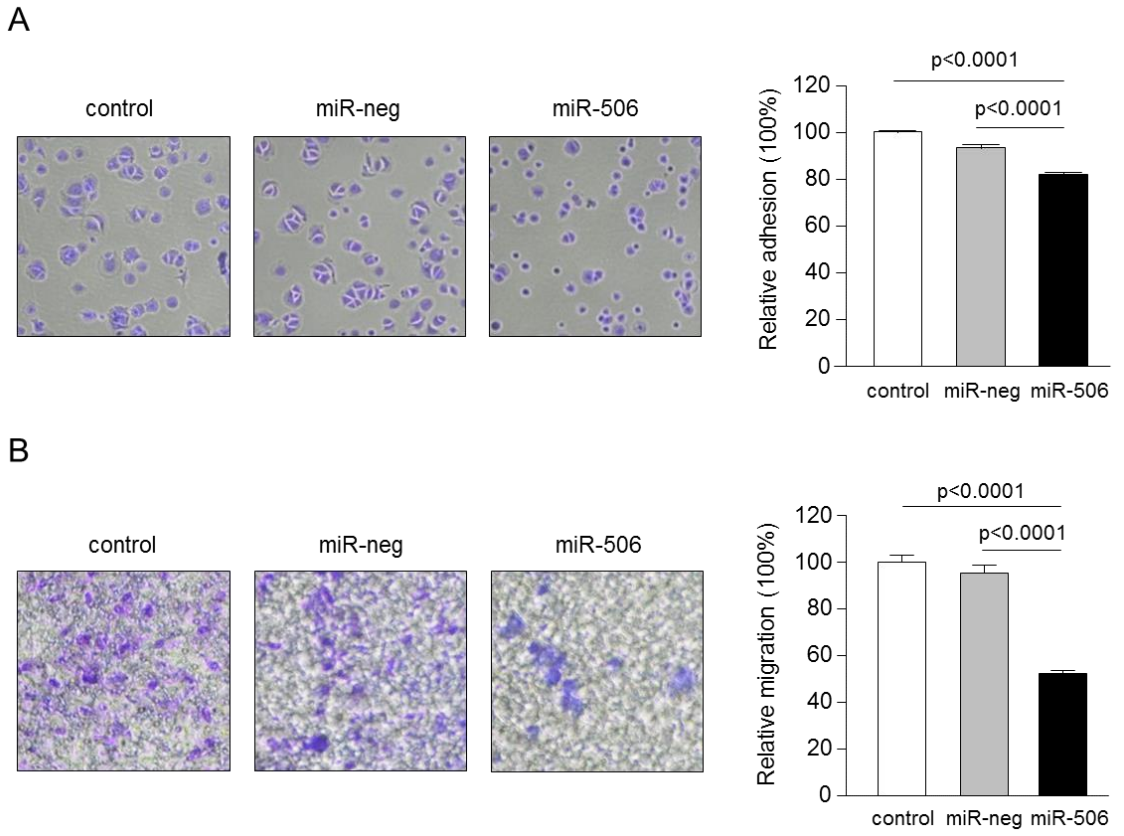

Figure 1.R.6. MiR-506 inhibits cholangiocyte adhesion and migration. **(A)** Representative images and corresponding quantification of the adhesion properties of H69, H69-miR-neg and H69-miR-506 cells (n=8). **(B)** Representative images and corresponding quantification of cell migration analysis using transwell assays (n=5).

1.R.6 *Involvement of miR-506 in cholangiocyte stress and apoptosis*

PBC cholangiocytes are characterized by cellular stress [135] and increased apoptosis [136, 137]. These PBC features are promoted by a downregulation of

AE2 and InsP3R3 in cholangiocytes. In this context, the lack of AE2 in PBC cholangiocytes sensitizes the cells to the apoptosis induced by cytotoxic apolar hydrophobic bile acids [138], and the downregulation of InsP3R3 leads to altered ER-related Ca^{2+} signaling [117, 120, 139]. Since miR-506 directly targets both AE2 and InsP3R3 mRNAs, cellular stress and apoptosis were evaluated in H69-miR-506 cells and controls. MiR-506 increased the levels of reactive oxidative species (ROS) in cholangiocytes (Figure 1.R.7A) and upregulated the expression of two key endoplasmic reticulum (ER) stress markers such as *IRE1*α and *CHOP* compared to controls (Figure 1.R.7B), while other markers such as *ATF6*, *PERK* or *XBP1* remained unaltered (Figure 1.R.7B).

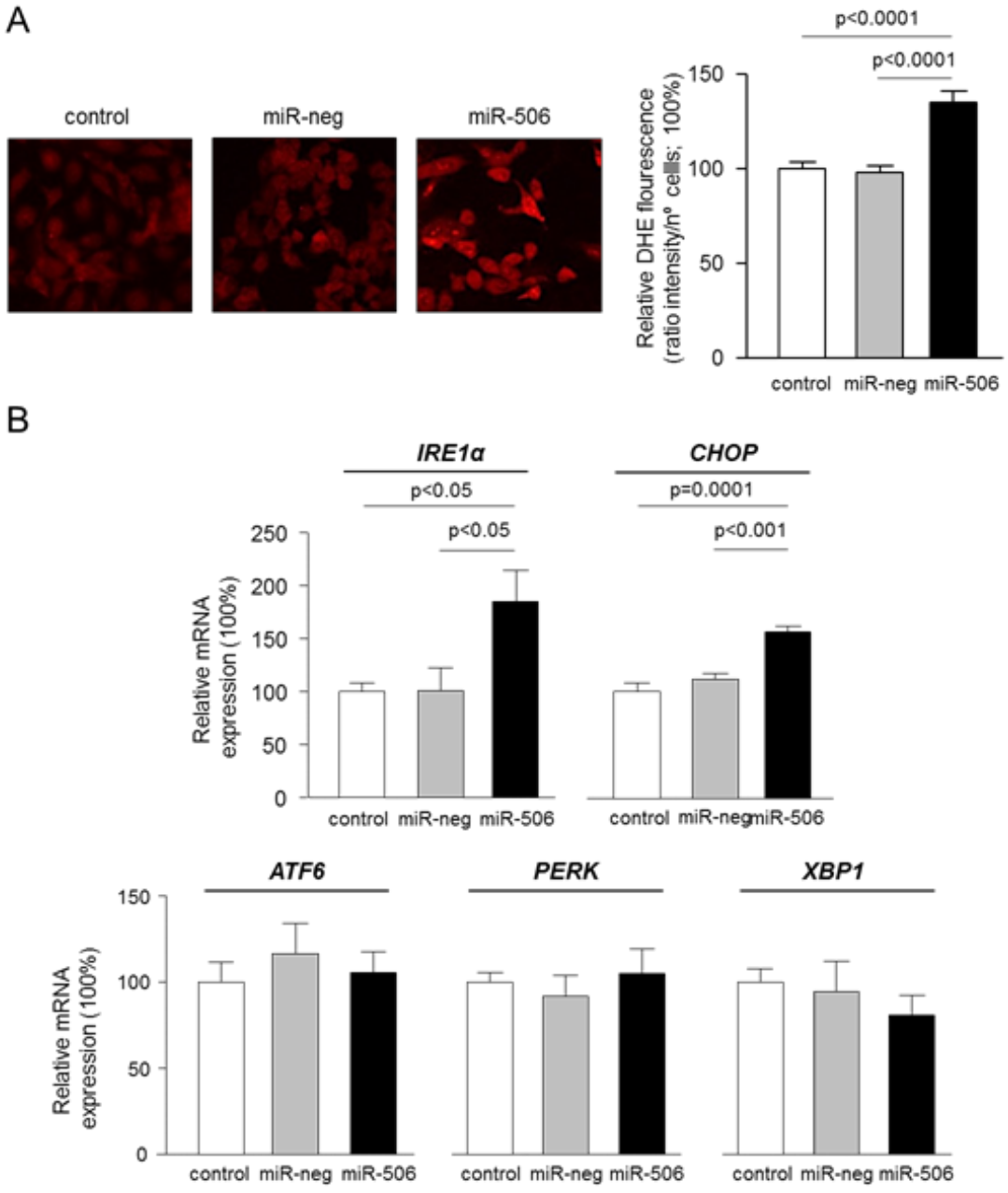

Figure 1.R.7. MiR-506 induces stress in cholangiocytes. (A) Representative fluorescence microscopy images and quantification of DHE staining (n=57-59 cells in each group). **(B)** mRNA expression of ER stress markers (n=6). *GAPDH* was used as a housekeeping control.

All these pathological events were associated with upregulation of the DNA damage marker γH2AX protein (Figure 1.R.8A) but did not affect the baseline apoptosis of cholangiocytes compared to controls (Figure 1.R.8B).

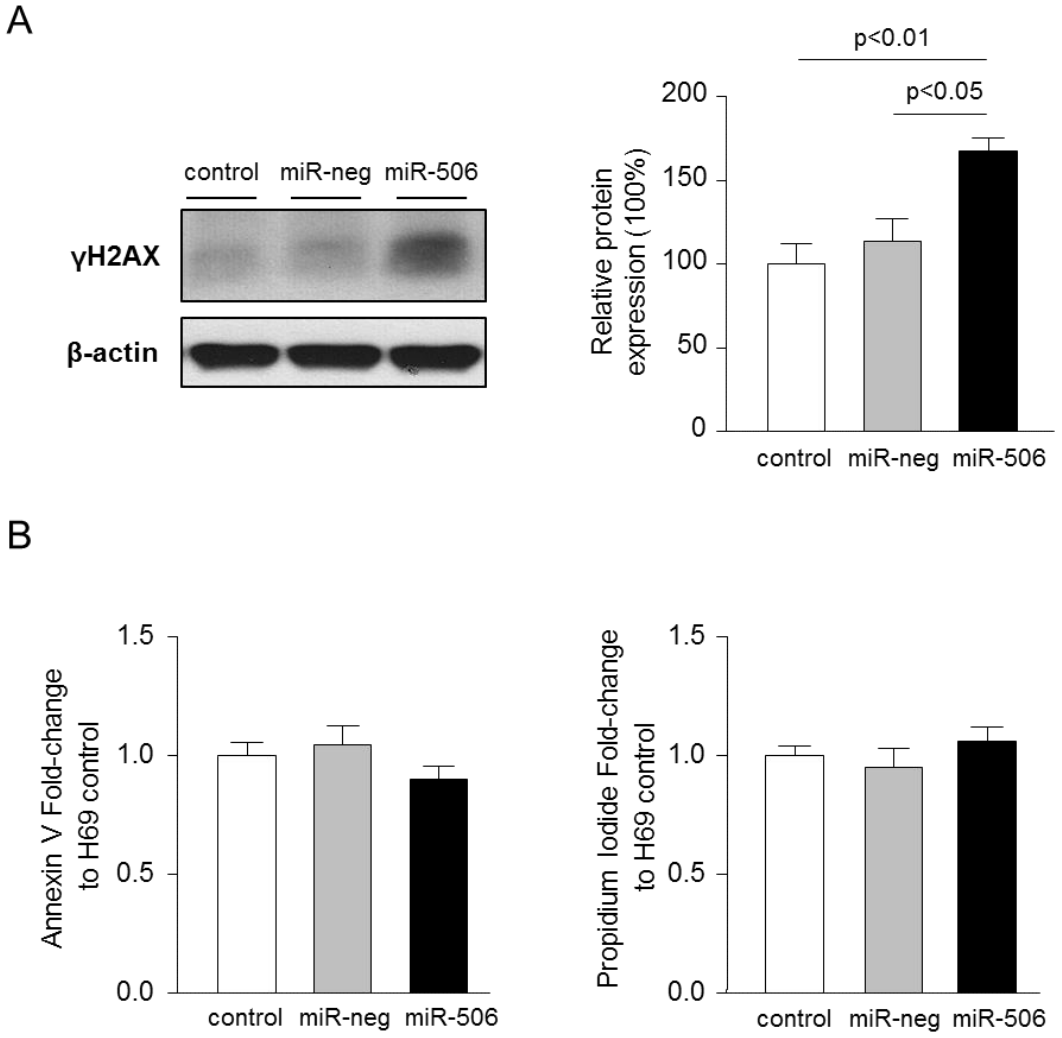

Figure 1.R.8. MiR-506 induces DNA damage in cholangiocytes but do not affect baseline apoptosis. (A) Representative immunoblot of γH2AX. Bar-graph showing the quantification relative to β-actin (n=4). **(B)** Baseline cell death determined by flow cytometry using annexin V and propidium iodide staining (n=6 from two independent experiments).

However, notably, miR-506 sensitized cholangiocytes to the apoptosis induced by the cytotoxic BAs CDCA or GCDCA measured by flow cytometry-based assays (i.e. annexin V and propidium iodide) compared to controls (Figure 1.R.9 A and B, respectively).

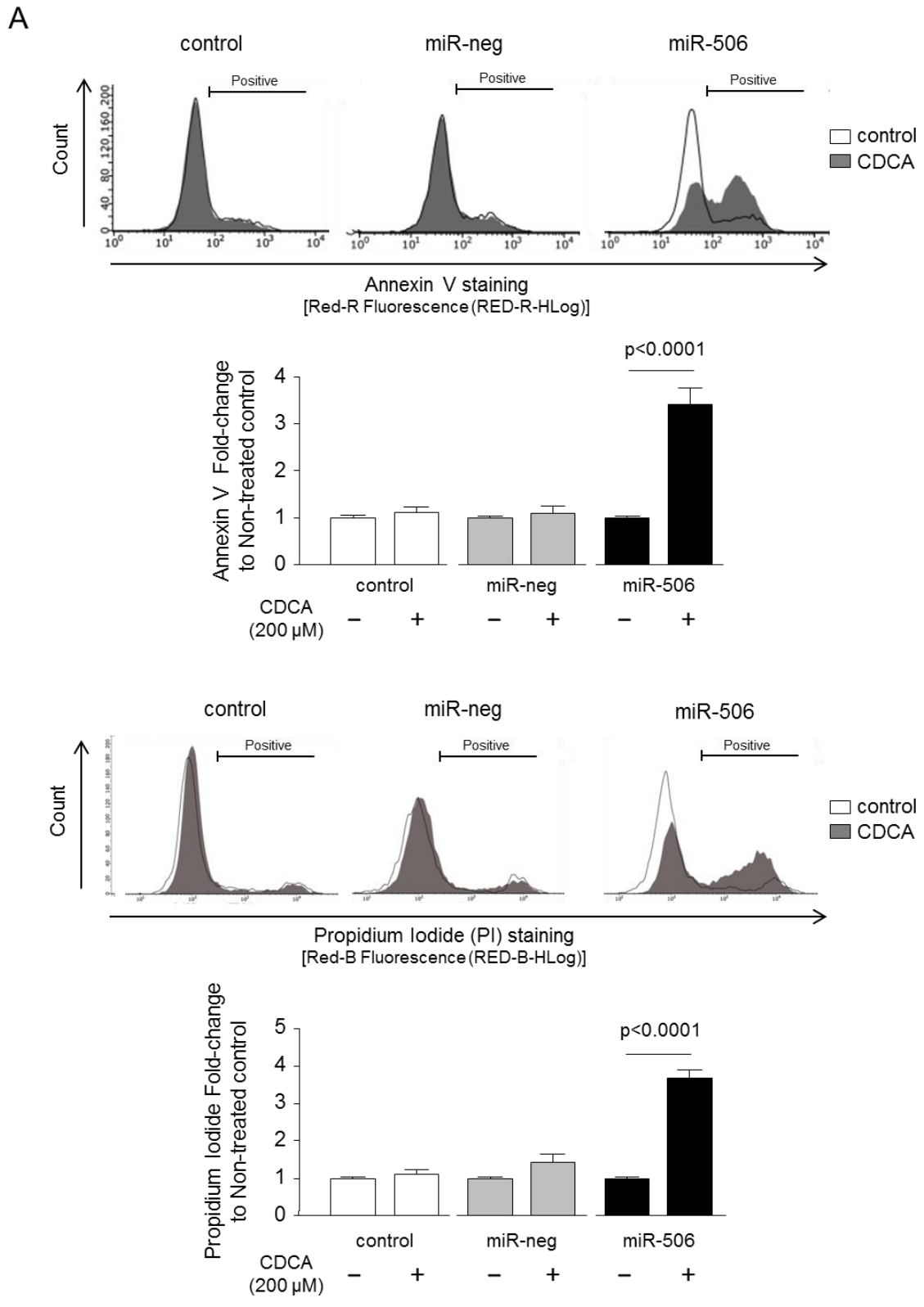

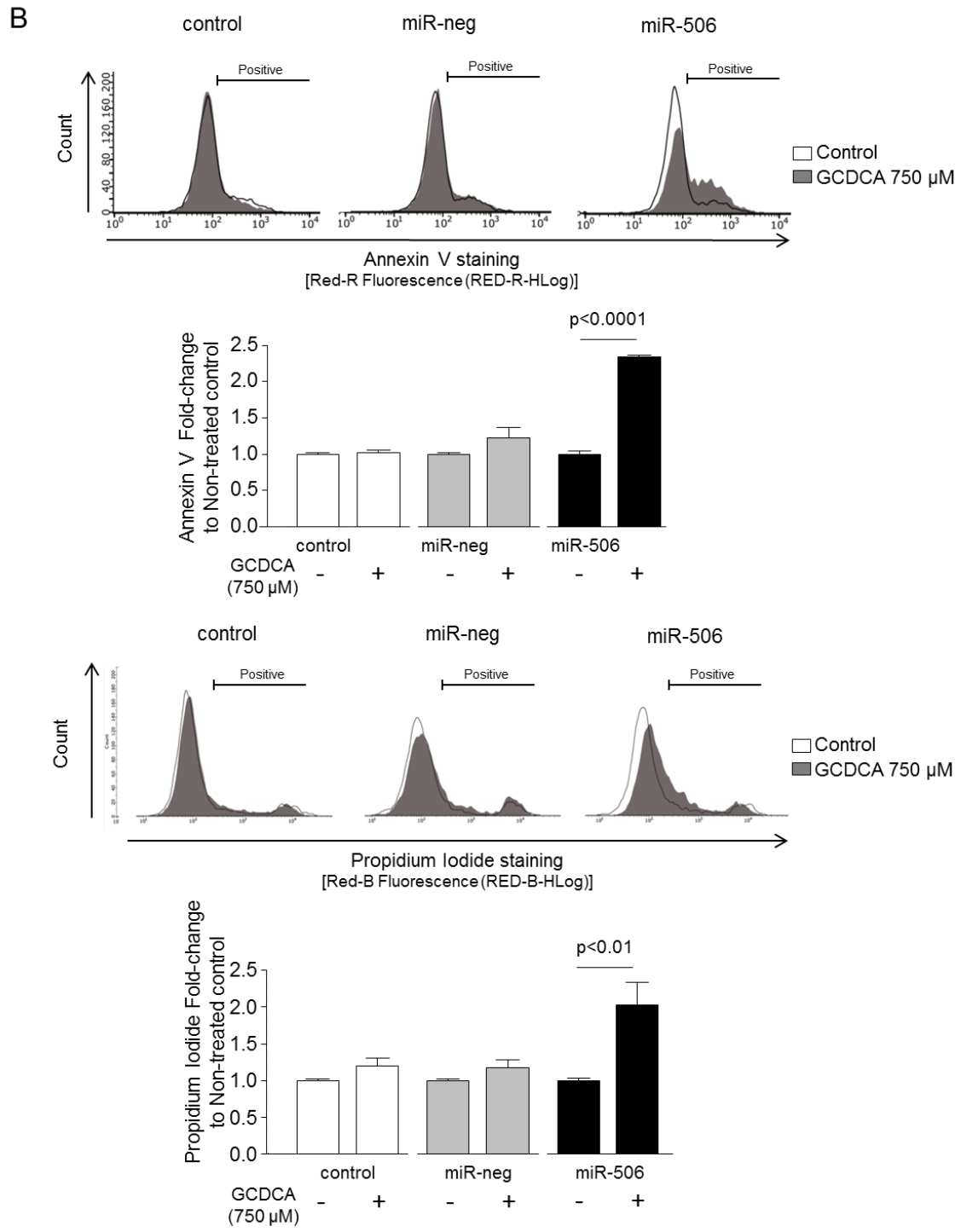

Figure 1.R.9. MiR-506 sensitizes cholangiocytes to cytotoxic bile acid-induced apoptosis. Flow cytometry-based apoptosis images and quantification of annexin V and propidium iodide staining under the presence of **(A)** 200 µM CDCA (n=6) or **(B)** 750 µM GCDCA (n=6).

In line with this, the presence of CDCA in the culture medium highly stimulated p21, cleaved caspase-3 and γH2AX expression in H69-miR-506 cholangiocytes (Figure 1.R.10).

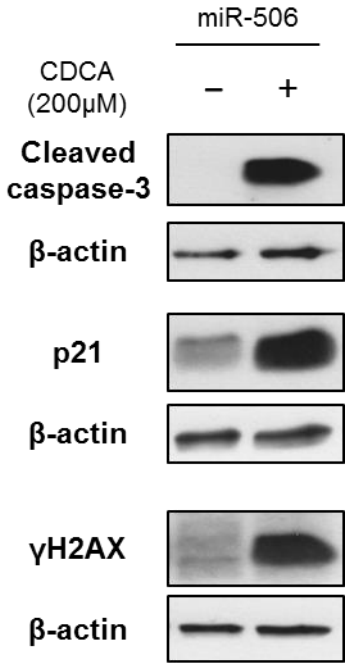

Figure 1.R.10. MiR-506 sensitizes cholangiocytes to toxic bile acid-induced DNA damage and apoptosis. Immunoblots of cleaved caspase-3, p21 and γH2AX in H69-miR-506 cells in the presence or absence of 200 μM CDCA. β-actin was used as a housekeeping control.

1.R.7 *Role of miR-506 in the mitochondrial energetic metabolism in cholangiocytes*

Since most of the proteins found dysregulated in cholangiocytes under miR-506 overexpression participate in metabolic processes (Figure 1.R.4), mitochondrial metabolism was investigated. Hence, oxygen consumption rate (OCR) and extracellular acidification rate (ECAR) were monitored upon sequential treatment of H69, H69-miR-neg and H69-miR-506 cells with different mitochondrial inhibitors in a *Seahorse XF96 Extracellular Flux Analyzer* (Figure 1.R.11A). MiR-506 altered the mitochondrial energetic metabolism in cholangiocytes which was characterized by increased baseline respiration, maximal respiration, ATP-linked respiration and non-mitochondrial respiration compared to controls (Figure 1.R.11B). In addition, H69-miR-506 cells showed

increased ECAR, glycolysis and oxidative phosphorylation (OXPHOS), and a more energetic phenotype compared to controls (Figure 1.R.11C).

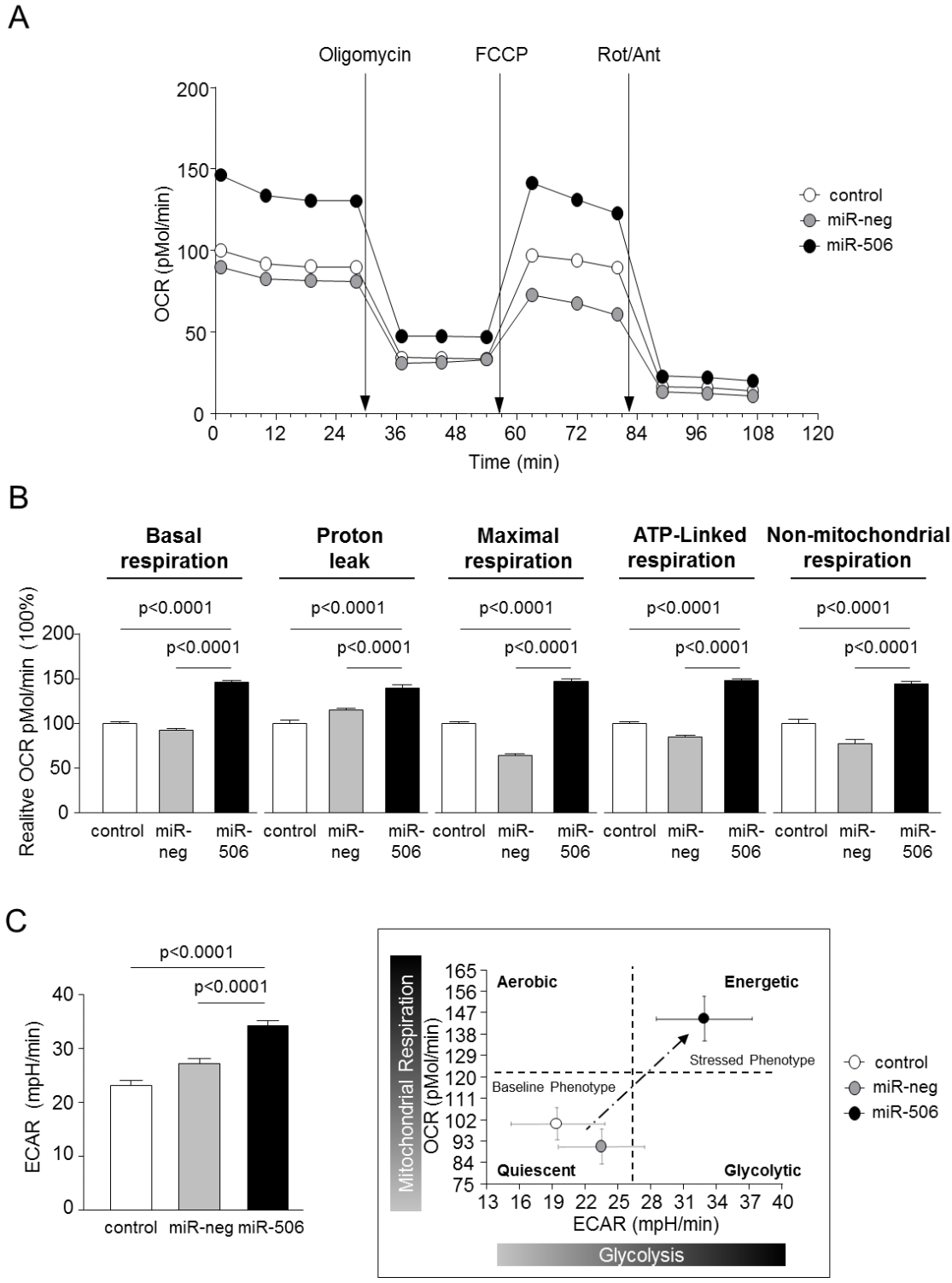

Figure 1.R.11. Cholangiocytes overexpressing miR-506 show increased mitochondrial metabolism. (A) Representative oxygen consumption rate (OCR) of H69, H69-miR-neg and H69-miR-506 cells during mitochondrial stress test analyzed by the Seahorse technology. **(B)** Metabolic parameters calculated upon OCR measurements. **(C)** Bar-graph showing

extracellular acidification rate (ECAR) during mitochondrial stress test and representation of OCR *vs* ECAR for determining the metabolic-switch. Seahorse data corresponds to n=22-30 wells in each group.

Notably, all these functional events in H69-miR-506 cells were associated with increased proton leak compared to controls (Figure 1.R.11B), indicating higher uncoupling of mitochondrial ATP production from respiration in H69-miR-506 cells that results in overall decreased ATP production (Figure 1.R.12A). The increased uncoupled respiration in H69-miR-506 cells was confirmed by the upregulation of the mitochondrial *uncoupling proteins 1* and *2* (*UCP1* and *UCP2)* gene expression in H69-miR-506 cells compared to controls (Figure 1.R.12B). These functional data were also supported by the fact that different proteins involved in metabolic processes were found altered by proteomic analysis in cholangiocytes under miR-506 overexpression, including proteins involved in the mitochondrial energetic metabolism.

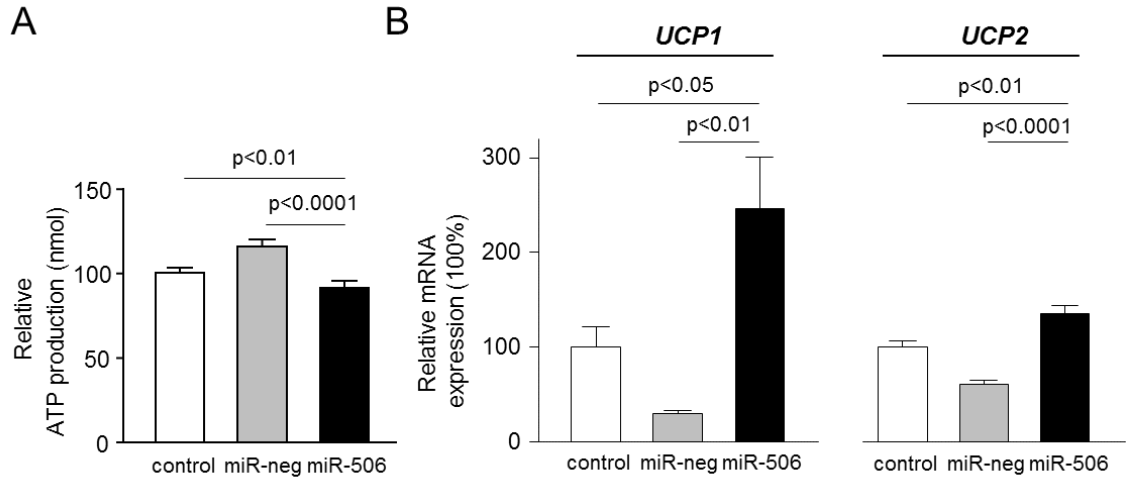

Figure 1.R.12. MiR-506 decreased ATP production in cholangiocytes and increased expression of mitochondrial uncoupling proteins (UCP). (A) ATP production rate (n=6). **(B)** *UCP1* and *UCP2* mRNA expression relative to *GAPDH* (n=6).

1.R.8 *Relevance of miR-506 on PDC-E2 expression in cholangiocytes and on immune regulation*

PBC patients are mostly characterized (~95%) by spontaneous development of AMA specific against PDC-E2, as a consequence of the overexpression and mislocalization of PDC-E2 in cholangiocytes, resulting in autoimmune

phenomena [35, 140]. Thus, we analyzed whether the miR-506 regulates PDC-E2 expression and its role in immunity. Here, we found that H69-miR-506 cells have PDC-E2 mRNA and protein overexpression (Figures 1.R.13 A and B, respectively), which was found located in both cytoplasm and plasma membrane compared to control conditions, where PDC-E2 was mainly localized into the cytoplasm (Figure 1.R.13B).

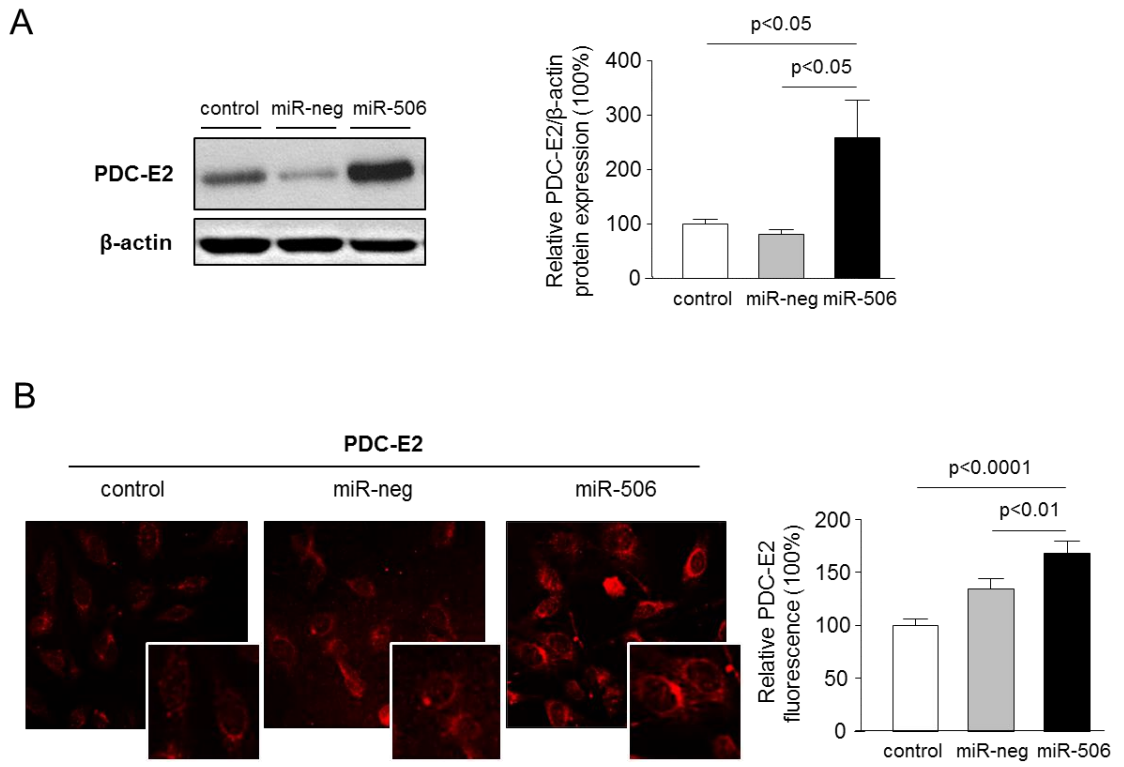

Figure 1.R.13. MiR-506 induces PDC-E2 overexpression in cholangiocytes. (A) Representative immunoblot and corresponding quantification (n=6) showing PDC-E2 protein overexpression in H69-miR-506 cells compared to controls. β-actin is used as a loading control. **(B)** Representative immunofluorescent microscopy images showing PDC-E2 protein expression and location, and corresponding fluorescence quantification (n=40-54 cells for each group).

Next, co-cultures of H69, H69-miR-neg or H69-miR-506 cells together with PBC peripheral blood mononuclear cells (PBMCs) were carried out and the proliferation and activation of PBMCs was studied. Co-cultures of H69-miR-506 cholangiocytes together with PBMCs from PBC patients induced the generation of higher number and size of lymphocyte-aggregates compared to control conditions (Figure 1.R.14A). Notably, these aggregates were characterized by increased proliferation (CFSE assay by flow-cytometry; Figure 1.R.14B) and

activation (CD25 marker by flow-cytometry; Figure 1.R.14C) of PBC PBMCs compared to controls.

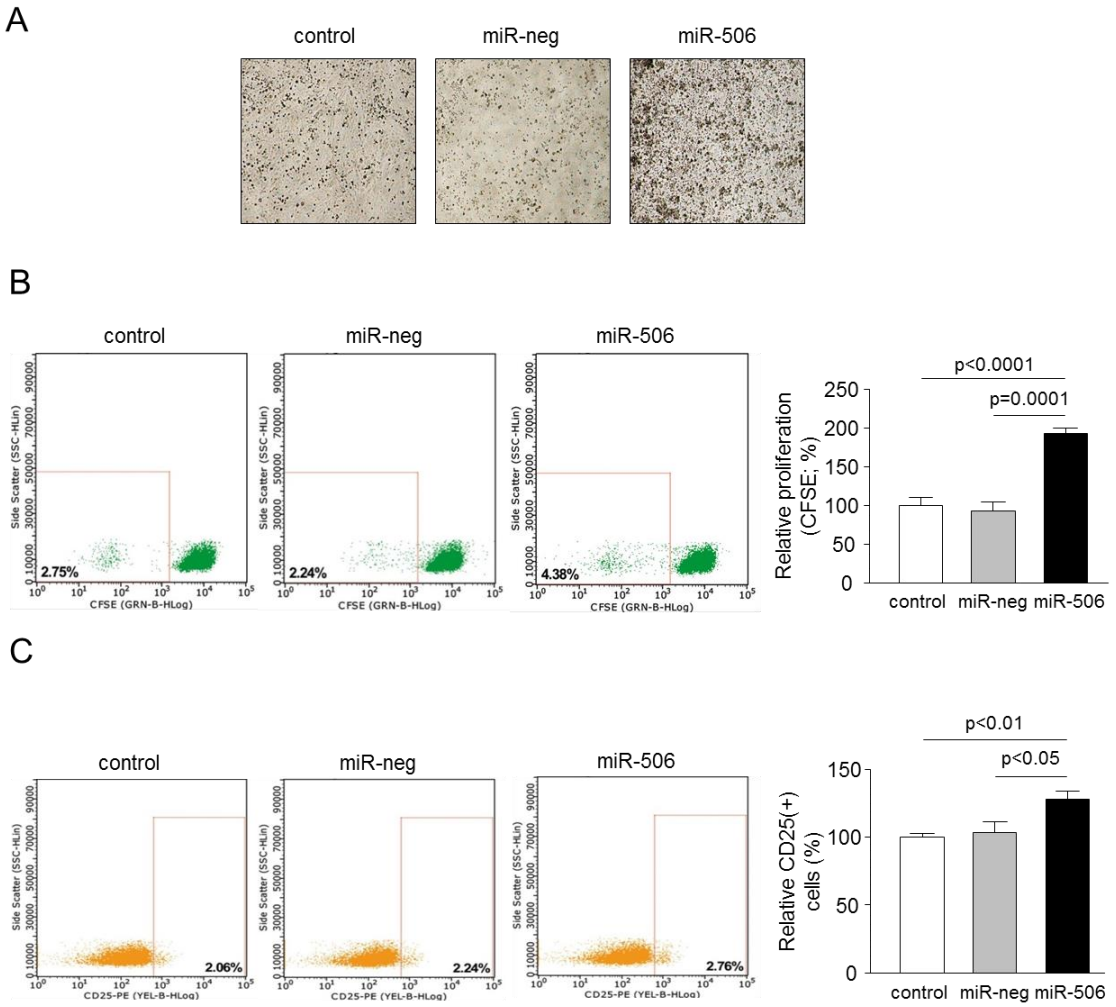

Figure 1.R.14. MiR-506 promotes immune activation. H69, H69-miR-neg and H69-miR-506 co-culture with PBMCs from a PBC patient was established (n=5). **(A)** Representative microscope images of the different co-culture conditions. **(B-C)** In PBMCs under co-culture conditions **(B)** proliferation rate (with CFSE staining), and **(C)** activation (by CD25 staining) were evaluated. Representative dot-blots are shown for each condition.

Additionally, the levels of cytokines involved in the immune response of PBC patients were evaluated in the supernatant of the cells cultured alone or co-cultured with PBMCs from a PBC patient. When co-cultured, H69-miR-506 cells showed higher IL-17A and IL-23 cytokine levels compared to controls and to the other co-culture conditions (Figure 1.R.15).

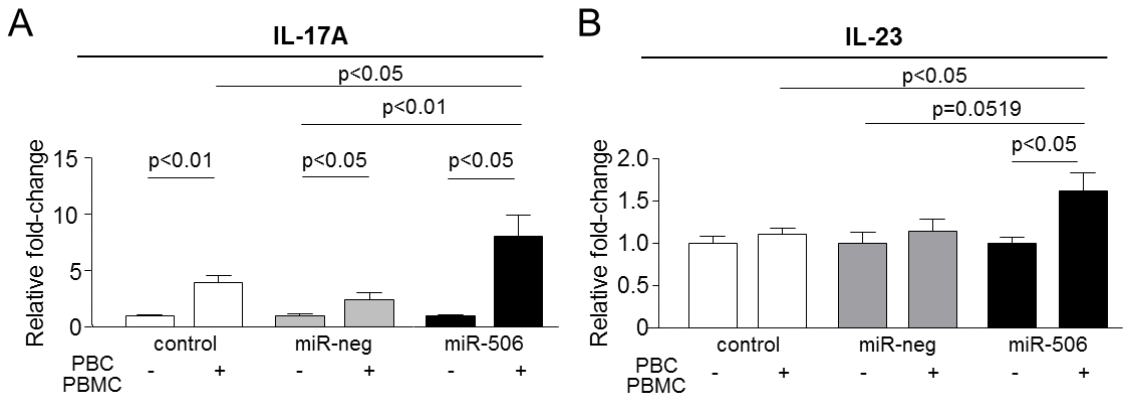

Figure 1.R.15. MiR-506 promotes the secretion of IL-17A and IL-23. Levels of **(A)** IL-17A and **(B)** IL-23 in the supernatant of H69, H69-miR-neg and H69-miR-506 co-cultured with PBC PBMCs (n=4-5).

1 - Discussion

PBC is characterized by a dysregulation of the miR expression profile in both liver and PBMCs [122, 141], but their functional relevance still remains mostly unknown. In this regard, we previously found that miR-506 is exclusively expressed in the bile duct epithelial cells of PBC livers and its expression is increased compared to the bile duct cells of normal controls [105]. In cholangiocytes, miR-506 directly targets both AE2 [105] and Ins3PR3 [120] leading to cholestasis [119, 120, 142]. However, the regulation of miR-506 expression and its role in cholangiocyte pathophysiology and immune regulation remain unknown. In the current report, the evaluation of different lengths of miR-506 promoter indicate that the full-length ~3 kb region of miR-506 promoter is required for its activation by pro-inflammatory cytokines found overexpressed in PBC livers such as IL-8, IL-12, IL-17, IL-18 and TNFα. These pro-inflammatory cytokines are involved in PBC immune response modulation and are associated with disease progression [133, 143-146]. Thus, in PBC patients, the cytokine profile in serum and liver samples suggests activation and liver recruitment of T-helper (Th)1 and Th17 cells [144]. lL-12 and IL-23, which are produced by antigen presenting cells, are responsible for promoting Th1 and Th17 immune responses, respectively. IL-12 primarily promotes the differentiation of Th0 to Th1 cells (which are known to produce IFN-γ, lL-18 and TNFα), whereas IL-23 is implicated in the differentiation of Th0 to Th17 that induces IL-17 secretion [40, 147]. In contrast, other pro-inflammatory or pro-fibrotic cytokines, as well as estrogens –believed to participate in the pathogenesis of this disease that mainly affects middle-aged women–, growth factors, immunosuppressors, and choleretic but potentially cytotoxic (i.e. CA) or hypercholeretic and hepatoprotective (i.e. UDCA and TUDCA) bile acids (BAs) did not show any effect on miR-506 expression. These data indicate that the full-length promoter sequence contains essential regulatory elements for the specific regulation of miR-506 expression in cholangiocytes under baseline and stimulated conditions, and highlight the importance of specific pro-inflammatory cytokines in the induction of miR-506 expression.

AE2 is critical for the maintenance of intracellular pH homeostasis in both cholangiocytes and CD8(+) T lymphocytes and for the modulation of immune

responses [109, 148]. In this sense, *Ae2*$^{-/-}$ mice spontaneously develop different PBC-like features such as portal infiltration of T lymphocytes and bile duct damage, increased oxidative stress in cholangiocytes, elevated production of IFNγ and IL-12, periductular hepatic fibrosis, an increase of IgM, IgG and hepatic alkaline phosphatase and specific AMA against PDC-E2, all favoring autoimmunity against cholangiocytes [109, 116]. Since the characteristic downregulation of AE2 in PBC cholangiocytes is, at least partially, mediated by miR-506, in the present work, we further evaluated the role of miR-506 in cholangiocyte pathophysiology. Experimental overexpression of miR-506 in cholangiocytes induced the dysregulation of proteins involved in fundamental biological processes. In particular, miR-506 decreased the expression of biliary/epithelial markers and upregulated the expression of mesenchymal and pro-inflammatory markers in cholangiocytes. In addition, miR-506 inhibited cholangiocyte proliferation, adhesion and migration. These results mimic the phenotype of PBC cholangiocytes, which are characterized by dedifferentiation and inflammation [40]. Senescence and oxidative stress have also been described to be involved in PBC. The damaged small bile ducts in PBC livers showed senescence-associated beta-galactosidase and increased levels of γH2AX-DNA-damage-foci, p16INK4a and p21WAF1/Cip1 by immunostaining, together with telomere shortening [149, 150]. Senescence is known to be related to ER stress. Biliary epithelial cells become senescent by increased ER stress and, moreover, senescent cells in PBC livers showed ER stress markers (i.e. glucose-regulated protein 78 [GRP78]) [135]. In agreement with these PBC features, our data indicate that miR-506 induces cell senescence by increasing p21 expression and stimulates cellular stress by increasing ROS levels, ER stress and DNA damage; this altered phenotype did not result in baseline cholangiocyte cell death but sensitized the cells against caspase-3-dependent apoptosis induced by toxic BAs. The pro-apoptotic effect of miR-506 may be related, to a certain degree, to its direct targeting of AE2 mRNA, as experimental downregulation of AE2 in cholangiocytes has been shown to favor bile salt-induced apoptosis (BSIA) [151]. Moreover, GCDC has been described to reduce AE2 expression in biliary epithelial cells by inducing ROS [152]. These data pointed out the relevant role of miR-506 regulating the so called “AE2-related biliary bicarbonate umbrella”. AE2 downregulation impairs this

protective barrier resulting in increased intracellular pH, accumulated toxic apolar hydrophobic BAs and cell apoptosis [13]. All these PBC-like features observed in miR-506 overexpressing cholangiocytes may be responsible, at least in part, of the progressive ductopenia which is characteristic of these patients [150].

On the other hand, the pro-apoptotic phenotype of miR-506 overexpressing cholangiocytes is in line with studies indicating that this miR acts as a tumor suppressor in different types of cancer such as colon, pancreas, hepatocellular (HCC), breast or glioblastoma [153]. Downregulation of miR-506 in cancer promotes cell survival, proliferation, invasion/migration and chemoresistance [153]. Data indicating the tumor suppressor capacity of miR-506 in different cancers may provide insights into the differential predisposition of different biliary diseases to the development of cholangiocarcinoma (CCA). PBC is rarely associated with biliary cancer development whereas primary sclerosing cholangitis (PSC), another biliary disease also associated with autoimmune phenomena targeting the bile duct epithelial cells, predisposes to the development of CCA in up to ~15% of patients [45]. We previously reported miR-506 overexpression in the bile duct cells of PBC patients but not in PSC patients [105]. Thus, whether miR-506 is involved on PSC should be analyzed, in order to determine if miR-506 overexpression could contribute to the differential pro-tumorigenic predisposition of PSC *vs* PBC. Future studies should clarify the role of miR-506 in hepatobiliary cancers.

The role of miR-506 was also evaluated on the mitochondrial metabolic activity and immune activation. Mitochondrial abnormalities are involved in the pathogenesis of PBC. Toxic BA accumulation during cholestasis leads to mitochondrial dysfunction through oxidative stress [154]. Our data showed that overexpression of miR-506 in cholangiocytes led to an altered mitochondrial energetic metabolism characterized by increased oxygen consumption and glycolysis but also with increased proton leak, indicating an increase of uncoupling respiration. This increase in uncoupling could be in line with the increase in ROS production and perhaps with DNA damage and ER stress. Of note, miR-506-dependent mitochondrial dysfunction in cholangiocytes was also associated with PDC-E2 overexpression, a typical PBC feature that may promote, at least in part, the immunogenicity of cholangiocytes [40]. Therefore,

we evaluated the capacity of miR-506 in cholangiocytes to modulate PBC lymphocytes under co-culture. Interestingly, miR-506 overexpressing cholangiocytes promoted the proliferation and activation of PBC PBMCs compared to cholangiocytes under control conditions, pointing out the relevance of miR-506 in the regulation of cholangiocyte immunogenicity and in the potential induction of auto-immunity. In addition, co-cultures of H69-miR-506 cells and PBMC increased both IL-17 and IL-23 levels, important cytokines in Th1 and Th17 immune responses and in PBC, as these pro-inflammatory cytokines are overexpressed in peripheral blood of PBC patients [145]. These data are consistent with previous reports indicating that PBC cholangiocytes are characterized by an overexpression and aberrant location, into the plasma membrane, of mitochondrial PDC-E2. Additionally, PBC cholangiocytes present increased apoptosis [136, 137] and immunologically active PDC-E2 due to the lack of glutathiolation [155], which may be present in apoptotic bodies (known as apotopes) [155, 156]. These two mechanisms of aberrant PDC-E2 presentation may be the base of the development of AMA and further promotion of autoimmunity against cholangiocytes.

In summary, this study provides novel insights of the important role of miR-506 in the pathogenesis of PBC. Different pro-inflammatory cytokines found overexpressed in PBC livers promote the upregulation of miR-506 expression in cholangiocytes, leading to the development of PBC-like features such as cell dedifferentiation, stress, predisposition to bile-salt induced apoptosis, alterations in mitochondrial function and PDC-E2 overexpression, which finally result in PBC immune activation (Figure 1.D.1). These effects are mediated, to a certain degree, by direct targeting of miR-506 to both AE2 and Ins3PR3, which play key roles in the maintenance of the biliary phenotype. However, the role of miR-506 directly regulating the expression of other genes must also be considered and determined in future studies.

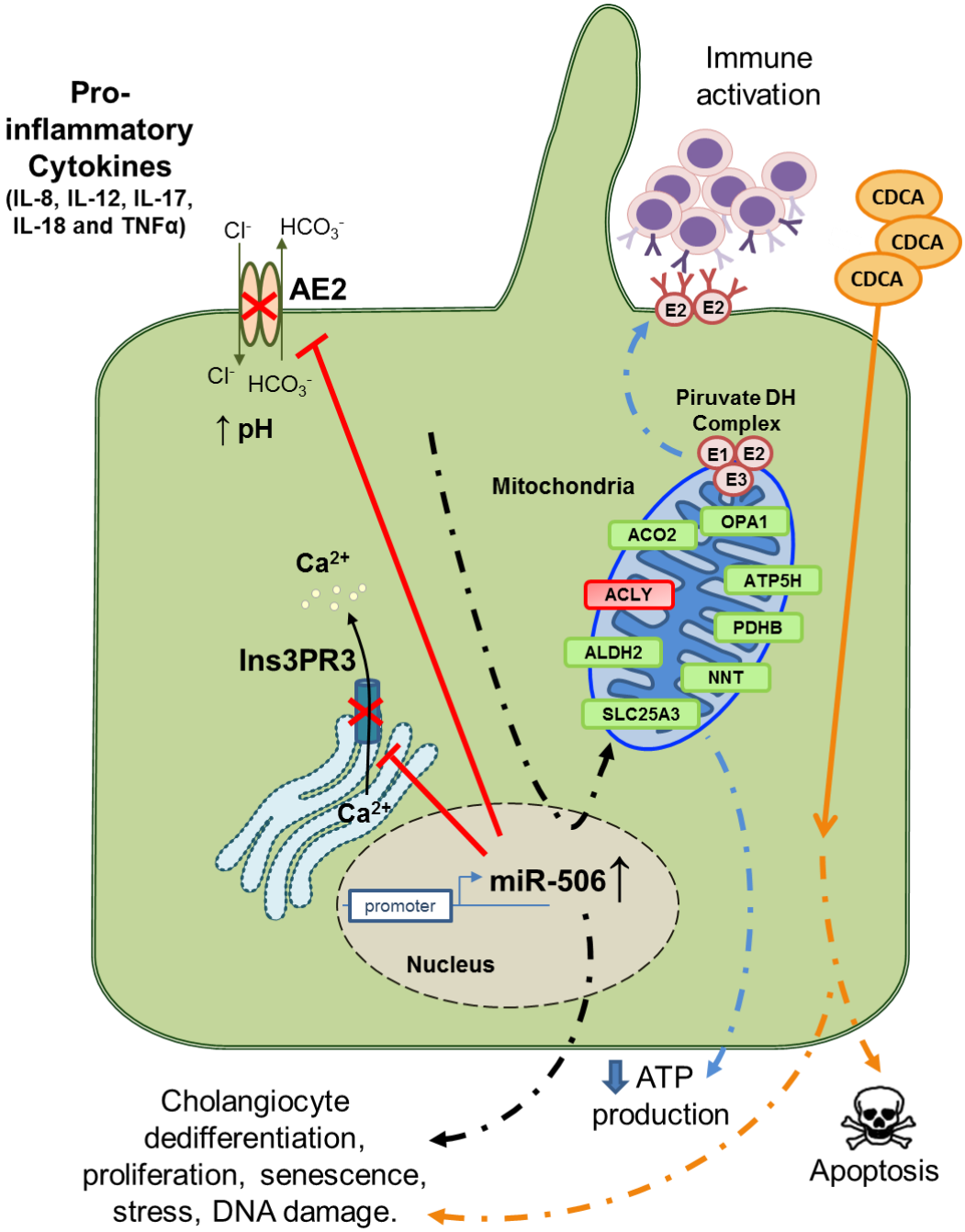

Figure 1.D.1. Working model. Pro-inflammatory cytokines such as IL-8, IL-12, IL-17, IL-18 and TNFα stimulate the promoter activity of *miR-506* gene. Overexpression of miR-506 in cholangiocytes inhibits AE2 and Ins3PR3 expression and activities, resulting in altered intracellular pH and Ca^{2+} concentration. MiR-506 leads to altered mitochondrial energetic metabolism associated with altered expression of proteins involved in such process; the resultant mitochondrial energetic metabolism fails and results in decreased ATP production and in overexpression and mislocalization of PDC-E2, leading to immune activation. MiR-506 decreases the expression of biliary and epithelial markers in cholangiocytes and increases the expression of mesenchymal, inflammatory and senescence genes, impairing cell proliferation, adhesion and migration, and stimulating ROS, ER stress and DNA damage. MiR-506 also sensitizes cholangiocytes against toxic BA-induced apoptosis.

1 - Conclusions

The key findings reported here are related to the role of miR-506 in cholangiocyte pathophysiology and immune regulation. Our data indicate that:

I. Different pro-inflammatory cytokines (i.e. IL-8, IL-12, IL-17, IL-18 and TNFα) found overexpressed in PBC livers stimulated the activity of miR-506 gene promoter, whereas bile acids, estrogens and growth factors had no effects.
II. MiR-506 in cholangiocytes inhibited AE2 protein expression and dysregulated the proteomic profile of the cells, particularly altering the expression of proteins involved in mitochondrial metabolism.
III. MiR-506 inhibited the expression of biliary and epithelial markers in cholangiocytes and induced the expression of mesenchymal, inflammatory and senescence/cell cycle inhibitory genes. This phenotype resulted in a decrease in cell proliferation, adhesion and migration.
IV. MiR-506 stimulated ROS, ER stress and DNA damage in cholangiocytes, and sensitized the cells to the apoptosis induced by toxic bile acids.
V. MiR-506 increased the mitochondrial metabolism and oxidative phosphorylation, events that were associated with an uncoupling of ATP production from mitochondrial respiration and with overexpression of PDC-E2.
VI. MiR-506 in cholangiocytes induced the proliferation and activation of PBC PBMCs, and stimulated the secretion of IL-17 and IL-18 cytokines, which participate in autoimmunity processes.

Our data are consistent with the notion that miR-506 is a key player in the pathogenesis of PBC and a potential target for therapy.

IV. CHAPTER 2

ROLE OF FXR AND TGR5 IN CHOLANGIOCARCINOMA

2 - Introduction

2.I.1 *Cholangiocarcinoma (CCA)*

Cholangiocarcinomas (CCAs) are heterogeneous cancers affecting the biliary tract, and some symptoms arise as a consequence of the biliary obstruction caused by the tumor [43, 53]. The etiology of most CCAs is currently unknown. However, CCA development has been associated to different risk factors including choledocal cysts and cholestatic conditions such as primary sclerosis cholangitis (PSC) and hepatolithiasis, and CCAs may themselves cause cholestasis by tumor-induced biliary obstruction [45]. The biliary obstruction can result in the accumulation of toxic bile acids (BAs) and increased BA concentration has been suggested as a potential event inducing CCA development and progression [72]. For instance, BAs regulate the secretion, proliferation, apoptosis and differentiation of cholangiocytes [157].

2.I.2 *Bile acids (BAs)*

Bile acids (BAs) are water-soluble and amphipathic molecules derived from cholesterol. BAs are mainly synthetized in the liver and then transformed by bacteria in the gut [158]. Cholesterol metabolism in the liver and fat digestion and absorption in the gut are the main functions for BAs. However, BAs participate in the regulation of multiple pathophysiological processes along the gastrointestinal tract.

There are two main biosynthetic pathways for primary BA formation. The “classical or neutral” is only present in the liver and is catalyzed by the enzymes *microsomal cholesterol 7α-hydroxylase* (CYP7A1) and *cytochrome P450 family 8 subfamily B member 1* (CYP8B1). The two primary BAs in humans are synthesized by this pathway: cholic acid (3α, 7α, 12α-trihydroxy-5β-cholanoic acid) (CA) and chenodeoxycholic acid (3α, 7α-dihydroxy-5β-cholanoic acid) (CDCA) [159] (Figure 2.I.1). This pathway is considered the most relevant for BA synthesis in humans. However, the “alternative or acidic” pathway has been also described. This pathway is catalyzed by the *sterol 27-hydroxylase* (CYP27A1) and the *oxysterol 7α-hydroxylase* (CYP7B1) and occurs in the liver;

however, it may also occur in the kidneys and brain due to their high expression of CYP7B1 [160]. In this process, CDCA is the main BA synthesized [161]. Over 99% of BAs are taurine- or glycine-conjugated, being these conjugated forms the major solutes in bile [162, 163]. The primary BAs (CA or CDCA) are then metabolized by intestinal microbiota resulting in the formation of the secondary bile acids: deoxycholic acid (3α acid, 12α-dihydroxy-5β-cholanoic) (DCA) and lithocholic acid (3α-hydroxy-5β-cholanoic) (LCA) [161] (Figure 2.I.1).

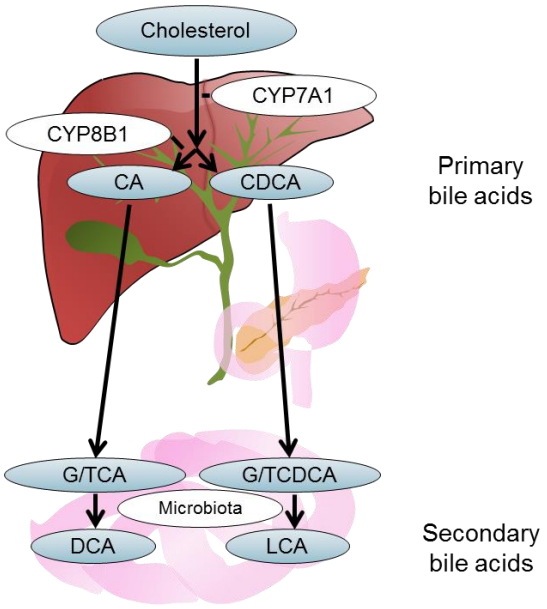

Figure 2.I.1. "Classical or neutral" pathway for BA synthesis. (Adapted from Qi *et al.*, 2014).

Once synthesized, BAs enter into the enterohepatic circulation and are transported by different carriers [158, 164] (Figure 2.I.2):

- **Bile salt export pump (BSEP)**: located into the bile canaliculus. BSEP is involved in the luminal secretion of BAs [165].
- **Apical sodium-dependent bile salt transporter (ASBT)**: located at the apical membrane of distal ileal epithelial cells, ASBT reabsorbs BAs from the gut [166].
- **Organic solute transporter α/β (OST α/β)**: located at the basolateral membrane of ileal epithelial cells, OST α/β is responsible for BA secretion into the portal circulation [167].
- **Na^+-taurocholate cotransporting polypeptide** (NTCP; also known as SLC10A1): a sodium/BA cotransporter located at the basolateral

membrane of hepatocytes and involved in BA absorption into the liver [168].

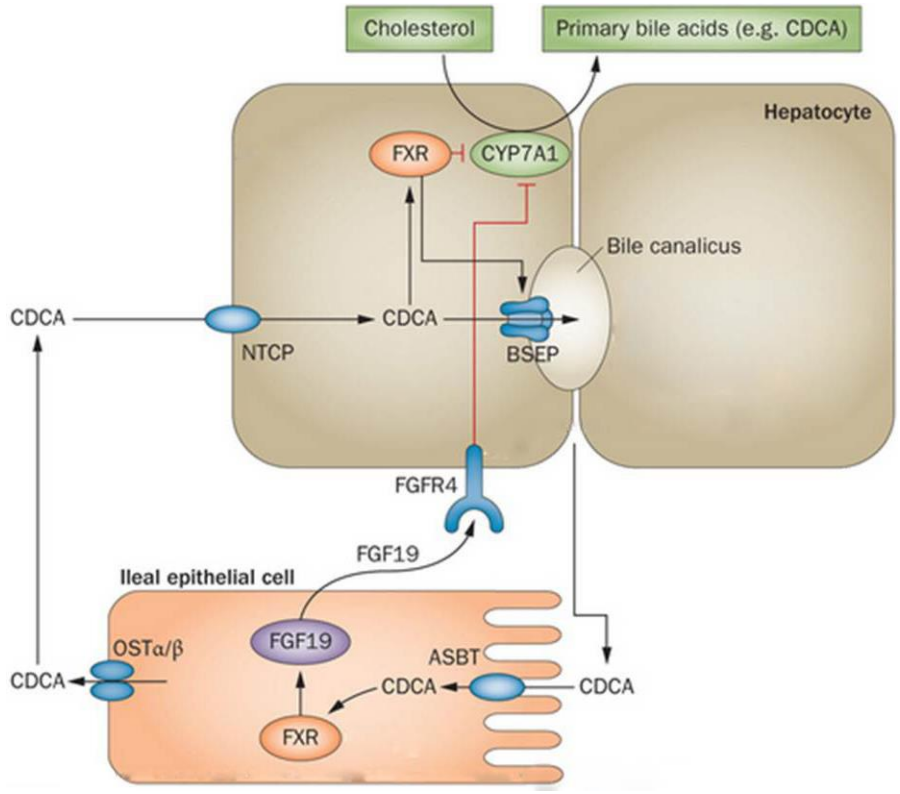

Figure 2.I.2. Enterohepatic circulation of BAs. BAs are secreted into the canaliculus by BSEP. ASBT reabsorbs BAs in the ileum and then are secreted to portal circulation via OST α/β. NTCP is responsible of the absorption of BAs to the liver (Adapted from Schaap *et al.,* 2014).

In addition, hepatocytes and cholangiocytes both have different important BA transporters. In the basolateral membrane of hepatocytes, the family of organic anion transporting polypeptides (OATP) is involved in the sinusoidal sodium-independent BA uptake [169]. BA efflux in the basolateral membrane of hepatocytes is carried out by the multidrug-resistance associated proteins MRP3 and MRP4, or by OST α/β [164]. In the canalicular membrane, apart from BSEP, MRP2 and ATP-binding cassette sub-family G member 2 (ABCG2 or BCRP) are found, which mediate the transport of conjugated BAs [161, 164, 170] (Figure 2.I.3A). Regarding cholangiocytes, BAs are absorbed by ASBT at the apical membrane and then effluxed by OST α/β at the basolateral membrane [164] (Figure 2.I.3B).

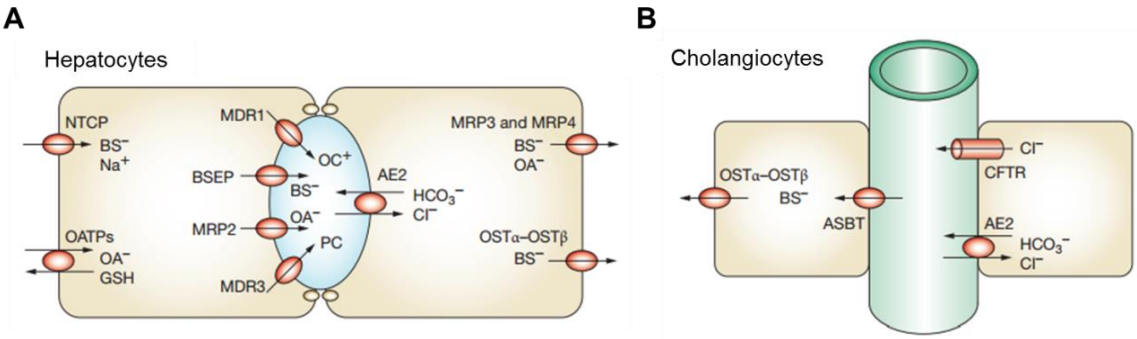

Figure 2.I.3. BA transporters in hepatocytes and cholangiocytes. Different transport systems are present in both hepatocytes and cholangiocytes for BAs and other solutes. **(A)** In hepatocytes, BAs are uptaken through NTCP and OATP and effluxed via BSEP, MRP2 and MDRs. **(B)** In cholangiocytes, ASBT and OST α/β are the main BA transporters (Adapted from Geier *et al.,* 2006).

Newly synthesized BAs are secreted into the canalicular lumen and then transported to the gallbladder, where BAs are stored. After food ingestion, BAs are secreted to the intestinal lumen for lipid and vitamin adsorption. Once digestive functions are performed, over 95% of the BAs are transported back to the liver [159, 162]. Furthermore, some BAs undergo what is called the cholehepatic shunting, where BAs in bile can be reabsorbed by cholangiocytes and then uptake by hepatocytes and further secreted to bile [171-173]. Finally, non-reabsorbed BAs enter the colon to be either converted to secondary BAs or eliminated with the feces [174]. The levels of BA have to be meticulously regulated, as BAs are essential for the hepatic elimination of toxic endogenous compounds and xenobiotics. Thus, maintaining BA homeostasis is crucial in order to avoid toxicity. BAs modulate cholesterol levels but also the levels of phospholipids [175].

BAs regulate pathophysiological processes in different cell types by binding to BA receptors. There is a group of nuclear hormone receptors (NHRs) for BA binding that include the farnesoid X receptor (FXR, encoded by *NR1H4*), pregnane X receptor (PXR, encoded by *NR1I2*), vitamin D_3 receptor (VDR, encoded by *NR1I3*) and constitutive androstane receptor (CAR, encoded by *NR1I3*) [176-179]. Additionally, BAs may bind to a cell-surface receptor termed TGR5 (also known as G protein-coupled BA receptor 1 -*GPBAR1*-) [180].

2.I.3 *BAs in cholangiocytes and CCA*

Besides the aforementioned functions, BAs modulate different functions in different cell types, including cholangiocytes [181]. In this regard, BAs are key molecules regulating physiological and pathological events in cholangiocytes [181]. The binding of BAs to their specific receptors lead to the regulation of cholangiocyte proliferation, secretion, dead and survival pathways [157]. Among the receptors, FXR and TGR5 are crucial for BA homeostasis [158]. On the other hand, accumulation of toxic BAs during cholestasis may promote the development and progression of gastrointestinal tumors [72]. In particular, intrahepatic accumulation of toxic BAs does not induce carcinogenesis directly, but facilitates a co-carcinogenic effect by inducing cholangiocyte inflammation and proliferation [182-185].

2.I.4 *BA receptors: FXR and TGR5*

2.I.4.1 *FXR*

FXR is the member of the NHR superfamily that preferentially mediates and regulates BA homeostasis and signaling [158, 176, 186-189]. Four FXR isoforms have been described, named as FXRα1+, FXRα1−, FXRα2+ and FXRα2− due to differences in exon 1 to 3 (α1 and α2) and the presence (+) or absence (−) of a 12 base pair insert at the end of exon 5 [190, 191]. FXR expression is higher in tissues exposed to high BA concentration, thus FXR levels increase along the enterohepatic circulation of BAs. Indeed, high FXR expression has been described in the intestine (particularly in the ileum), liver (both in hepatocytes and cholangiocytes) and in the kidneys [176, 192]. To exert its function on target genes, FXR forms a heterodimer with the retinoid X receptor α (RXRα, also known as NR2B1) [158]. FXR is crucial for BA homeostasis and modulates it at different levels [158]: i) repression of BA synthesis by indirect regulation of CYP7A1 expression, via upregulation of CYP7A1 inhibitor short heterodimer partner (SHP) in hepatocytes [193, 194] or by stimulating FGF19 transcription in the ileum that is further secreted into portal circulation, binds to its receptor in hepatocytes (i.e. FGFR4) and subsequently inhibits CYP7A1 [195]; ii) stimulation of BA secretion from

hepatocytes by stimulating BSEP [196]; iii) increase of basolateral efflux of BAs in the ileum by OST α/β upregulation [167]; and iv) stimulation of BA conjugation [163]. Importantly, FXR also mediates BA signaling in hepatobiliary pathophysiology, being involved in several processes such as lipid and glucose metabolism, immunomodulation, liver fibrosis, inflammation, regeneration, cell differentiation and tumorigenicity, among others [192, 197-201].

2.I.4.1.1 *FXR and CCA*

In the last decade, FXR was described to have a potential role in liver tumorigenesis since *Fxr* knockout mice (*Fxr*$^{-/-}$) spontaneously develop liver tumors [199, 202]. Regarding CCA, *FXR* expression was found to be downregulated in CCA samples compared to healthy livers [191], but the mechanisms by which this occurs is not clear. Several studies postulated that epigenetic silencing (i.e. by miR-421, SIRT1 or methylation) or the inflammatory microenvironment might be involved in FXR downregulation [203]. On note, simultaneous study of the hepatobiliary carcinogen thioacetamide (TAA) administration and/or experimental induction of obstructive cholestasis (i.e. bile duct ligation (BDL) showed a higher reduction of *FXR* expression in the liver upon BA accumulation in the BDL models, both alone or in combination with TAA, compared to rats that received TAA alone. Moreover, the combination of TAA and BDL or BDL alone increased the expression of CCA and inflammation markers in the liver compared to the administration of TAA alone, indicating that increased BA levels are not directly responsible of cholangiocarcinogenesis but they favour it [204].

2.I.4.1.2 *FXR agonists*

Given the assortment of functions of FXR and its implication in different liver diseases, targeting of this nuclear receptor appeared as a potential therapeutic tool. Several FXR ligands have been described and used for treating liver diseases. Among BAs, CDCA is the most potent FXR endogenous agonist, followed by DCA, LCA and finally CA, the less potent BA activator for FXR [158, 188]. Synthetic BA analogues have been developed for FXR activation, including obeticholic acid (OCA) [also known as INT-747 (6α-ethyl-

chenodeoxycholic acid)] [205] and INT-767 (6α-ethyl-3α,7α,23-trihydroxy-24-nor-5β-cholan-23-sulfate) [206]. Other nonsteroidal synthetic FXR agonists include GW4064, fexaramine, GSK2324, Way362450 or PX-102 [158].

OCA (Figure 2.I.4) is a synthetic BA derivative that activates FXR with high affinity and selectivity [205]. OCA is currently under clinical evaluation for the treatment of several diseases such as non-alcoholic steatohepatitis (NASH), PSC and biliary atresia [207, 208], and has recently been approved for the treatment of primary biliary cholangitis (PBC) [39].

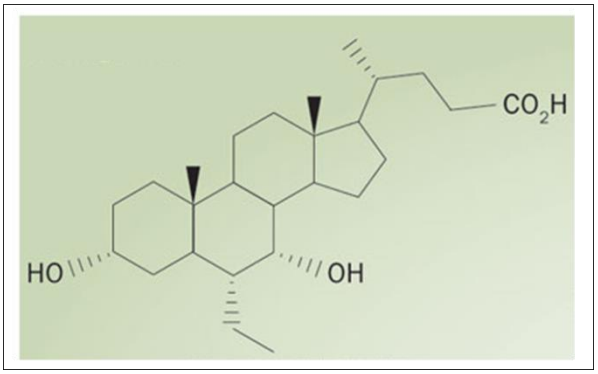

Figure 2.I.4. Molecular structure of obeticholic acid. OCA (also named INT-747 or 6-ECDCA) is synthetized by Intercept Pharmaceuticals (Adapted from Schaap *et al.*,2013).

2.I.4.2 *TGR5*

TGR5 is a G protein-coupled BA membrane receptor that is activated by BAs independently of transport systems [180, 209]. TGR5 is broadly expressed, but its expression is higher in tissues such as brown adipose tissue, brain, muscle, placenta, lung, intestine, spleen, stomach, gallbladder and liver [158, 210-212]. In the liver, TGR5 expression is found in sinusoidal epithelial cells, Kupffer cells and cholangiocytes [213-215]. In different tissues, activation of TGR5 leads to downstream adenylate cyclase stimulation and increases intracellular cAMP production subsequently activating protein kinase A and further downstream signaling activation [216]. Together with FXR, TGR5 is involved in the maintenance of BA homeostasis. In this regard, *Tgr5* knockout mice (*Tgr5*$^{-/-}$) have lower total BA pool concentration (in a liver, gallbladder and small intestine homogenate) compared to wild-type mice [216, 217]. Importantly, localized in the apical membrane and at the primary cilium of cholangiocytes, TGR5 functions as a sensor of bile composition and stimulates the generation of the

so-called “bicarbonate biliary umbrella”, which is crucial to avoid BA-induced toxicity [13]. TGR5 regulates the CFTR channel, increasing Cl^- secretion and further bicarbonate secretion into bile [13, 212]. Besides these functions, TGR5 is very important in metabolic disorders. TGR5 regulates glucose homeostasis and insulin-sensitivity, by modulating glucagon-like peptide-1 (GLP-1) release in the gut [218]. Studies using *Tgr5*$^{-/-}$ mice and TGR5 activation mechanisms pointed TGR5 as an important negative regulator in obesity, as TGR5 increases the energy expenditure and oxygen consumption in muscle and brown adipose tissue by a cAMP-dependent generation of active thyroid hormone (T3) [217, 219].

2.I.4.2.1 *TGR5 and cancer*

TGR5 expression and activity are altered in different cancers. In particular, increased TGR5 expression has been associated with pro-tumorigenic effects in gastrointestinal cancers, favouring cell proliferation and survival by regulating downstream targets such as EGFR, ERK1/2 or cyclin D1 [220]. However, regarding CCA, although TGR5 has been postulated to have pro-tumoral effects [221-223] no clear information is available yet. In this regard, TGR5 has been suggested to protect cholangiocytes against apoptosis as BAs known to be TGR5 ligands were described to protect cholangiocytes from induced-cell injury [221, 224, 225].

2.I.4.2.2 *TGR5 agonists*

Similar to FXR, TGR5 is considered a promising target for therapy in several diseases such as NASH, hypercholesterolaemia, hyperglyceridaemia and type 2 diabetes mellitus [158]. TGR5 activation by BAs is given as follows, in a decreasing order of potency: LCA, DCA, CDCA and CA. Of note, taurine-conjugated BAs activate TGR5 more effectively compared to unconjugated BAs [180, 211]. Regarding synthesized BA analogues for TGR5 activation, INT-777 (6α-ethyl-23(S)-methyl-3α,7α,12α-trihydroxyl-5β-cholan-24-oic acid or 6-EMCA) [226] and the dual FXR-TGR5 agonist INT-767 [206] are found.

INT-777 (Figure 2.I.5) is a synthetic BA derivative that with high affinity and selectivity activates TGR5. In different animal models, INT-777 has been reported to control glucose homeostasis, hamper atherosclerosis by

macrophage regulation, prevent diabetic kidney disease and control weight gain as well as adiposity modulating cAMP and energy expenditure [227-229].

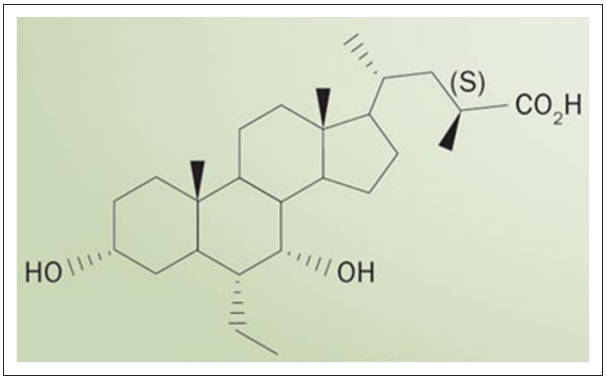

Figure 2.I.5. Molecular structure of INT-777. INT-777 (6-EMCA) is synthetized by Intercept Pharmaceuticals (Adapted from Schaap *et al.*,2013).

2 - Hypothesis and Objectives

The present study aimed to elucidate the role of FXR and TGR5 activation in CCA progression, using the specific agonists OCA and INT-777. We propose the following objectives:

I. Analysis of *FXR* and *TGR5* expression in CCA tissues of two independent cohorts of patients and elucidation of their association with tumor clinicopathology.
II. Evaluation of the expression of *FXR* and *TGR5* in normal and tumor human cholangiocytes in culture.
III. Determination of the effect of FXR and TGR5 agonists on CCA tumor growth in an orthotopic mouse model.
IV. Determination of the differential effects of FXR or TGR5 activation in CCA cell growth in culture.

2 - Materials and Methods

2.M.1 *Human liver biopsies*

CCA and surrounding non-tumoral human tissues of two independent cohorts of patients [Copenhagen (Denmark) and San Sebastian (Spain)] were studied. On the one hand, in collaboration with the group of Dr Jesper Andersen (Copenhagen), whole transcriptome profiling was performed in samples of a cohort of patients analyzed in Copenhagen (named as Copenhagen cohort), which included 104 CCA surgical specimens (68 intrahepatic and 36 perihilar CCAs) and 60 surrounding normal tissue samples, by using *humanRef-8v2 BeadChips* (Illumina) as previously described (GEO: GSE26566) [230].

Additionally, both *FXR* and *TGR5* mRNA expression was determined by qPCR in CCA human biopsies and surrounding normal human liver tissues obtained from the Basque Biobank of the Donostia University Hospital (named as San Sebastian cohort). The clinical information of the patients included in the analysis of *FXR* or *TGR5* expression is stated in Table 2.M.1.

Research protocols were approved by the *Clinical Research Ethics Committees* of supporting institutions, and all patients signed written consents for the use of their samples for biomedical research.

Table 2.M.1. Clinical information of the San Sebastian cohort of patients for *FXR* and *TGR5* expression analysis.

	Gender	Age		Disease	
		Average	Standard Deviation	iCCA	eCCA
FXR	Male Female	68,90 67,75	9,09 15,84	7 3	3 1
TGR5	Male Female	62,00 64,86	9,23 14,19	7 4	1 3

Abbreviations: iCCA, intrahepatic CCA; eCCA, extrahepatic CCA

2.M.2 *Cell culture*

Normal human cholangiocytes (i.e. NHC) and two CCA cell lines (i.e. EGI1 and TFK1) were used in the present study. Cells and culture conditions are described in general materials and methods section (see above).

2.M.3 *Cell treatments*

In vivo and *in vitro* assays were performed using specific FXR and TGR5 agonists produced by Intercept Pharmaceuticals. FXR and TGR5 agonists consist on obeticholic acid (OCA) and INT-777, respectively.

2.M.4 G*ene expression (mRNA)*

Gene expression was determined by qPCR from RNA isolated and retrotranscribed as described in general materials and methods section (see above). The primers used in the present study are grouped in Table 2.M.2.

Table 2.M.2. Primers used for RT-PCR of human mRNAs.

Primer	Sequences	
FXR	*Forward*	5'-ACAGAACAAGTGGCAGGTC-3'
	Reverse	5'-CTGAAGAAACCTTTACACCCCTC-3'
TGR5	*Forward*	5'-TTGGTCCACTTGTGCTCTTC-3'
	Reverse	5'-GCTGGTGTGTAGTGGTCTTC-3'
Ki67	*Forward*	5'-CCACGCAAACTCTCCTTGTA-3'
	Reverse	5'-TTGTCAACTGCGGTTGCTCC-3'
PCNA	*Forward*	5'-ACACTAAGGGCCGAAGATAACG-3'
	Reverse	5'-ACAGCATCTCCAATATGGCTGA-3'
Cyclin D1	*Forward*	5'-GCTGCGAAGTGGAAACCATC-3'
	Reverse	5'-CCTCCTTCTGCACACATTTGAA-3'
Cyclin D3	*Forward*	5'-TACCCGCCATCCATGATCG-3'
	Reverse	5'-AGGCAGTCCACTTCAGTGC-3'
Cdc25a	*Forward*	5'-CTGCCTGCACTCTCATGGAC-3'
	Reverse	5'-CTGTCCAGAGGCTTGCCATG-3'
GAPDH	*Forward*	5'-CCAAGGTCATCCATGACAAC-3'
	Reverse	5'-TGTCATACCAGGAAATGAGC-3'

2.M.5 *Liver orthotopic CCA model in vivo*

An orthotopic model of human CCA was generated in immunodeficient CD1 nude mice (Crl:CD1-*Foxn1*^{nu}, strain 086, homozygous) obtained from Charles River. In order to determine the effects of FXR or TGR5 activation on CCA progression, mice were fed with either a control chow diet or a chow diet supplemented with the FXR agonist OCA or the TGR5 agonist INT-777 (0,03%; both from Intercept Pharmaceuticals). Briefly, CCA human cells (i.e. EGI1) were subcutaneously injected (5x10^5 cells) in nude mice to generate CCA tumors. Seven weeks later, CCA tumors were resected and dissected into ~2-3 mm pieces, which were afterwards implanted in the liver of new immunodeficient mice. The CCA tumor volume in liver was determined and monitored overtime at the Molecular Imaging Unit of CIC biomaGUNE (San Sebastian, Spain) using a 7 Tesla Bruker Biospec 70/30 magnetic resonance imaging (MRI) system acquiring respiration synchronized T2 weighted images of the abdomen covering the whole liver. The volume was calculated from manual segmentation of the MRI images using the ImageJ 1.47 software. First, the tumor volume was measured by MRI one week after the orthotopic implantation of CCAs. Then, mice were homogeneously distributed into three different groups according to the initial tumor volume for the administration of control, OCA or INT-777 diet for 2 months. Subsequently, new MRI studies were performed 1 and 2 months after the beginning of diet administration. Animal experimental protocols were approved by the *Animal Experimentation Ethics Committee* of Biodonostia Health Research Institute and CIC biomaGUNE. Mice were weighted weekly.

2.M.5.1 *Mice sacrifice*

Mice were anesthetized and livers were extracted. Tumor samples were collected and some tissue was frozen for RNA isolation and other tissue was paraffin-embebed for immunohistochemistry.

2.M.6 *Immunohistochemistry*

Ki67 and PCNA staining were performed on formalin-fixed paraffin-embedded mouse liver tissue sections. Briefly, sections were deparaffined in xylene and hydrated using decreasing percentages of ethanol solutions. Thereafter,

endogenous peroxidase was blocked in 3.5% H_2O_2 in methanol for 15 min. Antigen-retrieval was performed with citrate buffer pH 6.0 and avidin and biotin sites were then blocked with *avidin-biotin blocking kit* (Vector laboratories). Next, slides were blocked with 20% FBS in PBS. Rabbit anti-human Ki67 (Abcam) and rabbit anti-human PCNA (Santa Cruz) antibodies were incubated overnight at 4ºC and were used at a dilution of 1:500 and 1:200 in PBS, respectively. Sections were then incubated with biotinylated swine anti-rabbit secondary antibody for 1 h and after PBS washing incubated with streptavidin biotin-peroxidase complex for 45 min (*Vectastain ABC kit*) (Vector laboratories) Positive cells were stained with *3,3-diaminobenzidine* (DAB) (Vector laboratories). Finally, sections were counterstained with hematoxylin and slides were dehydrated, mounted in DPX (Sigma) and visualized on a Nikon optical microscope (Eclipse E800).

2.M.7 *Determination of cell proliferation*

Cell proliferation was assessed by *CellTrace™ CFSE Cell Proliferation* staining, following the described protocol in general materials and methods section (see above). Cells were treated for 48 h with the FXR and TGR5 agonists in DMEM/F-12 supplemented with 3%FBS/1% P/S.

2.M.8 *Determination of cell death by flow cytometry*

Cell death was analyzed by flow cytometry using annexin V and propidium iodide staining as described in general materials and methods section (see above). Cells were treated for 48 h with the FXR and TGR5 agonists in DMEM/F-12 supplemented with 3%FBS/1% P/S.

2.M.9 *Mitochondrial function assessment by Seahorse Analyzer*

Oxygen consumption rate (OCR) was measured in an XF96 Extracellular Flux Analyzer (Seahorse Bioscience) using the *XF Cell Mito Stress Test Kit* following the manufacturer's instructions. Briefly, $8x10^3$ cells per well were seeded in a collagen-coated 96-well Seahorse microplate and cultured O/N in fully supplemented DMEM/F-12 media (Table I.2). Next, cells were pre-treated for 2 h with OCA or INT-777 (25 µM), and then cell culture medium was replaced by

Assay medium (Gibco) supplemented with glucose, L-glutamine and sodium pyruvate (Sigma) at pH = 7.4 with the corresponding BA receptor agonists (OCA or INT-777; 25 µM) or vehicle (DMSO) and cells were cultured for 1 h at 37°C without CO_2. Three initial measurements were performed in each cell culture, DMSO was injected, as this was the vehicle for the treatments, and three basal measurements were carried out. Next, mitochondrial inhibitors [i.e. 1 µM Oligomycin, 1.2 µM FCCP and 0.5 µM both Rotenone-Antimycin A (all from Sigma)] were sequentially added and three measurements were performed after the administration of each inhibitor. Metabolic parameters were calculated as indicated by Seahorse Bioscience and as described in general materials and methods section (see above).

2.M.10 *Determination of cell migration*

Cell migration was analyzed by wound-healing assays and by transwell migration chambers as stated in general materials and methods section (see above).

2.M.11 *Statistical analysis*

Results were statistically analyzed as stated in general materials and methods section (see above). For comparisons between two groups, parametric *unpaired T-test* or non-parametric *Mann-Whitney test* were used. For paired data comparisons, *paired T-test* or *Wilcoxon matched-paires signed rank test* were used. Differences were considered significant when $p<0.05$.

2 - Results

2.R.1 *Expression of FXR and TGR5 in CCA human tissue and cells*

We first tested the mRNA expression of *FXR* and *TGR5* in samples of two independent CCA patient cohorts. *FXR* and *TGR5* expression was analyzed in CCA human biopsies and surrounding normal human liver tissues by two approaches (i.e. mRNA microarray and qPCR) in both cohorts of patients (i.e. Copenhagen and San Sebastian), respectively. In agreement with previous observations, mRNA microarray analysis in samples of the Copenhagen cohort showed that *FXR* is significantly downregulated in whole tissue of 104 CCA tumor biopsies compared to 60 surrounding normal human liver tissues (Figure 2.R.1A). Notably, *FXR* expression correlated with the tumor differentiation degree; those CCAs with lower *FXR* expression presented less differentiation than those CCAs with higher *FXR* expression (Figure 2.R.1B). Similarly, *FXR* expression was also evaluated in the San Sebastian cohort of patients and qPCR data revealed that *FXR* levels are also lower in 14 CCA tissues compared to 12 surrounding non-tumoral liver tissues (Figure 2.R.1C). Besides, matched tumor/surrounding non-tumoral tissue samples showed decreased *FXR* mRNA expression in tumor tissue (n=12) (Figure 2.R.1D).

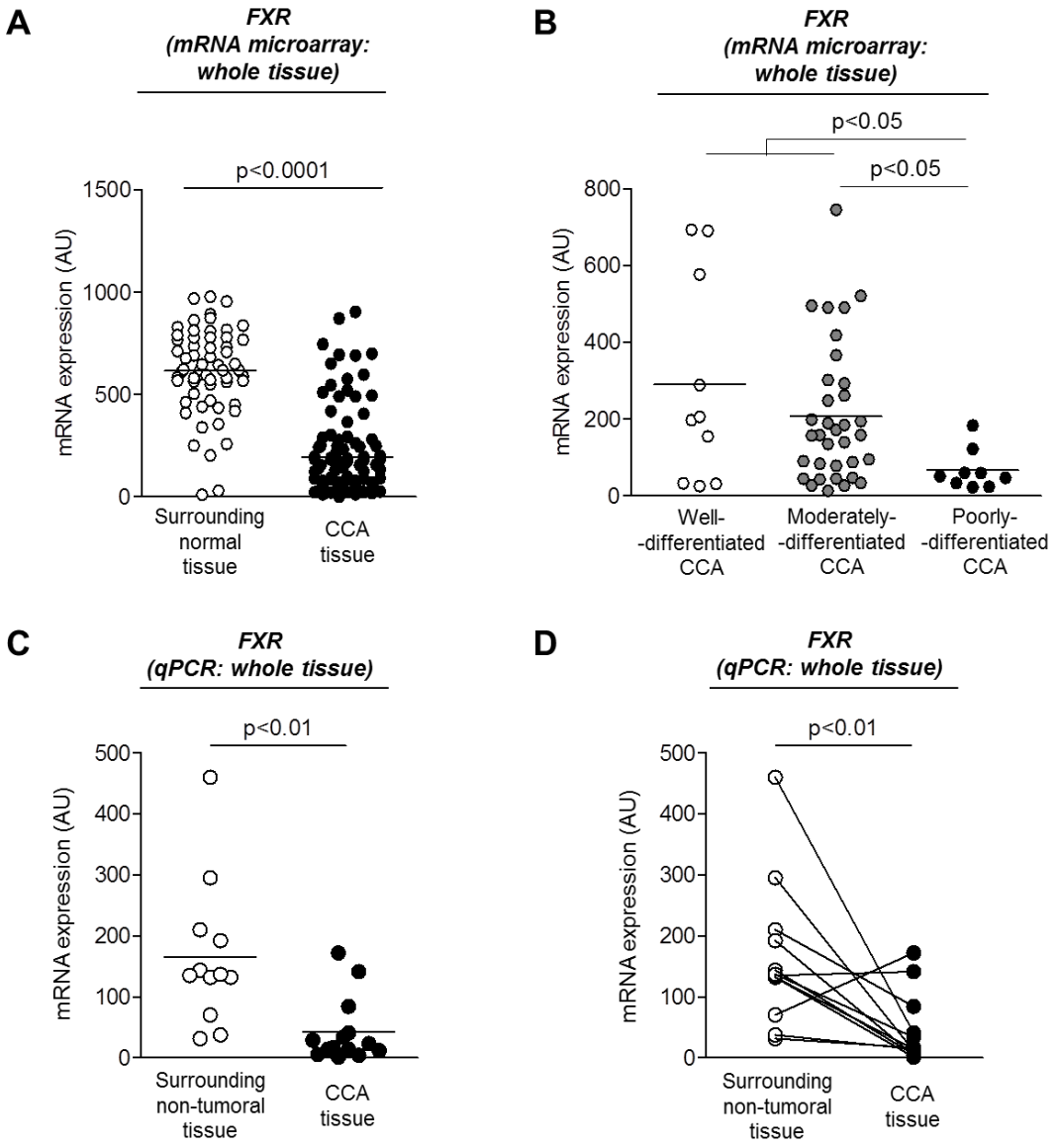

Figure 2.R.1. *FXR* expression is decreased in CCA tumors and correlates with tumor differentiation. (A) *FXR* mRNA (microarray) expression in CCA tumors (n=104) compared to surrounding normal human tissue (n=60) (Copenhagen cohort). **(B)** *FXR* mRNA (microarray) expression in CCA tumors grouped upon tumor differentiation grade: well-/moderately- (n=44) or poorly- (n=9) differentiated (Copenhagen cohort). **(C-D)** *FXR* mRNA expression (qPCR) **(C)** in CCA tumors (n=14) compared to surrounding non-tumoral human liver tissue (n=12) and **(D)** in matched-paired CCA tissue and surrounding tissue (n=12) (San Sebastian cohort).

In contrast, *TGR5* expression was found to be upregulated in 104 CCA human biopsies compared to 60 normal surrounding human liver tissues of the Copenhagen cohort (Figure 2.R.2A). *TGR5* expression was higher in perihilar (n=36) than in intrahepatic (n=68) CCAs, and in tumors with perineural invasion (n=42) compared to those without perineural invasion (n=50) (Figure 2.R.2B).

Likewise, qPCR evaluation of *TGR5* mRNA expression in the San Sebastian cohort of patients corroborated the increased *TGR5* expression in 15 CCA human tissues compared to 11 surrounding non-tumoral liver tissue (Figure 2.R.2C). Furthermore, in matched-paired samples, TGR5 expression was higher in CCA tissue than in matched-surrounding human liver tissue (n=11) (Figure 2.R.2D).

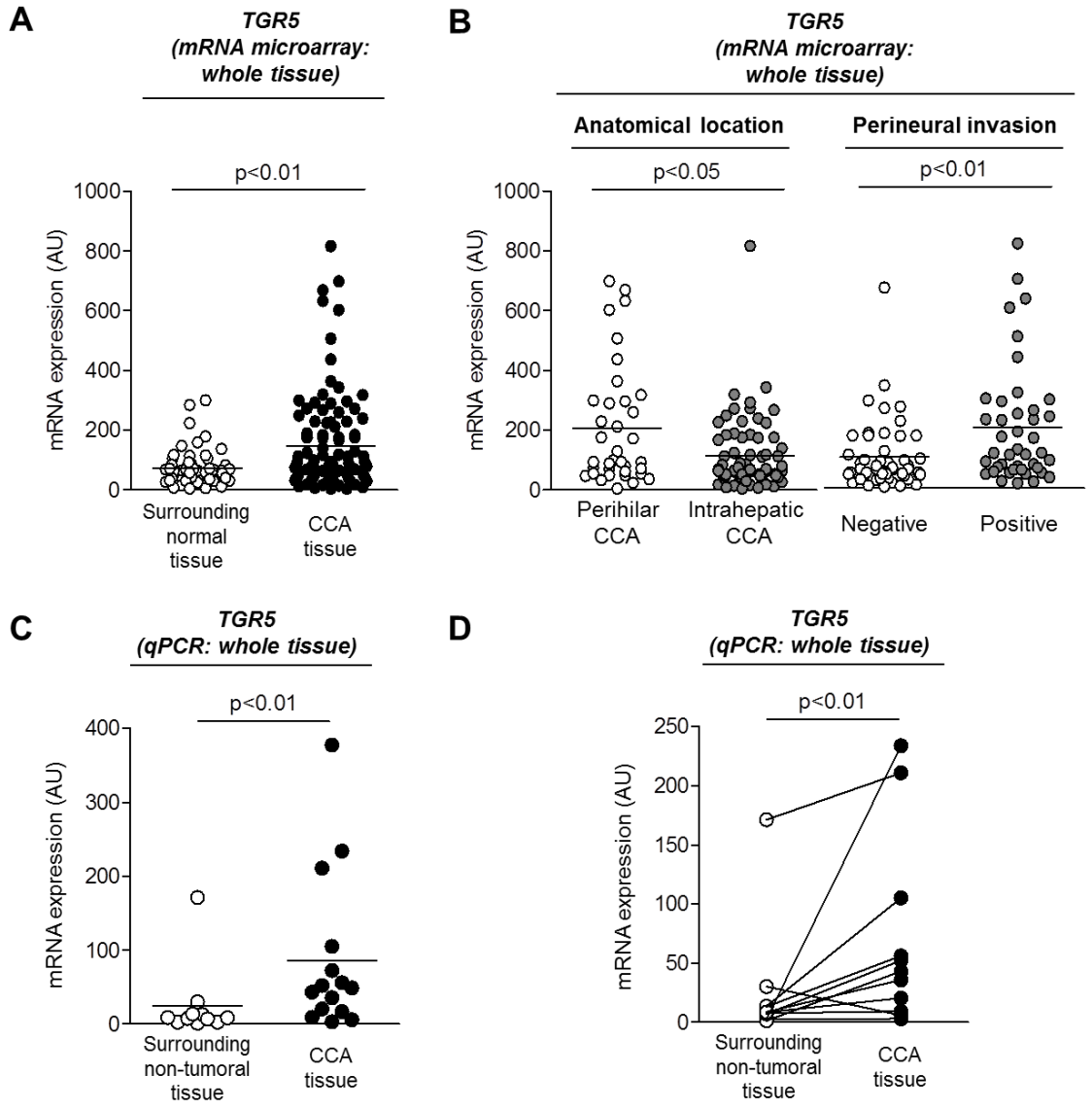

Figure 2.R.2. *TGR5* expression is increased in CCA tumors, been higher in perihilar than in intrahepatic CCAs, and correlates with perineural invasion. (A) *TGR5* mRNA (microarray) expression in CCA tumors (n=104) compared to surrounding normal human tissue (n=60) (Copenhagen cohort). **(B)** *TGR5* mRNA (microarray) expression in CCA tumors upon clinico-pathological parameters: anatomical location [perihilar (n=36) or intrahepatic (n=68)] and perineural invasion [negative (n=50) or positive (n=42)] (Copenhagen cohort). **(C-D)** *TGR5* mRNA expression (qPCR) **(C)** in CCA tumors (n=15) compared to surrounding non-tumoral

human liver tissue (n=11) and **(D)** in matched-paired CCA tissue and surrounding tissue (n=11) (San Sebastian cohort).

Next, we examined *FXR* and *TGR5* expression in CCA cell lines compared to NHCs, and cells exhibited similar *FXR* and *TGR5* expression patterns to that observed in human liver biopsies. *FXR* mRNA expression was downregulated and *TGR5* was upregulated in two human CCA cell lines (i.e. EGI1 and TFK1) compared to NHC *in vitro* (Figures 2.R.3A and B, respectively).

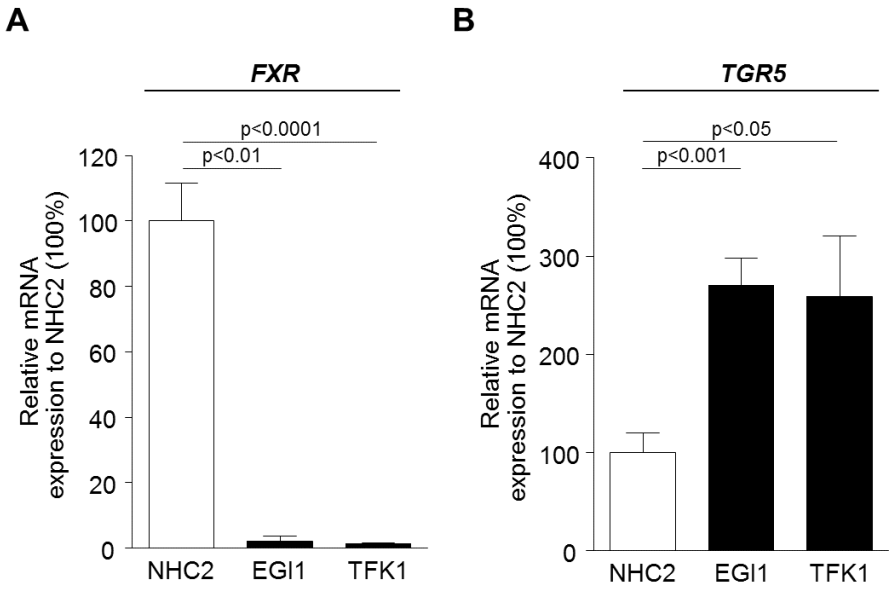

Figure 2.R.3. *FXR* expression is decreased and *TGR5* expression is increased in CCA cell lines compared to normal human cholangiocytes (NHCs). (A) *FXR* mRNA expression (qPCR) in NHCs and CCA cell lines (n=5-6). **(B)** *TGR5* mRNA expression (qPCR) in NHCs and CCA cell lines (n=4-6).

2.R.2 *Role of FXR or TGR5 activation on tumor growth in an orthotopic mouse model of human CCA*

The effect of FXR or TGR5 activation induced by OCA or INT-777, respectively, was evaluated on tumor growth in an orthotopic mouse model of CCA. Orthotopic CCA human tumors were generated by implantation of EGI1 CCA tumors in immunodeficient mice and control-, OCA- or INT-777- chow diet was administered. Tumors were monitored by MRI and they progressively grew overtime (Figure 2.R.4A). Of note, the tumor growth was lower in mice chronically treated with OCA compared to controls (Figure 2.R.4B and C).

Conversely, no differences on tumor volume were observed between mice chronically receiving INT-777 and control mice (Figure 2.R.4B and C).

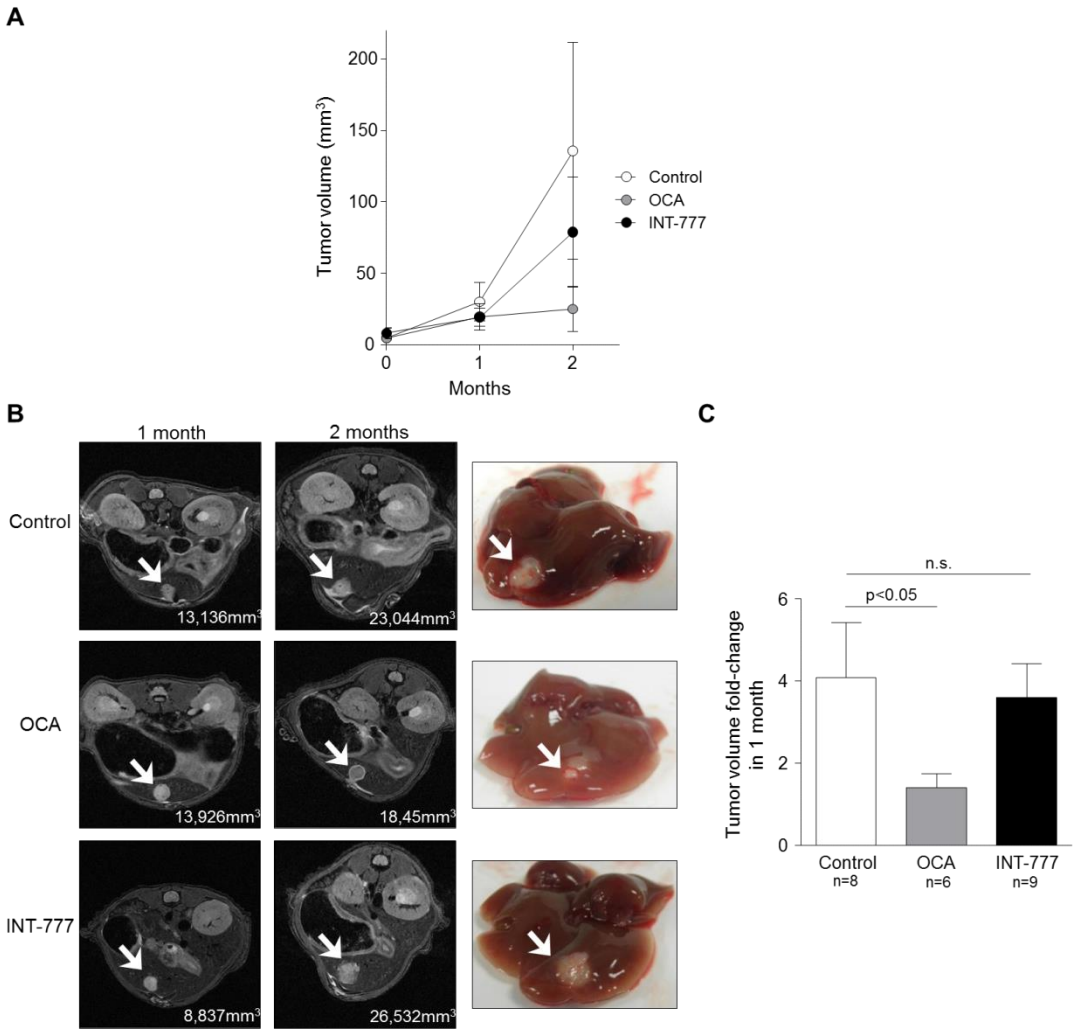

Figure 2.R.4. The FXR agonist obeticholic acid (OCA) inhibited tumor growth *in vivo.* (A) Tumor volume progression quantified by MRI during nude mice treatment with OCA, INT-777 or control diet. **(B)** Representative MRI and liver images of control mice, OCA-treated mice and INT-777-treated mice. **(C)** Bar-graph showing tumor volume fold-change in the last month of treatment quantified by MRI (Control n=8, OCA n=6 and INT-777 n=9).

To evaluate whether the FXR-dependent inhibition of CCA tumor growth *in vivo* could be related to the regulation of CCA cell proliferation, the expression of proliferation markers was analyzed in the tumors by qPCR and immunohistochemistry. In agreement with the inhibitory effect of FXR activation on tumor growth, CCA tumors from mice treated with OCA showed significantly decreased expression of the proliferation markers Ki67 and PCNA by both

strategies (Figures 2.R.5 and 6). A decreasing trend was observed in *Cdc25a*, *cyclin D1* and *cyclin D3* expression in the OCA treated group (Figure 2.R.5).

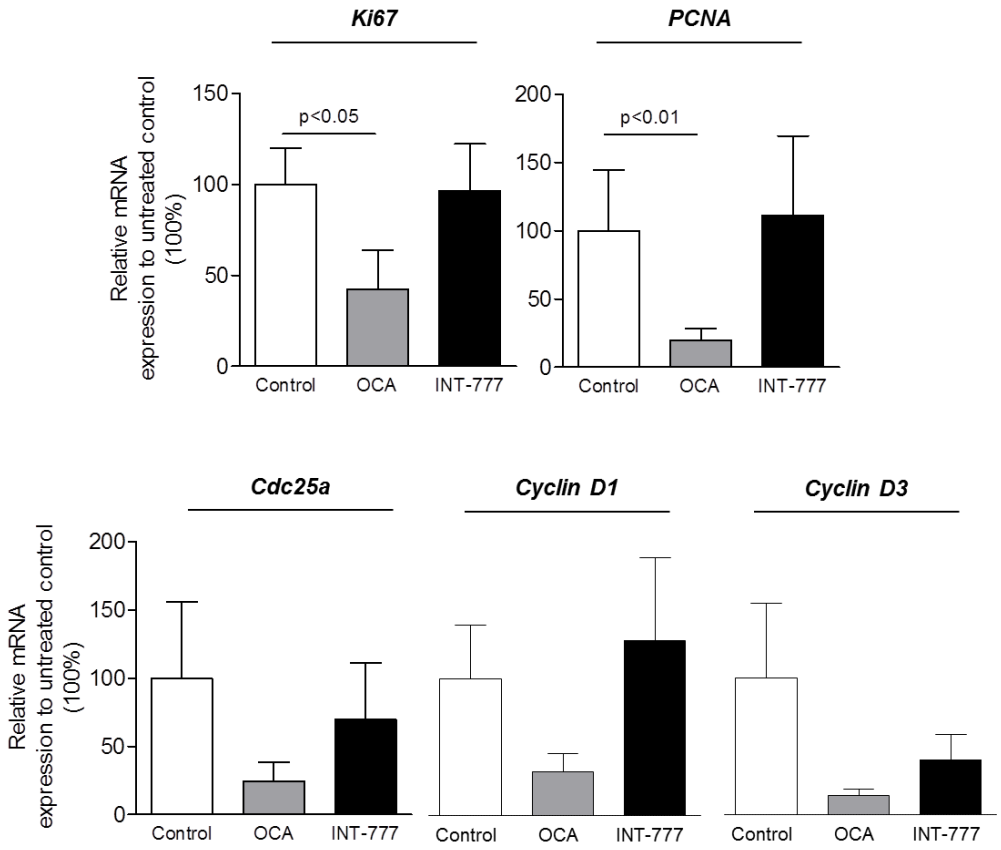

Figure 2.R.5. The FXR agonist obeticholic acid (OCA) decreased the mRNA expression of proliferation markers in CCA tumors *in vivo*. Analysis of proliferation markers (i.e. *Ki67, PCNA, Cdc25a, cyclin D1* and *cyclin D3*) within the tumors by qPCR (n=5-8).

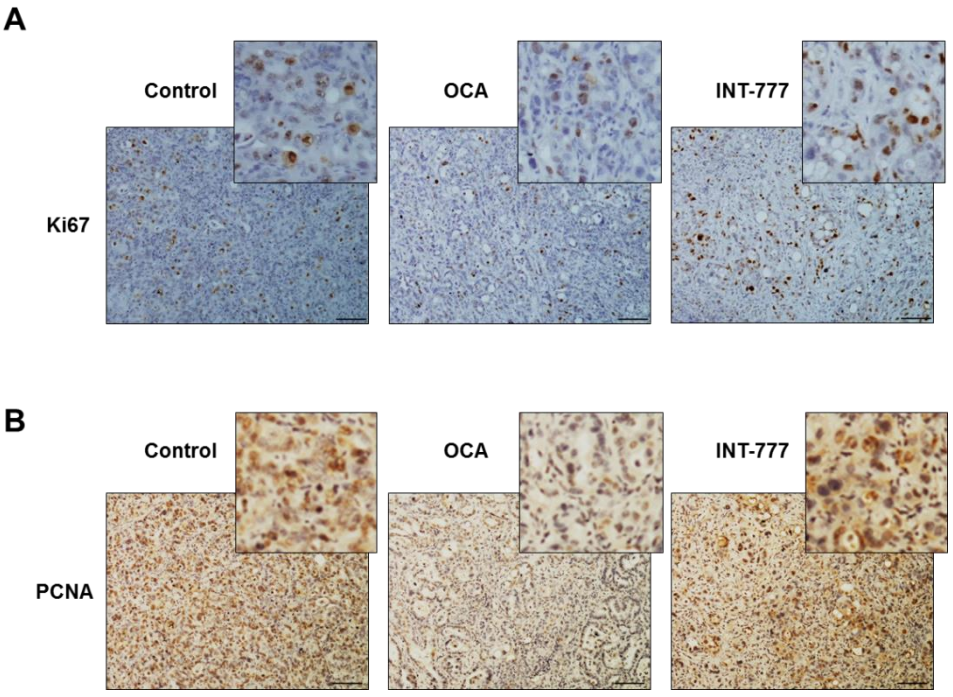

Figure 2.R.6. The FXR agonist obeticholic acid (OCA) decreased the protein expression of proliferation markers in CCA tumors *in vivo*. Immunohistochemical analysis of proliferation markers **(A)** *Ki67* and **(B)** *PCNA* within the tumors.

2.R.3 Effect of FXR activation on CCA cell proliferation, survival, migration and mitochondrial energy metabolism *in vitro*

To gain further insight on the influence of FXR or TGR5 activation on CCA cell biology, the effects of FXR or TGR5 agonists were evaluated in CCA cells and NHC *in vitro*. Our data indicate that OCA inhibits, in a dose-dependent manner (10, 25 and 50 µM), the proliferation of two different CCA cell lines (i.e. EGI1 and TFK1) compared to vehicle-treated control cells (Figure 2.R.7A). Moreover, the highest dose of OCA (i.e. 50 µM) was the only one that stimulated CCA cell (i.e. EGI1 and TFK1) apoptosis (evaluated by annexin V and propidium iodide staining) compared to control conditions (Figure 2.R.8A). In contrast, the inhibitory effect of OCA on NHC proliferation was only observed at the highest dose (50 µM) (Figure 2.R.7B), which was also associated with increased apoptosis (Figure 2.R.8B). Based on these data, further *in vitro* assays were performed with 25 µM OCA, which inhibits CCA cell proliferation but does not affect apoptosis. Under these conditions, OCA inhibited mRNA expression of different proliferation markers (i.e. *Ki67*, *PCNA*, *cyclin D1* and *cyclin D3*) in EGI1 CCA cells compared to controls (Figure 2.R.9).

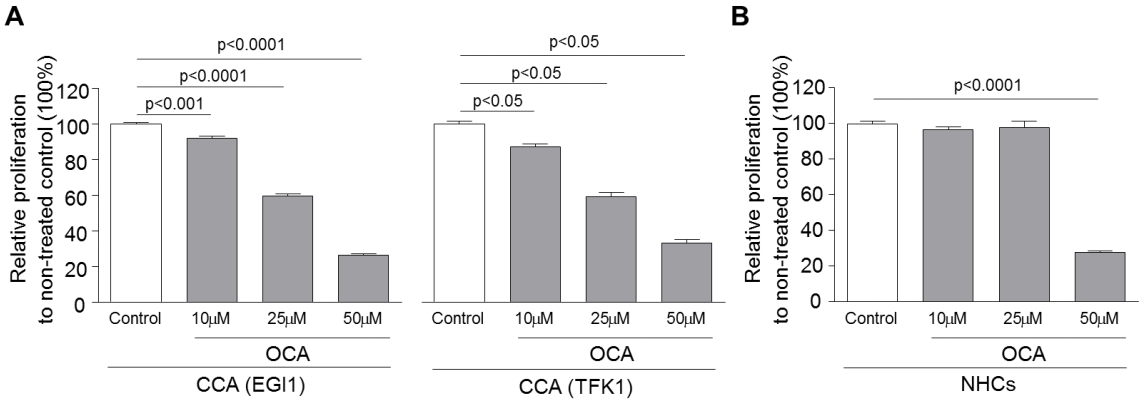

Figure 2.R.7. The FXR agonist OCA inhibits CCA cell proliferation in a dose-dependent manner. Flow cytometry-based cell proliferation (by CFSE) under increasing doses of OCA for 48 h. **(A)** Proliferation of CCA cells (i.e. EGI1 and TFK1, n=4-5) and **(B)** NHCs (n=7).

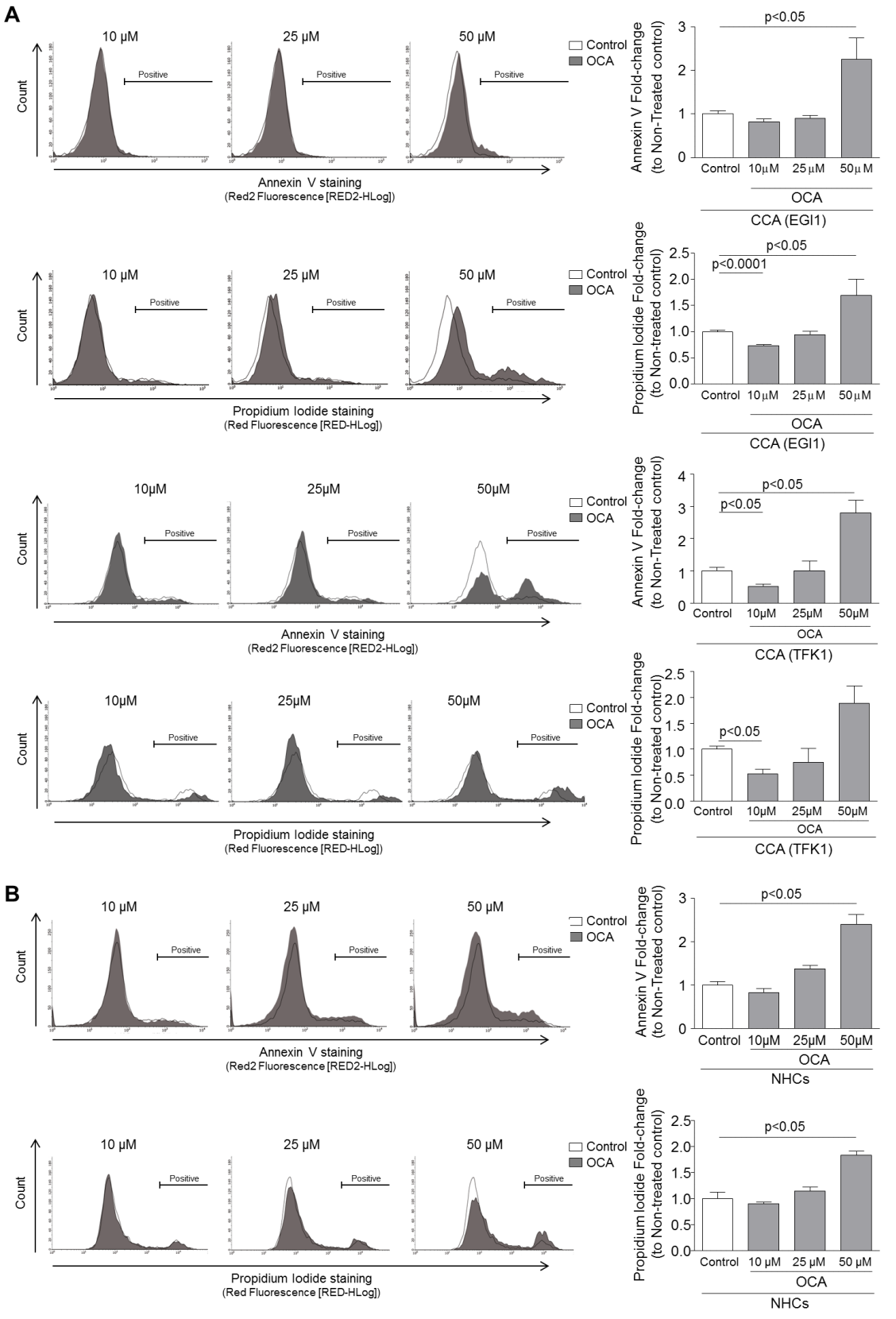

Figure 2.R.8: The FXR agonist does not induce apoptosis at low doses, but is toxic at the highest dose of 50 µM. Flow cytometry-based apoptosis assays (by Annexin V and Propidium Iodide staining) under increasing doses of OCA for 48 h. Cell death representative histograms

and corresponding quantification on **(A)** CCA cells (i.e. EGI1 and TFK1) (n=6-7 and n=3, respectively) and **(B)** NHCs (n=4).

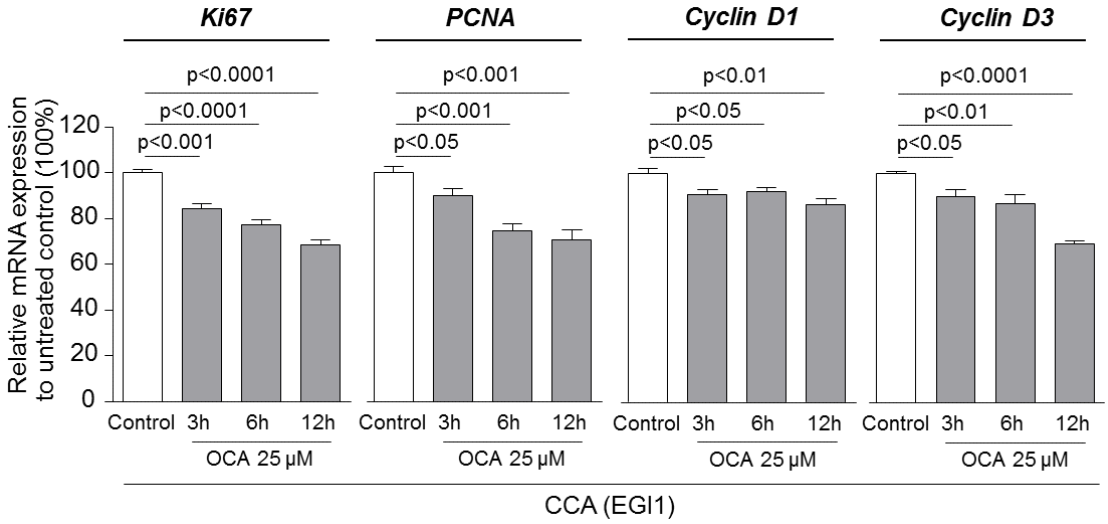

Figure 2.R.9: Inhibition of CCA cell proliferation by OCA is aasociated to decreased expression of proliferation-related genes. mRNA expression of proliferation markers (i.e. *Ki67*, *PCNA*, *cyclin D1* and *cyclin D3*) in CCA cells (i.e. EGI1) under OCA (25 µM) treatment for 3-6-12 h compared to vehicle-treated control cells (n=5-6).

Since cell migration is a characteristic event in metastatic tumors like CCA, the migratory properties of EGI1 CCA cells were analyzed in the presence or absence of OCA. OCA (25 µM) inhibited the migratory capacity of CCA cells compared to control conditions (Figure 2.R.10).

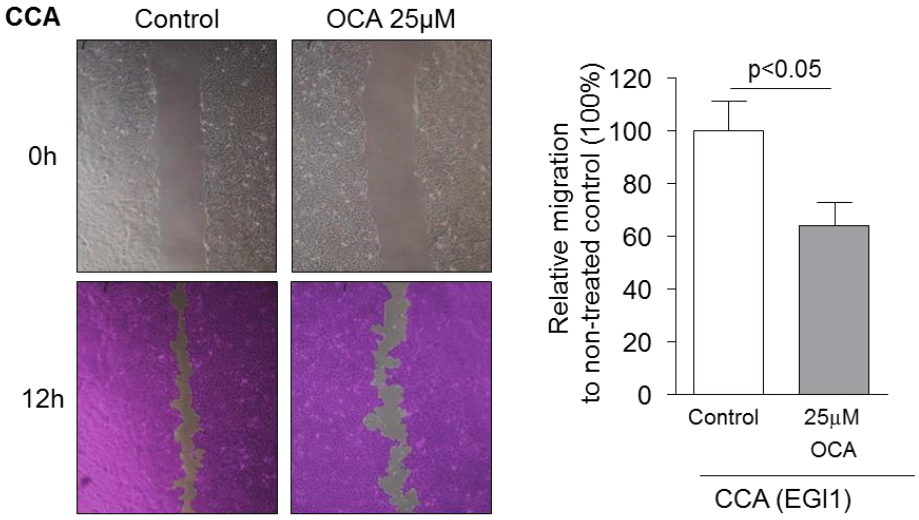

Figure 2.R.10: The FXR agonist OCA inhibits CCA cell migration. Representative microscope images and corresponding quantification of wound-healing assays at 12 h in vehicle-treated or OCA-treated (25 µM) EGI1 CCA cells (n=6).

Tumor cell features such as uncontrolled growth and invasiveness are mediated by the mitochondrial energy metabolism [231]. Accordingly, the inhibitory effect of OCA on CCA cell proliferation and migration was also associated with decreased mitochondrial energy metabolism compared to controls (Figure 2.R.11). In particular, OCA inhibited the basal, ATP-linked and maximal oxygen consumption rate (OCR) of CCA cells compared to control conditions, and increased proton-leak, suggesting increased mitochondrial stress (Figure 2.R.11B).

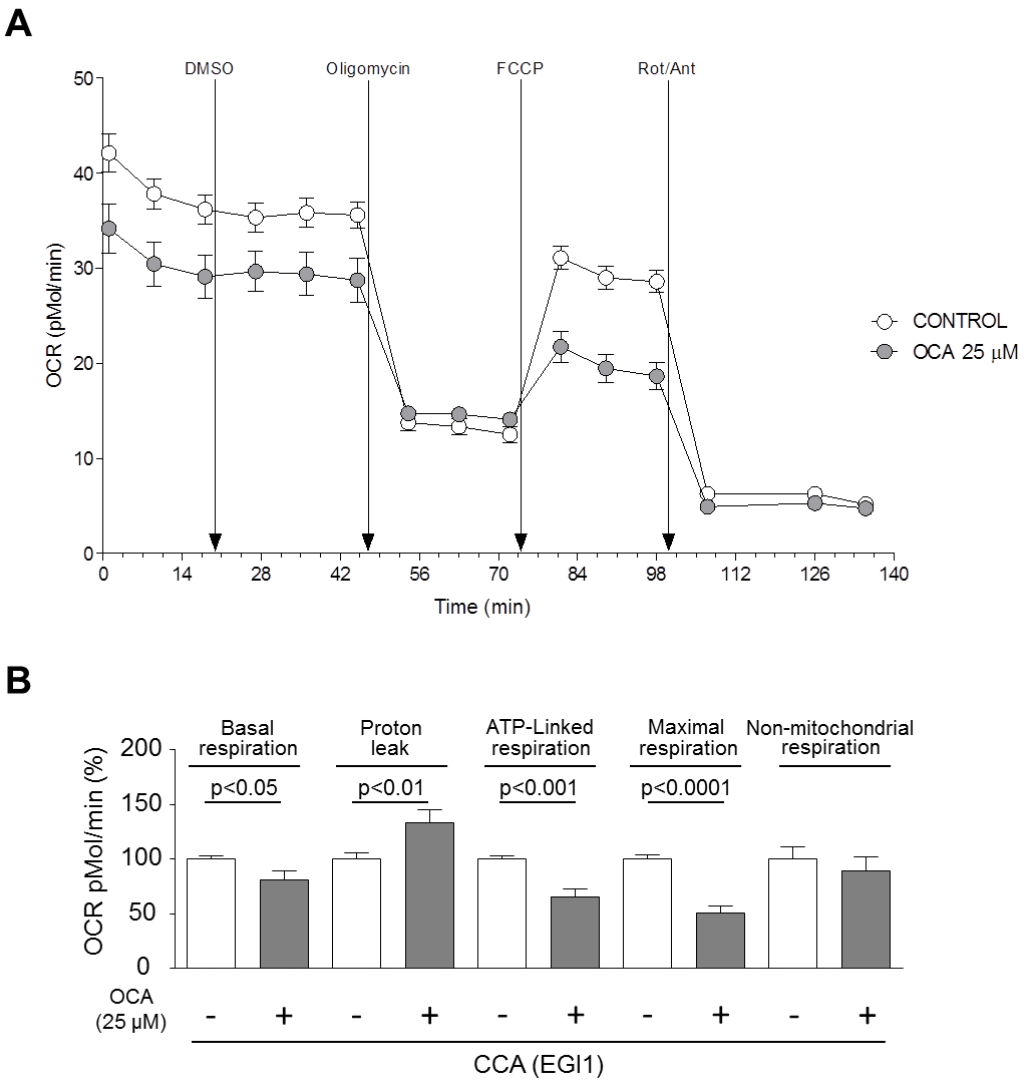

Figure 2.R.11: The FXR agonist OCA decreases mitochondrial metabolism in CCA cells. Seahorse oxygen consumption rate (OCR) using mitochondrial stress test kit in CCA cells (i.e. EGI1) vehicle-treated or treated with OCA (25 μM), with 3 h pre-treatment. **(A)** OCR profile and **(B)** bar-graph of metabolic parameters calculated upon OCR measurements (n=11-12).

2.R.4 Effect of TGR5 activation on CCA cell proliferation, migration and mitochondrial energy metabolism *in vitro*

Contrarily to FXR, it has been reported that TGR5 seems to be pro-tumorigenic and our data in *TGR5* expression and its *in vivo* activation is consistent with this idea. In this regard, our results showed that TGR5 agonists INT-777 and taurolitocholic acid (TLCA) stimulate CCA cell proliferation (Figures 2.R.12A and B) and migration (Figure 2.R.13) compared to control conditions, whereas INT-777 did not alter the proliferation of NHC (Figures 2.R.12C). The effects of TGR5 activation on CCA cell proliferation and migration were associated to a moderate increase of basal mitochondrial respiration and proton-leak compared to control conditions (Figure 2.R.14).

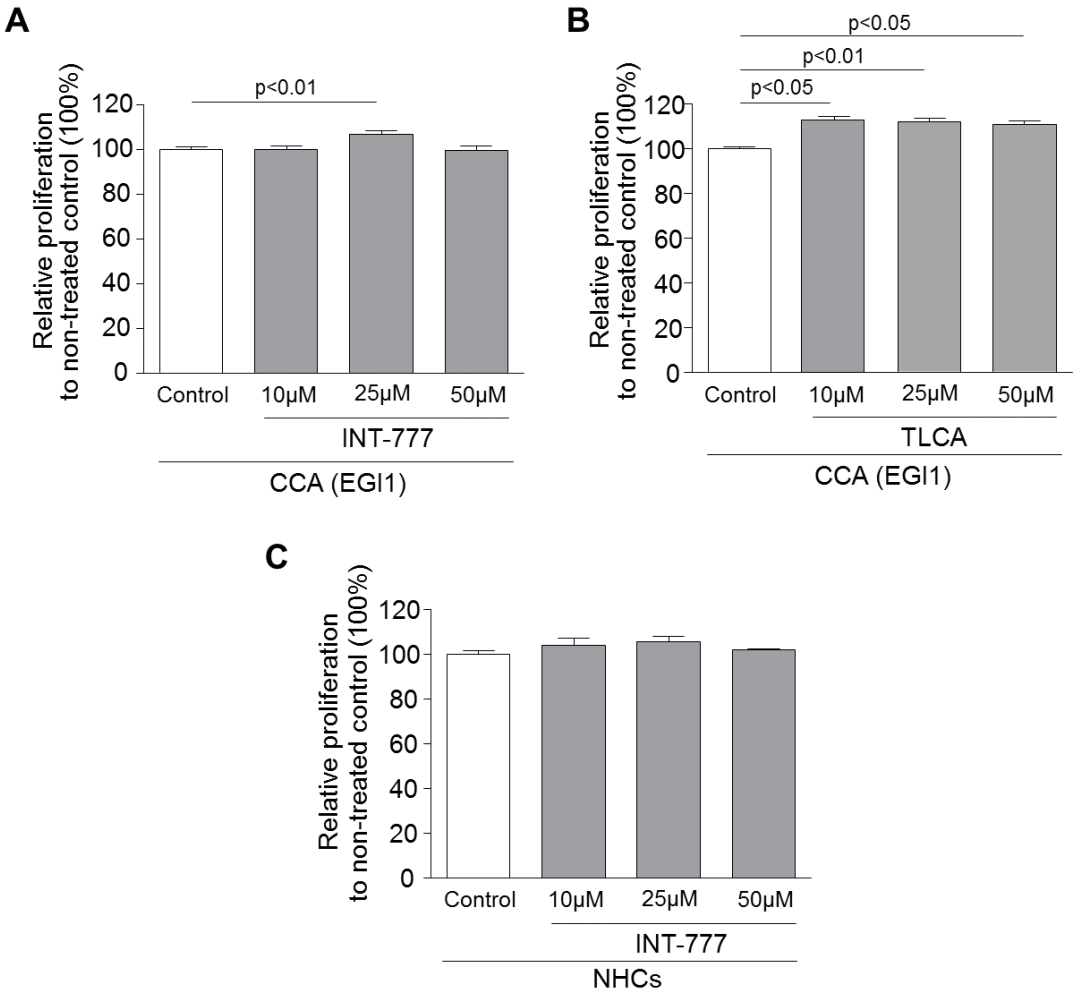

Figure 2.R.12: The TGR5 agonists slightly stimulate the proliferation of CCA cells. Flow cytometry-based cell proliferation assays (by CFSE) under increasing doses of TGR5 agonists

(i.e. INT777 or TLCA) for 48 h compared to vehicle-treated control cells. **(A-B)** CCA cells (i.e. EGI1) treated with **(A)** INT777 (n=5-6) and **(B)** TLCA (n=3-4). **(C)** NHCs (n=4-5).

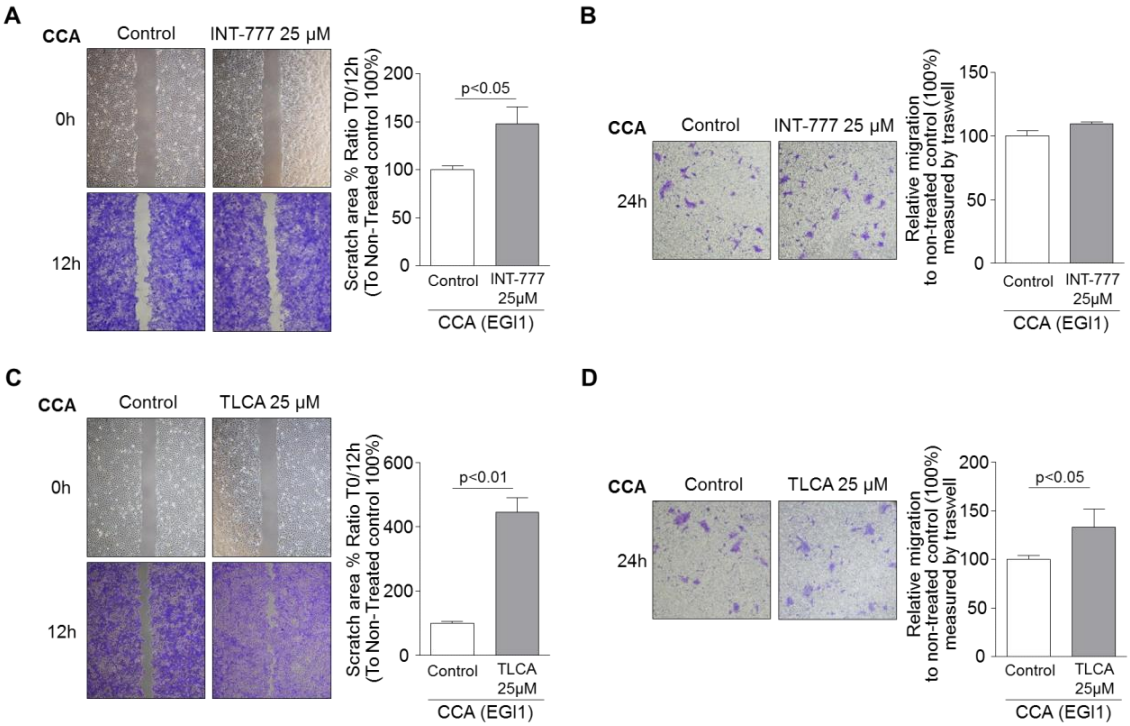

Figure 2.R.13: The TGR5 agonists stimulate the migration of CCA cells. Representative microscope images and corresponding quantification of wound-healing assays at 12 h and transwell migration chambers at 24 h in **(A-B)** OCA-treated (25 µM) (n=6-9 and 2-4, respectively) or **(C-D)** TLCA-treated (25 µM) EGI1 CCA cells compared to vehicle-treated cells (n=3 and 2-4, respectively).

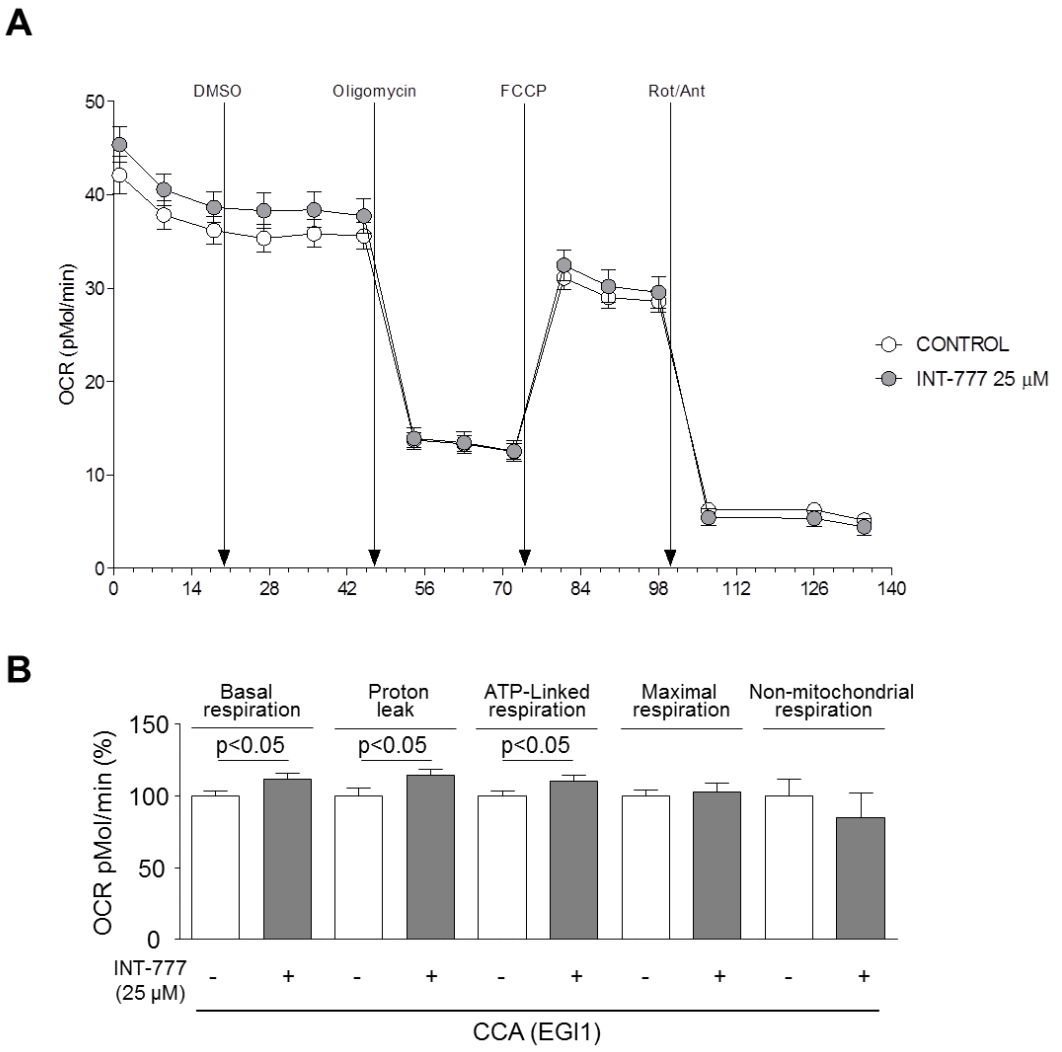

Figure 2.R.14: The TGR5 agonist INT-777 stimulates the mitochondrial metabolism of CCA cells. Seahorse oxygen consumption rate (OCR) using mitochondrial stress test kit in CCA cells (i.e. EGI1) vehicle-treated or treated with INT-777 (25 µM), with 3 h pre-treatment. **(A)** OCR profile and **(B)** Bar-graph of metabolic parameters calculated upon OCR measurements (n=11-12).

2 - Discussion

The key findings reported here are related to the role of BA receptors FXR and TGR5 in CCA progression. Our data are consistent with the notion that regulation of FXR and/or TGR5 activities in CCA tumor cells may have potential therapeutic value.

BAs are important organic molecules synthesized from cholesterol in hepatocytes, and their canaliculus secretion confers the driving force for the generation of the bile flow. In the last years, increasing number of evidence is expanding the knowledge of the role of BAs in health and disease. It is now clear that BAs are not mere detergent molecules mediating fat digestion and intestinal absorption of hydrophobic compounds (like liposoluble vitamins) after food intake, but they are also important regulators of different pathophysiological processes in the liver and extrahepatic tissues, including cell proliferation, survival, secretion, differentiation, metabolism, regeneration, fibrosis and inflammation, among others. The identification of FXR and TGR5 BA receptors has opened new and promising fields of research in physiology, pathology and pharmacology. FXR and TGR5 are differentially activated by distinct BAs and their activation mediates specific and complex responses regulating multiple pathophysiological processes. Moreover, there are four FXR isoforms, whose differential activation depends on their expression pattern and the BA pool composition [192].

The development of novel BA derivatives able to selectively target FXR or TGR5 (i.e. OCA and INT-777, respectively) has allowed to evaluate their therapeutic value for the treatment of liver diseases, including cholestatic, metabolic and cancer conditions. CCAs can arise as a consequence of prolonged cholestasis and inflammation in the liver [232, 233]. Although, novel tests have shown that BAs cannot be considered direct genotoxic agents [204], they may function as co-carcinogens by stimulating, via BA receptors, the proliferation, survival and inflammatory response of biliary epithelial cells [204]. We have confirmed in a larger number of CCA patients of two independent cohorts (Copenhagen and San Sebastian) the previously reported observations [191] indicating that *FXR* expression is lower in the tumors compared to

surrounding non-tumoral liver tissue. Interestingly, these results showed that *FXR* expression levels directly correlate with the degree of tumor differentiation. Additionally, our data indicated that *FXR* expression is lower in poorly-differentiated CCA tumors compared to moderate/well differentiated tumors. Since the tumor differentiation status has prognostic value [234], the analysis of *FXR* expression may help to characterize the CCA tumor features. On the other hand, our data indicated that, in both cohorts of patients, *TGR5* expression is enhanced in CCA tumors compared to surrounding normal liver tissue. Differences among subtypes were found as *TGR5* expression was higher in perihilar than in intrahepatic CCAs. Importantly, *TGR5* expression in CCA tumors correlated with their perineural invasion, which has important implications regarding the evolution of this cancer. Similarly, the expression of *FXR* and *TGR5* showed the same pattern in human CCA cells compared to normal human cholangiocytes *in vitro*. Therefore, the clinicopathological correlations for *FXR* and *TGR5* expression reported here may be helpful to better characterize human CCA tumors and may have potential prognostic value.

Next, we evaluated the effect of chronic activation of FXR or TGR5 on the tumor growth of an orthotopic mouse model of human CCA using the selective BA derivatives OCA and INT-777, respectively. Our results showed that chronic administration of OCA halts CCA tumor growth *in vivo* measured by MRI and inhibits the expression of pro-mitotic markers Ki67 and PCNA compared to controls. These results were expanded *in vitro* showing that OCA inhibits CCA cell proliferation in a dose-dependent manner compared to control conditions. Notably, NHCs were less sensitive to the effect of OCA and only the highest tested dose could inhibit cell proliferation *in vitro*. OCA also inhibited the migratory properties of CCA cells. These inhibitory effects of OCA on the proliferation and migration of CCA cells were associated with decreased mitochondrial energy metabolism. Conversely, although TGR5 activation by INT-777 did not modify CCA tumor growth *in vivo*, it stimulated proliferation and migration *in vitro*, which was associated with increased mitochondrial energy metabolism. These results indicate that the regulation of FXR and/or TGR5 activities may have important therapeutic value for CCA and suggest the potential use of OCA for the treatment of CCA patients. Moreover, the

development of selective TGR5 inhibitors will be of high importance to evaluate the potential therapeutic regulatory value of TGR5 activity in diseases like CCA.

OCA has recently been approved for the treatment of patients with PBC and is under study for diseases such as NASH, PSC and biliary atresia [207, 235]. Up to now, the beneficial effects of OCA have been related to its anti-cholestatic, anti-inflammatory and anti-fibrotic properties. Here, we have reported the therapeutic value of OCA in CCA by inhibiting orthotopic tumor growth in immunodeficient mice as well as proliferation, migration and mitochondrial energy metabolism of CCA tumor cells *in vitro*. These data are consistent with previous reports showing the inhibitory effect of the synthetic non-steroidal isoxazole-based FXR agonists GW4064 on the subcutaneous growth of CCA cells in nude mice [236]. Since FXR activation has been described to promote chemosensation [237], the effect of OCA together with chemotherapy should be evaluated in the near future. Based on our data, inhibition of TGR5 activity might also have therapeutic value for CCA. Previous studies have reported that TGR5 activation stimulates adenylate-cyclase and therefore increases cAMP generation, which subsequently activates protein kinase A (PKA) and cholangiocyte proliferation via EGFR/ERK [238]. In addition, TGR5 activation was reported to specifically stimulate the proliferation of non-ciliated cholangiocytes [239] as well as the survival to apoptosis in normal cholangiocytes [238]. CCA human cells are characterized by a shorter or even absent primary cilia compared to NHCs, thus, the pro-tumoral effects of TGR5 activation in CCA cells could be related to ciliary abnormalities in CCA cells. Our data indicating the pro-metastatic features of TGR5 activation in CCA cells are consistent with the fact that conjugated BAs such as taurocholate are known to increase CCA invasiveness [185] and INT-777 was reported to stimulate gastric cancer cell migration [240]. TGR5 has also been suggested to play a role in inflammation. Activation of TGR5 in hepatic Kupffer cells reduces LPS-induced pro-inflammatory cytokine production [214]. Based on these data and the fact that TGR5 activation in mice promotes protective mechanisms in biliary epithelial cells (as it contributes to the maintenance of the so-called ‘bicarbonate umbrella’) and reduces hepatic and systemic inflammation [241], TGR5 agonists were suggested for the treatment of PSC patients [241]. However, PSC is a well-known risk factor of CCA and 10-15 % of PSC patients

develop CCA [242]. As per our data TGR5 activation shows pro-tumorigenic properties in CCA progression and dissemination, the potential treatment of PSC patients with TGR5 agonists needs further investigation.

2 - Conclusions

The key findings reported here provide novel insights into the potential therapeutic value of regulating FXR and/or TGR5 activities in CCA. Our data indicate that:

I. FXR is downregulated in human CCA tissue compared to normal surrounding liver tissue as well as in CCA cells compared to normal human cholangiocytes. FXR expression correlated with tumor differentiation.

II. TGR5 is upregulated in human CCA tissue compared to normal surrounding liver tissue as well as in CCA cells compared to normal human cholangiocytes. TGR5 expression correlated with perineural invasion and the expression is higher in perihilar than in intrahepatic CCAs.

III. In mice with orthotopic implants of human CCA tumors, chronic administration of OCA inhibited the tumor growth compared to untreated control animals; this was accompanied by decreased expression of proliferation markers within the tumors. In contrast, chronic administration of INT-777 *in vivo* showed no effects on CCA tumor growth.

IV. *In vitro*, OCA inhibited CCA cell proliferation and migration, associated with decreased mitochondrial energetic metabolism, and did not affect apoptosis. In contrast, INT-777 stimulated proliferation and migration of CCA cells, associated with increased mitochondrial energetic metabolism.

Our data are consistent with the notion that FXR and TGR5 represent potential targets for therapy.

V. CHAPTER 3

ROLE OF KRÜPPEL-LIKE FACTOR 5 IN CHOLANGIOCARCINOMA

3 - Introduction

3.I.1 *Cholangiocarcinoma (CCA)*

Cholangiocarcinoma (CCA) is genomicaly heterogeneous and numerous genetic and epigenetic alterations have been described [45, 77]. Alterations in important regulatory genes involved in DNA repair mechanisms [78-80], cell proliferation pathways [43] or cholangiocyte differentiation [45], among others, are prevalent in CCA. Moreover, transcription factors (TFs) upstream of these important sets of genes are altered in CCA, contributing to the tumorigenic process [77]. A recent study has provided a number of TFs aberrantly expressed in CCA tissues by computational identification using the Gene Expression Omnibus (GEO) database [77].

3.I.2 *Transcription factors (TFs)*

Cancer is characterized by dysregulation of gene transcription. These alterations affect upstream signals and/or TFs [243]. In the last decades, the hallmarks of cancer have been well-established [244] and technological advances have permitted the better understanding of the function of TFs on these processes as well as their downstream targets and effectors [243] (Figure 3.I.1). Targeting of TFs involved in cancer development and progression may have potential therapeutic value [243] and, among them, the Krüppel-like factor (KLF) family seems to play an important role in different cancers.

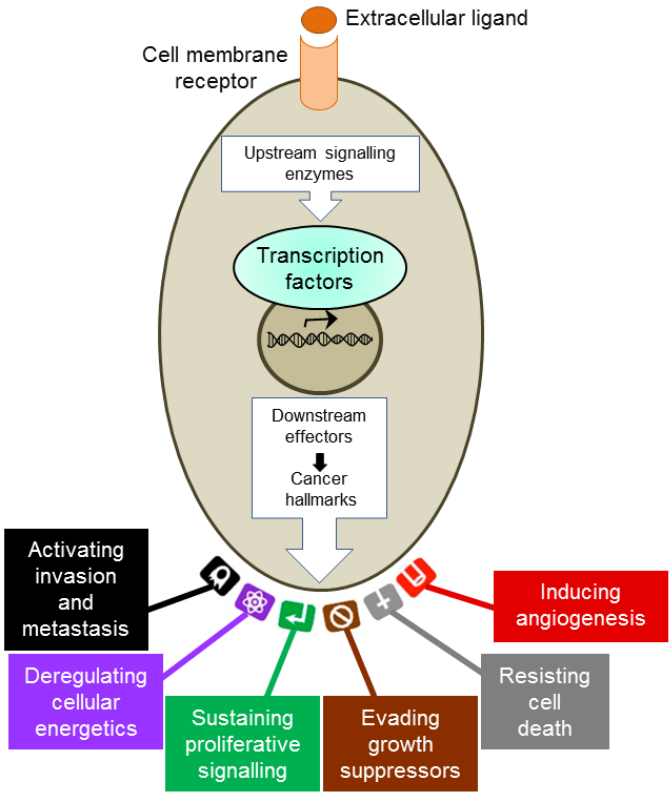

Figure 3.I.1. Transcription factors in cancer. Different cancer hallmarks may be regulated by TFs (Adapted from Johnston and Carroll, 2015).

3.I.3 *Krüppel-Like Factors (KLFs)*

3.I.3.1 *KLF family*

The first member of the actually termed Krüppel-like factor (KLF) family was described for the first time in 1993 [245]. *EKLF* (erythroid Krüppel-like factor; *KLF1*) was discovered as the mammalian homologue of the *Drosophila melanogaster* gene named *Krüppel* [245]. Up to now, 17 different KLF members have been described (Figure 3.I.2A), which consist in zinc finger-containing TFs. In particular, each KLF is formed by three C_2H_2 zinc-fingers in the carboxyl-terminal end of the proteins, a highly conserved region for DNA-binding of KLFs [246]. In contrast, the amino-terminal region is different along the KLF family members. These variations result in differential binding to co-activators, co-repressors and modifiers (i.e. histone acetyltransferases) [246]. KLFs are usually grouped upon the structural organization into groups with similar functionalities (Figure 3.I.2B). KLFs are also modified by post-

translational modifications (i.e. acetylation, phosphorylation, ubiquitination and sumoylation), modulating their transcriptional activity [246].

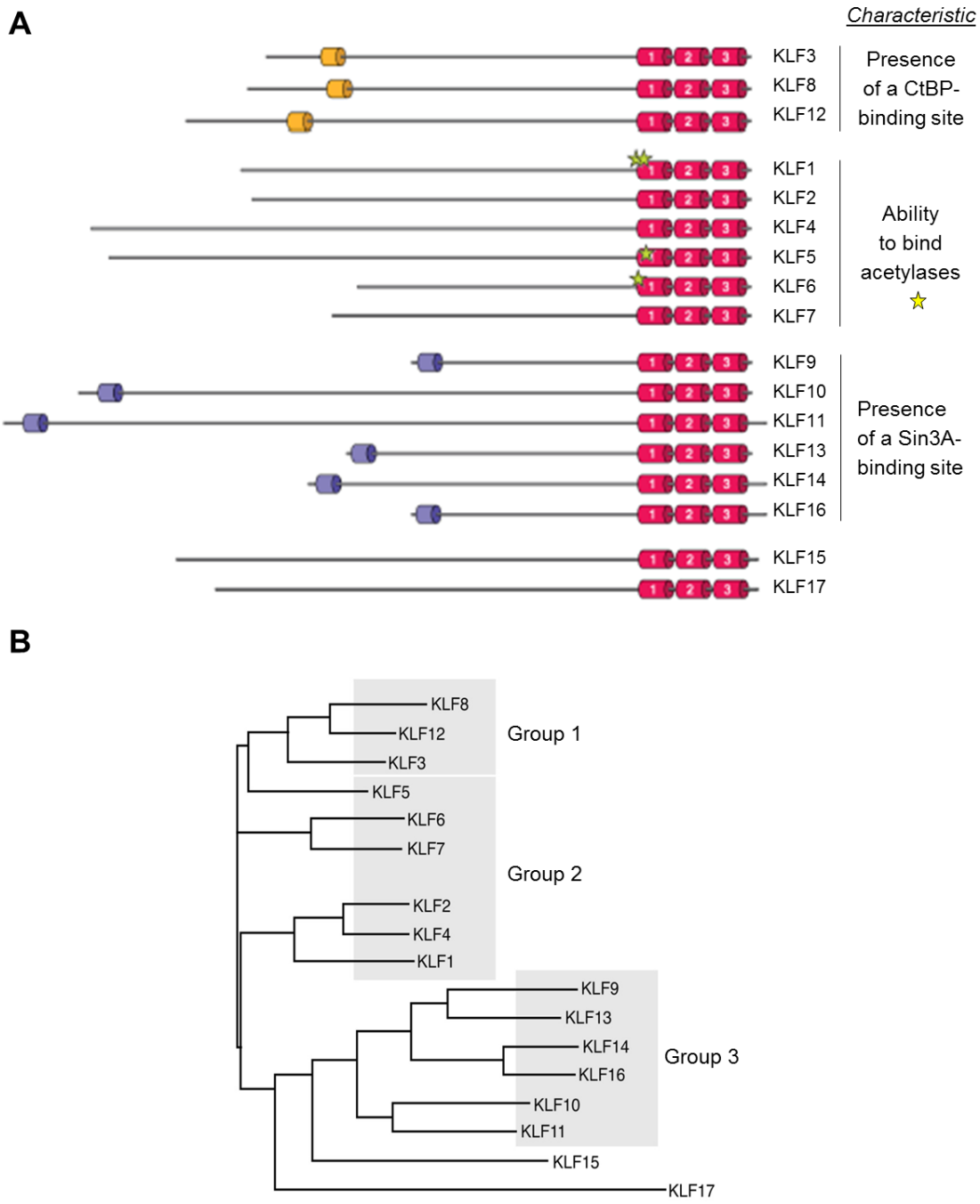

Figure 3.I.2. Human Krüppel-like factors (KLFs): structure and features. (A) KLFs grouped upon common structural and functional domains. High similarities are observed in the carboxyl-terminal DNA-binding regions, formed by three C_2H_2 zinc-finger motifs. **(B)** Phylogenetic representation of KLFs, performed by ClustalW tool-based multiple sequence alignment and phylogenetic analysis, grouping KLFs based on functional similarities (Adapted from McConnell and Yang, 2010).

Some KLFs are ubiquitously expressed, whereas others are tissue-specific [247]. Moreover, the expression of certain KLFs varies during developmental stages and diseases [247].

3.I.3.2 *Functions of KLFs*

KLFs regulate many normal biological processes. For instance, KLF4 inhibits the growth of damaged cells by inducing cell cycle arrest [248, 249], whereas KLF8 promotes cell cycle progression [250]. Cell differentiation and tissue homeostasis maintenance are also mediated by KLFs. As an example, KLF1 acts during erythropoiesis regulating the maturation of erythroid cells and simultaneously, a sumoylated form of KLF1 regulates megakaryopoiesis [251]. Differentiation in many other tissues (i.e. intestinal epithelium, adipocytes or cardiomyocytes) is also mediated by KLFs [246]. Importantly, KLFs are involved in almost any of the physiological processes of human biology and therefore, dysregulation of KLFs results in the development of diseases. Among the organs, KLFs are also involved in the homeostasis of the digestive system. In the liver, the initial activation of hepatic stellate cells (HSCs) upon liver injury induces KLF6 expression leading to fibrogenesis and extracellular matrix formation [252] by activating *collagen α1(I)* and *TGF-β* gene promoters [253].

3.I.3.3 *KLFs and cancer*

KLFs are dysregulated in cancer. The expression and/or function of certain KLFs vary depending on the cancer type or even also in the cancer stage [247]. Moreover, functional changes in KLFs are mediated by different mechanisms: *i*) under 'molecular switches', by changes in p53, p21 or SIN3a [247]; *ii*) by alternative splicing [254]; or *iii*) by post-translational modifications, which can regulate protein stability, determine protein localization or can also change KLFs function [247].

Cell proliferation is crucial for tumoral progression and some KLFs are able to regulate this process at different levels. Cell cycle regulators such as cyclins, cyclin-dependent kinases (CDKs) and CDK inhibitors are targeted by KLFs. (Figure 3.I.3) [247]. Moreover, proliferation signaling pathways, such as canonical WNT, RAS, TGFβ, NOTCH, and hormone receptor signaling, and

oncogenic transformation are all regulated by several KLFs [247] (Figure 3.I.3). On the other hand, apoptosis is also modulated by these TFs [247]. Several pro-apoptotic (i.e. BAX or NOXA), anti-apoptotic (i.e. BCL2 or MCL1) or pro-survival (i.e. BIRC5) regulators are directly targeted by KLFs like KLF4, 5 or 6 [247, 255-258]. Tumor cells are highly invasive and KLFs 2, 4, 5, 6, 8, 10, 12 or 17 have been reported to somehow regulate this process. Cell metastasis requires a joint work of mechanisms including epithelial-mesenchymal transition (EMT), invasion, immune cell recruitment and development of new vessels. For instance, the EMT regulators SNAIL, SLUG, TWIST1 or MMP9 are regulated by KLFs 4, 5, 6 or 8 [247]. Regarding angiogenesis, KLF functions are also variable, with several KLFs involved in its regulation [247]. Interestingly, KLFs have also been linked to pluripotency [259]. In 2006, KLF4 was described as part of the termed 'Yamanaka factors', that together with OCT4, SOX2 and c-MYC permitted the generation of pluripotent cells from differentiated adult somatic cells [260]. Recently, the cooperation of all three KLFs 2, 4 and 5 has been reported to be linked to pluripotency [261-263] (Figure 3.I.3).

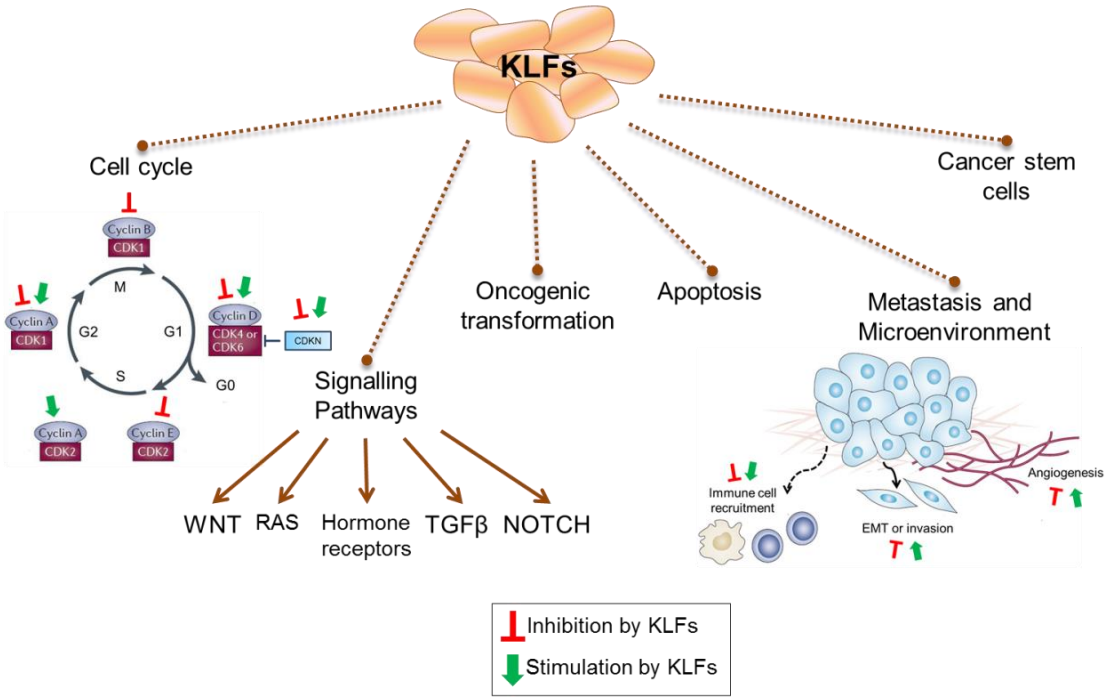

Figure 3.I.3. Functions of human Krüppel-like factors (KLFs) in cancer. KLFs regulate many cellular processes in cancer: i) cell cycle; ii) proliferation signaling pathways; iii) oncogenic transformation; iv) survival; v) metastasis and tumor microenvironment regulation; and vi) cancer stem cells (Adapted from Tetreault *et al*., 2013).

However, although important roles have been described for KLFs in cancer, there is no information about their role in CCA. Thus, the present study has analyzed the expression of KLFs in CCA, and then focused on Krüppel-like factor 5.

3.I.3.4 *Krüppel-like factor 5*

Human Krüppel-like factor 5 (KLF5, also known as IKLF or *BTEB2*) [264] is the fifth member of the KLF family. As a KLF member, three zinc-fingers are present in its carboxyl-terminus and it has a proline-rich motif E3 ubiquitin ligase WWP1 binding domain (Figure 3.I.4A) [265]. KLF5 is located in chromosome 13 at q22.1 position (Figure 3.I.4B) with ~22.6 kb and formed by four exons (Figure 3.I.4C). KLF5 protein is formed by 457 amino acids with a molecular mass of 50792 Da (from Genecards) (Figure 3.I.4C). However, KLF5 is modified by alternative splicing and to date, two transcript variants have been described. Transcript variant 1 represents the longer transcript (consisting of 3583 bp linear mRNA), whereas transcript variant 2 lacks a portion in the 5' UTR (consisting of 2969 bp linear mRNA) (according to NCBI/Nucleotide).

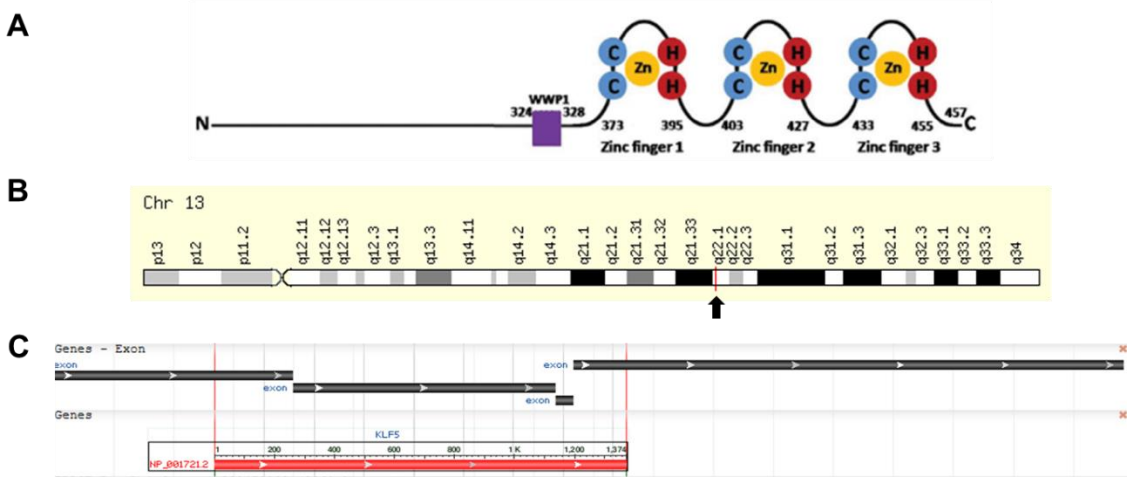

Figure 3.I.4. Structure of KLF5. (A) KLF5 consists of three zinc-fingers in the carboxyl-terminus and a proline-rich motif E3 ubiquitin ligase WWP1 binding domain. **(B)** KLF5 is located at q22.1 position in the chromosome 13. **(C)** KLF5 is formed by four exons and code for a 457 aminoacid protein with a molecular mass of 50792 Da.

KLF5 is highly expressed in the intestinal epithelium crypt cells [264] but it is also widely expressed among different tissues along the digestive tract or in others such as prostate or lung [266]. KLF5 regulates the expression of many

important downstream target genes binding to GC-rich DNA sequences through its zinc-finger domains [266, 267]. Nevertheless, KLF5 function is context-dependent, modulated in part by post-translational modifications (ubiquitination, SUMOylation, acetylation and phosphorylation) [266]. KLF5 mediates cell proliferation, apoptosis, migration or differentiation both in normal and tumoral cells and besides cancer, KLF5 is involved in cardiovascular diseases, inflammatory diseases or metabolic disorders like obesity [266].

KLF5 has been reported as pro-tumorigenic in different cancers such as bladder, breast, colon, lung or gastric cancers [246, 259], whereas studies in prostate cancer and esophageal squamous cell carcinoma pointed KLF5 as a tumor suppressor [268, 269]. However, the role of KLF5 in CCA has not been described yet.

3 - Hypothesis and Objectives

Krüppel-like factors (KLFs) are important TFs in different cancers, but there is no information about their role in CCA. Our preliminary analysis of KLFs expression in CCA pointed that KLF5 is overexpressed, being potentially relevant in cholangiocacinogenesis. Therefore, this study aims to elucidate the role of KLF5 in the pathogenesis of CCA and its potential therapeutic regulatory value. We propose the following objectives:

I. Analysis of KLFs expression in CCA cell lines compared to normal controls.
II. Analysis of KLFs expression in CCA human tissue compared to controls.
III. Evaluation of the role of KLF5 in the pathogenesis of CCA *in vitro*.
IV. Determination of the role of KLF5 in the CCA response to chemotherapy *in vitro*.
V. Analysis of the role of KLF5 in the pathogenesis of CCA *in vivo*.

3 - Materials and Methods

3.M.1 *Cell culture*

NHC primary cultures, non-tumoral SV-40 immortalized H69 cells and CCA human cell lines were used in the present study. Cells and culture conditions are described in general materials and methods section (see above).

3.M.2 *Human liver biopsies*

CCA and surrounding normal human tissues from three independent cohorts of patients were used. On the one hand, the here named “Copenhagen cohort” of patients was analyzed, where 104 CCA surgical specimens (68 intrahepatic and 36 perihilar CCAs) and 60 tumor adjacent normal tissue samples were analyzed in collaboration with Dr. Jesper Andersen (Copenhagen). Whole transcriptome profiling was performed using *humanRef-8v2 BeadChips* (Illumina) as previously described (GEO: GSE26566) [230]. The relationship between KLF5 expression and tumor clinical information (i.e. lymphatic invasion) was also analyzed. Data from The Cancer Genome Atlas (TCGA) was also used by the Andersen’s group for the analysis of KLF5 expression in 36 CCA tissue samples compared to 9 tumor adjacent tissues. Finally, the “San Sebastian cohort” of patients corresponded to 12 CCA samples and 10 tumor adjacent non-tumoral tissue samples. The clinical information of this cohort of patients is shown in Table 3.M.1. KLF5 expression was determined by qPCR. Research protocols were approved by the *Clinical Research Ethics Committees* of supporting institutions, and all patients signed written consents for the use of their samples for biomedical research.

Table 3.M.1. Clinical information of patients from the San Sebastian cohort.

Patient ID	Disease	Gender	Age	Stage	Size (cm)	CA19-9	CEA
1	iCCA	M	85	II	3.8	-	-
2	iCCA	M	62	II	2.7	2963	2.3
3	iCCA	F	78	IVB	6	43.2	1.2
4	iCCA	M	70	II	2	19.7	1.9
5	iCCA	F	82	IIIA	5.5	3528	307.9
6	pCCA	F	47	II	3.2	394.1	1.6
7	iCCA	M	61	II	4	0.6	2.8
8	iCCA	F	64	IIIA	5	374	2.9
9	dCCA	M	78	IIIA	2.3	16112	4.4
10	iCCA	M	68	IV	1.7	4.5	0.8
11	iCCA	M	60	II	5.2	19	2.9
12	pCCA	M	64	III	2	582.4	4.2

Abbreviations: iCCA: intrahepatic CCA; pCCA: perihilar CCA; dCCA: distal CCA; M: male; F: female

3.M.3 *Gene expression (mRNA)*

Gene expression was determined by qPCR from RNA isolated and retrotranscribed as described in general materials and methods section (see above). The primers used in the present study are grouped in Table 3.M.2.

Table 3.M.2. Human primers used for qRT-PCR.

Primer	Sequences	
KLF2	*Forward*	5'-GCATCTGAAGGCGCATCTGC-3'
	Reverse	5'-CACGATCGCACAGATGGCAC-3'
KLF3	*Forward*	5'-AGAACCTGGGATCGAACCAC-3'
	Reverse	5'-CACATCTGTGTATCCTCCGC-3'
KLF4	*Forward*	5'-CTTCCTGCCCGATCAGATGC-3'
	Reverse	5'-CCTGGTCAGTTCATCTGAGC-3'
KLF5	*Forward*	5'-AACGACGCATCCACTACTGC-3'
	Reverse	5'-CAGTGCTCAGTTCTGGTGCC-3'
KLF6	*Forward*	5'-AGGAGCTCCAGATCGTGCAC-3'
	Reverse	5'-AAACATAGCAGGGCTCGCTC-3'
KLF7	*Forward*	5'-ATGAGCTCACGAGGCACTAC-3'

	Reverse	5'-ACACTAGCCGATGCCATGGC-3'
KLF8	*Forward*	5'-ATCCCAGTGGTAGTGCAGTC-3'
	Reverse	5'-GTAGTCCCTGCAGACTCTGC-3'
KLF9	*Forward*	5'-ACAAGTGCCCCTACAGTGGC-3'
	Reverse	5'-GTGGTCACTCCTCATGAAGC-3'
KLF10	*Forward*	5'-GGAGTCACATCTGTAGCCAC-3'
	Reverse	5'-ATGGTCACTCCTCATGAACC-3'
KLF11	*Forward*	5'-CAGTGTTCATCACCTCTAGC-3'
	Reverse	5'-ATGCTTCGTCAGGTGGTCAC-3'
KLF12	*Forward*	5'-ACAAGACGCCAGAGACGGTC-3'
	Reverse	5'-CAGGTAGCATTCCTCACACC-3'
KLF13	*Forward*	5'-AAGCACAAGTGCCACTACGC-3'
	Reverse	5'-CTTGTTGCAGTCCTGCCAGC-3'
KLF15	*Forward*	5'-GCTGCAGCAAGATGTACACC-3'
	Reverse	5'-CTTCACACCTGAGTGCGAGC-3'
KLF16	*Forward*	5'-CTTTGGATGGCACTGGTGTG-3'
	Reverse	5'-GAGAACACAGAGAGCCGAGG-3'
KLF17	*Forward*	5'-GGAGTTCATGAGGTCTGACC-3'
	Reverse	5'-CTTGAAGACTGCCTCTCCTC-3'
Cyclin B1	*Forward*	5'-AAGGCGAAGATCAACATGGC-3'
	Reverse	5'-GTTACCAATGTCCCCAAGAG-3'
Cyclin D1	*Forward*	5'-GCTGCGAAGTGGAAACCATC-3'
	Reverse	5'-CCTCCTTCTGCACACATTTGAA-3'
Cyclin D3	*Forward*	5'-TACCCGCCATCCATGATCG-3'
	Reverse	5'-AGGCAGTCCACTTCAGTGC-3'
PCNA	*Forward*	5'-ACACTAAGGGCCGAAGATAACG-3'
	Reverse	5'-ACAGCATCTCCAATATGGCTGA-3'
Cdc25a	*Forward*	5'-CTGCCTGCACTCTCATGGAC-3'
	Reverse	5'-CTGTCCAGAGGCTTGCCATG-3'
Ki67	*Forward*	5'-CCACGCAAACTCTCCTTGTA-3'
	Reverse	5'-TTGTCAACTGCGGTTGCTCC-3'
VEGF	*Forward*	5'-AGGGCAGAATCATCACGAAGT-3'
	Reverse	5'-AGGGTCTCGATTGGATGGCA-3'
MMP9	*Forward*	5'-AAGGATACAGTTTGTTCCTCGTG-3'
	Reverse	5'-GCCCCTCAGTGAAGCGGTACAT-3'
RhoA	*Forward*	5'-GAATGATGAGCACACAAGGC-3'

	Reverse	5'-GCTGAACACTCCATGTACCC-3'
Rac1	*Forward*	5'-ATGTCCGTGCAAAGTGGTATC-3'
	Reverse	5'-CTCGGATCGCTTCGTCAAACA-3'
Cdc42	*Forward*	5'-GACAACTATGCAGTCACAG-3'
	Reverse	5'-GCAGTCTCTGGAGTGATAGG-3'
GAPDH	*Forward*	5'-CCAAGGTCATCCATGACAAC-3'
	Reverse	5'-TGTCATACCAGGAAATGAGC-3'

3.M.4 *Immunoblot and immunofluorescence*

Protein expression was analyzed by immunoblot as well as by immunofluorescence. The antibodies used for both methodologies are listed in Table 3.M.3.

Table 3.M.3. Antibodies used for immunoblot and/or immunofluorescence.

Antibody	Company	Reference	Use
Rabbit polyclonal to KLF5	Abcam	ab24331	WB 1:500 – IF 1:50
Rabbit polyclonal to GAPDH	Abcam	ab22555	WB 1:1000
Rabbit polyclonal to Histone H3	Santa Cruz	sc-10809	WB 1:1000
Mouse monoclonal anti-KRT19 (CK19)	ARP	03-61029	IF 1:50
Anti-rabbit IgG, HRP-linked Antibody	Cell signaling	7074	WB 1:5000
Donkey anti-Rabbit IgG (H+L) Secondary Antibody, Alexa Fluor® 488 conjugate	ThermoFisher	A21206	IF 1:1000
Donkey anti-Mouse IgG Secondary Antibody, Alexa Fluor® 568 conjugate	ThermoFisher	A10037	IF 1:1000

Abbreviations: WB: western blot; IF: immunofluorescence

3.M.4.1 *Immunoblot*

Total protein extracts and nuclear protein extracts were used in this study. Proteins were harvested, quantified and the expression determined by western blotting as described in general materials and methods section (see above).

3.M.4.2 *Immunofluorescence*

Liver tissue samples and cells in culture were used for immunofluorescence studies following a similar protocol but with some variations. Both methods were performed in a moist chamber and at end samples were mounted with a drop of VECTASHIELD^{TM} mounting medium (Vector) with 40,6-diamidino-2-phenyindole (DAPI, Vector laboratories). Finally, pictures were taken with a Nikon Digital Sight camera under a fluorescence microscope (Eclipse 80i, Nikon) with the NIS-elements AR 3.2 software.

3.M.4.2.1 *Immunofluorescence in liver tissue samples*

Paraffin-embedded tissue samples were deparaffined at 60ºC for 30 min and de-waxed in xylene. Decreasing grades of ethanol (100%, 96%, 70% and 50%) were used for tissue rehydration. Antigen retrieval was performed with *antigen unmaskin solution* (Vector), boiling the tissue samples for 15 min. Blocking solution (1% BSA/5% FBS/0.5% Triton/PBS 1x) was added for 1 h at room temperature. Samples were incubated O/N at 4ºC with the primary antibody (1:50) in a solution containing 1% BSA/0.1% Triton/PBS 1X. After 3 washes with PBS Tween 0.5%, samples were incubated with the corresponding fluorescent secondary antibody (1:400) for 1 h in darkness and then washed 3 times with PBS/0.5% Tween. Next, slides were mounted using a coverslip as above indicated.

3.M.4.2.2 *Immunofluorescence in cell cultures*

Cells ($5x10^4$) were cultured O/N on the top of collagen-coated coverslips (Menzel-Gläser). Then, cells were fixed adding 1 mL of cold methanol for 10 min at -20ºC. Samples were washed 3 times and incubated for 20 min with permeabilizing solution (0.5% Triton/PBS 1X) at room temperature. Next, blocking solution (5% FBS/1% BSA/0.5%Triton/PBS 1X) was added for 30 min at room temperature and the primary antibody (1:50) was then added in a solution containing 0.1% Triton/1% BSA/PBS 1X for 1h. Afterwards, cells were washed 3 times with 1% BSA/PBS 1X solution and incubated with the corresponding fluorescent secondary antibody (1:1000) diluted in the same solution for 2 h in the darkness. Finally, cells were washed 3 times with 1%

BSA/PBS 1X solution and coverslips were mounted and visualized as described above.

3.M.5 *Lentiviral vectors for KLF5 silencing*

The present study aimed to determine the effects of KLF5 in CCA. For that purpose, different approaches were followed for KLF5 silencing in CCA cell lines.

3.M.5.1 *KLF5 silencing with short hairpin RNA (shRNA) lentiviruses*

KLF5 was experimentally downregulated in CCA cells by using short hairpin RNAs (shRNAs) specific for KLF5. A non-target shRNA control was used as control. The Lent-shRNA-KLF5 contains a specific sequence designed to knock-down *KLF5* gene expression: CCGGCCTATAATTCCAGAGCAT AAACTCGAGTTTATGCTCTGGAATTATAGGTTTTTG. The non-target shRNAs are produced from sequence-verified lentiviral plasmid vectors that should not target any known human gene. The shRNAs were cloned in a pLKO.1-puro-CMV-tGFP vector, which is shown in Figure 3.M.1. The plasmid contains a region for puromycin resistance and GFP expression, which allow the selection of the infected cells. The shRNA-KLF5 and shRNA-control were purchased in glycerol stock and plasmid DNA formats, respectively (both from MISSION Sigma). Therefore, different methodologies were followed for plasmid amplification and lentiviral production.

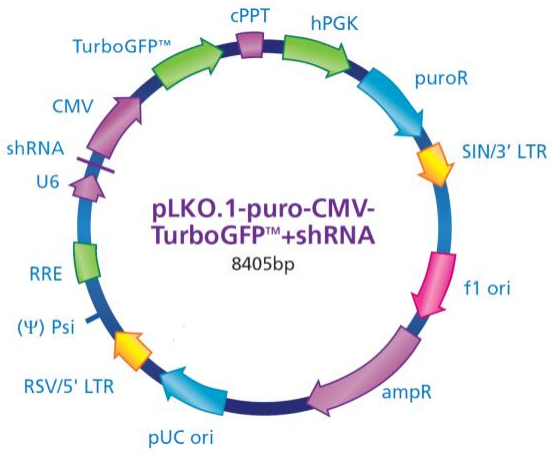

Figure 3.M.1. The shRNAs were cloned in a pLKO.1-puro-CMV-tGFP vector. Map of the pLKO.1-puro-CMV-tGFP (MISSION Sigma).

3.M.5.1.1 *Plasmid amplification*

ShRNA-control lentiviruses were obtained in plasmid DNA format, so an initial bacterial transformation was needed. Next, bacteria were amplified for both shRNA-control and shRNA-KLF5.

3.M.5.1.1.1 Bacterial transformation

Plasmid DNA and XL1-Blue competent bacteria were thaw on ice. 80 ng of plasmid DNA was added into a vial of competent bacteria and mixed by inverting the tube. The mixture was incubated for 30 min on ice. Then, the cells were exposed to a heat shock at 42°C for 2 min and the tubes were immediately chilled on ice, facilitating the entrance of the plasmid into the bacteria. Next, 250 µL of room temperature LB Broth (1231.00, Conda) was added and the tube was placed horizontally in a shaker at 200 rpm and incubated at 37°C for 1-2 h. An appropriate volume (50-200 µL) of the transformation volume was spread on a pre-warmed plate of LB Agar (1083.00, Conda) supplemented with 100 µg/mL ampicillin (624619.1, Lab. Normon) to be able to obtain well-spaced colonies. Plates were incubated O/N at 37°C. Plasmids were then amplified and purified.

3.M.5.1.1.2 Bacterial amplification

For both shRNA-control and shRNA-KLF5 lentiviruses, the surface of the glycerol stock was scratched with a sterile tip and the culture was spread onto a plate containing LB Agar supplemented with 100 µg/mL ampicillin. Plates were incubated O/N at 37°C and then an independent colony was picked from the plate in sterile conditions and it was inoculated in 3-5 mL of LB Broth supplemented with 100 µg/mL ampicillin. Samples were incubated in a shaker at 37°C for 4-8 h. Next, 100-250 mL of LB Broth with 100 µg/mL ampicillin were inoculated with an aliquot of each recombinant bacteria in sterile conditions. Bacteria were grown O/N in a shaker at 37°C. Plasmid DNA was purified using NucloBond Xtra Midi Plus kit (740412, Macherey-Nagel) following manufacturer's instructions and quantified by ultraviolet (UV) spectrophotometry using the *NanoDrop® ND-1000* apparatus (Thermo Scientific). Samples were stored at -20ºC for further viral production.

3.M.5.1.2 *Lentiviral production*

Next, lentiviral particles were produced. For that purpose, $2x10^6$ HEK293T cells (ATCC) were seeded in P100 plates in DMEM/F-12 media containing 10% FBS and 1% P/S. The next day, transfection was performed by using three packaging plasmids (Addgene) (Figure 3.M.2) and TurboFect (ThermoScientific).

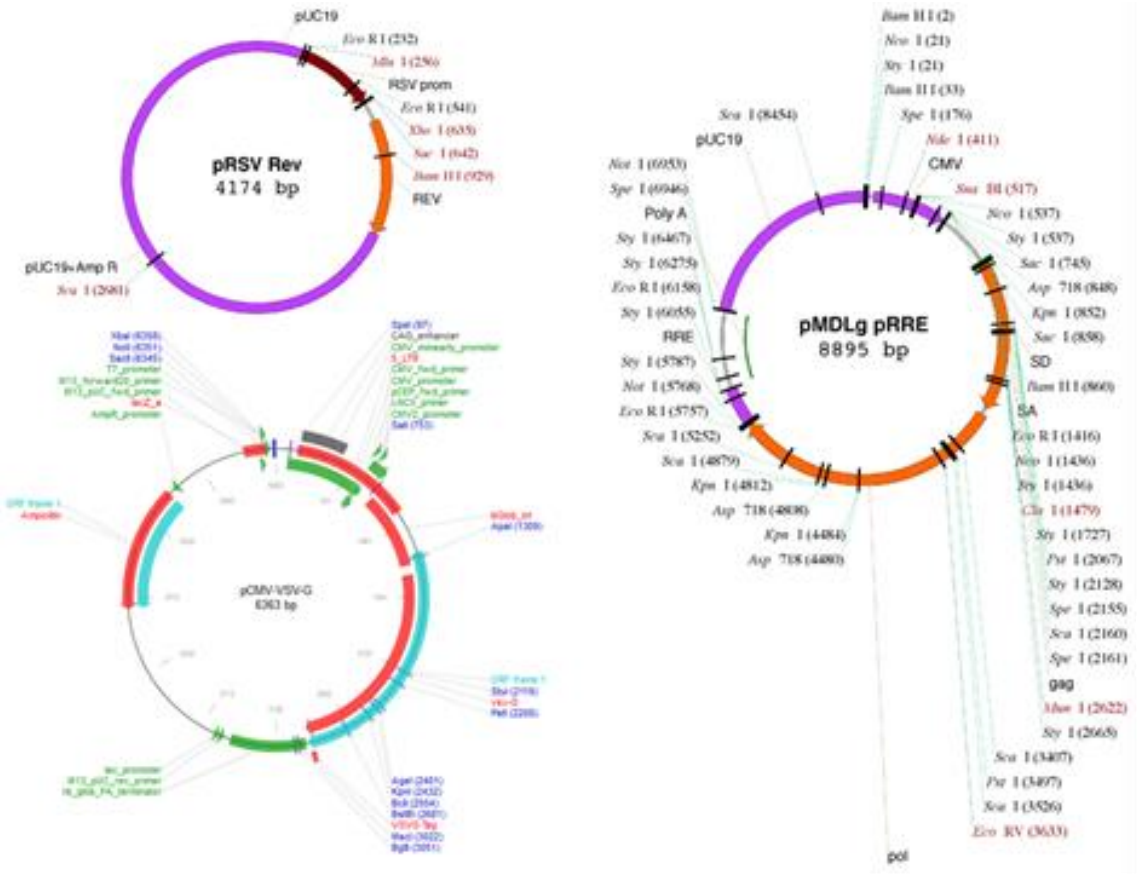

Figure 3.M.2. Packaging plasmids. Map of the vectors (Addgene).

The packaging plasmids and the transfer vector were thawed on ice. The transfection mix containing DMEM/F-12 (1.2 mL), plasmids (3.25 µg pMDLg-pRRE, 1.25 µg pRSV-REV and 1.75 µg pCMV-VSV-G) and transfer vector (5 µg) was first prepared in a sterile 1.5 mL Eppendorf tube. Afterwards, TurboFect was vortexed and 24 µL were added into the mix and immediately mixed by vortexing. The transfection mix was incubated for 15-20 min at room temperature. The mix was added dropwise along the surface of the plate with HEK293T cells containing 5 mL of DMEM/F-12 supplemented with 10%

FBS/1% P/S. Next, 16-18 h post-transfection, media was carefully replaced for 10 mL of DMEM/F-12 10% FBS/1% P/S. The following day lentiviruses were harvested and 10 mL of DMEM/F-12 10% FBS/1% P/S were added again to cells for 24 h culture for a second harvest. Harvested media was centrifuged at 1,500 rpm for 5 min for debris removal. Lentiviral particles were concentrated adding Lenti-X Concentrator reagent (ClonTech) (1 volume of reagent for 3 volumes of media). Tubes were mixed by gentle inversion and placed at 4ºC O/N. Afterwards, samples were centrifuged at 1,500 g at 4ºC for 45 min and supernatant was discarded. The pellet was resuspended in 100-400 µL DMEM/F-12, aliquoted and stored at -80ºC. Lentiviral particles were titrated by flow-cytometry using GFP expression as follows.

3.M.5.1.3 *Lentiviral titration*

In order to determine the concentration of each lentiviral production, CCA cells (i.e. EGI1; $2x10^4$ cells) were seeded in 24-well plates and incubated O/N at 37ºC. Culture media (fully-supplemented DMEM/F-12) was replaced by culture media containing polybrene (6 µg/µL) (Santa Cruz) and different amount of the lentiviruses (ranging 0.01 – 6 µL) were added to each well. A well without virus was used as a negative control. Plates were centrifuged at 1,800 g at 32ºC for 90 min. Then, cells were cultured O/N at 37ºC, and media was replaced. After, 72 h post-infection, cells were trypsinized, harvested in PBS with 20% FBS and GFP was checked by flow-cytometry. Thus the multiplicity of infection (MOI) was determined.

3.M.6 *Lentiviral infection of cells*

Similar to the titration protocol, CCA cells (i.e. EGI1 and Witt) were seeded in appropriate collagen-coated plates and left to attach at 37ºC. Culture media (fully-supplemented DMEM/F-12) was replaced by culture media containing polybrene (6 µg/µL) (Santa Cruz) and shRNA-control or shRNA-KLF5 lentiviruses were added at different multiplicity of infection (MOI) to each well. Cells without any lentivirus were maintained as negative control. Plates were centrifuged at 1,800 g at 32ºC for 90 min and cultured at 37ºC as needed. Puromycin dihydrochloride (Sigma) at 2 µg/mL was added 72 h post-infection

for selecting the cells infected with shRNA-KLF5 or shRNA-control and cells were amplified and used for functional assays.

3.M.7 *KLF5 knockout by CRISPR/Cas9 technology*

The novel clustered regularly interspaced short palindromic repeats (CRISPR) technology has been recently described. The RNA-guided CRISPR-associated nuclease Cas9 permits to introduce targeted mutations at specific sites in the genome leading to loss-of function [270, 271]. CRISPR/Cas is an adaptive immune system found in bacteria and archaea, which helps in the defense against invading genetic elements (virus or plasmid) [272] (Figure 3.M.3).

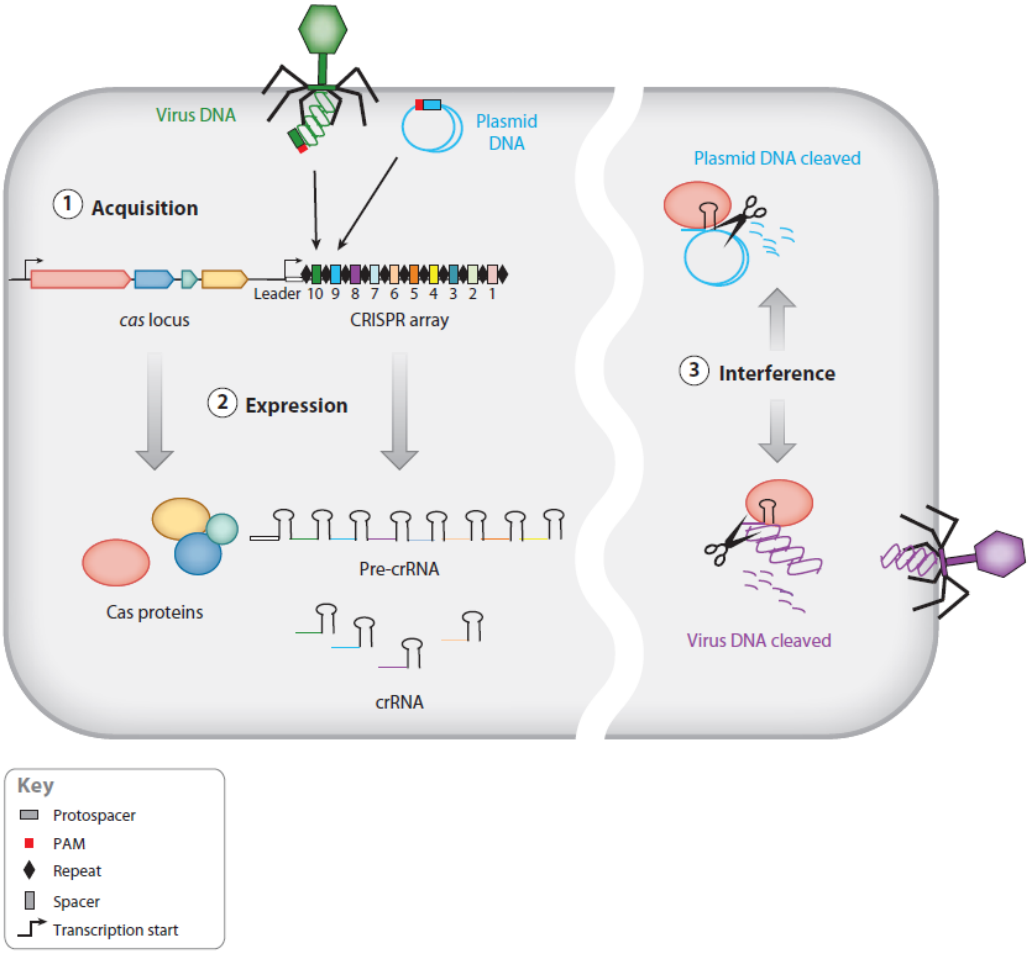

Figure 3.M.3. CRISPR-Cas adaptive immune system. 1) Foreign double stranded DNA are incorporated into CRISPR array. **2)** Cas proteins are transcribed and traduced, and CRISPR array is transcribed, generating small CRISPR RNAs. **3)** CRISPR RNAs guide Cas proteins towards complementary foreign DNA and Cas proteins cleave virus or plasmid DNA inactivating them (Adapted from D Bhaya, M Davison and R Barrangou, 2011).

Based on this system, human genome engineering was achieved by heterologous expression of a guide RNA (gRNA), which guides the Cas9 nuclease to the genomic location of interest for cleaving DNA [273]. Thus, in the present study, KLF5 was knocked-out by CRISPR/Cas9 methodology in CCA cells, in collaboration with Prof. Charles Lawrie's Lab (Biodonostia). The CRISPR/Cas9 technology allows the specific editing of the genome with a complete knockout, instead of the partial knockdown obtained by shRNA, thus enhancing the phenotypic effects [270, 271]. This methodology has also some off-targets – which are less than those observed with shRNAs – and can be predicted in the guide design and further checked to ensure there are no undesirable off-target effects. One issue whilst using this methodology might be the need of cell individualization for obtaining individual clones, as each clone could act differently, but this can be avoided by using several clones with verified gene knockout, as performed in the present study (see below).

3.M.7.1 *Guide design and oligo ordering*

Specific guides for KLF5 were designed using the CRISPR Design Tool in Genome-Engineering webpage (http://crispr.mit.edu/). Guides are designed in exons in order to ensure changes in protein expression. Single guide "sense" and "antisense" oligos (sgRNA_FW and sgRNA_RV, respectively) were ordered. In particular, the sense oligo must be 5' to 3' towards the protospacer adjacent motif (PAM). We selected the exon 2, as the forward KLF5 primer used in the present study was there. The program suggests several guides, specifying the genomic sequence, locus, score and offtargets, thus guides with higher scores and less offtargets were selected. Once the guides are selected, both "sense" and "antisense" sequences are designed as single guide RNAs (sgRNA) following the format showed in Table 3.M.4. This format allows a better transcriptional activity of the DNA polymerase III and a perfect annealing and reconstitution of the overhands generated by the BsbI enzyme.

Table 3.M.4. Format of the guides for CRISPR/Cas9 editing.

Oligo	Format
sgRNA_FW	5' - CACCG**G**_$N_{19\ (sense)}$- 3' (towards PAM)
sgRNA_RV	5' - AAAC_$N_{19\ (antsense)}$_CC - 3'

In the present study, five different guides were initially selected according to the quality score and the number and location of offtarget sites. Oligos (0.025 µmol) were ordered (Sigma). The specific sequences are shown in Table 3.M.5.

Table 3.M.5. KLF5 guide sequences.

KLF5 oligos	Sequence 5'-3'
Guide 1	*Forward* 5'-CACCGGTGTGTTACGCACGGTCTCT-3' *Reverse* 5'-AAACAGAGACCGTGCGTAACACACC-3'
Guide 2	*Forward* 5'-CACCGGTAGAAGGAGTAACCCCGATT-3' *Reverse* 5'-AAACAATCGGGGTTACTCCTTCTACC-3'
Guide 3	*Forward* 5'-CACCGGTGCGTCGTTTCTCCAAATCG-3' *Reverse* 5'-AAACCGATTTGGAGAAACGACGCACC-3'
Guide 4	*Forward* 5'-CACCGGTGCGCTCGCGGTTCTCTCG-3' *Reverse* 5'-AAACCGAGAGAACCGCGAGCGCACC-3'
Guide 5	*Forward* 5'-CACCGGCGCGTCGCGGGCCGGATTCG-3' *Reverse* 5'-AAACCGAATCCGGCCCGCGACGCGCC-3'

3.M.7.2 *Cloning of the guides in the Cas9 expressing plasmid*

To begin with, the guides have to be cloned in a pX330 EGFP/2A NEO-NEO (addgene) plasmid. For that purpose, first 10 µg of the plasmid were digested with a mix containing the BbsI restriction enzyme (NEB), 10X NEBuffer and DNase-RNase-free-H_2O (free-dH_2O), at 37ºC for 15 min, followed by a 20 min inactivation at 65ºC. Next, the digested plasmid was gel-purified by running the digestion product in a 0.8% agarose gel, harvesting the bands under UV light and extracting de DNA using the QUIaquick Gel Extraction Kit (Cat. No 28704, QIAGEN). The purified plasmid DNA was quantified by NanoDrop (Thermo

Scientific). Subsequently, double stranded oligos (dsOligo) were generated from the single stranded DNA guides. Forward and reverse stranded oligos (100 µM of each) in 10X NEBuffer 2.1 and free-dH_2O were subjected to 99ºC for 5 min, followed by a slow cool down until placing samples on ice. The dsOligo were precipitated using 3M NaOAc at pH 5.6 and 100% ethanol, with a 30 min centrifugation at 14000 rpm at 2ºC. The pellet was washed with 70% ethanol, centrifuged at 14000 rpm at room temperature for 10 min, dried and resuspended in free-dH_2O. The dsOligo DNA was then measured by Nanodrop.

In order to ligate the dsOligo and the digested plasmid, a previous kinase of the dsOligos is needed. 1 µg of the dsOligo was kinased using a T4 polynucleotide kinase (NEB) and the corresponding 10x buffer. The samples were incubated for 1 h at 37ºC. In this process, gamma-phosphates are transferred from ATP to the 5' end of the DNA, being ready for the ligation. The ligation reaction was performed with 20 µg of the plasmid opened backbone and 0.5 µL of the dsOligo using a T4 ligase (NEB) and associated 10x buffer, incubated for 1 h at room temperature. The ligation product (5 µL) was transformed in XL1-blue competent bacteria following these steps: 20 min on ice, 2 min at 42ºC and 3 min on ice. Next, LB Broth media (without antibiotics) was added and incubated for 1 h at 37ºC shaking, for bacteria recovery. Bacteria were grown O/N at 37ºC in LB Agar plates with ampicillin. Individual colonies were picked and grown O/N at 37ºC in LB Broth with ampicillin. Glycerol stocks of the samples were harvested and the plasmids were isolated using the QIAprep Spin Miniprep kit (QIAGEN), following manufacturer's instructions. DNA was quantified in a Nanodrop. Samples were then Sanger sequenced, using a forward primer for the plasmid (sequence: 5'-GCCTGGTATCTTTATAGTCC-3') in order to verify the correct cloning of the guides into the plasmid. Once the cloning was verified and one colony was selected, bacteria were picked from the glycerol stock for further amplification in LB Broth with ampicillin and subsequent plasmid isolation using the NucleoBond® Xtra Midi Plus (Macherey-Nagel).

3.M.7.3 *Cell transfection and selection by cell sorting*

CCA cells were seeded in P100 plates (Corning; $5x10^5$ cells per plate) with fully-supplemented DMEM/F-12 medium (Table I.2) and allowed growing O/N. The day after, cells were transfected using Opti-MEM (Gibco) medium, plasmid DNA (500 ng per 3 x 10^4 cells) and lipofectamine®2000 (Invitrogen)(1 µL per 3 x 10^4 cells). Transfection was left for 6 h and media was replaced by fully-supplemented DMEM/F-12 medium. 72 h post-transfection, cells were sortened in a FACSAria III Sorting Cytometer (BD) upon positive GFP expression, and each cell was seeded in a well of a collagen-coated V-bottom 96-well plate Cellstar® (Greiner) and cells were allowed to grow.

3.M.7.4 *Amplification of clones and detection of mutations in KLF5*

Individual cell clones were expanded and DNA was isolated using the NucleoSpin® Tissue kit (Macherey-Nagel), following manufacturer's instructions. Nanodrop quantified DNA was then amplified on the genomic regions of interest using specific primers for each guide, shown in Table 3.M.6. A master mix was prepared with 10x buffer, MgCl, dNTPs, Taq polymerase (all from Bioline), free-H_2O and the corresponding forward and reverse primers and mixed with the DNA. PCR conditions were set as follows in a Veriti Thermal Cycler: 1 min at 95ºC; 35 cycles of 30 seconds at 95ºC, 30 seconds at 64ºC and 30 seconds at 72ºC; 5 min at 72ºC; and placed at 4ºC. Samples were run in a 1.8% agarose gel in TBE using gel red in order to verify the amplification of the region. Subsequently, PCR products were Sanger sequenced, using the corresponding forward primers for each guide, for detection of mutations in KLF5.

Table 3.M.6. Specific primers used for amplification of the genomic region of interest for each KLF5 guide.

***KLF5* guide amplification primers**	**Sequence 5'-3'**
Guide 1	*Forward* 5'-CACTGAGGAGTTTGCCCTAGTACC-3' *Reverse* 5'-CTTCCAGGCTCTGAGCTTGGTGG-3'
Guides 2 and 3	*Forward* 5'-ACCTCTGCTGTTCCGCAGACTGC-3' *Reverse* 5'-CTGCCTGCAACCTCCACTTCACC-3'
Guide 4	*Forward* 5'-CTGCCTCTCTCCCTGCTCATAGGC-3' *Reverse* 5'-CGGCTCTTCCTACCTGGACCAGG-3'
Guide 5	*Forward* 5'-TGAGGAGTCCACCCGAAACCTCCC-3' *Reverse* 5'-TGGAGAGCGGTACAGGCGAAGGC-3'

3.M.7.5 *Confirmation by immunoblot*

Clones containing specific homozygous mutations were selected for KLF5 silencing confirmation at protein level by immunoblot.

3.M.8 ***Cell proliferation and cell cycle analysis***

Cell proliferation markers were analyzed by qPCR as previously stated (see above) and cell cycle profile was determined as explained below.

3.M.8.1 *Cell cycle analysis*

The cell cycle profile was analyzed by flow cytometry using TO-PRO-3 which allows distinguishing G0/G1, S and G2/M phases. Briefly, $1x10^6$ cells were harvested, washed with PBS and then resuspended in 300 µL of cold PBS for further fixation by adding 700 µL of cold (-20ºC) 100% ethanol dropwise while cells were being vortexed. Cells were incubated O/N at -20ºC. Next, samples were centrifuged at 1,000 g for 5 min and the pellet was washed with PBS in a 5 min centrifugation at 1,000 g. Cell pellets were subsequently stained with a PBS solution (470 µL) containing TO-PRO-3 (25 µL of a 1 µM stock; Life Technologies) and RNAse A (5 µL of 10 mg/mL stock; Sigma). Samples were incubated for 30 min at 37ºC in darkness. Samples were then transferred to a

U-bottom 96-well plate and cell cycle analysis was performed using a Guava® easyCyte HT Flow Cytometer (Merck Millipore).

3.M.9 *Determination of cell migration*

Cell migration was analyzed by wound-healing and transwell assays as stated in general materials and methods section (see above).

3.M.10 *Determination of cell viability by WST-1*

Cells ($2x10^4$) were seeded and, once attached, 6 h starvation was performed in DMEM/F-12 supplemented with 1 or 3% FBS and 1% P/S, as stated in each assay. Cell viability under the treatment with toxic bile acids or chemotherapeutics (shown in Table 3.M.7) was determined using WST-1 (Roche) as described in general materials and methods (see above).

Table 3.M.7. Molecules evaluated on CCA cell viability.

Drug (abbreviation)	Solvent	Concentration	Reference	Company
Chenodeoxycholic acid (CDCA)	DMSO	100 µM	C9377	Sigma
Gemcitabine (Gem)	H_2O	0.05 to 2 µM	G6423	Sigma
Cis-Diammineplatinum (II) dichloride or Cisplatin (Cis)	H_2O	5 and 10 µM	P4394	Sigma
5-Fluorouracil (5-FU)	DMSO	1 and 3 µM	F6627	Sigma
Doxorubicin hydrochloride (Doxo)	DMSO	20 to 100 nM	D1515	Sigma

3.M.11 *In vivo CCA model*

The role of KLF5 was studied *in vivo* using a subcutaneous xenograph model of CCA. These studies were performed in collaboration with the group of Dr. Maite Garcia (CIMA, Pamplona). To achieve this objective, KLF5 wild-type and KLF5 knockout CCA cells were previously transfected with a luciferase expressing vector (a kind gift from Dr. Maite Garcia). Once luciferase expression was

verified a subcutaneous model of CCA was established to determine the role of KLF5 in CCA tumor growth. Immunodeficient CD1 nude mice (Crl:CD1-*Foxn1*^{nu}, strain 086, homozygous) (from Charles River) were employed for the generation of the xenograph models. All experimental procedures were approved by the Ethical Committee for Animal Experimentation of the supporting institution and were used in conformity with the institution's guidelines for the use of laboratory animals.

3.M.11.1 *Luciferase transfection and verification*

A luciferase expressing vector with a CMV promoter (addgene) was used for CCA cell (EGI1) transfection. Cells were transfected as aforementioned using Opti-MEM (Gibco) medium and lipofectamine®2000 (Invitrogen). Transfection was left for 6 h and media was replaced by fully-supplemented DMEM medium. Luciferase expression was checked using the Dual-Luciferase® Reporter Assay system (Promega), following manufacturer's instructions, in a PHERAstar apparatus (BMG LABTECH).

3.M.11.2 *Subcutaneous model of CCA*

EGI1 control and CRISPR-KLF5 cells ($1x10^6$) were subcutaneously injected in both flanks of five nude mice each. Tumor volumes were monitored initially by luciferase expression in a PhotonImager after intraperitoneal injection of luciferine and later also by measuring the tumor size with a caliper. Tumor volume (V) was calculated using the following formula: $V = (D \times d^2)/2$ (where "D" represents the largest diameter measured and "d" the shortest).

3.M.12 ***Statistical analysis***

Statistical comparisons were performed as described in general materials and methods (see above). *Unpaired T-test* or *Mann-Whitney test* were used for comparisons between two groups. For paired samples, the *paired T-test* or the equivalent *Wilcoxon matched-paires signed ranks test* were used. Differences were considered significant when $p<0.05$.

3 - Results

3.R.1 *Expression of KLFs in normal and tumor cholangiocytes in culture*

The expression of 15 members of the KLF family was analyzed by qPCR in three CCA human cells (i.e. EGI1, TFK1 and Witt) and NHC (i.e. NHC2, NHCSS and C324). Data showed that *KLF5* is overexpressed in all CCA human cell lines compared to NHC, whereas the expression of *KLFs 7*, 8, *12, 13 and 15* is decreased in all CCA cell lines compared to NHC (Figure 3.R.1). On the other hand, the expression of KLFs 2, 3, 6, 9, 10, 11, 16 and 17 varies between cell lines (Figure 3.R.1). Since KLF5 was the only KLF found overexpressed in all CCA human cell lines compared to NHC, we put our attention in this TF. KLF5 studies in other cancers pointed it as a potential tumor promoter and therefore, as potential therapeutic target [266, 274] and nothing was known about its role in CCA.

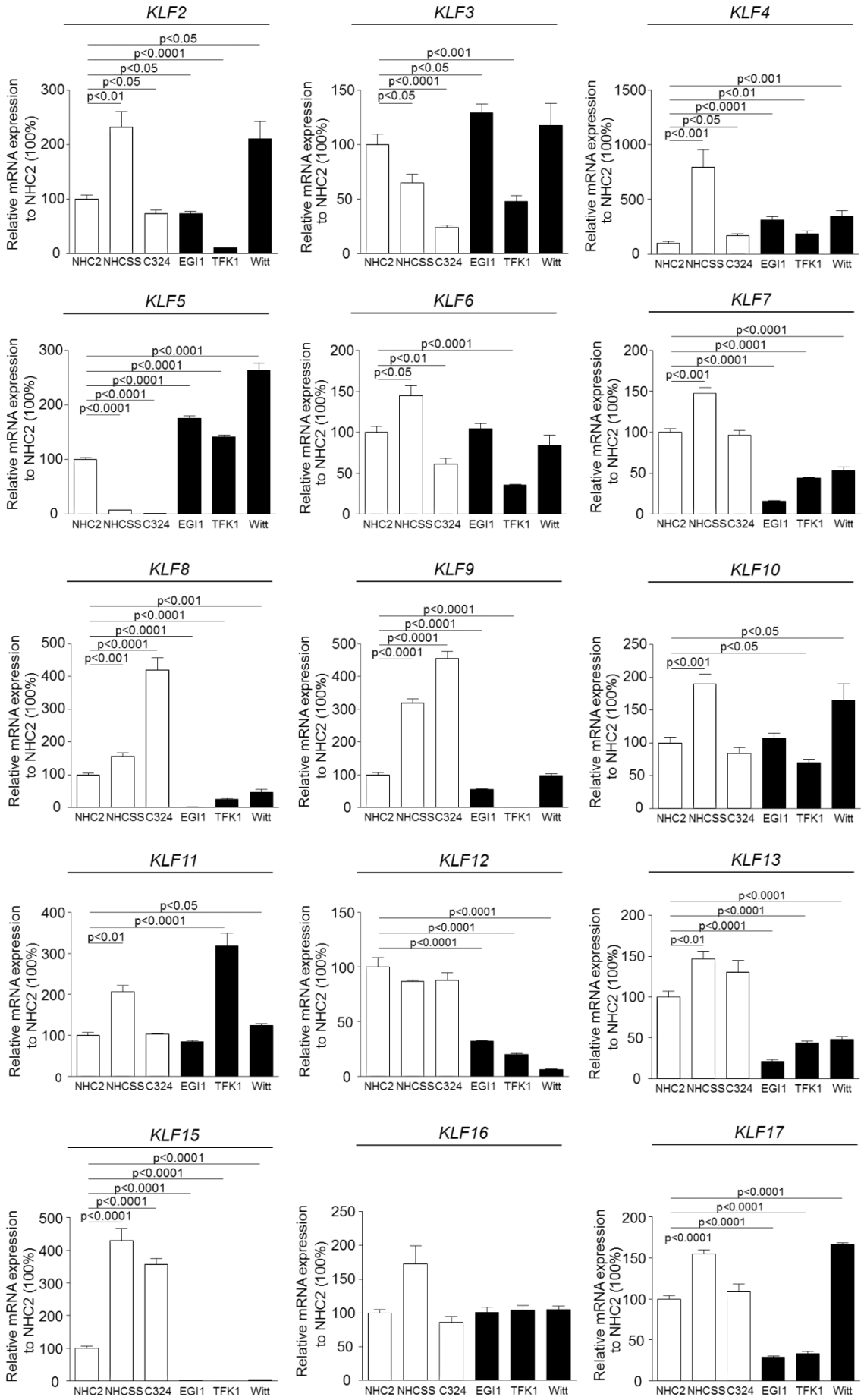
KLF2
p<0.05
p<0.0001
p<0.05
p<0.05
p<0.01
KLF3
p<0.001
p<0.05
p<0.0001
p<0.05
KLF4
p<0.001
p<0.01
p<0.0001
p<0.05
p<0.001
KLF5
p<0.0001
p<0.0001
p<0.0001
p<0.0001
p<0.0001
KLF6
p<0.0001
p<0.01
p<0.05
KLF7
p<0.0001
p<0.0001
p<0.0001
p<0.001
KLF8
p<0.001
p<0.0001
p<0.0001
p<0.0001
p<0.001
KLF9
p<0.0001
p<0.0001
p<0.0001
p<0.0001
KLF10
p<0.05
p<0.05
p<0.001
KLF11
p<0.05
p<0.0001
p<0.01
KLF12
p<0.0001
p<0.0001
p<0.0001
KLF13
p<0.0001
p<0.0001
p<0.0001
p<0.01
KLF15
p<0.0001
p<0.0001
p<0.0001
p<0.0001
p<0.0001
KLF16
KLF17
p<0.0001
p<0.0001
p<0.0001
p<0.0001
Relative mRNA expression to NHC2 (100%)
NHC2 NHCSS C324 EGI1 TFK1 Witt

Figure 3.R.1. Expression of *KLFs* in normal and tumor cholangiocytes in culture. Relative mRNA expression of *KLFs 2-13 and 15-17* in CCA human cell lines (i.e. EGI1, TFK1 and Witt) compared to NHCs (i.e. NHC2, NHCSS and C324) (n=5-6). Statistical comparisons are compared to NHC2.

3.R.2 *Expression of KLF5 normal and tumor cholangiocytes in culture*

KLF5 expression was then studied more in detail by analyzing its expression in eight CCA human cell lines, H69 cells and four NHC. In this regard, we found that KLF5 is overexpressed in all human CCA cell lines compared to H69 cells and all NHC (Figure 3.R.2). Thus, KLF5 appears to be overexpressed in all CCA human cells independent of the genetic background (i.e. KRAS-mutated or wild-type) and type of CCA (i.e.iCCA, mixed HCC-CCA or eCCA).

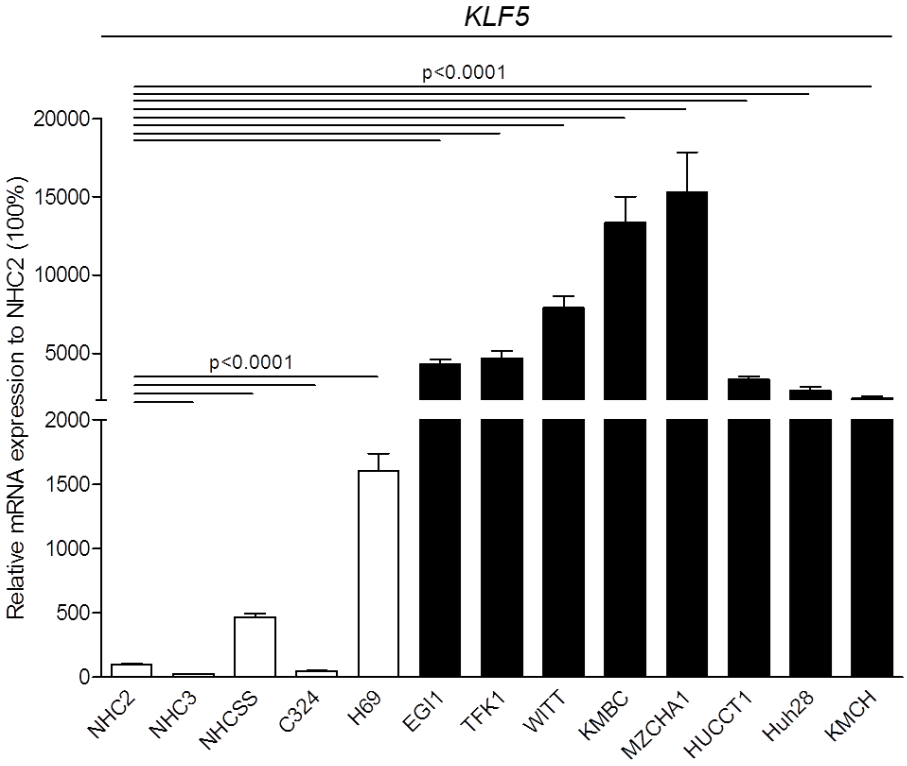

Figure 3.R.2. *KLF5* is overexpressed in CCA human cells compared to NHC in culture. Relative mRNA expression of *KLF5* in eight different CCA cell lines (black bars) and NHC (four different NHC primary cultures and H69 cells, which are non-tumor SV-40 inmortalized human cholangiocytes) (n=5-6).

Then, the protein expression of KLF5 was evaluated in both CCA human cell lines and NHC by immunoblotting (Figure 3.R.3) and immunofluorescence

(Figure 3.R.4). Since KLF5 is a nuclear TF, its protein levels were determined by immunoblotting in proteins isolated from total cell or nuclear extracts. Data showed that KLF5 protein is also overexpressed in all CCA human cell lines compared to NHC, and this overexpression is localized in the nuclei of CCA cells (Figure 3.R.3)

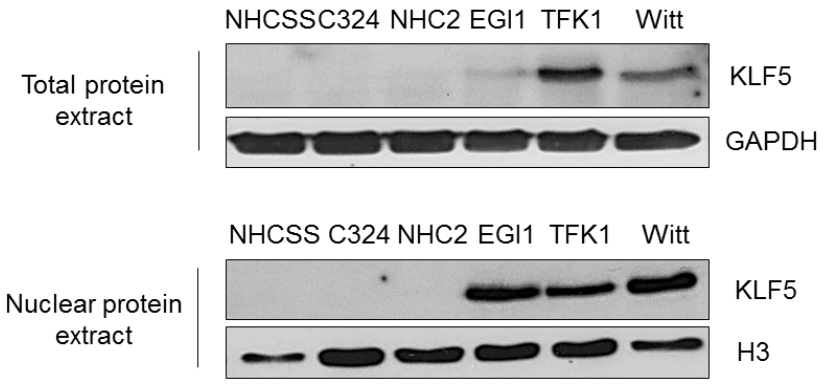

Figure 3.R.3. KLF5 protein is overexpressed in CCA human cell lines compared to NHC in culture. Representative immunoblot images showing KLF5 expression in both total protein cell extracts and nuclear protein extract from CCA cell lines (i.e. EGI1, TFK1 and Witt) and NHC (i.e. NHCSS, C324 and NHC2). GAPDH and H3 were used as housekeeping controls for total and nuclear protein extracts, respectively.

In addition, these results were confirmed by immunofluorescence analysis showing overexpression of KLF5 in the nuclei of CCA cells compared to NHC (Figure 3.R.4).

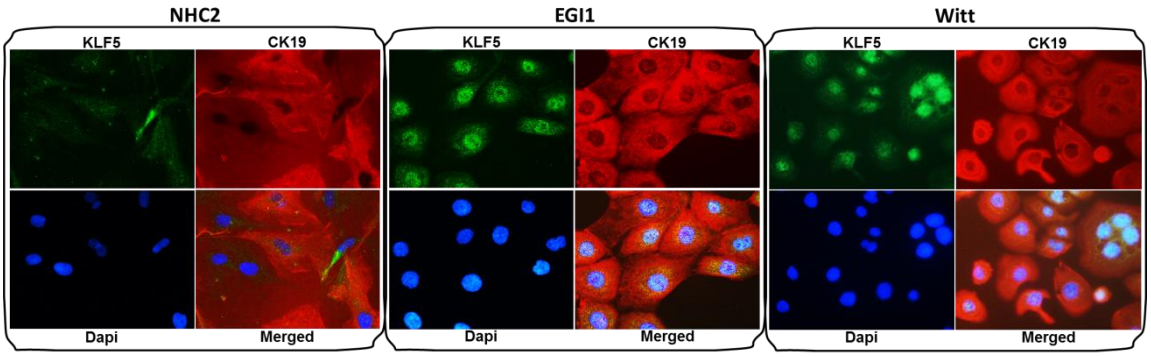

Figure 3.R.4. KLF5 is overexpressed in the nuclei of CCA human cells compared to NHC in culture by immunofluorescence. Representative immunofluorescence images showing KLF5 (green) expression in NHC (i.e. NHC2) and CCA cells (i.e. EGI1 and Witt). CK19 (red) was used as a marker of cholangiocytes and nuclei were stained with Dapi (blue). Pictures were taken with the 40x objective.

3.R.3 Expression of *KLF5 in CCA and normal liver human tissues*

KLF5 expression was also evaluated in CCA and normal liver human tissue from three different cohorts of patients, i.e. “Copenhagen cohort”, “tissue genome atlas (TCGA)” and “San Sebastian cohort”. The “Copenhagen cohort” showed KLF5 overexpression in tumoral CCA samples (n=104) compared to tumor adjacent normal tissue (TAN; n=60) by whole transcriptome profiling (Figure 3.R.5A). Moreover, *KLF5* expression was analyzed upon several clinicopathologic parameters on samples from the “Copenhagen cohort”. Data showed that tumor samples with higher *KLF5* expression are associated to lymphatic invasion (Figure 3.R.5B). *KLF5* was also checked by RNA-seq in a cohort from the tissue genome atlas (TCGA) and higher *KLF5* expression was observed in CCA tissue samples compared to TAN (Figure 3.R.5C).

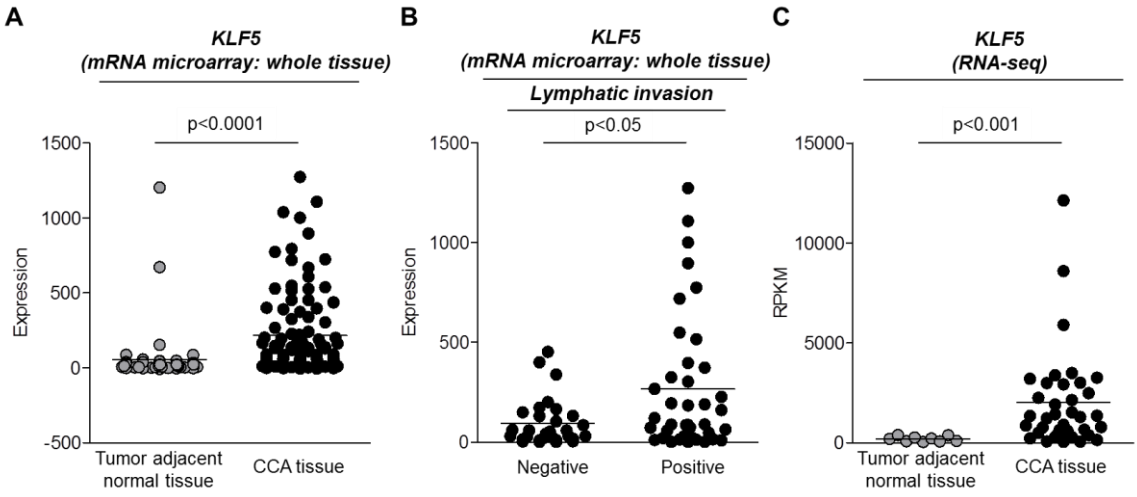

Figure 3.R.5. *KLF5* is overexpressed in CCAs from three different cohorts of patients and is associated to lymphatic invasion. (A-B) *KLF5* expression was analyzed in the Copenhagen cohort of patients by mRNA microarray in **(A)** CCA tissue and tumor adjacent normal tissue samples and **(B)** in CCA samples from individuals with negative or positive lymphatic invasion. **(C)** KLF5 expression analysis by RNAseq in a cohort from TCGA. Dots: number of patients.

Additionally, the expression of *KLF5* was evaluated by qPCR in the “San Sebastian cohort” and the same expression pattern was observed. Data showed that KLF5 is overexpressed in CCA tissue compared to non-tumoral surrounding liver tissue and NHC in culture (i.e. NHC2) in culture (Figure 3.R.6A). Of note, paired non-tumoral and CCA tumor samples from the same

patients also showed increased *KLF5* mRNA expression in CCA tissues (Figure 3.R.6B).

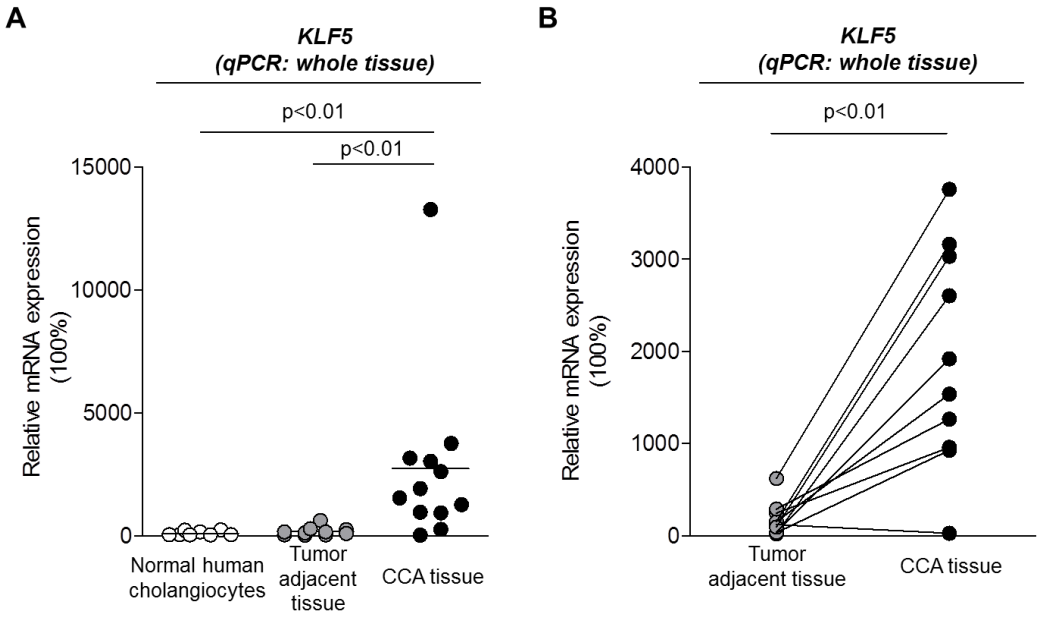

Figure 3.R.6. *KLF5* is overexpressed in CCA human tissue compared to normal surrounding liver tissue and normal human cholangiocytes in culture. (A) Relative mRNA expression of *KLF5* in NHCs and liver biopsies (tumor adjacent non-tumoral tissue and CCA tissue) from CCA patients of the "San Sebastian cohort" analyzed by qPCR. **(B)** Matched-paired samples of CCA and surrounding tissue showing increased *KLF5* levels in CCA tissue. Dots: number of patients.

On the other hand, immunofluorescence of KLF5 in liver biopsies from CCA patients also showed higher KLF5 expression in CCA tissue than in normal human bile ducts (Figure 3.R.7).

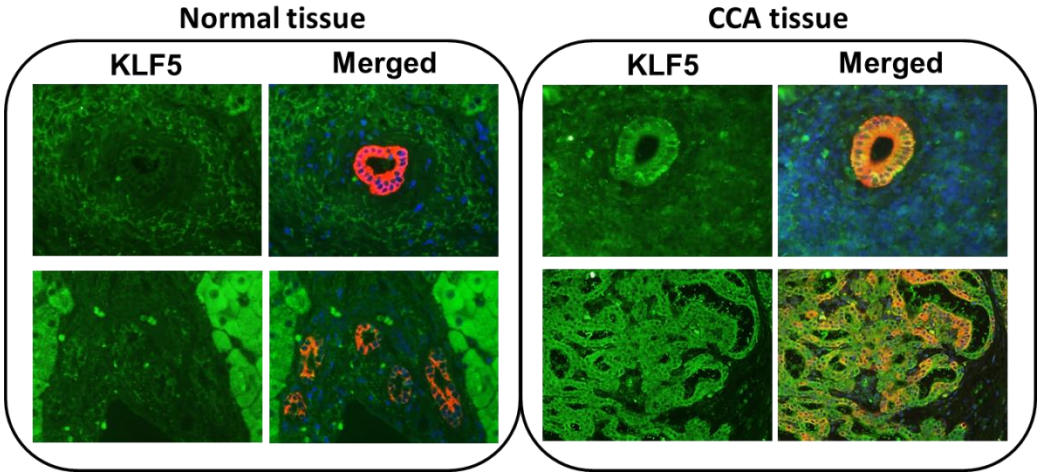

Figure 3.R.7. KLF5 expression in CCA and normal liver human tissue by immunofluorescence. Representative Immunofluorescence images showing KLF5 (green) expression in normal and CCA liver tissue. CK19 (red) was used as a cholangiocyte marker and nuclei were stained with Dapi (blue). Pictures were taken with the 40x objective.

3.R.4 *Experimental downregulation of KLF5 in CCA cell lines*

The role of KLF5 in the pathogenesis of CCA was then evaluated by using experimental *KLF5* knock down and knock out approaches in CCA cells.

3.R.4.1 *KLF5 silencing by short hairpin RNA lentiviruses*

KLF5 was knocked down with specific short hairpin RNAs (shRNAs) for KLF5. For that purpose, we produced lentiviral particles from a glycerol stock of shRNA in a pLKO.1-puro-CMV-tGFP vector (from Sigma). A non-target control was also purchased and control lentiviruses were produced in parallel. All procedures were performed as described in materials and methods section (see above). Two different CCA cell lines (i.e. EGI1 and WITT) were employed for evaluating KLF5 silencing. EGI1 CCA cells were infected with shRNA-KLF5 or shRNA-control lentiviruses at different multiplicity of infection (MOI) and selected with puromycin. We determined that at MOI of 5 cells were properly infected with both lentiviruses and that KLF5 was effectively silenced with shRNA-KLF5 lentiviruses (Figure 3.R.8). Therefore, a MOI of 5 was used along the study.

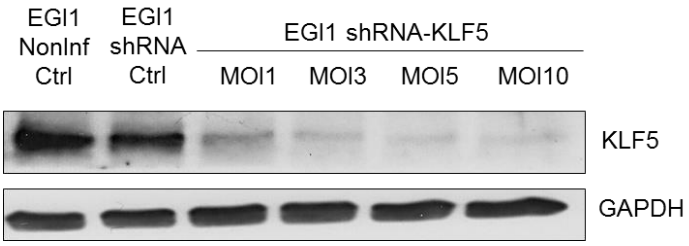

Figure 3.R.8. Experimental silencing of KLF5 expression with shRNA lentiviruses in CCA (EGI1) cells. Representative immunoblot of KLF5 expression in total protein extracts of CCA (EGI1) cells non-infected or infected with shRNA-control or shRNA-KLF5 lentiviruses at the indicated MOIs. GAPDH was used as housekeeping control.

Moreover, KLF5 expression was determined along the CCA (EGI1) cell passages after infection with shRNA-KLF5 or shRNA-control lentiviruses. The

expression of KLF5 was partially recovered 5 passages post-infection in CCA cells infected with shRNA-KLF5 lentiviruses (Figure 3.R.9). Therefore, all the experiments were performed using CCA cells with less than 5 passages post-infection.

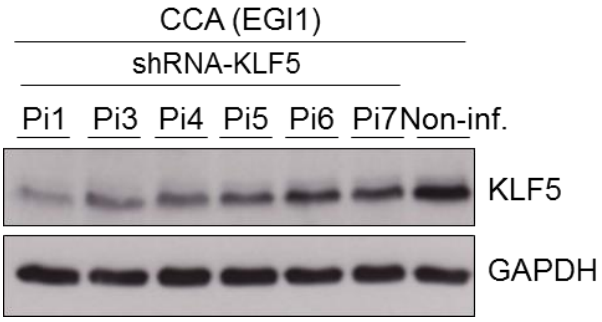

Figure 3.R.9. Expression of KFL5 protein in CCA (EGI1) cells along the cell passages *in vitro* after infection with specific shRNA lentiviruses. Representative immunoblot of KLF5 expression in total protein extracts of CCA (EGI1) cells along the cell passages *in vitro* after infection with specific shRNA lentiviruses. Non-infected cells were used as control. GAPDH was used as housekeeping control.

In addition, experimental KLF5 knock down was also carried out in another type of CCA human cells, i.e. Witt, compared both to non-infected cells and cells infected with shRNA-control lentiviruses (Figures 3.R.10).

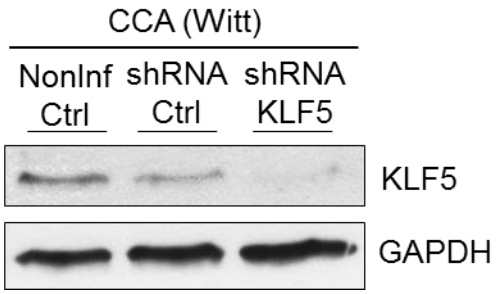

Figure 3.R.10. Expression of KFL5 protein in Witt CCA cells after infection with specific shRNA lentiviruses. Representative immunoblot of KLF5 expression in total protein extracts of CCA (Witt) cells after infection with specific shRNA lentiviruses. Non-infected or shRNA-control-infected cells were used as control. GAPDH was used as housekeeping control.

3.R.4.2 *Genetic knock out of KLF5 by CRISPR/Cas9 technology in CCA cells*

CRISPR/Cas9 is a novel methodology that enables to specifically knock out a particular gene of interest. The development of specific KLF5 knock out CCA

cells through CRISPR/Cas9 would allow us to obtain stable cells without KLF5 and compare the cell phenotype with the results obtained by knocking down KLF5 with specific shRNA-KLF5. Five different guides were first designed as described in the materials and methods section (see above) and cloned in the Cas9 expressing plasmid (i.e. px330). Three out of five guides were successfully cloned (see Figure 3.R.11 as an example).

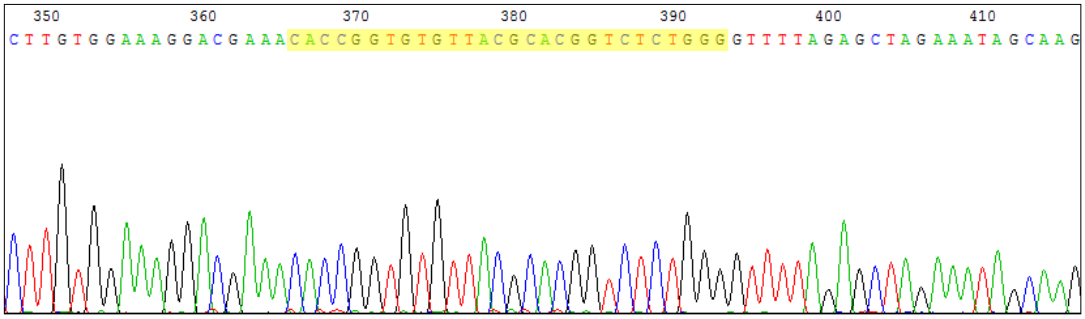

Figure 3.R.11. Guide cloning in the Cas9 expressing plasmid. Example of a cloned guide highlighted in yellow. Three different guides were successfully cloned into the px330 vector.

Next, CCA (EGI1) cells were transfected and selected by GFP-sorting. Individual clones were expanded and Sanger sequencing was performed in the KLF5 gene sequence. Samples with no mutations and with heterozygous mutations were discarded and only clones with homozygous mutations were selected. Of note, five CCA cell clones with different KLF5 mutations were obtained by using the guide 2. Changes in each clone are described in Table 3.R.1.

Table 3.R.1. Mutations in *KLF5* gene sequence by Sanger sequencing.

	Clone number	Alteration
CRISPR/Cas9 Guide 2	Clone 2	Removal of 30 bases
	Clone 3	Insertion of a new base: heterozygous C/G
	Clone 12	Removal of 2 bases
	Clone 16	Removal of 9 bases
	Clone 20	Removal of 23 bases

The expression of KLF5 was then evaluated at protein level in all five KLF5-mutated clones. Immunoblot analysis showed that at least four clones had

alterations on KLF5 expression and/or changes in the protein size (Figure 3.R.12A). Taking into account the alteration produced in the *KLF5* gene sequence and subsequent KLF5 protein expression and size, both clone 2 and 20 were selected for further analysis.

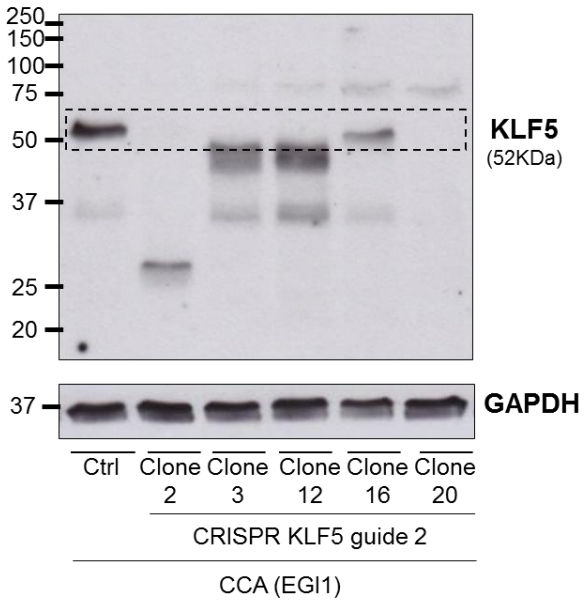

Figure 3.R.12. KLF5 is effectively mutated by CRISPR/Cas9 technology in CCA (EGI1) cells. Representative immunoblot of KLF5 expression in total protein extracts of wild-type or CRISPR/Cas9-KLF5 CCA (EGI1) cells. GAPDH was used as housekeeping control.

3.R.5 *Role of KLF5 in CCA progression in vitro*

Different assays were carried out to test the role of KLF5 in CCA. For this purpose, KLF5-silenced CCA (EGI1 and Witt) cells were used. For KLF5 silencing, both shRNA- and CRISPR/Cas9-based methodologies were employed. Since the results obtained with both methodologies were similar, this report only shows the data on CRISPR/Cas9 as representative.

3.R.5.1 *Role of KLF5 in CCA cell proliferation*

We analyzed the cell cycle profile using the CRISPR/Cas9 cells or the control cells and results showed that *KLF5* knock out induces cell cycle arrest in G0/G1 phase (Figure 3.R.13).

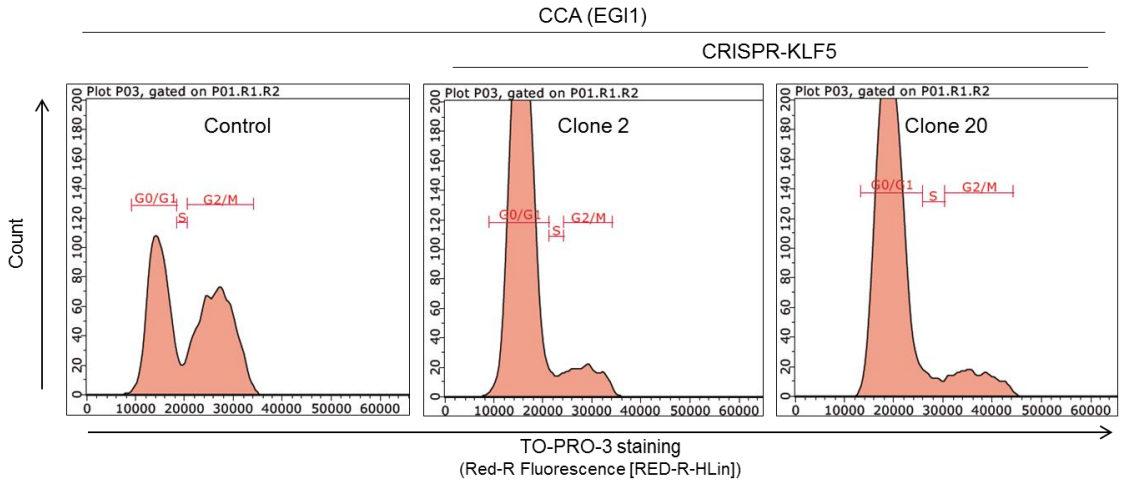

Figure 3.R.13. *KLF5* knock out induces G0/G1 cell cycle arrest in CCA cells. Flow-cytometry based analysis by TO-PRO-3 staining of cell cycle profile in wild-type or CRISPR/Cas9-KLF5 CCA cells.

Next, the expression of genes related to proliferation was determined by qPCR. The expression of the several proliferation markers (i.e. *cyclin D1, Cdc25a, PCNA,* and *Ki67*) was determined and found downregulated in CCA cells knocked out for *KLF5* (Figure 3.R.14).

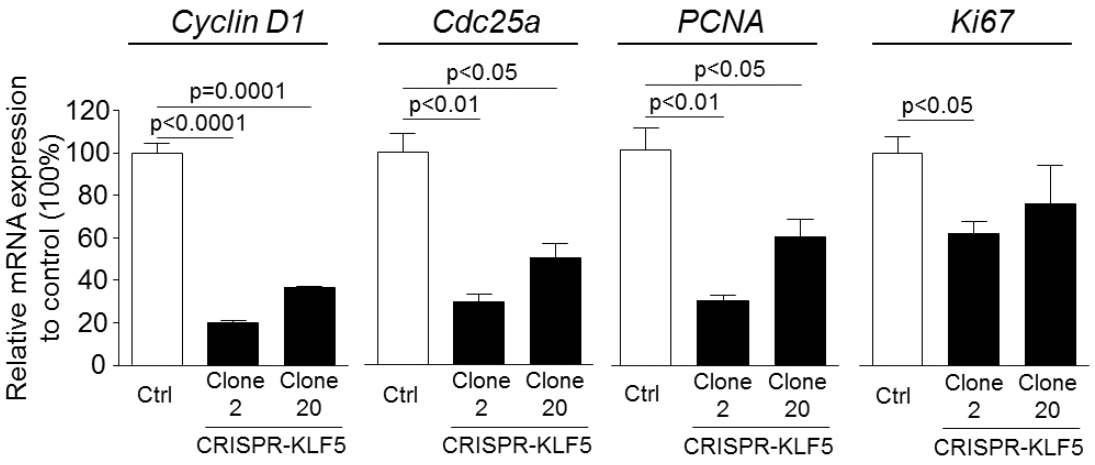

Figure 3.R.14. Expression of cell proliferation markers in CCA cells upon CRISPR/Cas9-based *KLF5* knock out. The mRNA expression of proliferation genes (i.e. *cyclin D1*, *Cdc25a, PCNA*, and *Ki67*) in wild-type or CRISPR/Cas9-KLF5 CCA cells (n=3).

3.R.5.2 *Role of KLF5 in CCA migration*

KLF5 knock out CCA (EGI1) cells have decreased migration properties compared to wild-type cells by using both wound-healing and transwell migration assay (Figure 3.R.15A and B, respectively).

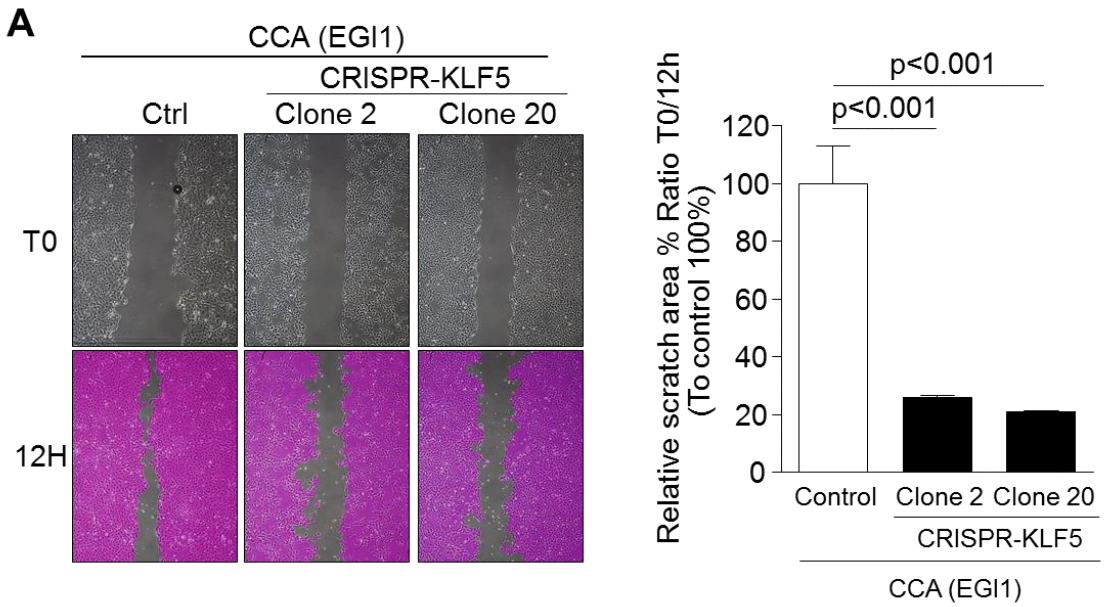

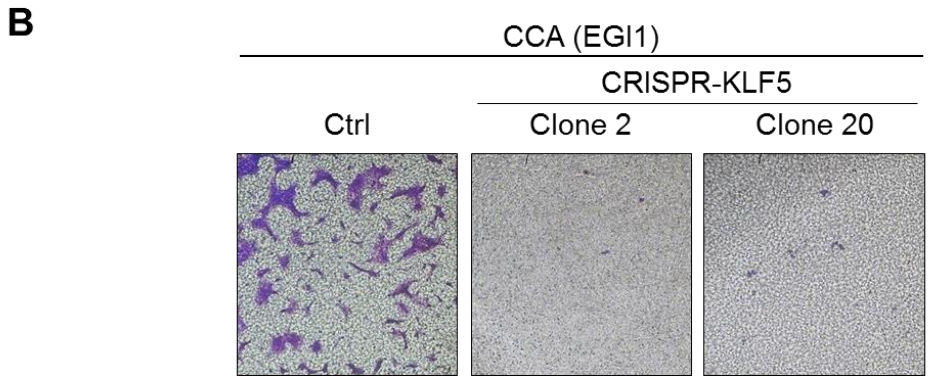

Figure 3.R.15. KLF5 regulates cholangiocyte migration in CCA cells *in vitro*. Migration was determination by wound-healing and transwell migration assays in wild-type or CRISPR/Cas9-*KLF5* CCA cells. **(A)** Representative wound-healing images and corresponding quantification at 12 h (n=6). **(B)** Representative transwell migration chamber images at 24 h.

Migration-related genes were also analyzed by qPCR in wild-type and CRISPR/Cas9-KLF5 CCA cells. Data showed decreased expression of *RhoA* and *Rac1* in *KLF5* knockout clones compared to control CCA cells (Figure 3.R.16).

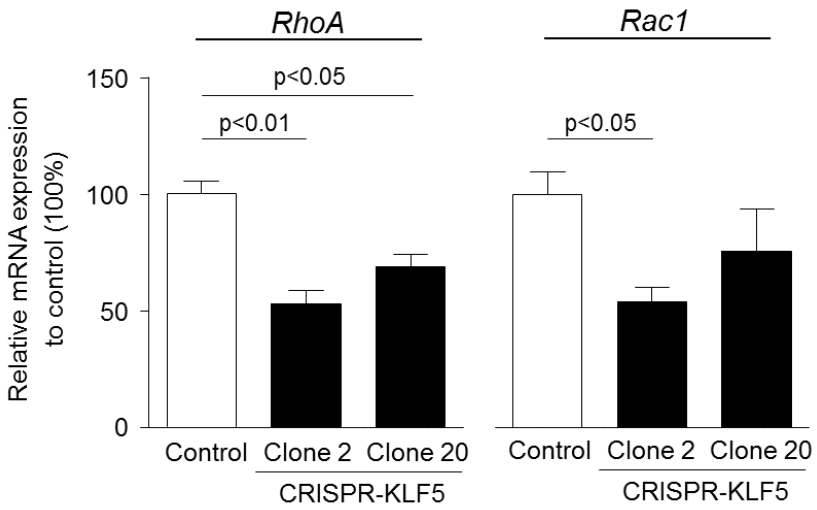

Figure 3.R.16 Expression of migration-related genes under *KLF5* silencing in CCA cells. Relative mRNA expression of genes involved in cell migration (i.e. *RhoA* and *Rac1*) in wild-type or CRISPR/Cas9-KLF5 CCA cells (n=3).

3.R.5.3 *Role of KLF5 in CCA response to cytotoxic bile acids*

Since CCA arises more frequently under cholestatic conditions [45], the role of KLF5 was evaluated on cell viability under the presence or absence of toxic bile acids (BAs) (i.e. CDCA 100 µM) that induces apoptosis. Data showed that CDCA reduced cell viability in wild-type CCA cells, but this effect was more marked in *KLF5* knock out CCA cells (Figure 3.R.17).

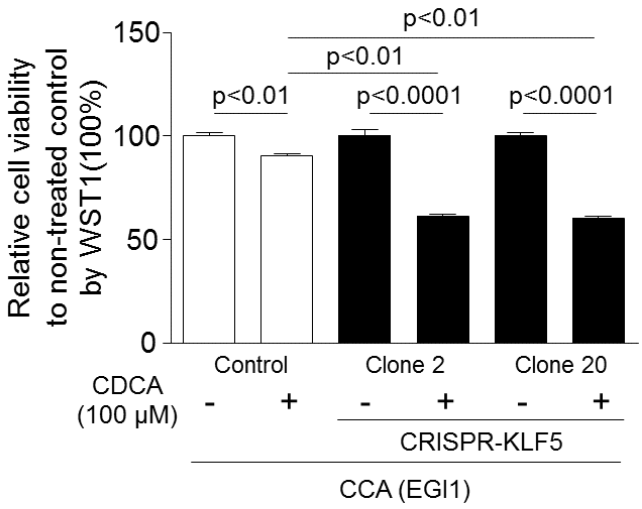

Figure 3.R.17. KLF5 promotes cell viability in CCA cells under the presence of toxic bile acids. Quantification of cell viability in wild-type *vs* CRISPR-KLF5 CCA cells under the presence or absence of CDCA in DMEM/F-12 supplemented with 3% FBS/1% P/S (n=6).

3.R.6 *Role of KLF5 in the CCA response to chemotherapy*

The effect of four different chemotherapeutics (i.e. gemcitabine, 5-fluorouracil, cisplatin and doxorubicin) was evaluated on the survival of wild-type and *KLF5* knock out CCA cells. Dose-dependent studies were carried out with each drug in wild-type CCA cells and specific doses were selected for further experiments (data not shown). Data showed that *KLF5* knock out CCA cells showed decreased cell viability under the presence of gemcitabine, cisplatin, gemcitabine+cisplatin, or doxorubicin than wild-type cells (Figure 3.R.18). In contrast, this effect was not observed under the presence of 5-FU.

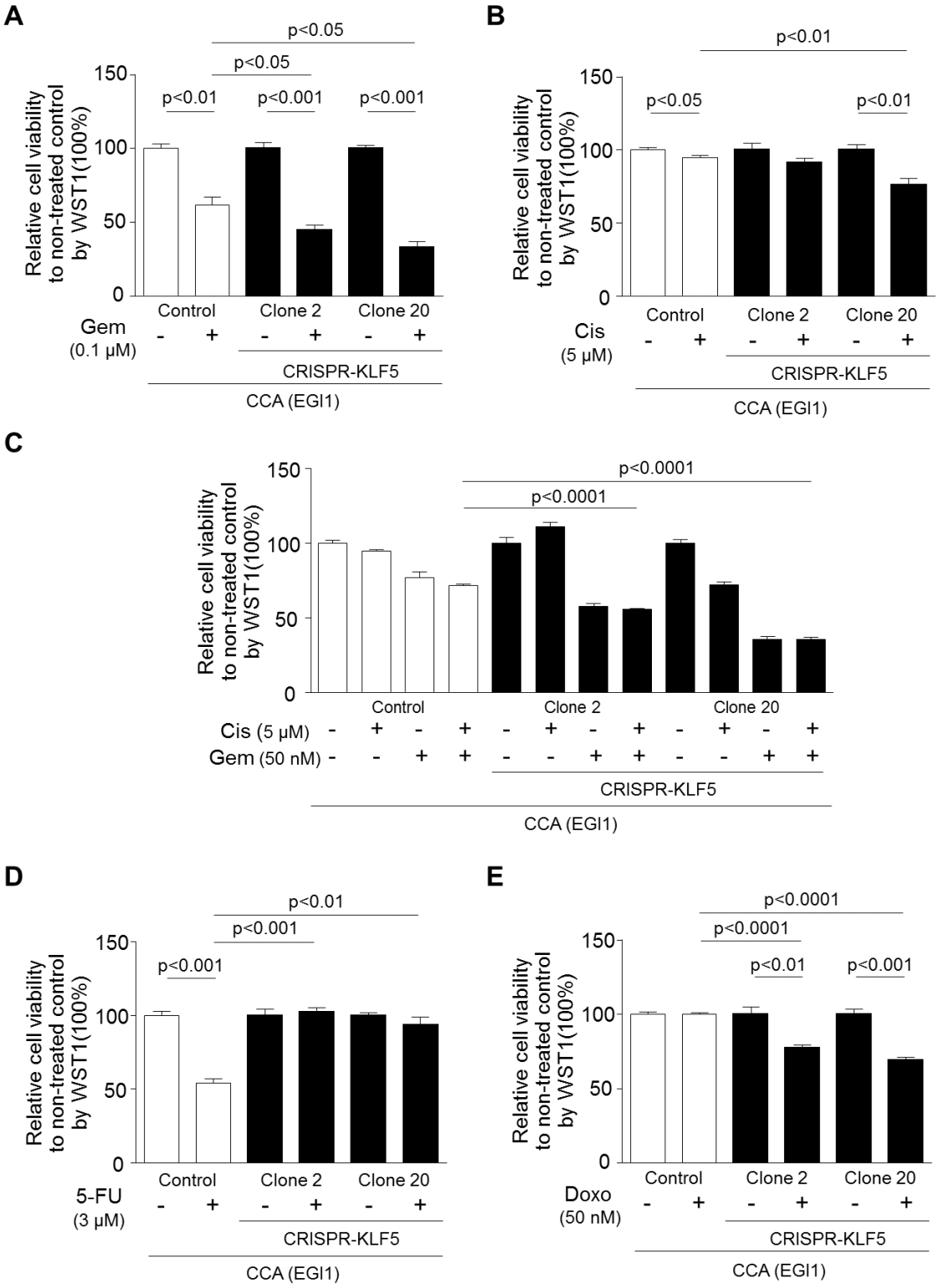

Figure 3.R.18. Cell viability under treatment with chemotherapy. Cell viability was tested in EGI1 CCA cells with CRISPR/Cas9-mediated *KLF5* silencing or EGI1 wild-type cells by WST-1 assays upon treatment with different chemotherapeutics for 72 h in DMEM/F-12 supplemented with 1% FBS/ 1% P/S. **(A)** 0.1 µM gemcitabine (Gem) treatment (n=3). **(B)** 5 µM cisplatin (Cis) treatment (n=4). **(C)** 5 µM Cis and 50 nM Gem treatment (n=4-6). **(D)** 3 µM 5-fluorouracil (5-FU) treatment (n=3). **(E)** 50 nM doxorubicin (Doxo) treatment (n=4).

3.R.7 *Role of KLF5* in the subcutaneous implantation and growth of CCA cells in immunodeficient mice

Wild-type and CRISPR/Cas9-KLF5 CCA (EGI1) cells transfected with a luciferase expressing vector were subcutaneously injected in the flanks of immunodeficient mice and tumor growth was monitored by luciferase expression and by tumor size measurement using a caliber. For this purpose, the CRISPR/Cas9-KLF5 CCA clone 20 was selected. Results showed that *KLF5* knock out dramatically impaired the CCA cell implantation and/or growth subcutaneously in immunodeficient mice compared to wild-type cells (Figure 3.R.19).

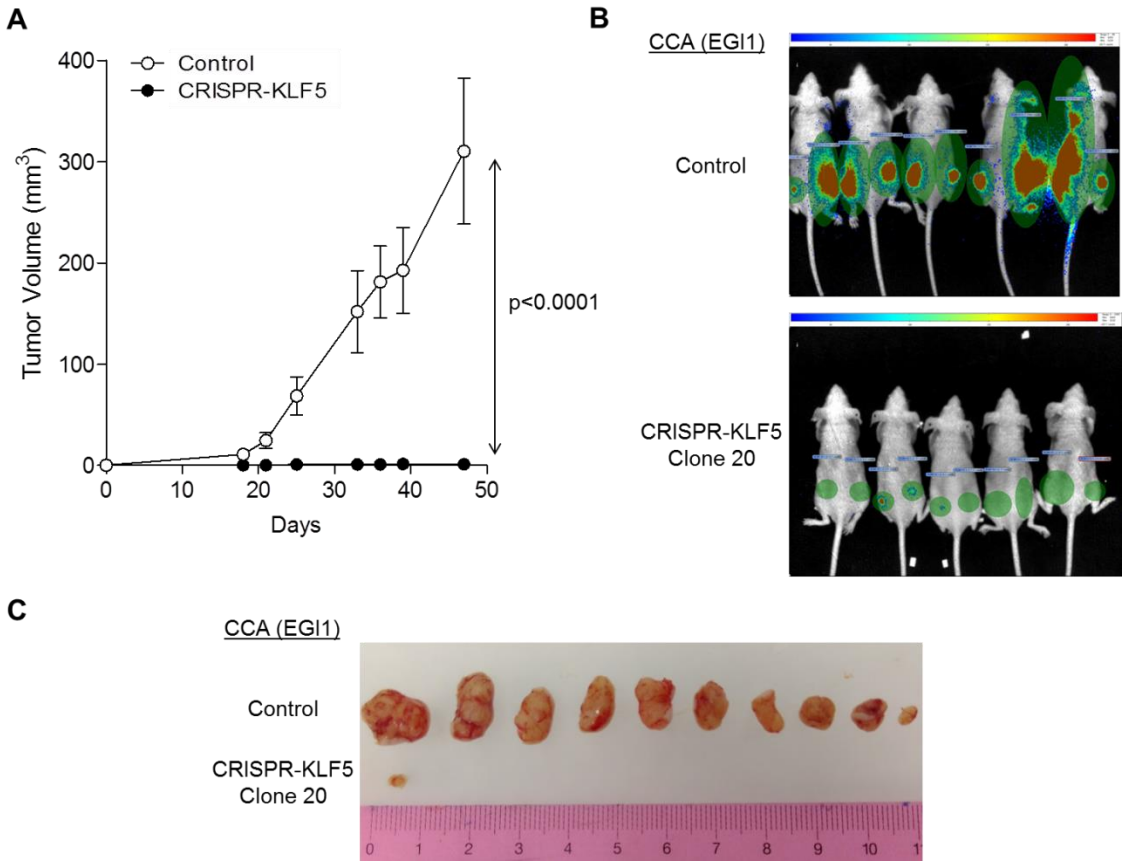

Figure 3.R.19. KLF5 promotes CCA implantation and grow subcutaneously in immunodeficient mice. (A) Tumor volume growth in wild-type *vs* CRISPR-KLF5 CCA cells injected subcutaneously in immunodeficient mice. **(B)** Luciferase expression of wild-type *vs* CRISPR-KLF5 CCA tumors. **(C)** Image of wild-type and CRISPR-KLF5 CCA tumors extracted at the end of the experiment.

3 - Discussion

CCAs, similarly to other cancers, are characterized by alterations in transcription factors (TFs) upstream of genes involved in tumorigenesis [77, 243]. The family of TFs Krüppel-like factors (KLFs) are widely expressed in human tissue and play important roles in health and disease [246], and for instance the expression and activity of certain KLFs are altered in some types of cancer [247]. However, very limited information is available about their role in biliary pathophysiology and particularly in CCA. The analysis of the expression of the different KLFs in normal and tumor cholangiocytes in culture revealed a differential expression pattern between both types of cells. In particular, *KLF5* was the only *KLF* significantly and homogeneously overexpressed in all CCA cell lines compared normal human cholangiocytes (NHC) in culture. The expression of *KLF5* was also found upregulated in CCA human tissue from three independent CCA cohorts of patients compared to controls. These results are in line with previous observations in other cancer types such as breast cancer [275], prostate cancer [276] and stem-like esophageal cancer cells [277], where KLF5 was also found overexpressed. Moreover, our data also indicate that *KLF5* expression in CCA is associated with some clinicopathological features of the tumors such as lymph node invasion. Those CCA tumors with lymph node invasion presented higher expression levels of KLF5 than those tumors without lymph node invasion, suggesting KLF5 as a potential prognostic marker. In this regard, KLF5 has previously been suggested as a potential prognostic factor for disease-free survival and overall survival in breast cancer [275].

The relevant role of KLF5 in CCA pathology was highlighted here by using KLF5 loss-of-function studies in CCA cells. The results revealed that KLF5 promotes CCA cell cycle progression and migration, events associated with overexpression of different genes involved in both processes. KLF5 has been previously described to promote cell proliferation via cyclin D1 stimulation [278] or both p27 and p15 repression [279]. Regarding migration, our data are consistent with a recent report in breast cancer describing that the *tumor necrosis factor-α (TNFα)-induced gene TNFAIP2* is a direct target of KLF5, and that both regulate *Rac-1* and *Cdc42* genes, which are members of the Rho

superfamily of GTPases that, among other functions, regulate cell motility [267, 280]. Moreover, KLF5 modulates the sensitivity of CCA cells to cytotoxic BAs, which are elevated under cholestasic conditions. Indeed, experimental silencing of KLF5 expression decreased the viability of CCA cells under the presence of toxic-BA compared to control CCA cells. The anti-apoptotic effect of KLF5 in CCA cells is in agreement with reports showing that KLF5 targets the apoptosis inhibitor survivin (also known as BIRC5) in ovarian cancer [281] or leukemia [258] and the survival kinase Pim1 [282].

On the other hand, our data strongly indicated that KLF5 may be important in response to chemotherapy. CCAs are highly chemoresistant tumors and chemotherapy is only administered as adjuvant after transplantation or as a palliative strategy for patients with unresectable or metastatic disease [43, 45]. Thus, chances of success for CCA patients with current available drugs are very low and this is related to the mechanisms of chemoresistance (MOCs) present on these tumors [45]. Our results indicated that KLF5 in CCA cells induces resistance to doxorubicin, cisplatin also gemcitabine. Doxorubicin is an anthracycline with topoisomerase II inhibition properties that induces double-strand break in the DNA [283] and is widely used as anti-tumor therapy [284, 285], although it is not commonly used in CCA clinical practice. However, *in vitro* studies showed CCA cells are sensitive to it, with beneficial effects upon combination with approaches such as NF-kB activity inhibition [286]. Cisplatin is a platinum compound approved by the FDA for cancer treatment, which overall acts binding to purine residues, subsequently causing DNA damage, impairing cell division and inducing cell apoptosis [287]. Gemcitabine is a nucleoside analog used against a wide variety of tumors, including CCA [288] which mainly inhibits DNA synthesis through blocking cytidine during DNA replication and arresting cell growth [289]. In CCA, combination of cisplatin and gemcitabine (CisGem) is the referent chemotherapy for CCA patients, which slightly improves their overall survival [288, 290]. Of note, KLF5-silenced CCA cells were more sensitive to CisGem than control CCA cells; albeit the benefits with the combination *vs* monotherapy are small, as low additive effect was observed. The MOCs induced by KLF5 in CCA cells should be analyzed in detail in the next future. These relevant results are rather novel since little information is available on the role of KFL5 in the regulation of response to chemotherapy in

cancer, and, indeed, the available studies pointed KLF5 might be involved in chemoresistance in ovarian cancer and in breast cancer [281, 291, 292], what is in accordance to our results in CCA.

Furthermore, the *in vivo* studies revealed that KLF5 is crucial for CCA tumor implantation and growth subcutaneously in immunodeficient mice. In our model, only 1 out of 10 tumors was able to grow in the CRISPR-KLF5 group compared to 10/10 tumors in the control group. In this regard, we are currently evaluating the role of KLF5 in CCA under intravenous or intrahepatic injection of cells, i.e. models of metastasis or liver cancer, respectively.

Altogether, these data strongly suggest KLF5 as a potential therapeutic target in CCA. In the last years, several studies have focused on identifying selective KLF5 inhibitors. In this regard, KLF5 expression or activity is indirectly regulated by different inhibitors of general key cellular pathways such as RAR-ligands or some MEK, HDAC or PI3K inhibitors. Moreover, specific KLF5 inhibitors have been developed by ultra-high-throughput screening (uHTS) in colon cancer cell lines and are under study [265]. Recently, ML264 (Sigma) has been produced as the most promising KLF5 inhibitor, showing effective antitumoral activity in colorectal cancer [274]. Therefore, future studies will be carried out by using this new inhibitor in experimental (*in vitro* and *in vivo*) models of CCA.

KLF5 gain-of-function studies using lentiviruses overexpressing KLF5 in NHCs would help to further elucidate the role of this TF in the process of CCA development. In this regard, our preliminary data (not shown) indicate that KLF5 promotes migration and confers resistance to chemotherapy in NHCs, highlighting the role of KLF5 in the malignant transformation of cholangiocytes.

It was previously reported that KLF5 expression is stimulated by RAS/MAPK/PI3K and WNT signaling pathways [274], and whether certain growth factors (i.e. EGF and Wnt3a) and pro-inflammatory (i.e. IL1β) or pro-fibrogenic (i.e. TGFβ) cytokines found commonly overexpressed in the CCA microenvironment participate in its regulation should be clarified. For instance, both IL1β and HIF1α have been described as promoters of KLF5 expression in pancreatic cancer [257]. On the other hand, TGFβ-mediated acetylation of KLF5 results in differential KLF5 function in epidermal cells. In the presence of TGFβ, this recruits acetylase p300 to acetylate KLF5, and this leads to altered binding

of KLF5 to the promoter of the cell cycle inhibitor p15, resulting in the reversal of KLF5 function [293]. On the other hand, studies in breast cancer pointed KLF5 as a potential target for triple negative breast cancer and have shown that its expression is regulated by miR-217 [294]. Thus, it would be interesting to analyze how KLF5 becomes overexpressed in CCA. Importantly, FBW7 (F-box and WD repeat domain-containing 7, also known as CDC4, AGO and SEL10) targets KLF5 for its degradation through the proteasome [295]. FBW7 is part of the E3 ubiquitin ligase complex and mediates the ubiquitin-dependent proteolysis, targeting many substrates including *cyclin E*, *c-Myc* or *Mcl-1*, [295]. Mutations in FBW7 resulted in the inactivation of this gene and FBW7 is known as a tumor suppressor gene. Of note, CCAs are the tumors with the highest rates in FBW7 mutations, with a 35% of frequency [296]. In this regard, FBW7 was seen downregulated in CCA cells and biopsies and was associated to tumor metastasis [297]. Additionally, a recent work has shown that the isoform α of FBW7 is important in CCA progression, as its experimental overexpression using lentiviruses resulted in the inhibition of CCA cell proliferation as well as in CCA growth impairment *in vivo* [298].

3 - Conclusions

The key findings reported here are related to the role of Krüppel-like factors (KLFs) in the etiopathogenesis of CCA and indicate that KLF5 acts as an oncogene promoting CCA progression. Our data indicate that:

I. The expression of *KLF* family members is dysregulated in CCA cells compared to NHC in culture.
II. KLF5 is overexpressed in different CCA cell lines compared to primary cultures of NHC. This KLF5 overexpression was mainly found in the nucleus of CCA cells.
III. In three different cohorts of patients, *KLF5* was found overexpressed in human CCA tissue compared to normal surrounding liver tissue. *KLF5* expression correlated with lymph node invasion.
IV. Experimental *KLF5*-silenced CCA cells showed reduced cell cycle progression, migration and viability under the presence of toxic bile acids or different chemotherapeutics.
V. *KLF5* knock out CCA cells presented impaired subcutaneous implantation and/or growth in immunodeficient mice compared to controls.

Our results are consistent with the notion that KLF5 is a relevant TF in CCA development and progression, as well as a potential diagnostic/prognostic biomarker and a target for therapy.

VI. SUMMARY IN SPANISH (RESUMEN EN ESPAÑOL)

INTRODUCCIÓN GENERAL

El hígado es uno de los órganos más importantes del cuerpo humano, realizando funciones claves tales como el metabolismo de proteínas, aminoácidos y lípidos, detoxificación y producción de bilis [1, 2]. El hígado está formado por dos tipos de células epiteliales, hepatocitos y colangiocitos, que representan el ~70% y ~3-5% de la población celular hepática, respectivamente [3, 4]. Los colangiocitos, pese a ser una pequeña proporción de todas las células del hígado, participan en procesos clave para el correcto funcionamiento del hígado, tales como la fuidificación y alcalinización de la bilis generada en el canalículo de los hepatocitos [5-8]. Para ello, contienen diversos transportadores específicos de membrana que participan en el intercambio de electrolitos, ácidos biliares y metabolitos, entre otros [4, 9-11].

Las enfermedades que afectan a los colangiocitos se conocen como colangiopatías, y se clasifican en: *i*) inmuno-asociadas, *ii*) infecciosas, *iii*) genéticas, *iv*) asociadas con alteraciones vasculares, *v*) neoplásicas, *vi*) inducidas por sustancias tóxicas, o *vii*) idiopáticas [15]. Se trata de un grupo heterogéneo de enfermedades que suelen estar caracterizadas por procesos inflamatorios crónicos y por presencia de colestasis. Sin embargo, dichas enfermedades presentan sus propias particularidades que determinan la historia natural de cada enfermedad [15]. Pese a ser enfermedades poco frecuentes, las colangiopatías presentan elevada morbilidad y mortalidad [15]. En la actualidad, debido a la escasez de tratamientos eficaces frente a las distintas colangiopatías, es clave investigar en detalle la etiopatogenia de estas enfermedades para poder así aportar nuevas dianas y estrategias terapéuticas.

Este trabajo de tesis doctoral se centra en el estudio de dos enfermedades biliares, como lo son la colangitis biliar primaria (CBP) (del inglés *primary biliary cholangitis*, PBC) – asociada con procesos autoinmunes frente a los colangiocitos – y en el colangiocarcinoma (CCA) – cáncer biliar–. En concreto, se han llevado a cabo 3 trabajos, evaluando el papel del miR-506 en la etiopatogenia de la PBC y el de los receptores de ácidos biliares FXR y TGR5, así como del factor de transcripción KLF5, en el CCA.

CAPÍTULO 1: PAPEL DEL MIR-506 EN LA COLANGITIS BILIAR PRIMARIA (PBC)

Introducción

La colangitis biliar primaria (CBP, en inglés *primary biliary colangitis* o PBC) es una enfermedad hepática colestásica crónica asociada con procesos auto-inmunes frente a los conductos biliares intrahepáticos pequeños y medianos [22, 24]. Existen varios estadios de la enfermedad caracterizados por un aumento progresivo de colestasis y fibrosis hepática [25], que sin tratamiento efectivo pueden evolucionar en cirrosis hepática [26-29]. La etiología de la PBC permanece todavía desconocida pero se cree que es multifactorial. Afecta mayoritariamente a mujeres de mediana edad [30, 31] y está caracterizada por el desarrollo (en el ~95% de los casos) de auto-anticuerpos anti-mitocondriales (en inglés *anti-mitochondrial autoantibodies*, AMAs) específicos frente a la subunidad E2 del complejo piruvato deshidrogenasa mitocondrial (en inglés *E2 component of the pyruvate dehydrogenase complex*, PDC-E2) [35]. Es importante destacar que, pese a ser una enfermedad asociada con procesos auto-inmunes, los inmunosupresores habituales no presentan eficacia terapéutica. Actualmente, el único tratamiento aprobado por la "*food and drug administration"* (FDA de Estados Unidos) para el tratamiento de la PBC es la administración diaria y crónica de ácido ursodesoxicólico (en inglés *ursodeoxycholic acid*, UDCA). Se ha comprobado que el UDCA mejora el pronóstico en ~2/3 de pacientes con PBC tratados en estadíos iniciales de la enfermedad [24, 36-38]. Sin embargo, para los pacientes que no responden a la monoterapia con UDCA, se están estudiando tratamientos alternativos con ciertos beneficios terapéuticos, como es el caso del ácido obeticólico (del inglés *obeticholic acid*, OCA), el cual parece mejorar ciertos parámetros de colestasis aunque presenta efectos secundarios importantes [39].

La colestasis de los pacientes con PBC está caracterizada con alteraciones en la secreción biliar de bicarbonato [111, 112], la cual es clave para la fluidificación y alcalinización de la bilis y para proteger al epitelio biliar frente al efecto dañino de los ácidos biliares tóxicos. En humanos, el intercambiador Cl^-/HCO_3^- AE2 (en inglés *anion exchanger 2*, AE2, también conocido como

SLC4A2) es el responsable de la secreción biliar de bicarbonato, estando localizado en la membrana apical de los colangiocitos. Además, AE2 participa en la regulación del pH intracelular (pH_i) de las células biliares [113-115]. Los pacientes con PBC presentan una disminución muy notable en la expresión de AE2 en los colangiocitos, lo cual favorece la colestasis [105]. El papel de AE2 parece ser clave en la etiopatogenia de la PBC, ya que ratones $Ae2^{-/-}$ desarrollan diversas características hepato-biliares e inmunológicas típicas de los pacientes con PBC, incluyendo la presencia de AMAs frente a PDC-E2 [116]. Por otro lado, el receptor inositol 1,4,5-trifosfato tipo 3 (Ins3PR3) parece tener un papel importante en la colestasis de los pacientes con PBC. El Ins3PR3 es una proteína integral de membrana localizada en la región subapical del retículo endoplasmático (en inglés *endoplasmic reticulum*, ER) que favorece la secreción biliar de bicarbonato dependiente de AE2 en los colangiocitos a través de la salida de calcio (Ca^{2+}) desde el ER al citoplasma celular [117, 118]. Al igual que AE2, la expresión del Ins3PR3 se encuentra disminuida en los colangiocitos PBC, favoreciendo también la colestasis [119]. En este sentido, cabe destacar que fue recientemente comprobado que el descenso de expresión de AE2 e Ins3PR3 en los colangiocitos PBC es inducido, al menos en parte, por el miR-506, el cual se encuentra sobre-expresado [105, 120].

Hipótesis y objetivos

El miR-506 parece tener un papel fundamental en la etiopatogénesis de la PBC. Sin embargo, hasta el momento se desconocen los mecanismos que regulan su expresión en los colangiocitos así como el papel del miR-506 en la patogenia de los colangiocitos y en la regulación inmune. Este trabajo pretende estudiar la regulación de la expresión del miR-506 en los colangiocitos y su papel en la patología y activación inmune de la PBC. Para ello, nos propusimos los siguientes objetivos:

I. Análisis de la regulación de la actividad promotora del miR-506 en colangiocitos.

II. Determinación del efecto directo del miR-506 en la fisiopatología de los colangiocitos.

III. Estudio del papel del miR-506 en la regulación inmune en PBC.

Material y métodos

1. *Estudio de la regulación de la actividad del promotor del miR-506 en colangiocitos humanos normales*

Para determinar los mecanismos de regulación de la actividad del promotor del gen humano *miR-506* (hsa-miR-506) en colangiocitos humanos normales se clonaron tres regiones de distinto tamaño del promotor (~3000, ~2000 y ~1000 bp, denominadas Z1, Z2 y Z3, respectivamente) en un vector de expresión que contiene el gen de la luciferasa. Posteriormente se transfectaron colangiocitos humanos (H69) con los tres vectores recombinantes. Tras 6 h de transfección, las células fueron tratadas durante 24 h con diversos estímulos: citoquinas pro-inflamatorias, [en inglés *interleukins (IL) 1β, 6, 8, 12, 17, 18*, *tumor necrosis factor alpha* (TNFα), e *interferon gamma* (IFNγ)], factores pro-fibróticos [en inglés *transforming growth factor beta 1* (TGFβ1)], estrógenos (17β-estradiol), glucocorticoides [dexametasona (DEX)], factores de crecimiento [en inglés *epidermal growth factor* (EGF)] y ácidos biliares [ácidos cólico (CA), ursodesoxicólico (UDCA) y tauroursodesoxicólico (TUCA)]. Posteriormente, las células fueron lisadas y se determinó la actividad luciferasa utilizando un kit de luciferasa (Promega).

2. *Estudio del efecto de la sobre-expresión del miR-506 en colangiocitos humanos normales*

Los colangiocitos humanos H69 fueron transfectados de manera estable utilizando vectores de expresión que contienen la secuencia del miR-506 (H69-miR-506) o una secuencia control (H69-miR-neg) (Thermo Fisher Scientific). Además, se utilizaron también células tratadas con el vehículo de transfección como control. Se determinó el perfil proteómico de las células mediante espectrometría de masas y se analizó la expresión génica de marcadores biliares y epiteliales, así como de marcadores mesenquimales y pro-inflamatorios. Además, se analizó el efecto de la sobre-expresión del miR-506 en la proliferación, adhesión, migración y muerte celular, en el estrés oxidativo y en la actividad metabólica mitocondrial. Por último, se llevaron a cabo co-

cultivos de colangiocitos con sobre-expresión del miR-506 junto con células mononucleares de sangre periférica (en inglés *peripheral blood mononuclear cells*, PBMCs) de una paciente con PBC para determinar el efecto de la sobre-expresión del miR-506 en los colangiocitos sobre la regulación inmunológica.

Resultados y discusión

Diversas citoquinas pro-inflamatorias cuya expresión está aumentada en hígados de pacientes con PBC (i.e. IL8, IL12, IL17, IL18 y TNFα) estimularon la actividad del promotor del gen *miR-506* en colangiocitos humanos normales. Sin embargo, los ácidos biliares, estrógenos y factores de crecimiento evaluados no mostraron efecto sobre la actividad promotora del gen *miR-506*.

La sobre-expresión del miR-506 en colangiocitos inhibió la expresión proteica de AE2 y alteró el perfil proteómico de las células, particularmente afectando a la expresión de proteínas implicadas en procesos metabólicos. Además, el miR-506 inhibió la expresión de diversos marcadores biliares y epiteliales en colangiocitos, y promovió la expresión de genes mesenquimales, inflamatorios y de senescencia. Este fenotipo alterado dio como resultado una disminución de la proliferación, adhesión y migración celular. Por otro lado, el miR-506 estimuló el estrés celular, mediante el aumento de los niveles de especies reactivas de oxígeno (en inglés *reactive oxigen species*, ROS), del estrés de ER y del daño del ADN en los colangiocitos, y sensibilizó a las células a la apoptosis inducida por ácidos biliares citotóxicos habitualmente aumentados en hígados de pacientes con PBC. Los efectos del miR-506 se vieron también asociados a un aumento del metabolismo mitocondrial y de la fosforilación oxidativa – eventos que se dieron junto con un desacoplamiento de la producción de ATP de la respiración mitocondrial –, y también con sobreexpresión de PDC-E2. Finalmente, el miR-506 en colangiocitos promovió la proliferación y activación de los PBMCs de PBC, y estimuló la secreción de las citoquinas pro-inflamatorias IL-17A e IL-23, que participan en procesos de autoinmunidad.

Conclusión

Los hallazgos descritos en este estudio indican que el ambiente inflamatorio presente en el hígado de pacientes con PBC favorece la expresión del miR-506 en los colangiocitos. Dicho miRNA promueve el desarrollo de características fenotípicas típicas de PBC en los colangiocitos, favoreciendo asimismo la activación inmune. Nuestros datos apoyan la idea de que el miR-506 juega un papel clave en la patogenia de la PBC, siendo una posible diana terapéutica.

CAPÍTULO 2: PAPEL DE FXR Y TGR5 EN EL COLANGIOCARCINOMA (CCA)

Introducción

Los CCAs agrupan a un conjunto heterogéneo de tumores que afectan a los colangiocitos [41, 42]. Se trata del segundo tipo de tumor hepático primario más frecuente detrás del carcinoma hepatocelular (en inglés *hepatocellular carcinoma*, HCC), representado el ~3% de los cánceres gastrointestinales [41, 43]. Se trata de tumores asintomáticos en estadios iniciales, siendo generalmente diagnosticados en fases avanzadas, lo cual compromete las posibles opciones terapéuticas [45, 62]. En la actualidad, las únicas opciones potencialmente curativas son la resección quirúrgica del tumor o el trasplante hepático, aunque solo están indicadas en un número reducido de casos que cumplen con criterios estrictos de estadio tumoral [98]. Este hecho, junto con la elevada quimioresistencia que presentan estos tumores [101], hace que el pronóstico de los pacientes CCA sea muy malo a corto plazo. Por ello, es clave esclarecer los mecanismos moleculares involucrados en el desarrollo y progresión de estos tumores para aportar nuevas estrategias terapéuticas efectivas.

En la actualidad, la etiología de la mayoría de los CCAs se desconoce. Sin embargo, un gran número de CCAs aparece en presencia de colestásis [45]. La acumulación de ácidos biliares (ABs) tóxicos puede favorecer el desarrollo y la progresión de tumores gastrointestinales [72]. En este sentido, los ABs tóxicos no inducen carcinogénesis directamente en los colangiocitos, pero pueden favorecer el desarrollo y progresión de los CCAs mediante la estimulación de la inflamación y proliferación de los colangiocitos [183-185]. Los ABs son

moléculas que regulan diversos procesos fisiológicos y patológicos en los colangiocitos, tales como proliferación, secreción o supervivencia celular [157, 181], a través de su unión selectiva por dos tipos de receptores de ABs: el receptor nuclear farnesoide X (del inglés *farnesoid X receptor*, FXR, también conocido como *NR1H4*) [176-179] y el receptor de membrana tipo 1 acoplado a proteína G (TGR5, también conocido como *GPBAR1*) [180].

FXR es el miembro de la superfamilia de receptores nucleares de hormonas más específico para la regulación de la homeostasis y señalización de ABs [158, 176, 186-189]. La expresión de FXR se encuentra aumentada en aquellas células y tejidos expuestos a altas concentraciones de ABs, incluyendo los colangiocitos. FXR está involucrado en funciones tales como el metabolismo de lípidos y glucosa, inflamación, inmumodulación, fibrosis, así como regeneración, diferenciación y proliferación celular [197-201]. TGR5 también es un importante mediador en la homeostasis de ABs y su expresión es más generalizada, con mayor expresión en tejidos como tejido adiposo pardo, cerebro, músculo, placenta, pulmón, intestino, bazo, estómago, vesícula biliar e hígado [158, 210-212]. En los colangiocitos, TGR5 se expresa en la membrana apical, favoreciendo la secreción biliar de bicarbonato [13].

Tanto FXR como TGR5 parecen estar involucrados en el desarrollo y progresión de distintos tipos de cánceres. En este sentido, FXR parece funcionar como supresor tumoral [200] mientras que TGR5 parece ser un promotor tumoral mediante la estimulación de la proliferación y supervivencia celular en diversos tipos de cáncer [220, 240]. Por lo tanto, la regulación funcional de estos receptores de ABs se presenta como posible opción terapéutica para diversas enfermedades. En este sentido, se han desarrollado nuevos derivados de ABs capaces de activar de forma selectiva FXR o TGR5, entre los que se encuentran el ácido obeticólico (en inglés *obeticholic acid*, OCA) y el INT-777, respectivamente. OCA (también conocido como INT-747 o ácido 6α-etil-chenodesoxicólico) es un derivado sintético de AB que activa FXR con gran afinidad y selectividad [205] y que está bajo evaluación clínica para el tratamiento de diversas enfermedades tales como esteatohepatitis no alcohólica (del inglés *non-alcoholic steatohepatitis*, NASH), la colangitis esclerosante primaria (del inglés *primary sclerosing colangitis*, PSC) y atresia biliar [207, 208]. Además, el OCA ha sido aprobado recientemente para el

tratamiento de pacientes con PBC. Por otro lado, el INT-777 (ácido 6α-etil-23(S)-metil-3α,7α,12α-trihidroxil-5β-colan-24-oico) [226] es otro derivado sintético de AB que en este caso activa TGR5 de forma selectiva. Estudios con animales han mostrado que el INT-777 controla la homeostasis de glucosa, previene la aterosclerosis y enfermedad renal diabética, y controla también el aumento de peso y la adiposidad mediante la regulación del AMP cíclico y el consumo energético [227-229].

Hipótesis y objetivos

Dada la importancia de los ABs en el desarrollo y progresión del CCA, este estudio pretende investigar el papel de FXR y TGR5 en la patogenia del CCA, para lo cual evaluará el efecto diferencial de su activación en la progresión tumoral utilizando los agonistas selectivos OCA e INT-777. Para ello, nos propusimos los siguientes objetivos:

I. Análisis de la expresión de FXR y TGR5 en tejido de CCA de 2 cohortes independientes de pacientes y determinación de su asociación con parámetros clinicopatológicos tumorales.

II. Evaluación de la expresión de FXR y TGR5 en colangiocitos humanos normales y tumorales en cultivo.

III. Determinación del efecto de los agonistas de FXR o TGR5 sobre el crecimiento del CCA en un modelo ortotópico en ratones inmunodeficientes.

IV. Estudio de los efectos diferenciales de la activación de FXR o TGR5 en el crecimiento de células de CCA en cultivo.

Material y métodos

1. *Expresión de FXR y TGR5*

La expresión génica de *FXR* y *TGR5* fue determinada mediante PCR cuantitativa en tejido de CCA e hígado normal de 2 cohortes diferentes de pacientes – cohortes de ‘San Sebastian’ y ‘Copenhagen’ –, así como en líneas celulares humanas de CCA (EGI1 y TFK1) y colangiocitos humanos normales (NHC) en cultivo.

2. *Efecto de OCA e INT-777 sobre un modelo animal de CCA humano ortotópico*

Se estableció un modelo de CCA humano en hígado de ratones inmunodeficientes mediante la implantación de tumores derivados de células humanas de CCA (EGI1). El crecimiento tumoral en el hígado fue monitorizado mediante resonancia magnética (en inglés *magnetic resonance imaging*, MRI) durante 2 meses de tratamiento con OCA o INT-777 (Intercept Pharmaceuticals) en dieta (0.03%). Posteriormente, se analizó la expresión de marcadores de proliferación en los tumores mediante PCR cuantitativa e inmunohistoquímica.

3. *Efecto de la administración de OCA e INT-777 en colangiocitos normales y tumorales en cultivo*

Se utilizaron células de CCA (EGI1 y TFK1) y NHC en cultivo para determinar el efecto de OCA e INT-777 sobre su proliferación, apoptosis (ambos por citometría de flujo), migración (por "*wound-healing*" y "*transwell*") y/o metabolismo energético mitocondrial (por Seahorse).

Resultados y discusión

La expresión de *FXR* se encuentra disminuida y la de TGR5 aumentada en tejido tumoral de CCA humano en comparación con tejido hepático sano adyacente. La expresión de *FXR* correlaciona con el grado de diferenciación tumoral mientras que la de *TGR5* correlaciona con la invasión tumoral perineural. La expresión de *TGR5* es mayor en CCAs perihilares que en intrahepáticos. *In vitro*, la expresión de *FXR* está disminuida mientras que la de *TGR5* está aumentada en células de CCA en relación a NHC en cultivo. En ratones con implantes ortotópicos de tumores de CCA humanos, la administración crónica de OCA inhibió el crecimiento tumoral en comparación con animales control no tratados. Este hecho fue acompañado por una disminución de la expresión de marcadores de proliferación en los tumores. Por el contrario, la administración crónica de INT-777 *in vivo* no mostró efectos en el crecimiento tumoral. *In vitro*, OCA inhibió la proliferación y migración de las células de CCA, evento asociado con una disminución del metabolismo

energético mitocondrial, y sin afectar a la apoptosis. Por el contrario, INT-777 estimuló la proliferación y la migración de las células de CCA, evento asociado con el aumento del metabolismo energético mitocondrial.

Conclusiones

Este estudio proporciona nuevo conocimiento sobre el potencial valor terapéutico de la regulación de la actividad de FXR y/o TGR5 en CCA. La activación de FXR por OCA inhibe el crecimiento del CCA, mientras que la activación de TGR5 mediante INT-777 no muestra actividad inhibidora e incluso puede promover la progresión del CCA. Estos efectos están mediados, al menos en parte, por el efecto diferencial de la activación de FXR o TGR5 sobre la proliferación, migración y metabolismo energético mitocondrial en las células de CCA. Además, la correlación de la expresión de FXR o TGR5 con importantes características clínico-patológicas como la diferenciación tumoral y la invasión perineural, respectivamente, pueden tener importante valor pronóstico. Por lo tanto, nuestros resultados indican que FXR y TGR5 son posibles dianas terapéuticas para el tratamiento de los pacientes con CCA.

CAPÍTULO 3: PAPEL DEL FACTOR DE TRANSCRIPCIÓN KLF5 EN EL COLANGIOCARCINOMA (CCA)

Introducción

El desarrollo y progresión del colangiocarcinoma (CCA), al igual que otros tumores, está regulado por factores de transcripción (FT) involucrados en procesos de proliferación, diferenciación y supervivencia, entre otros. Se han descrito alteraciones en la expresión de diversos FT que regulan diferentes características del CCA [77], siendo su regulación potencialmente terapéutica. En los últimos años se ha descrito el papel de la familia de FT tipo Krüppel (en inglés *Krüppel-like factor*, KLF) en diversos procesos biológicos y patológicos, incluido el cáncer. Sin embargo, su papel en la fisiopatología del epitelio biliar y en el CCA permanece prácticamente desconocido. La familia de KLFs consta de 17 miembros, los cuales contienen tres dedos de zinc con una región bien

conservada en su región carboxi-terminal para la unión al DNA y una región amino-terminal variable entre los miembros [246]. Es esta última región la que determina la función de cada KLF a través de su unión a co-activadores, co-represores o modificadores como las histona acetiltransferasas. Además, los KLFs pueden sufrir modificaciones post-transduccionales que regulan su función y actividad transcripcional [246]. Este trabajo se centra en el estudio de la expresión de los KLFs en colangiocitos normales y tumorales en cultivo, y en particular en el análisis del papel de KLF5 en la etiopatogenia del CCA.

Hipótesis y objetivos

Los factores de transcripción KLF están involucrados en el desarrollo y progresión de diversos cánceres, no obstante, su papel en CCA es desconocido. Nuestros datos preliminares de expresión de KLFs en CCA mostraron que KLF5 se encuentra altamente sobre-expresado en colangiocitos tumorales en comparación con colangiocitos normales, indicando su posible relevancia en la colangiocarcinogénesis. Este estudio pretende analizar el papel de KLF5 en la patogenia del CCA y determinar el posible valor terapéutico de su regulación. Los objetivos del estudio son:

I. Analizar la expresión de los distintos KLF en líneas celulares de CCA en comparación con colangiocitos normales.

II. Analizar la expresión de KLF5 en tejido de CCA en comparación con controles hepáticos no tumorales.

III. Evaluar el papel de KLF5 en la patogénesis del CCA *in vitro*.

IV. Estudiar el papel de KLF5 en la respuesta del CCA a la quimioterapia *in vitro*.

V. Determinar el papel de KLF5 en la patogénesis de CCA *in vivo*.

Material y métodos

1. *Expresión de KLFs en colangiocitos normales y tumorales, así como en tejido de pacientes con CCA e hígado normal*

*S*e llevaron a cabo análisis de expresión de los distintos KLFs a nivel de RNA mensajero mediante PCR cuantitativa. Para ello, se utilizaron líneas celulares

de CCA humano (EGI1, TFK1 y Witt, entre otras) así como cultivos primarios de colangiocitos humanos normales (NHC2, NHC3, NHC-SS y C324) y colangiocitos humanos no tumorales inmortalizados con el oncogen SV-40 (células H69). Por otro lado, se analizaron muestras de tejido de CCA e hígado sano adyacente al tumor de 3 cohortes diferentes de pacientes ("Copenhagen", "TCGA" y "San Sebastian") para la determinación de la expresión génica de *KLF5*. Además, se analizó la expresión proteica de KLF5 mediante inmunoblot e inmunofluorescencia en los colangiocitos normales y tumorales en cultivo, y también mediante inmunofluorescencia en tejido de pacientes con CCA.

2. *Inhibición de la expresión de KLF5 en células de CCA mediante RNA de interferencia y tecnología CRISPR/Cas9 y análisis de su papel funcional in vitro*

Tras la determinación de la expresión de los KLFs en colangiocitos normales y tumorales en cultivo, se comprobó que KLF5 se encuentra altamente sobre-expresado en diversas líneas celulares de CCA en comparación con NHC. Para poder estudiar el efecto funcional de dicha sobre-expresión, se procedió a la inhibición o anulación de la expresión de KLF5 mediante partículas lentivirales con shRNAs específicos o tecnología CRISPR/Cas9, respectivamente. Posteriormente, se analizó el efecto de la pérdida de expresión de KLF5 sobre la proliferación, migración, y supervivencia celular en presencia de ácidos biliares tóxicos o quimioterápicos.

3. Efecto de la pérdida de expresión de KLF5 sobre la tumorogénesis del CCA *in vivo*

Se analizó el papel de la pérdida de expresión de KLF5 en células de CCA (tecnología CRISPR/Cas9) sobre la implantación y crecimiento tumoral subcutáneo en ratones inmunodeficientes.

Resultados y discusión

La expresión de diferentes miembros de la familia de factores de transcripción KLF se encuentra alterada en colangiocitos humanos tumorales en comparación con colangiocitos normales en cultivo. Entre los KLFs cuya expresión se encuentra alterada en células de CCA destacó KLF5, el cual se

encuentra altamente sobre-expresado en 8 líneas celulares de CCA en comparación con 4 cultivos primarios de NHC. La expresión de KLF5 se encuentra particularmente elevada en el núcleo de las células de CCA. La expresión de KLF5 se encontró también aumentada en tejido de CCA de pacientes de 3 cohortes independientes en comparación con tejido hepático adyacente no tumoral. Curiosamente, los tumores que presentaban invasión de nódulos linfáticos mostraron mayores niveles de expresión de *KLF5* en comparación con los tumores de CCA que no presentaban dicha invasión de nódulos linfáticos, indicando su posible valor pronóstico. El silenciamiento experimental de la expresión de KLF5 en células de CCA en cultivo mediante tecnología CRISPR/Cas9 y/o lentivirus shRNA específicos provocó una parada en el ciclo celular e inhibición de la migración, así como una menor viabilidad celular en presencia de ácidos biliares tóxicos y diversos agentes quimioterápicos. Por último, los estudios llevados a cabo en ratones inmunodeficientes mostraron que las células de CCA deficientes de KLF5 inyectadas de manera subcutánea presentan una drástica disminución en la capacidad de implantación y crecimiento tumoral en comparación con las células control.

Conclusiones

Los hallazgos descritos en este estudio demuestran que las células de CCA presentan alteraciones en la expresión de distintos KLF, entre los que destaca KLF5. La expresión de *KLF5* se encuentra aumentada en tumores de pacientes con CCA y particularmente en tumores con invasión de nódulos linfáticos (asociado a un estadio avanzado de la enfermedad). Los estudios experimentales *in vitro* e *in vivo* demuestran que KLF5 promueve la proliferación, migración y tumorogénesis de las células de CCA y favorece su supervivencia y quimioresistencia. Por tanto, KLF5 puede ser un importante marcador diagnóstico y pronóstico, así como una diana terapéutica en CCA. Serán necesarios futuros estudios para validar y expandir dichos resultados, así como para evaluar la posible regulación terapéutica de KLF5 en pacientes con CCA.

VII. REFERENCES

1. Juza, R.M. and E.M. Pauli, *Clinical and surgical anatomy of the liver: a review for clinicians.* Clin Anat, 2014. **27**(5): p. 764-9.
2. Hall, C., et al., *Regulators of Cholangiocyte Proliferation.* Gene Expr, 2017. **17**(2): p. 155-171.
3. Boyer, J.L., *Bile formation and secretion.* Compr Physiol, 2013. **3**(3): p. 1035-78.
4. Glaser, S.S., et al., *Cholangiocyte proliferation and liver fibrosis.* Expert Rev Mol Med, 2009. **11**: p. e7.
5. Saxena, R. and N. Theise, *Canals of Hering: recent insights and current knowledge.* Semin Liver Dis, 2004. **24**(1): p. 43-8.
6. Tabibian, J.H., et al., *Physiology of cholangiocytes.* Compr Physiol, 2013. **3**(1): p. 541-65.
7. Kanno, N., et al., *Functional heterogeneity of the intrahepatic biliary epithelium.* Hepatology, 2000. **31**(3): p. 555-61.
8. Han, Y., et al., *Recent advances in the morphological and functional heterogeneity of the biliary epithelium.* Exp Biol Med (Maywood), 2013. **238**(5): p. 549-65.
9. Lazaridis, K.N., M. Strazzabosco, and N.F. Larusso, *The cholangiopathies: disorders of biliary epithelia.* Gastroenterology, 2004. **127**(5): p. 1565-77.
10. Jensen, K., et al., *Autocrine regulation of biliary pathology by activated cholangiocytes.* Am J Physiol Gastrointest Liver Physiol, 2012. **302**(5): p. G473-83.
11. Bogert, P.T. and N.F. LaRusso, *Cholangiocyte biology.* Curr Opin Gastroenterol, 2007. **23**(3): p. 299-305.
12. Maroni, L., et al., *Functional and structural features of cholangiocytes in health and disease.* Cell Mol Gastroenterol Hepatol, 2015. **1**(4): p. 368-380.
13. Beuers, U., et al., *The biliary HCO(3)(-) umbrella: a unifying hypothesis on pathogenetic and therapeutic aspects of fibrosing cholangiopathies.* Hepatology, 2010. **52**(4): p. 1489-96.
14. Alvaro, D., et al., *Proliferating cholangiocytes: a neuroendocrine compartment in the diseased liver.* Gastroenterology, 2007. **132**(1): p. 415-31.
15. Lazaridis, K.N. and N.F. LaRusso, *The Cholangiopathies.* Mayo Clin Proc, 2015. **90**(6): p. 791-800.
16. Haque, S., et al., *Identification of bipotential progenitor cells in human liver regeneration.* Lab Invest, 1996. **75**(5): p. 699-705.
17. Roskams, T., *Progenitor cell involvement in cirrhotic human liver diseases: from controversy to consensus.* J Hepatol, 2003. **39**(3): p. 431-4.
18. Roskams, T.A., L. Libbrecht, and V.J. Desmet, *Progenitor cells in diseased human liver.* Semin Liver Dis, 2003. **23**(4): p. 385-96.
19. O'Hara, S.P., et al., *The dynamic biliary epithelia: molecules, pathways, and disease.* J Hepatol, 2013. **58**(3): p. 575-82.
20. Fabris, L., et al., *Revisiting Epithelial-to-Mesenchymal Transition in Liver Fibrosis: Clues for a Better Understanding of the "Reactive" Biliary Epithelial Phenotype.* Stem Cells Int, 2016. **2016**: p. 2953727.
21. Invernizzi, P. and I.R. Mackay, *Autoimmune liver diseases.* World J Gastroenterol, 2008. **14**(21): p. 3290-1.

22. Beuers, U., et al., *Changing nomenclature for PBC: from 'cirrhosis' to 'cholangitis'.* Gastroenterology, 2015. **149**(6): p. 1627-9.
23. Hirschfield, G.M. and M.E. Gershwin, *Primary biliary cirrhosis: one disease with many faces.* Isr Med Assoc J, 2011. **13**(1): p. 55-9.
24. Poupon, R., *Primary biliary cirrhosis: a 2010 update.* J Hepatol, 2010. **52**(5): p. 745-58.
25. Kaplan, M.M. and M.E. Gershwin, *Primary biliary cirrhosis.* N Engl J Med, 2005. **353**(12): p. 1261-73.
26. Hohenester, S., R.P. Oude-Elferink, and U. Beuers, *Primary biliary cirrhosis.* Semin Immunopathol, 2009. **31**(3): p. 283-307.
27. Lleo, A., et al., *Etiopathogenesis of primary biliary cirrhosis.* World J Gastroenterol, 2008. **14**(21): p. 3328-37.
28. Crosignani, A., et al., *Clinical features and management of primary biliary cirrhosis.* World J Gastroenterol, 2008. **14**(21): p. 3313-27.
29. Juran, B.D. and K.N. Lazaridis, *Genetics and genomics of primary biliary cirrhosis.* Clin Liver Dis, 2008. **12**(2): p. 349-65; ix.
30. Griffiths, L., J.K. Dyson, and D.E. Jones, *The new epidemiology of primary biliary cirrhosis.* Semin Liver Dis, 2014. **34**(3): p. 318-28.
31. Invernizzi, P., et al., *Antinuclear antibodies in primary biliary cirrhosis.* Semin Liver Dis, 2005. **25**(3): p. 298-310.
32. Triger, D.R., P.A. Berg, and J. Rodes, *Epidemiology of primary biliary cirrhosis.* Liver, 1984. **4**(3): p. 195-200.
33. Marzorati, S., et al., *The epigenetics of PBC: The link between genetic susceptibility and environment.* Clin Res Hepatol Gastroenterol, 2016. **40**(6): p. 650-659.
34. Lindor, K.D., et al., *Primary biliary cirrhosis.* Hepatology, 2009. **50**(1): p. 291-308.
35. Surh, C.D., R. Coppel, and M.E. Gershwin, *Structural requirement for autoreactivity on human pyruvate dehydrogenase-E2, the major autoantigen of primary biliary cirrhosis. Implication for a conformational autoepitope.* J Immunol, 1990. **144**(9): p. 3367-74.
36. Poupon, R.E., et al., *A multicenter, controlled trial of ursodiol for the treatment of primary biliary cirrhosis. UDCA-PBC Study Group.* N Engl J Med, 1991. **324**(22): p. 1548-54.
37. Beuers, U., *Drug insight: Mechanisms and sites of action of ursodeoxycholic acid in cholestasis.* Nat Clin Pract Gastroenterol Hepatol, 2006. **3**(6): p. 318-28.
38. Lindor, K., *Ursodeoxycholic acid for the treatment of primary biliary cirrhosis.* N Engl J Med, 2007. **357**(15): p. 1524-9.
39. Markham, A. and S.J. Keam, *Obeticholic Acid: First Global Approval.* Drugs, 2016. **76**(12): p. 1221-6.
40. Dyson, J.K., et al., *Novel therapeutic targets in primary biliary cirrhosis.* Nat Rev Gastroenterol Hepatol, 2015. **12**(3): p. 147-58.
41. Fitzmaurice, C., et al., *The Global Burden of Cancer 2013.* JAMA Oncol, 2015. **1**(4): p. 505-27.
42. Nakeeb, A., et al., *Cholangiocarcinoma. A spectrum of intrahepatic, perihilar, and distal tumors.* Ann Surg, 1996. **224**(4): p. 463-73; discussion 473-5.

43. Erice, O., et al., *Molecular Mechanisms of Cholangiocarcinogenesis: New Potential Targets For Therapy.* Curr Drug Targets, 2015. **[Epub ahead of print]**.
44. Nakamura, H., et al., *Genomic spectra of biliary tract cancer.* Nat Genet, 2015. **47**(9): p. 1003-10.
45. Banales, J.M., et al., *Expert consensus document: Cholangiocarcinoma: current knowledge and future perspectives consensus statement from the European Network for the Study of Cholangiocarcinoma (ENS-CCA).* Nat Rev Gastroenterol Hepatol, 2016. **13**(5): p. 261-80.
46. Mosconi, S., et al., *Cholangiocarcinoma.* Crit Rev Oncol Hematol, 2009. **69**(3): p. 259-70.
47. Malhi, H. and G.J. Gores, *Cholangiocarcinoma: modern advances in understanding a deadly old disease.* J Hepatol, 2006. **45**(6): p. 856-67.
48. Bridgewater, J., et al., *Guidelines for the diagnosis and management of intrahepatic cholangiocarcinoma.* J Hepatol, 2014. **60**(6): p. 1268-89.
49. Razumilava, N. and G.J. Gores, *Cholangiocarcinoma.* Lancet, 2014. **383**(9935): p. 2168-79.
50. Han, J.K., et al., *Cholangiocarcinoma: pictorial essay of CT and cholangiographic findings.* Radiographics, 2002. **22**(1): p. 173-87.
51. Nguyen, K. and J.T. Sing, Jr., *Review of endoscopic techniques in the diagnosis and management of cholangiocarcinoma.* World J Gastroenterol, 2008. **14**(19): p. 2995-9.
52. Sripa, B., et al., *Liver fluke induces cholangiocarcinoma.* PLoS Med, 2007. **4**(7): p. e201.
53. Blechacz, B., et al., *Clinical diagnosis and staging of cholangiocarcinoma.* Nat Rev Gastroenterol Hepatol, 2011. **8**(9): p. 512-22.
54. Yamasaki, S., *Intrahepatic cholangiocarcinoma: macroscopic type and stage classification.* J Hepatobiliary Pancreat Surg, 2003. **10**(4): p. 288-91.
55. Alvaro, D., et al., *Cholangiocarcinoma in Italy: A national survey on clinical characteristics, diagnostic modalities and treatment. Results from the "Cholangiocarcinoma" committee of the Italian Association for the Study of Liver disease.* Dig Liver Dis, 2011. **43**(1): p. 60-5.
56. De Rose, A.M., et al., *Prognostic significance of tumor doubling time in mass-forming type cholangiocarcinoma.* J Gastrointest Surg, 2013. **17**(4): p. 739-47.
57. Aishima, S. and Y. Oda, *Pathogenesis and classification of intrahepatic cholangiocarcinoma: different characters of perihilar large duct type versus peripheral small duct type.* J Hepatobiliary Pancreat Sci, 2015. **22**(2): p. 94-100.
58. Komuta, M., et al., *Histological diversity in cholangiocellular carcinoma reflects the different cholangiocyte phenotypes.* Hepatology, 2012. **55**(6): p. 1876-88.
59. Liau, J.Y., et al., *Morphological subclassification of intrahepatic cholangiocarcinoma: etiological, clinicopathological, and molecular features.* Mod Pathol, 2014. **27**(8): p. 1163-73.
60. Nakanuma, Y., et al., *Pathological classification of intrahepatic cholangiocarcinoma based on a new concept.* World J Hepatol, 2010. **2**(12): p. 419-27.

61. Palmer, W.C. and T. Patel, *Are common factors involved in the pathogenesis of primary liver cancers? A meta-analysis of risk factors for intrahepatic cholangiocarcinoma.* J Hepatol, 2012. **57**(1): p. 69-76.
62. Patel, T., *Cholangiocarcinoma--controversies and challenges.* Nat Rev Gastroenterol Hepatol, 2011. **8**(4): p. 189-200.
63. Burak, K., et al., *Incidence and risk factors for cholangiocarcinoma in primary sclerosing cholangitis.* Am J Gastroenterol, 2004. **99**(3): p. 523-6.
64. Kobayashi, M., et al., *Incidence of primary cholangiocellular carcinoma of the liver in japanese patients with hepatitis C virus-related cirrhosis.* Cancer, 2000. **88**(11): p. 2471-7.
65. Lee, T.Y., et al., *Hepatitis B virus infection and intrahepatic cholangiocarcinoma in Korea: a case-control study.* Am J Gastroenterol, 2008. **103**(7): p. 1716-20.
66. Shin, H.R., et al., *Hepatitis B and C virus, Clonorchis sinensis for the risk of liver cancer: a case-control study in Pusan, Korea.* Int J Epidemiol, 1996. **25**(5): p. 933-40.
67. Kaewpitoon, N., et al., *Opisthorchis viverrini: the carcinogenic human liver fluke.* World J Gastroenterol, 2008. **14**(5): p. 666-74.
68. Plentz, R.R. and N.P. Malek, *Clinical presentation, risk factors and staging systems of cholangiocarcinoma.* Best Pract Res Clin Gastroenterol, 2015. **29**(2): p. 245-52.
69. Zhou, H.B., J.Y. Hu, and H.P. Hu, *Hepatitis B virus infection and intrahepatic cholangiocarcinoma.* World J Gastroenterol, 2014. **20**(19): p. 5721-9.
70. Nishihara, K., et al., *Intrahepatic calculi associated with cholangiocarcinoma.* Jpn J Surg, 1986. **16**(5): p. 367-70.
71. Soreide, K., et al., *Bile duct cysts in adults.* Br J Surg, 2004. **91**(12): p. 1538-48.
72. Bernstein, H., et al., *Bile acids as endogenous etiologic agents in gastrointestinal cancer.* World J Gastroenterol, 2009. **15**(27): p. 3329-40.
73. Blechacz, B. and G.J. Gores, *Cholangiocarcinoma: advances in pathogenesis, diagnosis, and treatment.* Hepatology, 2008. **48**(1): p. 308-21.
74. Aljiffry, M., et al., *Evidence-based approach to cholangiocarcinoma: a systematic review of the current literature.* J Am Coll Surg, 2009. **208**(1): p. 134-47.
75. Maroni, L., et al., *The significance of genetics for cholangiocarcinoma development.* Ann Transl Med, 2013. **1**(3): p. 28.
76. Patel, T., *New insights into the molecular pathogenesis of intrahepatic cholangiocarcinoma.* J Gastroenterol, 2014. **49**(2): p. 165-72.
77. Yang, L., S. Feng, and Y. Yang, *Identification of transcription factors (TFs) and targets involved in the cholangiocarcinoma (CCA) by integrated analysis.* Cancer Gene Ther, 2016. **23**(12): p. 439-445.
78. Jiao, Y., et al., *Exome sequencing identifies frequent inactivating mutations in BAP1, ARID1A and PBRM1 in intrahepatic cholangiocarcinomas.* Nat Genet, 2013. **45**(12): p. 1470-3.
79. Zou, S., et al., *Mutational landscape of intrahepatic cholangiocarcinoma.* Nat Commun, 2014. **5**: p. 5696.

80. Ong, C.K., et al., *Exome sequencing of liver fluke-associated cholangiocarcinoma.* Nat Genet, 2012. **44**(6): p. 690-3.
81. Boulter, L., et al., *WNT signaling drives cholangiocarcinoma growth and can be pharmacologically inhibited.* J Clin Invest, 2015. **125**(3): p. 1269-85.
82. Borad, M.J., et al., *Integrated genomic characterization reveals novel, therapeutically relevant drug targets in FGFR and EGFR pathways in sporadic intrahepatic cholangiocarcinoma.* PLoS Genet, 2014. **10**(2): p. e1004135.
83. Fujimoto, A., et al., *Whole-genome mutational landscape of liver cancers displaying biliary phenotype reveals hepatitis impact and molecular diversity.* Nat Commun, 2015. **6**: p. 6120.
84. Sia, D., et al., *Massive parallel sequencing uncovers actionable FGFR2-PPHLN1 fusion and ARAF mutations in intrahepatic cholangiocarcinoma.* Nat Commun, 2015. **6**: p. 6087.
85. Haga, H. and T. Patel, *Molecular diagnosis of intrahepatic cholangiocarcinoma.* J Hepatobiliary Pancreat Sci, 2015. **22**(2): p. 114-23.
86. Rizvi, S. and G.J. Gores, *Pathogenesis, diagnosis, and management of cholangiocarcinoma.* Gastroenterology, 2013. **145**(6): p. 1215-29.
87. Arai, Y., et al., *Fibroblast growth factor receptor 2 tyrosine kinase fusions define a unique molecular subtype of cholangiocarcinoma.* Hepatology, 2014. **59**(4): p. 1427-34.
88. Kajiyama, K., et al., *The significance of stromal desmoplasia in intrahepatic cholangiocarcinoma: a special reference of 'scirrhous-type' and 'nonscirrhous-type' growth.* Am J Surg Pathol, 1999. **23**(8): p. 892-902.
89. Sirica, A.E. and G.J. Gores, *Desmoplastic stroma and cholangiocarcinoma: clinical implications and therapeutic targeting.* Hepatology, 2014. **59**(6): p. 2397-402.
90. Sirica, A.E., *The role of cancer-associated myofibroblasts in intrahepatic cholangiocarcinoma.* Nat Rev Gastroenterol Hepatol, 2011. **9**(1): p. 44-54.
91. Angulo, P. and K.D. Lindor, *Primary sclerosing cholangitis.* Hepatology, 1999. **30**(1): p. 325-32.
92. Boberg, K.M., et al., *Cholangiocarcinoma in primary sclerosing cholangitis: risk factors and clinical presentation.* Scand J Gastroenterol, 2002. **37**(10): p. 1205-11.
93. Morris-Stiff, G., et al., *Cholangiocarcinoma complicating primary sclerosing cholangitis: a 24-year experience.* Dig Surg, 2008. **25**(2): p. 126-32.
94. Bjornsson, E. and P. Angulo, *Cholangiocarcinoma in young individuals with and without primary sclerosing cholangitis.* Am J Gastroenterol, 2007. **102**(8): p. 1677-82.
95. Khan, S.A., et al., *Guidelines for the diagnosis and treatment of cholangiocarcinoma: an update.* Gut, 2012. **61**(12): p. 1657-69.
96. Bledsoe, J.R., S.A. Shinagare, and V. Deshpande, *Difficult Diagnostic Problems in Pancreatobiliary Neoplasia.* Arch Pathol Lab Med, 2015. **139**(7): p. 848-57.

97. Rullier, A., et al., *Cytokeratin 7 and 20 expression in cholangiocarcinomas varies along the biliary tract but still differs from that in colorectal carcinoma metastasis.* Am J Surg Pathol, 2000. **24**(6): p. 870-6.
98. Adam, A. and I.S. Benjamin, *The staging of cholangiocarcinoma.* Clin Radiol, 1992. **46**(5): p. 299-303.
99. Williams, T.M., et al., *Defining the role of adjuvant therapy: cholangiocarcinoma and gall bladder cancer.* Semin Radiat Oncol, 2014. **24**(2): p. 94-104.
100. Rizvi, S. and G.J. Gores, *Current diagnostic and management options in perihilar cholangiocarcinoma.* Digestion, 2014. **89**(3): p. 216-24.
101. Herraez, E., et al., *Expression of SLC22A1 variants may affect the response of hepatocellular carcinoma and cholangiocarcinoma to sorafenib.* Hepatology, 2013. **58**(3): p. 1065-73.
102. Smith, A.C., et al., *Randomised trial of endoscopic stenting versus surgical bypass in malignant low bileduct obstruction.* Lancet, 1994. **344**(8938): p. 1655-60.
103. Martin, R.C., 2nd, et al., *Cost comparison of endoscopic stenting vs surgical treatment for unresectable cholangiocarcinoma.* Surg Endosc, 2002. **16**(4): p. 667-70.
104. Liberato, M.J. and J.M. Canena, *Endoscopic stenting for hilar cholangiocarcinoma: efficacy of unilateral and bilateral placement of plastic and metal stents in a retrospective review of 480 patients.* BMC Gastroenterol, 2012. **12**: p. 103.
105. Banales, J.M., et al., *Up-regulation of microRNA 506 leads to decreased Cl-/HCO3- anion exchanger 2 expression in biliary epithelium of patients with primary biliary cirrhosis.* Hepatology, 2012. **56**(2): p. 687-97.
106. Salter, K.D., et al., *Modified culture conditions enhance expression of differentiated phenotypic properties of normal rat cholangiocytes.* Lab Invest, 2000. **80**(11): p. 1775-8.
107. Divakaruni, A.S., et al., *Analysis and interpretation of microplate-based oxygen consumption and pH data.* Methods Enzymol, 2014. **547**: p. 309-54.
108. Schneider, C.A., W.S. Rasband, and K.W. Eliceiri, *NIH Image to ImageJ: 25 years of image analysis.* Nat Methods, 2012. **9**(7): p. 671-5.
109. Concepcion, A.R., et al., *CD8+ T cells undergo activation and programmed death-1 repression in the liver of aged Ae2a,b-/- mice favoring autoimmune cholangitis.* Oncotarget, 2015. **6**(30): p. 28588-606.
110. Lleo, A., et al., *Biliary apotopes and anti-mitochondrial antibodies activate innate immune responses in primary biliary cirrhosis.* Hepatology, 2010. **52**(3): p. 987-98.
111. Melero, S., et al., *Defective regulation of cholangiocyte Cl-/HCO3(-) and Na+/H+ exchanger activities in primary biliary cirrhosis.* Hepatology, 2002. **35**(6): p. 1513-21.
112. Prieto, J., et al., *Assessment of biliary bicarbonate secretion in humans by positron emission tomography.* Gastroenterology, 1999. **117**(1): p. 167-72.
113. Banales, J.M., et al., *Bicarbonate-rich choleresis induced by secretin in normal rat is taurocholate-dependent and involves AE2 anion exchanger.* Hepatology, 2006. **43**(2): p. 266-75.

114. Arenas, F., et al., *Combination of ursodeoxycholic acid and glucocorticoids upregulates the AE2 alternate promoter in human liver cells.* J Clin Invest, 2008. **118**(2): p. 695-709.
115. Martinez-Anso, E., et al., *Immunohistochemical detection of chloride/bicarbonate anion exchangers in human liver.* Hepatology, 1994. **19**(6): p. 1400-6.
116. Salas, J.T., et al., *Ae2a,b-deficient mice develop antimitochondrial antibodies and other features resembling primary biliary cirrhosis.* Gastroenterology, 2008. **134**(5): p. 1482-93.
117. Minagawa, N., et al., *Cyclic AMP regulates bicarbonate secretion in cholangiocytes through release of ATP into bile.* Gastroenterology, 2007. **133**(5): p. 1592-602.
118. Hirata, K. and M.H. Nathanson, *Bile duct epithelia regulate biliary bicarbonate excretion in normal rat liver.* Gastroenterology, 2001. **121**(2): p. 396-406.
119. Shibao, K., et al., *Loss of inositol 1,4,5-trisphosphate receptors from bile duct epithelia is a common event in cholestasis.* Gastroenterology, 2003. **125**(4): p. 1175-87.
120. Ananthanarayanan, M., et al., *Post-translational regulation of the type III inositol 1,4,5-trisphosphate receptor by miRNA-506.* J Biol Chem, 2015. **290**(1): p. 184-96.
121. Martinelli, I., et al., *The transition G to A at position 20210 in the 3'-untranslated region of the prothrombin gene is not associated with cerebral ischemia.* Blood, 1997. **90**(9): p. 3806.
122. Padgett, K.A., et al., *Primary biliary cirrhosis is associated with altered hepatic microRNA expression.* J Autoimmun, 2009. **32**(3-4): p. 246-53.
123. Lee, R.C., R.L. Feinbaum, and V. Ambros, *The C. elegans heterochronic gene lin-4 encodes small RNAs with antisense complementarity to lin-14.* Cell, 1993. **75**(5): p. 843-54.
124. Wightman, B., I. Ha, and G. Ruvkun, *Posttranscriptional regulation of the heterochronic gene lin-14 by lin-4 mediates temporal pattern formation in C. elegans.* Cell, 1993. **75**(5): p. 855-62.
125. Bartel, D.P., *MicroRNAs: target recognition and regulatory functions.* Cell, 2009. **136**(2): p. 215-33.
126. Garzon, R., G. Marcucci, and C.M. Croce, *Targeting microRNAs in cancer: rationale, strategies and challenges.* Nat Rev Drug Discov, 2010. **9**(10): p. 775-89.
127. Esparza-Baquer, A., et al., *MicroRNAs in cholangiopathies: Potential diagnostic and therapeutic tools.* Clin Res Hepatol Gastroenterol, 2016. **40**(1): p. 15-27.
128. Herraez, E., et al., *Cisplatin-induced chemoresistance in colon cancer cells involves FXR-dependent and FXR-independent up-regulation of ABC proteins.* Mol Pharm, 2012. **9**(9): p. 2565-76.
129. Unwin, R.D., J.R. Griffiths, and A.D. Whetton, *Simultaneous analysis of relative protein expression levels across multiple samples using iTRAQ isobaric tags with 2D nano LC-MS/MS.* Nat Protoc, 2010. **5**(9): p. 1574-82.
130. Zelaya, M.V., et al., *Olfactory bulb proteome dynamics during the progression of sporadic Alzheimer's disease: identification of common*

and distinct olfactory targets across Alzheimer-related co-pathologies. Oncotarget, 2015. **6**(37): p. 39437-56.
131. Shilov, I.V., et al., *The Paragon Algorithm, a next generation search engine that uses sequence temperature values and feature probabilities to identify peptides from tandem mass spectra.* Mol Cell Proteomics, 2007. **6**(9): p. 1638-55.
132. McDaniel, K., et al., *Forkhead box A2 regulates biliary heterogeneity and senescence during cholestatic liver injury in micedouble dagger.* Hepatology, 2017. **65**(2): p. 544-559.
133. Huang, Q., et al., *Interleukin-17A-Induced Epithelial-Mesenchymal Transition of Human Intrahepatic Biliary Epithelial Cells: Implications for Primary Biliary Cirrhosis.* Tohoku J Exp Med, 2016. **240**(4): p. 269-275.
134. Robertson, H., et al., *Biliary epithelial-mesenchymal transition in posttransplantation recurrence of primary biliary cirrhosis.* Hepatology, 2007. **45**(4): p. 977-81.
135. Sasaki, M., et al., *A possible involvement of endoplasmic reticulum stress in biliary epithelial autophagy and senescence in primary biliary cirrhosis.* J Gastroenterol, 2015. **50**(9): p. 984-95.
136. Harada, K., et al., *Enhanced apoptosis relates to bile duct loss in primary biliary cirrhosis.* Hepatology, 1997. **26**(6): p. 1399-405.
137. Koga, H., et al., *Nuclear DNA fragmentation and expression of Bcl-2 in primary biliary cirrhosis.* Hepatology, 1997. **25**(5): p. 1077-84.
138. Hohenester, S., et al., *A biliary HCO3- umbrella constitutes a protective mechanism against bile acid-induced injury in human cholangiocytes.* Hepatology, 2012. **55**(1): p. 173-83.
139. Hirata, K., et al., *Regulation of Ca(2+) signaling in rat bile duct epithelia by inositol 1,4,5-trisphosphate receptor isoforms.* Hepatology, 2002. **36**(2): p. 284-96.
140. Gershwin, M.E., et al., *Identification and specificity of a cDNA encoding the 70 kd mitochondrial antigen recognized in primary biliary cirrhosis.* J Immunol, 1987. **138**(10): p. 3525-31.
141. Qin, B., et al., *Analysis of altered microRNA expression profiles in peripheral blood mononuclear cells from patients with primary biliary cirrhosis.* J Gastroenterol Hepatol, 2013. **28**(3): p. 543-50.
142. Medina, J.F., et al., *Decreased anion exchanger 2 immunoreactivity in the liver of patients with primary biliary cirrhosis.* Hepatology, 1997. **25**(1): p. 12-7.
143. Chuang, Y.H., et al., *Increased killing activity and decreased cytokine production in NK cells in patients with primary biliary cirrhosis.* J Autoimmun, 2006. **26**(4): p. 232-40.
144. Yang, C.Y., et al., *IL-12/Th1 and IL-23/Th17 biliary microenvironment in primary biliary cirrhosis: implications for therapy.* Hepatology, 2014. **59**(5): p. 1944-53.
145. Qian, C., et al., *Increased IL-23 and IL-17 expression by peripheral blood cells of patients with primary biliary cirrhosis.* Cytokine, 2013. **64**(1): p. 172-80.
146. Yamano, T., et al., *Serum interferon-gamma-inducing factor/IL-18 levels in primary biliary cirrhosis.* Clin Exp Immunol, 2000. **122**(2): p. 227-31.
147. Kikly, K., et al., *The IL-23/Th(17) axis: therapeutic targets for autoimmune inflammation.* Curr Opin Immunol, 2006. **18**(6): p. 670-5.

148. Concepcion, A.R., et al., *Role of AE2 for pHi regulation in biliary epithelial cells.* Front Physiol, 2013. **4**: p. 413.
149. Sasaki, M., et al., *Frequent cellular senescence in small bile ducts in primary biliary cirrhosis: a possible role in bile duct loss.* J Pathol, 2005. **205**(4): p. 451-9.
150. Sasaki, M., et al., *Telomere shortening in the damaged small bile ducts in primary biliary cirrhosis reflects ongoing cellular senescence.* Hepatology, 2008. **48**(1): p. 186-95.
151. Chang, J.C., et al., *Soluble Adenylyl Cyclase Regulates Bile Salt-Induced Apoptosis in Human Cholangiocytes.* Hepatology, 2016. **64**(2): p. 522-34.
152. Hisamoto, S., et al., *Hydrophobic bile acids suppress expression of AE2 in biliary epithelial cells and induce bile duct inflammation in primary biliary cholangitis.* J Autoimmun, 2016.
153. Li, J., et al., *The emerging role of miR-506 in cancer.* Oncotarget, 2016.
154. Perez, M.J. and O. Briz, *Bile-acid-induced cell injury and protection.* World J Gastroenterol, 2009. **15**(14): p. 1677-89.
155. Odin, J.A., et al., *Bcl-2-dependent oxidation of pyruvate dehydrogenase-E2, a primary biliary cirrhosis autoantigen, during apoptosis.* J Clin Invest, 2001. **108**(2): p. 223-32.
156. Lleo, A., et al., *Apotopes and the biliary specificity of primary biliary cirrhosis.* Hepatology, 2009. **49**(3): p. 871-9.
157. Xia, X., et al., *Bile acid interactions with cholangiocytes.* World J Gastroenterol, 2006. **12**(22): p. 3553-63.
158. Schaap, F.G., M. Trauner, and P.L. Jansen, *Bile acid receptors as targets for drug development.* Nat Rev Gastroenterol Hepatol, 2014. **11**(1): p. 55-67.
159. Qi, Y., et al., *Bile acid signaling in lipid metabolism: metabolomic and lipidomic analysis of lipid and bile acid markers linked to anti-obesity and anti-diabetes in mice.* Biochim Biophys Acta, 2015. **1851**(1): p. 19-29.
160. Lefebvre, P., et al., *Role of bile acids and bile acid receptors in metabolic regulation.* Physiol Rev, 2009. **89**(1): p. 147-91.
161. Monte, M.J., et al., *Bile acids: chemistry, physiology, and pathophysiology.* World J Gastroenterol, 2009. **15**(7): p. 804-16.
162. Cuperus, F.J., et al., *The role of canalicular ABC transporters in cholestasis.* Drug Metab Dispos, 2014. **42**(4): p. 546-60.
163. Pircher, P.C., et al., *Farnesoid X receptor regulates bile acid-amino acid conjugation.* J Biol Chem, 2003. **278**(30): p. 27703-11.
164. Geier, A., P. Fickert, and M. Trauner, *Mechanisms of disease: mechanisms and clinical implications of cholestasis in sepsis.* Nat Clin Pract Gastroenterol Hepatol, 2006. **3**(10): p. 574-85.
165. Gerloff, T., et al., *The sister of P-glycoprotein represents the canalicular bile salt export pump of mammalian liver.* J Biol Chem, 1998. **273**(16): p. 10046-50.
166. Craddock, A.L., et al., *Expression and transport properties of the human ileal and renal sodium-dependent bile acid transporter.* Am J Physiol, 1998. **274**(1 Pt 1): p. G157-69.
167. Boyer, J.L., et al., *Upregulation of a basolateral FXR-dependent bile acid efflux transporter OSTalpha-OSTbeta in cholestasis in humans and rodents.* Am J Physiol Gastrointest Liver Physiol, 2006. **290**(6): p. G1124-30.

168. Hagenbuch, B. and P.J. Meier, *Molecular cloning, chromosomal localization, and functional characterization of a human liver Na+/bile acid cotransporter.* J Clin Invest, 1994. **93**(3): p. 1326-31.
169. Kullak-Ublick, G.A., et al., *Organic anion-transporting polypeptide B (OATP-B) and its functional comparison with three other OATPs of human liver.* Gastroenterology, 2001. **120**(2): p. 525-33.
170. Akita, H., et al., *Characterization of bile acid transport mediated by multidrug resistance associated protein 2 and bile salt export pump.* Biochim Biophys Acta, 2001. **1511**(1): p. 7-16.
171. Alpini, G., et al., *Secretin activation of the apical Na+-dependent bile acid transporter is associated with cholehepatic shunting in rats.* Hepatology, 2005. **41**(5): p. 1037-45.
172. Halilbasic, E., et al., *Side chain structure determines unique physiologic and therapeutic properties of norursodeoxycholic acid in Mdr2-/- mice.* Hepatology, 2009. **49**(6): p. 1972-81.
173. Glaser, S.S. and G. Alpini, *Activation of the cholehepatic shunt as a potential therapy for primary sclerosing cholangitis.* Hepatology, 2009. **49**(6): p. 1795-7.
174. Hofmann, A.F., *The enterohepatic circulation of bile acids in mammals: form and functions.* Front Biosci (Landmark Ed), 2009. **14**: p. 2584-98.
175. Smit, J.J., et al., *Homozygous disruption of the murine mdr2 P-glycoprotein gene leads to a complete absence of phospholipid from bile and to liver disease.* Cell, 1993. **75**(3): p. 451-62.
176. Forman, B.M., et al., *Identification of a nuclear receptor that is activated by farnesol metabolites.* Cell, 1995. **81**(5): p. 687-93.
177. Baes, M., et al., *A new orphan member of the nuclear hormone receptor superfamily that interacts with a subset of retinoic acid response elements.* Mol Cell Biol, 1994. **14**(3): p. 1544-52.
178. Makishima, M., et al., *Vitamin D receptor as an intestinal bile acid sensor.* Science, 2002. **296**(5571): p. 1313-6.
179. Choi, H.S., et al., *Differential transactivation by two isoforms of the orphan nuclear hormone receptor CAR.* J Biol Chem, 1997. **272**(38): p. 23565-71.
180. Kawamata, Y., et al., *A G protein-coupled receptor responsive to bile acids.* J Biol Chem, 2003. **278**(11): p. 9435-40.
181. Marin, J.J., et al., *Bile Acids in Physiology, Pathology and Pharmacology.* Curr Drug Metab, 2015. **17**(1): p. 4-29.
182. Herraez, E., et al., *Role of macrophages in bile acid-induced inflammatory response of fetal lung during maternal cholestasis.* J Mol Med (Berl), 2014. **92**(4): p. 359-72.
183. Yoon, J.H., et al., *Bile acids induce cyclooxygenase-2 expression via the epidermal growth factor receptor in a human cholangiocarcinoma cell line.* Gastroenterology, 2002. **122**(4): p. 985-93.
184. Dai, J., et al., *Bile acids affect the growth of human cholangiocarcinoma via NF-kB pathway.* Cancer Invest, 2013. **31**(2): p. 111-20.
185. Liu, R., et al., *Conjugated bile acids promote cholangiocarcinoma cell invasive growth through activation of sphingosine 1-phosphate receptor 2.* Hepatology, 2014. **60**(3): p. 908-18.

186. Seol, W., H.S. Choi, and D.D. Moore, *Isolation of proteins that interact specifically with the retinoid X receptor: two novel orphan receptors.* Mol Endocrinol, 1995. **9**(1): p. 72-85.
187. Wang, H., et al., *Endogenous bile acids are ligands for the nuclear receptor FXR/BAR.* Mol Cell, 1999. **3**(5): p. 543-53.
188. Parks, D.J., et al., *Bile acids: natural ligands for an orphan nuclear receptor.* Science, 1999. **284**(5418): p. 1365-8.
189. Makishima, M., et al., *Identification of a nuclear receptor for bile acids.* Science, 1999. **284**(5418): p. 1362-5.
190. Eloranta, J.J. and G.A. Kullak-Ublick, *The role of FXR in disorders of bile acid homeostasis.* Physiology (Bethesda), 2008. **23**: p. 286-95.
191. Martinez-Becerra, P., et al., *No correlation between the expression of FXR and genes involved in multidrug resistance phenotype of primary liver tumors.* Mol Pharm, 2012. **9**(6): p. 1693-704.
192. Vaquero, J., et al., *Differential activation of the human farnesoid X receptor depends on the pattern of expressed isoforms and the bile acid pool composition.* Biochem Pharmacol, 2013. **86**(7): p. 926-39.
193. Chiang, J.Y., et al., *Farnesoid X receptor responds to bile acids and represses cholesterol 7alpha-hydroxylase gene (CYP7A1) transcription.* J Biol Chem, 2000. **275**(15): p. 10918-24.
194. Goodwin, B., et al., *A regulatory cascade of the nuclear receptors FXR, SHP-1, and LRH-1 represses bile acid biosynthesis.* Mol Cell, 2000. **6**(3): p. 517-26.
195. Inagaki, T., et al., *Fibroblast growth factor 15 functions as an enterohepatic signal to regulate bile acid homeostasis.* Cell Metab, 2005. **2**(4): p. 217-25.
196. Ananthanarayanan, M., et al., *Human bile salt export pump promoter is transactivated by the farnesoid X receptor/bile acid receptor.* J Biol Chem, 2001. **276**(31): p. 28857-65.
197. Gadaleta, R.M., et al., *Farnesoid X receptor activation inhibits inflammation and preserves the intestinal barrier in inflammatory bowel disease.* Gut, 2011. **60**(4): p. 463-72.
198. Zhang, L., et al., *Promotion of liver regeneration/repair by farnesoid X receptor in both liver and intestine in mice.* Hepatology, 2012. **56**(6): p. 2336-43.
199. Kim, I., et al., *Spontaneous hepatocarcinogenesis in farnesoid X receptor-null mice.* Carcinogenesis, 2007. **28**(5): p. 940-6.
200. Deuschle, U., et al., *FXR controls the tumor suppressor NDRG2 and FXR agonists reduce liver tumor growth and metastasis in an orthotopic mouse xenograft model.* PLoS One, 2012. **7**(10): p. e43044.
201. Zhu, C., et al., *Bile acids in regulation of inflammation and immunity: friend or foe?* Clin Exp Rheumatol, 2016. **34**(4 Suppl 98): p. 25-31.
202. Yang, F., et al., *Spontaneous development of liver tumors in the absence of the bile acid receptor farnesoid X receptor.* Cancer Res, 2007. **67**(3): p. 863-7.
203. Huang, X.F., W.Y. Zhao, and W.D. Huang, *FXR and liver carcinogenesis.* Acta Pharmacol Sin, 2015. **36**(1): p. 37-43.
204. Lozano, E., et al., *Cocarcinogenic effects of intrahepatic bile acid accumulation in cholangiocarcinoma development.* Mol Cancer Res, 2014. **12**(1): p. 91-100.

205. Pellicciari, R., et al., *6alpha-ethyl-chenodeoxycholic acid (6-ECDCA), a potent and selective FXR agonist endowed with anticholestatic activity.* J Med Chem, 2002. **45**(17): p. 3569-72.
206. Rizzo, G., et al., *Functional characterization of the semisynthetic bile acid derivative INT-767, a dual farnesoid X receptor and TGR5 agonist.* Mol Pharmacol, 2010. **78**(4): p. 617-30.
207. Matsubara, T., F. Li, and F.J. Gonzalez, *FXR signaling in the enterohepatic system.* Mol Cell Endocrinol, 2013. **368**(1-2): p. 17-29.
208. Williamson, K.D. and R.W. Chapman, *New Therapeutic Strategies for Primary Sclerosing Cholangitis.* Semin Liver Dis, 2016. **36**(1): p. 5-14.
209. Chen, X., et al., *TGR5: a novel target for weight maintenance and glucose metabolism.* Exp Diabetes Res, 2011. **2011**: p. 853501.
210. Tiwari, A. and P. Maiti, *TGR5: an emerging bile acid G-protein-coupled receptor target for the potential treatment of metabolic disorders.* Drug Discov Today, 2009. **14**(9-10): p. 523-30.
211. Calmus, Y. and R. Poupon, *Shaping macrophages function and innate immunity by bile acids: mechanisms and implication in cholestatic liver diseases.* Clin Res Hepatol Gastroenterol, 2014. **38**(5): p. 550-6.
212. Keitel, V., et al., *The membrane-bound bile acid receptor TGR5 is localized in the epithelium of human gallbladders.* Hepatology, 2009. **50**(3): p. 861-70.
213. Keitel, V., et al., *The G-protein coupled bile salt receptor TGR5 is expressed in liver sinusoidal endothelial cells.* Hepatology, 2007. **45**(3): p. 695-704.
214. Keitel, V., et al., *Expression and function of the bile acid receptor TGR5 in Kupffer cells.* Biochem Biophys Res Commun, 2008. **372**(1): p. 78-84.
215. Keitel, V., C. Ullmer, and D. Haussinger, *The membrane-bound bile acid receptor TGR5 (Gpbar-1) is localized in the primary cilium of cholangiocytes.* Biol Chem, 2010. **391**(7): p. 785-9.
216. Pols, T.W., et al., *The bile acid membrane receptor TGR5 as an emerging target in metabolism and inflammation.* J Hepatol, 2011. **54**(6): p. 1263-72.
217. Maruyama, T., et al., *Targeted disruption of G protein-coupled bile acid receptor 1 (Gpbar1/M-Bar) in mice.* J Endocrinol, 2006. **191**(1): p. 197-205.
218. Thomas, C., et al., *TGR5-mediated bile acid sensing controls glucose homeostasis.* Cell Metab, 2009. **10**(3): p. 167-77.
219. Watanabe, M., et al., *Bile acids induce energy expenditure by promoting intracellular thyroid hormone activation.* Nature, 2006. **439**(7075): p. 484-9.
220. Tsuei, J., et al., *Bile acid dysregulation, gut dysbiosis, and gastrointestinal cancer.* Exp Biol Med (Maywood), 2014. **239**(11): p. 1489-504.
221. Keitel, V. and D. Haussinger, *TGR5 in the biliary tree.* Dig Dis, 2011. **29**(1): p. 45-7.
222. Alpini, G., et al., *Bile acids stimulate proliferative and secretory events in large but not small cholangiocytes.* Am J Physiol, 1997. **273**(2 Pt 1): p. G518-29.

223. Alpini, G., et al., *Bile acid feeding induces cholangiocyte proliferation and secretion: evidence for bile acid-regulated ductal secretion.* Gastroenterology, 1999. **116**(1): p. 179-86.
224. Marzioni, M., et al., *Taurocholate prevents the loss of intrahepatic bile ducts due to vagotomy in bile duct-ligated rats.* Am J Physiol Gastrointest Liver Physiol, 2003. **284**(5): p. G837-52.
225. Marzioni, M., et al., *Cytoprotective effects of taurocholic acid feeding on the biliary tree after adrenergic denervation of the liver.* Liver Int, 2007. **27**(4): p. 558-68.
226. Pellicciari, R., et al., *Discovery of 6alpha-ethyl-23(S)-methylcholic acid (S-EMCA, INT-777) as a potent and selective agonist for the TGR5 receptor, a novel target for diabesity.* J Med Chem, 2009. **52**(24): p. 7958-61.
227. de Oliveira, M.C., et al., *Bile acid receptor agonists INT747 and INT777 decrease oestrogen deficiency-related postmenopausal obesity and hepatic steatosis in mice.* Biochim Biophys Acta, 2016. **1862**(11): p. 2054-2062.
228. Wang, X.X., et al., *G Protein-Coupled Bile Acid Receptor TGR5 Activation Inhibits Kidney Disease in Obesity and Diabetes.* J Am Soc Nephrol, 2016. **27**(5): p. 1362-78.
229. Pols, T.W., et al., *TGR5 activation inhibits atherosclerosis by reducing macrophage inflammation and lipid loading.* Cell Metab, 2011. **14**(6): p. 747-57.
230. Andersen, J.B., et al., *Genomic and genetic characterization of cholangiocarcinoma identifies therapeutic targets for tyrosine kinase inhibitors.* Gastroenterology, 2012. **142**(4): p. 1021-1031 e15.
231. Chattopadhyay, E. and B. Roy, *Altered Mitochondrial Signalling and Metabolism in Cancer.* Front Oncol, 2017. **7**: p. 43.
232. de Groen, P.C., et al., *Biliary tract cancers.* N Engl J Med, 1999. **341**(18): p. 1368-78.
233. Sirica, A.E., et al., *Pathobiology of biliary epithelia and cholangiocarcinoma: proceedings of the Henry M. and Lillian Stratton Basic Research Single-Topic Conference.* Hepatology, 2008. **48**(6): p. 2040-6.
234. Demarez, C., et al., *Expression of Molecular Differentiation Markers Does Not Correlate with Histological Differentiation Grade in Intrahepatic Cholangiocarcinoma.* PLoS One, 2016. **11**(6): p. e0157140.
235. Trauner, M., et al., *New therapeutic concepts in bile acid transport and signaling for management of cholestasis.* Hepatology, 2017. **65**(4): p. 1393-1404.
236. Dai, J., et al., *Impact of bile acids on the growth of human cholangiocarcinoma via FXR.* J Hematol Oncol, 2011. **4**: p. 41.
237. Wang, W., et al., *FXR agonists enhance the sensitivity of biliary tract cancer cells to cisplatin via SHP dependent inhibition of Bcl-xL expression.* Oncotarget, 2016. **7**(23): p. 34617-29.
238. Reich, M., et al., *TGR5 is essential for bile acid-dependent cholangiocyte proliferation in vivo and in vitro.* Gut, 2016. **65**(3): p. 487-501.
239. Masyuk, A.I., et al., *Ciliary subcellular localization of TGR5 determines the cholangiocyte functional response to bile acid signaling.* Am J Physiol Gastrointest Liver Physiol, 2013. **304**(11): p. G1013-24.

240. Carino, A., et al., *The bile acid receptor GPBAR1 (TGR5) is expressed in human gastric cancers and promotes epithelial-mesenchymal transition in gastric cancer cell lines.* Oncotarget, 2016. **7**(38): p. 61021-61035.
241. Keitel, V., M. Reich, and D. Haussinger, *TGR5: pathogenetic role and/or therapeutic target in fibrosing cholangitis?* Clin Rev Allergy Immunol, 2015. **48**(2-3): p. 218-25.
242. Saich, R. and R. Chapman, *Primary sclerosing cholangitis, autoimmune hepatitis and overlap syndromes in inflammatory bowel disease.* World J Gastroenterol, 2008. **14**(3): p. 331-7.
243. Johnston, S.J. and J.S. Carroll, *Transcription factors and chromatin proteins as therapeutic targets in cancer.* Biochim Biophys Acta, 2015. **1855**(2): p. 183-92.
244. Hanahan, D. and R.A. Weinberg, *The hallmarks of cancer.* Cell, 2000. **100**(1): p. 57-70.
245. Miller, I.J. and J.J. Bieker, *A novel, erythroid cell-specific murine transcription factor that binds to the CACCC element and is related to the Kruppel family of nuclear proteins.* Mol Cell Biol, 1993. **13**(5): p. 2776-86.
246. McConnell, B.B. and V.W. Yang, *Mammalian Kruppel-like factors in health and diseases.* Physiol Rev, 2010. **90**(4): p. 1337-81.
247. Tetreault, M.P., Y. Yang, and J.P. Katz, *Kruppel-like factors in cancer.* Nat Rev Cancer, 2013. **13**(10): p. 701-13.
248. Zhang, W., et al., *The gut-enriched Kruppel-like factor (Kruppel-like factor 4) mediates the transactivating effect of p53 on the p21WAF1/Cip1 promoter.* J Biol Chem, 2000. **275**(24): p. 18391-8.
249. Yoon, H.S., et al., *Kruppel-like factor 4 prevents centrosome amplification following gamma-irradiation-induced DNA damage.* Oncogene, 2005. **24**(25): p. 4017-25.
250. Zhao, J., et al., *Identification of transcription factor KLF8 as a downstream target of focal adhesion kinase in its regulation of cyclin D1 and cell cycle progression.* Mol Cell, 2003. **11**(6): p. 1503-15.
251. Siatecka, M., L. Xue, and J.J. Bieker, *Sumoylation of EKLF promotes transcriptional repression and is involved in inhibition of megakaryopoiesis.* Mol Cell Biol, 2007. **27**(24): p. 8547-60.
252. Ratziu, V., et al., *Zf9, a Kruppel-like transcription factor up-regulated in vivo during early hepatic fibrosis.* Proc Natl Acad Sci U S A, 1998. **95**(16): p. 9500-5.
253. Kim, Y., et al., *Transcriptional activation of transforming growth factor beta1 and its receptors by the Kruppel-like factor Zf9/core promoter-binding protein and Sp1. Potential mechanisms for autocrine fibrogenesis in response to injury.* J Biol Chem, 1998. **273**(50): p. 33750-8.
254. Camacho-Vanegas, O., et al., *Shaking the family tree: identification of novel and biologically active alternatively spliced isoforms across the KLF family of transcription factors.* FASEB J, 2013. **27**(2): p. 432-6.
255. Li, Z., et al., *KLF4 promotes hydrogen-peroxide-induced apoptosis of chronic myeloid leukemia cells involving the bcl-2/bax pathway.* Cell Stress Chaperones, 2010. **15**(6): p. 905-12.
256. Zhang, G., et al., *Kruppel-like factor 4 represses transcription of the survivin gene in esophageal cancer cell lines.* Biol Chem, 2009. **390**(5-6): p. 463-9.

257. Mori, A., et al., *Up-regulation of Kruppel-like factor 5 in pancreatic cancer is promoted by interleukin-1beta signaling and hypoxia-inducible factor-1alpha.* Mol Cancer Res, 2009. **7**(8): p. 1390-8.
258. Zhu, N., et al., *KLF5 Interacts with p53 in regulating survivin expression in acute lymphoblastic leukemia.* J Biol Chem, 2006. **281**(21): p. 14711-8.
259. Farrugia, M.K., et al., *Kruppel-like Pluripotency Factors as Modulators of Cancer Cell Therapeutic Responses.* Cancer Res, 2016. **76**(7): p. 1677-82.
260. Takahashi, K. and S. Yamanaka, *Induction of pluripotent stem cells from mouse embryonic and adult fibroblast cultures by defined factors.* Cell, 2006. **126**(4): p. 663-76.
261. Jiang, J., et al., *A core Klf circuitry regulates self-renewal of embryonic stem cells.* Nat Cell Biol, 2008. **10**(3): p. 353-60.
262. Nichols, J. and A. Smith, *Pluripotency in the embryo and in culture.* Cold Spring Harb Perspect Biol, 2012. **4**(8): p. a008128.
263. Aksoy, I., et al., *Klf4 and Klf5 differentially inhibit mesoderm and endoderm differentiation in embryonic stem cells.* Nat Commun, 2014. **5**: p. 3719.
264. Conkright, M.D., et al., *A gene encoding an intestinal-enriched member of the Kruppel-like factor family expressed in intestinal epithelial cells.* Nucleic Acids Res, 1999. **27**(5): p. 1263-70.
265. Gao, Y., et al., *Targeting Kruppel-like factor 5 (KLF5) for cancer therapy.* Curr Top Med Chem, 2015. **15**(8): p. 699-713.
266. Dong, J.T. and C. Chen, *Essential role of KLF5 transcription factor in cell proliferation and differentiation and its implications for human diseases.* Cell Mol Life Sci, 2009. **66**(16): p. 2691-706.
267. Jia, L., et al., *KLF5 promotes breast cancer proliferation, migration and invasion in part by upregulating the transcription of TNFAIP2.* Oncogene, 2016. **35**(16): p. 2040-51.
268. Yang, Y., et al., *KLF4 and KLF5 regulate proliferation, apoptosis and invasion in esophageal cancer cells.* Cancer Biol Ther, 2005. **4**(11): p. 1216-21.
269. Chen, C., et al., *KLF5 is frequently deleted and down-regulated but rarely mutated in prostate cancer.* Prostate, 2003. **55**(2): p. 81-8.
270. Gaj, T., C.A. Gersbach, and C.F. Barbas, 3rd, *ZFN, TALEN, and CRISPR/Cas-based methods for genome engineering.* Trends Biotechnol, 2013. **31**(7): p. 397-405.
271. Shalem, O., et al., *Genome-scale CRISPR-Cas9 knockout screening in human cells.* Science, 2014. **343**(6166): p. 84-7.
272. Bhaya, D., M. Davison, and R. Barrangou, *CRISPR-Cas systems in bacteria and archaea: versatile small RNAs for adaptive defense and regulation.* Annu Rev Genet, 2011. **45**: p. 273-97.
273. Cong, L., et al., *Multiplex genome engineering using CRISPR/Cas systems.* Science, 2013. **339**(6121): p. 819-23.
274. Ruiz de Sabando, A., et al., *ML264, A Novel Small-Molecule Compound That Potently Inhibits Growth of Colorectal Cancer.* Mol Cancer Ther, 2016. **15**(1): p. 72-83.

275. Tong, D., et al., *Expression of KLF5 is a prognostic factor for disease-free survival and overall survival in patients with breast cancer.* Clin Cancer Res, 2006. **12**(8): p. 2442-8.
276. Chaib, H., et al., *Profiling and verification of gene expression patterns in normal and malignant human prostate tissues by cDNA microarray analysis.* Neoplasia, 2001. **3**(1): p. 43-52.
277. Huang, D., et al., *Isolation and identification of cancer stem-like cells in esophageal carcinoma cell lines.* Stem Cells Dev, 2009. **18**(3): p. 465-73.
278. Nandan, M.O., et al., *Kruppel-like factor 5 mediates the transforming activity of oncogenic H-Ras.* Oncogene, 2004. **23**(19): p. 3404-13.
279. Chen, C., et al., *KLF5 promotes cell proliferation and tumorigenesis through gene regulation and the TSU-Pr1 human bladder cancer cell line.* Int J Cancer, 2006. **118**(6): p. 1346-55.
280. Ellenbroek, S.I. and J.G. Collard, *Rho GTPases: functions and association with cancer.* Clin Exp Metastasis, 2007. **24**(8): p. 657-72.
281. Dong, Z., L. Yang, and D. Lai, *KLF5 strengthens drug resistance of ovarian cancer stem-like cells by regulating survivin expression.* Cell Prolif, 2013. **46**(4): p. 425-35.
282. Zhao, Y., et al., *Kruppel-like factor 5 modulates p53-independent apoptosis through Pim1 survival kinase in cancer cells.* Oncogene, 2008. **27**(1): p. 1-8.
283. Patel, S., et al., *Identification of yeast DNA topoisomerase II mutants resistant to the antitumor drug doxorubicin: implications for the mechanisms of doxorubicin action and cytotoxicity.* Mol Pharmacol, 1997. **52**(4): p. 658-66.
284. Tacar, O., P. Sriamornsak, and C.R. Dass, *Doxorubicin: an update on anticancer molecular action, toxicity and novel drug delivery systems.* J Pharm Pharmacol, 2013. **65**(2): p. 157-70.
285. Zhang, S., et al., *Identification of the molecular basis of doxorubicin-induced cardiotoxicity.* Nat Med, 2012. **18**(11): p. 1639-42.
286. Seubwai, W., et al., *Inhibition of NF-kappaB Activity Enhances Sensitivity to Anticancer Drugs in Cholangiocarcinoma Cells.* Oncol Res, 2016. **23**(1-2): p. 21-8.
287. Dasari, S. and P.B. Tchounwou, *Cisplatin in cancer therapy: molecular mechanisms of action.* Eur J Pharmacol, 2014. **740**: p. 364-78.
288. Valle, J., et al., *Cisplatin plus gemcitabine versus gemcitabine for biliary tract cancer.* N Engl J Med, 2010. **362**(14): p. 1273-81.
289. Mini, E., et al., *Cellular pharmacology of gemcitabine.* Ann Oncol, 2006. **17 Suppl 5**: p. v7-12.
290. Valle, J.W., et al., *Cisplatin and gemcitabine for advanced biliary tract cancer: a meta-analysis of two randomised trials.* Ann Oncol, 2014. **25**(2): p. 391-8.
291. Farrugia, M.K., et al., *Regulation of anti-apoptotic signaling by Kruppel-like factors 4 and 5 mediates lapatinib resistance in breast cancer.* Cell Death Dis, 2015. **6**: p. e1699.
292. Li, Z., et al., *Dexamethasone induces docetaxel and cisplatin resistance partially through up-regulating Kruppel-like factor 5 in triple-negative breast cancer.* Oncotarget, 2017. **8**(7): p. 11555-11565.

293. Guo, P., et al., *Pro-proliferative factor KLF5 becomes anti-proliferative in epithelial homeostasis upon signaling-mediated modification.* J Biol Chem, 2009. **284**(10): p. 6071-8.
294. Zhou, W., et al., *miR-217 inhibits triple-negative breast cancer cell growth, migration, and invasion through targeting KLF5.* PLoS One, 2017. **12**(4): p. e0176395.
295. Luan, Y. and P. Wang, *FBW7-mediated ubiquitination and degradation of KLF5.* World J Biol Chem, 2014. **5**(2): p. 216-23.
296. Akhoondi, S., et al., *FBXW7/hCDC4 is a general tumor suppressor in human cancer.* Cancer Res, 2007. **67**(19): p. 9006-12.
297. Yang, H., et al., *FBXW7 suppresses epithelial-mesenchymal transition, stemness and metastatic potential of cholangiocarcinoma cells.* Oncotarget, 2015. **6**(8): p. 6310-25.
298. Li, M., et al., *E3 ubiquitin ligase FBW7alpha inhibits cholangiocarcinoma cell proliferation by downregulating c-Myc and cyclin E.* Oncol Rep, 2017. **37**(3): p. 1627-1636.